Title
Boundary control laws and observer design for convective, turbulent and magnetohydrodynamic flows

Author
Vazquez Valenzuela, Rafael

Publication Date
2006

Peer reviewed|Thesis/dissertation

UNIVERSITY OF CALIFORNIA, SAN DIEGO

Boundary Control Laws and Observer Design for Convective, Turbulent and Magnetohydrodynamic Flows

A dissertation submitted in partial satisfaction of the requirements for the degree
Doctor of Philosophy

in

Engineering Sciences (Aerospace Engineering)

by

Rafael Vazquez Valenzuela

Committee in charge:

Professor Miroslav Krstić, Chair
Professor Thomas Bewley
Professor William Helton
Professor Juan Lasheras
Professor William McEneaney

2006

The dissertation of Rafael Vazquez Valenzuela is approved, and it is acceptable in quality and form for publication on microfilm:

Chair

University of California, San Diego

2006

DEDICATION

To my mom

EPIGRAPH

Everything is vague to a degree you do not realize
till you have tried to make it precise.

Bertrand Russell

A mathematician who is not also something of a poet
will never be a complete mathematician.

Karl Weierstrass

A child of five would understand this...
Send someone to fetch a child of five!

Groucho Marx

TABLE OF CONTENTS

LIST OF FIGURES

ACKNOWLEDGMENTS

This dissertation would not have been possible without the help and support of many people, to whom I owe far more gratitude than I can possibly express here.

First and foremost I want to express my deepest gratitude to my advisor, Professor Miroslav Krstić, whose technical and editorial advice has been essential to the completion of this dissertation. He has provided me with endless support, patience, and encouragement during the course of my graduate studies, and his relentless pursuit of academic perfection has been a reference model for me.

I gratefully acknowledge the members of my committee for reading this manuscript and for their valuable remarks. I am particullary indebted to Professors Tom Bewley and William Helton with whom I have enjoyed helpful discussions about some of my research topics, and to Professor Juan Lasheras who helped me in getting admitted to UCSD.

I would like to acknowledge the support of a EU Marie Curie CTS Fellowship that allowed me to visit the Mathematics Department in the Université Paris-Sud, France, during most of the year 2005 . I want to express my most sincere gratitude to Professors Jean-Michel Coron and Emmanuel Trélat who managed my stay and provided great advice and research support.

I am specially indebted to my colleague Andrey Smyshlyaev, whose work laid a solid foundation for this dissertation, and whose friendship and support was of great value during these years. I also want to thank the rest of my former and current fellow graduate students Lawrence Yuan, Olga Koroleva, Nick Killingsworth, Marco Luethi, Denis Jacquet and Antranik Siranosian for helpful discussions and a friendly environment in the lab, and especially Professor Eugenio Schuster and Jennie Cochran, with whom I had the pleasure to collaborate in research.

I would like to express my gratitude to my former mentors in the School of Engineering in Seville, in particular Professors Javier Aracil, Enrique Ponce, Emilio Freire and Antonio Barrero, whose teachings have had a lasting influence on my work.

In addition, I would like to thank all those who have helped me and supported me in many ways during my graduate studies, especially Dr. Gonzalo del Álamo, Professor Alberto Aliseda, Professor Carlos Canudas de Wit, Professor Eduardo F. Camacho, Dr. Laura Cerviño, Professor Enrique Fernández-Cara, Professor Mihailo R. Jovanovic, Dr. Juan Pedro Mellado, Professor Françoise Lamnabhi-Lagarrigue, Professor Costas Pozrikidis, Dr. F. Javier Rubio-Sierra, Dr. Masashi Shimada, Dr. Robert Stark, Professor Enrique Zuazua, and many other people.

Finally, my most profound thanks go to my mother, María Dolores, who has always been a role model and inspired me to pursuit a career in academia; to my father, Luis, who taught me the qualities of imagination, dedication and integrity, so important in research and in life; to Mercedes, with whom I found love when I least expected it—and needed it the most; to Miguel, whose unrelenting friendship across the ocean supported me in moments of distress; and last, but not least, to the rest of my family and loved ones in Spain, for their generous support, understanding, and patience during all this time half a world away from them.

This dissertation includes reprints or adaptations of the following papers:

R. Vazquez and M. Krstic, "Explicit integral operator feedback for local stabilization of nonlinear thermal convection loop PDEs," *Systems and Control Letters*, vol. 55, pp. 624–632, 2006. (Chapter 2)

R. Vazquez and M. Krstic, "Explicit output feedback stabilization of a thermal convection loop by continuous backstepping and singular perturbations," submitted, *2007 American Control Conference*, New York, 2007. (Chapter 3)

R. Vazquez and M. Krstic, "A closed-form feedback controller for stabilization of linearized Navier-Stokes equations: the 2D Poiseuille flow," *Proc. of the 2005 CDC*, Sevilla, Spain, 2005. (Chapter 4)

R. Vazquez and M. Krstic, "Higher order stability properties of a 2D Navier-Stokes system with an explicit boundary controller," *Proc. of the 2006 ACC*, Minneapolis, 2006. (Chapter 4)

R. Vazquez and M. Krstic, "A closed-form observer for the channel flow Navier-Stokes system," *Proc. of the 2005 CDC*, Sevilla, Spain, 2005. (Chapter 5)

R. Vazquez, E. Schuster and M. Krstic, "A closed-form feedback controller for stabilization of magnetohydrodynamic channel flow," submitted, *2007 European Control Conference*, Kos, Greece, 2007. (Chapter 6)

R. Vazquez, E. Schuster and M. Krstic, "A closed-form observer for the 3D inductionless MHD and Navier-Stokes channel flow," *Proc. of the 2006 CDC*, San Diego, 2006. (Chapter 7)

R. Vazquez, E. Trélat and J.-M. Coron, "Stable Poiseuille flow transfer for a Navier-Stokes system," *Proc. of the 2006 ACC*, Minneapolis, 2006. (Chapter 8)

R. Vazquez and M. Krstic, "Control of 1-D parabolic PDEs with Volterra nonlinearities —Part I: Design," in preparation, 2006. (Chapter 9)

R. Vazquez and M. Krstic, "Control of 1-D parabolic PDEs with Volterra nonlinearities —Part II: Analysis," in preparation, 2006. (Chapter 9)

The dissertation author was the primary author and the co–authors listed in these publications directed and supervised the research.

VITA

1999	B.S. in Electrical Engineering, School of Engineering, University of Seville, Spain
2000-2001	System Administrator and Systems Engineer, Telvent Interactiva, Seville, Spain
2003	B.S. in Mathematics, University of Seville, Spain
2004	M.S. in Aerospace Engineering, University of California, San Diego
2002–2006	Research Assistant, Department of MAE University of California, San Diego
2005	Marie-Curie CTS Fellow, Department of Mathematics Université Paris-Sud, France
2006	Ph.D. in Aerospace Engineering University of California, San Diego

PUBLICATIONS

R. Vazquez and M. Krstic, "Explicit integral operator feedback for local stabilization of nonlinear thermal convection loop PDEs," *Systems and Control Letters*, vol. 55, pp. 624–632, 2006.

R. Vazquez and M. Krstic, "A closed-form feedback controller for stabilization of linearized Navier-Stokes equations: the 2D Poiseuille flow," *Proc. of the 2005 CDC*, Sevilla, Spain, 2005.

F. J. Rubio-Sierra, R. Vazquez and R. Stark, "Transfer function analysis of the micro cantilever used in atomic force microscopy," *IEEE Transactions on Nanotechnology*, vol. 5, pp. 692–700, 2006.

R. Vazquez, E. Trélat and J.-M. Coron, "Stable Poiseuille flow transfer for a Navier-Stokes system," *Proc. of the 2006 ACC*, Minneapolis, 2006.

R. Vazquez, F. J. Rubio-Sierra and R. Stark, "Transfer function analysis of a surface coupled atomic force microscope cantilever system," *Proc. of the 2006 ACC*, Minneapolis, 2006.

R. Vazquez, E. Schuster and M. Krstic, "A closed-form observer for the 3D inductionless MHD and Navier-Stokes channel flow," *Proc. of the 2006 CDC*, San Diego, 2006.

FIELDS OF STUDY

Major Field: Engineering

Studies in Control Theory.
Professors Miroslav Krstić, Robert Bitmead, and William McEneaney

Studies in Fluid Mechanics.
Professors Paul Linden, Stefan Llewellyn Smith and Sutanu Sarkar

Studies in Differential Equations.
Professors Jean-Michel Coron, William Helton and Bruce Driver.

Studies in Numerical Methods.
Professor Costas Pozrikidis

ABSTRACT OF THE DISSERTATION

Boundary Control Laws and Observer Design
for Convective, Turbulent and Magnetohydrodynamic Flows

by

Rafael Vazquez Valenzuela
Doctor of Philosophy in Engineering Sciences (Aerospace Engineering)
University of California, San Diego, 2006
Professor Miroslav Krstić, Chair

The dissertation introduces a constructive and rigorous approach to design boundary controllers and boundary estimators for flow control problems.

We study several flow control applications, including thermal fluids with convective-type instabilities, Navier-Stokes channel flow, and magnetohydrodynamic channel flow, which are considered benchmark models to problems such as turbulence control, drag reduction, model-based turbulence estimation, cooling systems (computer systems, fusion reactors), hypersonic flight and propulsion. For all systems considered, we solve both the problem of (full state) boundary stabilization and boundary estimation, and the combination of the two, output feedback boundary stabilization. We also consider a tracking problem for the Navier-Stokes channel flow.

While some of these problems have been solved in the past, previous solutions were mainly done for spatially discretized versions of the models; however, controllers designed for a discretized plant do not always converge (when the grid size goes to zero) to stabilizing controllers for the continuous plant. In addition, the computational complexity of discretization-based methods may become overwhelming if a very fine grid is necessary in the discretizations to accurately describe the system (for example, in the case of very large Reynolds numbers in the channel flow stabilization problem).

In contrast, our method uses a continuum approach and does not require discretization. Our approach exploits the spatially invariant geometry of our model problems to apply the backstepping control/observer design method for 1-D infinite-dimensional linear parabolic systems. Backstepping produces explicitly computable control and output injection gains, which are found from the solutions of linear hyperbolic PDEs. For all considered problems we show stability of the closed-loop system (for stabilization problems) and observer estimate convergence (for estimation problems).

Finally, we also provide an extension of the backstepping method that allows to solve boundary control problems for a class of nonlinear parabolic PDEs. While boundary control of linear parabolic PDEs is a well established subject, boundary control of nonlinear parabolic PDEs is still an open problem as far as general classes of systems are concerned. Applications of interest include not only fluids but also many others like flexible structures, atomic force microscopy, aeroelasticity, chemical systems and quantum systems.

Chapter 1

Introduction

Motivation

Recent years have been marked by dramatic advances in the field of *active flow control*. This explosion can be credited not only to advances in the various fields that intersect at the discipline (such as control theory, fluid mechanics, PDE theory, and numerical methods), but also to technological developments such as Micro-Electro-Mechanical Systems (MEMS) sensors and actuators and the ever-increasing prowess of last-generation computers, that have augmented the possibilities of effective implementation in both real-life and numerical experiments. However, the area is far from being mature with still many opportunities and challenging open problems. See for instance the survey [21] for a friendly and balanced perspective on the state of the field.

When looking at the flow control literature, one finds countless papers with a wealth of applications and methods, but most results roughly fit into one of the following two categories:

1. *Constructive* results [3–9, 20, 23, 32, 42, 62, 63, 77, 78, 86, 87, 109], which range from theoretically-inspired designs (usually borrowing from well-established finite-dimensional control techniques) to hands-on experimentally-driven designs; both are mostly problem- and geometry-specific and share the objective

of obtaining an *implementable* solution, in many cases without a mathematically sound proof. Usually, a discretization-based approach is used and the results are proven by simulations or experiments.

2. *Controllability/Stabilizability* results [13–17,35,46,50,53–55,57,64,88,96,104, 106, 110], which are usually given for broad classes of systems in general geometries, but generally fail to produce an *effective* solution, being mostly existence-and-uniqueness type of results in the framework of functional analysis. However general and precise these results may be, they do not go very far, considering there are still very basic open questions such as the well-posedness of the *open-loop* 3-D Navier-Stokes equations [48], still a (million-dollar) open problem.

These two schools of research certainly benefit from some interaction; on the one hand controllability results give a clue about which problems are actually *solvable* (and sometimes point in the right direction to solve it), while on the other hand the more application-oriented research community provides controllability theorists with an endless supply of models of relevant, physically meaningful systems.

This dissertation aims towards providing results which are both *constructive* and *rigorous* from a mathematical point of view. Our work is based on the recently developed continuous backstepping control/observer design method for 1-D infinite-dimensional linear parabolic systems [101–103]. Backstepping exploits the structure of parabolic systems, and has the striking property that it both produces explicitly computable (symbolically, numerically, and in some cases, even in closed-form) gains, and at the same time provides a flexible framework that greatly facilitates mathematical proofs of stability and well-posedness even for complex systems. We exploit the spatially invariant [12] geometry of several benchmark flow control problems to apply the backstepping method.

Our applications include thermal fluids with convective-type instabilities, Navier-Stokes channel flow, and magnetohydrodynamic channel flow, which are considered benchmark models to problems such as turbulence control, drag reduction, model-based turbulence estimation, cooling systems (computer systems, fusion reactors), hypersonic flight and propulsion. In all the systems we consider both the problem of (full state) boundary stabilization and boundary estimation, and the combination of the two: output feedback boundary stabilization. We also consider a tracking problem for the Navier-Stokes channel flow. Many of these problems have been solved in the past, but previous solutions were mainly done for spatially discretized versions of the models; it is known [124] that controllers designed for a discretized plant do not always converge (when the grid size goes to zero) to stabilizing controllers for the continuous plant (specially for those of hyperbolic type).

The continuum approach also has computational advantages; the computational complexity of any discretization-based approach may become overwhelming if a very fine grid is necessary in the discretizations to accurately describe the system (for example, in the case of very large Reynolds numbers in the channel flow stabilization problem). In contrast, control and output injection gains in the backstepping method are computed solving *linear* hyperbolic PDEs in very simple domains.

We also provide an extension of the backstepping method that allows to solve boundary control problems for a class of nonlinear parabolic PDEs. While boundary control of linear parabolic PDEs is a well established subject, boundary control of nonlinear parabolic PDEs is still an open problem as far as general classes of systems are concerned. Potential applications include not only fluids but also many other interesting physical problems like flexible structures, atomic force microscopy, aeroelasticity, chemical systems, electromagnetic systems and quantum systems.

Contributions

1. **Boundary Stabilization and Boundary Estimation for a Thermal-Fluid Convection Loop ([112,120], Chapters 2, 3).** We consider a 2-D model of thermal fluid convection that exhibits the prototypical Rayleigh-Bernard convective instability. We design boundary controllers and observers for a collocated setup, with actuation and measurements located at the outer boundary. Our design is based on a combination of singular perturbation theory and the backstepping dual control/observer method, allowing to prove system stability in the L^2 and observer error convergence in the H^1 norm in the case of a large Prandtl number. The results are illustrated with simulations for a physically meaningful case.

2. **Boundary Stabilization and Boundary Estimation for 2-D Navier-Stokes Channel Flow ([113–115], Chapters 4, 5).** We present an explicit formula for a boundary control law which stabilizes the 2-D infinite channel flow benchmark problem for arbitrary Reynolds numbers. Our result uses backstepping and a Fourier transform approach, achieving exponential stabilization in the L^2, H^1 and H^2 norms for the linearized Navier-Stokes equations. Explicit solutions are obtained for the closed loop system, which is shown well-posed. We also introduce a nonlinear PDE observer that estimates the velocity and pressure fields in the channel using measurements of pressure and skin friction at one of the walls, at arbitrary Reynolds numbers. The observer structure is similar to an Extended Kalman Filter, with gains designed to guarantee observer error convergence for the linearized observer. Finally, combining the state feedback controller and the observer, an stabilizing output feedback controller for the linearized channel flow is derived.

3. **Boundary Stabilization and Boundary Estimation for 3-D Magnetohydrodynamic Channel Flow ([117, 121], Chapters 6, 7).** We

design a boundary controller that stabilizes the velocity, pressure, and electromagnetic fields in a magnetohydrodynamic 3-D channel flow, a benchmark model for applications such as cooling systems, hypersonic flight and propulsion. We also present an observer to estimate the various electromagnetic and mechanical fields inside the channel from measurements at the walls. The design is based on an extension of the 2-D non-conducting case, and deals with some issues unique to 3-D. For example, the velocity field equations (and the velocity error system for the observer), written in some appropriate coordinates, is very similar to the Orr-Sommerfeld-Squire system of PDE's and presents the same difficulties (non-normality leading to transient growth). Thus we use actuation (output injection gains in the case of the observer) not only to guarantee stability but also to decouple the system in order to prevent transients. For zero magnetic field or non-conducting fluids, the problem reduces to the 3-D Navier-Stokes channel flow and the control and observer design still hold.

4. **Stable Poiseuille Flow Transfer for 2-D Navier-Stokes Channel Flow ([116], Chapter 8).** We consider the problem of stable flow transfer between two arbitrary steady-state profiles in a 2-D periodic channel flow (for example, rest to fully developed profile for a given Reynolds number). We generate an exact velocity trajectory of the nonlinear Navier-Stokes equations that approaches exponentially the objective. A boundary control law guarantees then that the error between the state and the trajectory decays exponentially in the L^2, H^1, and H^2 norms and that the closed-loop system is well-posed. The result is first proved for the linearized Navier-Stokes equations, then shown to hold for the fully nonlinear Navier-Stokes system.

5. **Boundary Control of a Class of 1-D Parabolic Nonlinear PDEs ([118,119], Chapter 9).** Boundary control of nonlinear parabolic PDEs is a completely open problem as far as general classes of systems are concerned.

In this paper we present results identifying a broad class of systems that is stabilizable, at least locally, by a feedback law designed constructively. Our approach is a direct infinite dimensional extension of the feedback linearization/backstepping approach and employs Volterra series nonlinear operators both in the transformation to a stable linear PDE and in the feedback law. We present in full detail our design method and give several examples, analytical and numerical, for which we include simulations. We study some theoretical properties of the transformation, showing that the nonlinear Volterra operators are globally well-defined, and explicitly construct a local inverse of the feedback linearizing Volterra transformation; this, in turn, allows us to prove L^2 and H^1 local exponential stability and derive explicit closed loop solutions for the nonlinear system.

Chapter 2

Boundary Stabilization of a Thermal-Fluid Convection Loop

2.1 Introduction

In this chapter we consider a 2-D model of thermal fluid convection that exhibits the prototypical Rayleigh-Bernard convective instability [44]. The fluid is enclosed between two cylinders, heated from above and cooled from below. Imposing a temperature gradient induces density differences, which creates a circular motion that is opposed by viscosity and thermal diffusivity. For a large enough Rayleigh number, which is a function of physical constants of the system, geometry and temperature difference between the top and the bottom, the plant develops an instability.

Stabilizing controllers have been designed for this problem in the past, including an LQG controller by Burns et al [30] who formulated the problem, and a nonlinear backstepping design for a discretized version of the plant [24]. The present design is *simpler* than the former, not needing a solution of Ricatti equations, only a linear hyperbolic equation; and more *rigorous* than the latter, which does not hold in the limit when the discrete grid approaches the continuous domain.

The main ingredients of our design are singular perturbation theory and the backstepping method for infinite dimensional linear systems. Singular perturbation theory is a mature area [70] with a wealth of control applications, while backstepping for linear parabolic PDEs is a recent development [101, 102] but has already found other applications in flow control [3]. Combining both methods it is possible to design a feedback control law which stabilizes the closed loop; this is proved for a large enough Prandtl number, which is the ratio between kinematic viscosity and thermal difussivity. In this problem, the inverse of the Prandtl number plays the role of the singular perturbation parameter. Using the methods of [101], a highly accurate approximation to the control law is found in closed form

The theoretical result is suported by a simulation study for physically meaningful plant parameters, in which numerical computations of the evolution of the closed loop *nonlinear* plant and control effort is shown. In these simulations the Rayleigh number is large enough for the plant to go open loop unstable, but the controller is able to overcome the instability

2.2 Problem Statement

For the convection loop we employ the model derived in [24]. The geometry of the problem is shown in Fig. 2.1, and consists of fluid confined between two concentric cylinders standing in a vertical plane. The main assumption of this model is that the gap between the cylinders is small compared to the radius of the cylinders, i.e. $R_2 - R_1 \ll R1 < R2$. Then, introducing the Boussinesq approximation, other standard assumptions for the velocity in this 2D configuration, and integrating the momentum equation along circles of fixed radius r, the following plant equations are derived

$$v_t = \frac{\gamma}{2\pi} \int_0^{2\pi} T(t, s, \phi) \cos\phi d\phi + \nu \left(-\frac{v}{r^2} + \frac{v_r}{r} + v_{rr} \right), \tag{2.2.1}$$

$$T_t = -\frac{v}{r} T_\theta + \chi \left(\frac{T_{\theta\theta}}{r^2} + \frac{T_r}{r} + T_{rr} \right), \tag{2.2.2}$$

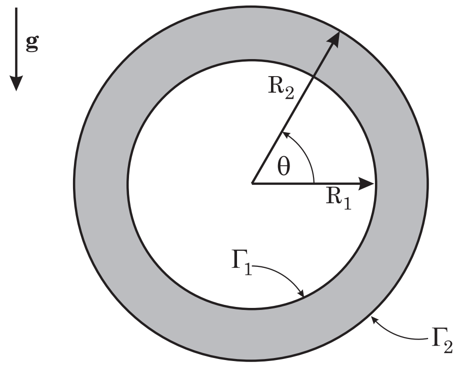

Figure 2.1: Convection Loop.

where v stands for velocity, which only depends on the radius r, T for the temperature, which depends on both r and the angle θ, ν is the kinematic viscosity, χ the thermal diffusivity, and $\gamma = g\beta$, with g representing the acceleration due to gravity and β the coefficient of thermal expansion. The boundary conditions are Dirichlet for velocity, with actuation by rotating the outer boundary, while the temperature has Neumann boundary conditions, namely $T_r(t, R_1, \theta) = \Gamma_1$, $T_r(t, R_2, \theta) = \Gamma_2$, with $\Gamma_1 = K \sin\theta$ and $\Gamma_2 = \Gamma + K \sin\theta$, where K a constant parameter representing the imposed heating and cooling in the boundaries and Γ is the actuation variable. Thus we actuate the heat flux in the outer boundary, which is more realistic than direct temperature actuation.

Defining $\tau = T - Kr\sin\theta$ we shift the equilibrium to the origin. Then, we introduce nondimensional coordinates and variables, $r' = r/d$, $t' = t\chi/d^2$, $v' = vd/\chi$, $\tau' = \tau/\Delta T$, $\Gamma' = \Gamma/\Delta T$, $R_a = (1/C)\gamma\Delta d^3/2\nu\chi$, $P = \nu/\chi$, where $d = R2 - R1$, $\Delta T = -(4/\pi)K(R_1 + R_2/2)$, C is a constant to be defined, and R_a and P are respectively the Rayleigh and Prandtl numbers. The nondimensional plant equations are, dropping primes, as follows:

$$v_t = \frac{1}{\pi} P R_a C \int_0^{2\pi} \tau(t, s, \phi) \cos\phi d\phi + P\left(-\frac{v}{r^2} + \frac{v_r}{r} + v_{rr}\right), \tag{2.2.3}$$

$$\tau_t = \frac{d\pi}{2(R_1 + R_2)} v\cos\theta - \frac{v}{r}\tau_\theta + \frac{\tau_{\theta\theta}}{r^2} + \frac{\tau_r}{r} + \tau_{rr}. \tag{2.2.4}$$

The boundary conditions are

$$v(t, R_1) = 0, \quad v(t, R_2) = V(t), \tag{2.2.5}$$

$$\tau_r(t, R_1, \theta) \ = \ 0, \quad \tau_r(t, R_2, \theta) = \Gamma(t, \theta), \tag{2.2.6}$$

where V and Γ are, respectively, the nondimensional velocity and temperature control. Note that for a given time V is an scalar, while Γ is a (periodic) function of the angle.

Following the lines of the stability study of these equations in [24], the value of C is set so the system is stable for Rayleigh numbers less than unity and unstable otherwise.

Defining $\epsilon = P^{-1}$, $A_1 = R_a C/\pi$, $A_2 = d\pi/2(R_1 + R_2)$, dropping time dependence, and neglecting the nonlinear term, the linearized plant equations are the following:

$$\epsilon v_t \ = \ A_1 \int_0^{2\pi} \tau(r, \phi) \cos\phi d\phi - \frac{v}{r^2} + \frac{v_r}{r} + v_{rr}, \tag{2.2.7}$$

$$\tau_t \ = \ A_2 v \cos\theta + \frac{\tau_{\theta\theta}}{r^2} + \frac{\tau_r}{r} + \tau_{rr}, \tag{2.2.8}$$

with the same boundary conditions.

We will stabilize this linearized plant around its equilibrium at zero, therefore stabilizing —at least locally— the full nonlinear plant.

2.3 Reduced Model

For dealing with this plant assume that the parameter ϵ is small enough so we can use singular perturbation theory.

For obtaining the value for the quasi-steady-state, we set $\epsilon = 0$ and solve (2.2.7):

$$0 = A_1 \int_0^{2\pi} \tau \cos\phi d\phi - \frac{v}{r^2} + \frac{v_r}{r} + v_{rr}. \tag{2.3.9}$$

The general solution for (2.3.9) is [100]:

$$v \ = \ C_1 r + C_2 \frac{1}{r} - \frac{A_1}{2} \int_{R_1}^{r} \int_0^{2\pi} \frac{r^2 - s^2}{r} \cos\phi \tau(s, \phi) ds d\phi.$$

The values of C_1 and C_2 depend on the boundary conditions, and therefore on the velocity actuation. The quasi-steady-state, substituted into (2.2.8), gives the reduced system, which will be stabilized via the backstepping method. For this procedure to be applicable we need the quasy-steady-state to have a strict integral feedback form [71], i.e., $v(t,r)$ should not depend on any value of τ after r. Based on this consideration we set the velocity actuation:

$$V = -\frac{A_1}{2}\int_{R_1}^{R_2}\int_0^{2\pi}\frac{R_2^2-s^2}{R_2}\cos\phi\tau(s,\phi)dsd\phi, \tag{2.3.10}$$

and then the final expression for the quasi-steady-state is

$$v = -\frac{A_1}{2}\int_{R_1}^{r}\int_0^{2\pi}\frac{r^2-s^2}{r}\cos\phi\tau(t,s,\phi)dsd\phi, \tag{2.3.11}$$

which plugged into equation (2.2.8) renders the following reduced system:

$$\tau_t = -A_{12}\int_{R_1}^{r}\int_0^{2\pi}\frac{r^2-s^2}{r}\cos\phi\cos\theta\tau(s,\phi)dsd\phi + \frac{\tau_{\theta\theta}}{r^2} + \frac{\tau_r}{r} + \tau_{rr}, \tag{2.3.12}$$

where $A_{12} = A_1A_2/2$. Note that the reduced system has an integral term which is in the desired strict feedback form.

2.4 Backstepping Controller for Temperature

For stabilization of the reduced system we apply the backstepping technique for parabolic PDEs [101], which allows for compensation of integral terms like the one that appears in (2.3.12).

2.4.1 Target system

The target system is going to be:

$$w_t = \frac{w_{\theta\theta}}{r^2} + \frac{w_r}{r} + w_{rr}, \tag{2.4.13}$$

with w periodic in θ and the following boundary conditions in r:

$$w_r(R_1) = 0, \quad w_r(R_2) = qw(R_2), \tag{2.4.14}$$

where q is negative and used for tweaking. Note that this system is exponentially stable, which follows from a standard argument taking as a Lyapunov functional the L^2 norm of w.

2.4.2 Backstepping transformation

For transforming (2.3.12) into (2.4.13) we are going to use the following change of variables:

$$w(r,\theta) = \tau(r,\theta) - \int_{R_1}^{r} \int_{0}^{2\pi} k(r,\theta,s,\phi)\tau(s,\phi)dsd\phi. \tag{2.4.15}$$

For calculating the kernel, we introduce (2.4.15) into (2.4.13) and then we apply integration by parts to arrive at an ultra-hyperbolic PDE which must be verified by the kernel,

$$\begin{aligned} k_{rr} &= -\frac{k_{\theta\theta}}{r^2} - \frac{k_r}{r} + \frac{k_{\phi\phi}}{s^2} - \frac{k_s}{s} + k_{ss} + \frac{k}{s^2} + A_{12}\left(\int_s^r \int_0^{2\pi} k(r,\theta,\rho,\psi)\right. \\ &\quad \left. \times \frac{\rho^2 - s^2}{\rho} \cos\psi d\rho d\psi - \frac{r^2 - s^2}{r}\cos\theta\right)\cos\phi, \end{aligned} \tag{2.4.16}$$

with periodic boundary conditions in both ϕ and ψ, and the following boundary conditions in the radial variables:

$$k_s(r,\theta,R_1,\phi) = \frac{k(r,\theta,R_1,\phi)}{R_1}, \tag{2.4.17}$$

$$k(r,\theta,r,\phi) = 0. \tag{2.4.18}$$

By inspection of (2.4.16) and looking for a solution, we insert the following particular shape of the kernel:

$$k(r,\theta,s,\phi) = \cos\theta\cos\phi\bar{k}(r,s), \tag{2.4.19}$$

which verifies the periodic boundary conditions, and substituted in (2.4.16) yields:

$$\bar{k}_{rr} = \frac{\bar{k}}{r^2} - \frac{\bar{k}_r}{r} - \frac{\bar{k}_s}{s} + \bar{k}_{ss} - A_{12}\left(\frac{r^2 - s^2}{r} - \pi\int_s^r \bar{k}(r,\rho)\frac{\rho^2 - s^2}{\rho}d\rho\right), \tag{2.4.20}$$

completely eliminating the angular dependence. Also, introducing $\bar{k} = \sqrt{\frac{s}{r}}\hat{k}(r,s)$ in the last equation we get:

$$\hat{k}_{rr} - \hat{k}_{ss} = \frac{3}{4}\left(\frac{1}{r^2} - \frac{1}{s^2}\right)\hat{k} - A_{12}\left(\frac{r^2 - s^2}{\sqrt{rs}} - \pi\int_s^r \hat{k}(r,\rho)\frac{\rho^2 - s^2}{\sqrt{\rho s}}d\rho\right), \tag{2.4.21}$$

a hyperbolic partial integro-differential equation, in the region $\mathcal{T}_R = \{(r,s) : R_1 \leq r \leq R_2, R_1 \leq s \leq r\}$ with boundary conditions:

$$\hat{k}_s(r,R_1) = \frac{\hat{k}(r,R_1)}{2R_1}, \tag{2.4.22}$$

$$\hat{k}(r,r) = 0. \tag{2.4.23}$$

The kernel in this form can be calculated numerically, using a simple finite difference scheme, or rewritten into an integral equation (useful for proving well-posedness and smoothness). This last step can be done introducing the following variables $\xi = r+s$, $\eta = r-s$, and denoting

$$G(\xi,\eta) = \hat{k}(r,s) = \hat{k}\left(\frac{\xi+\eta}{2}, \frac{\xi-\eta}{2}\right) \tag{2.4.24}$$

transforming the problem into the following PIDE:

$$\begin{aligned} G_{\xi\eta} &= 3\left(\frac{\xi\eta}{(\xi^2-\eta^2)^2}\right)G - A_{12}\left(\frac{\xi\eta}{2\sqrt{\xi^2-\eta^2}} - \pi\int_0^{2\eta} G\left(\xi+\frac{\rho}{2}, \eta-\frac{\rho}{2}\right)\right. \\ &\quad \left.\times\frac{(\rho+\xi-\eta)^2-(\xi-\eta)^2}{2\sqrt{(\rho+\xi-\eta)(\xi-\eta)}}d\rho\right). \end{aligned} \tag{2.4.25}$$

This equation can be transformed into a pure integral equation, doing several integrations and employing the boundary conditions, arriving at

$$\begin{aligned} G &= -A_{12}\left(\int_{2R_1+\eta}^{\xi}\int_0^{\eta}\frac{\gamma\sigma}{2\sqrt{\sigma^2-\gamma^2}}d\gamma d\sigma + \int_0^{\eta}\int_0^{\sigma} e^{\frac{\eta-\sigma}{R_1}}\right. \\ &\quad \left.\times\frac{(2R_1+\sigma)\gamma}{\sqrt{(2R_1+\sigma)^2-\gamma^2}}d\gamma d\sigma\right) + \int_{2R_1+\eta}^{\xi}\int_0^{\eta}\left(3\left(\frac{\gamma\sigma}{(\sigma^2-\gamma^2)^2}\right)G(\gamma,\sigma)\right. \\ &\quad \left.+\int_0^{2\gamma} A_{12}\pi G\left(\sigma+\frac{\rho}{2}, \gamma-\frac{\rho}{2}\right)\frac{(\rho+\sigma-\gamma)^2-(\sigma-\gamma)^2}{2\sqrt{(\rho+\sigma-\gamma)(\sigma-\gamma)}}d\rho\right)d\gamma d\sigma \\ &\quad +\int_0^{\eta}\int_0^{\sigma} 6\mathrm{e}^{\frac{\eta-\sigma}{R_1}}\left(\int_0^{2\gamma} A_{12}\pi\frac{(\rho+2R_1+\sigma-\gamma)^2-(2R_1+\sigma-\gamma)^2}{6\sqrt{(\rho+2R_1+\sigma-\gamma)(2R_1+\sigma-\gamma)}}\right. \\ &\quad \left.\times G\left(2R_1+\sigma+\frac{\rho}{2}, \gamma-\frac{\rho}{2}\right)d\rho + \frac{G(\gamma,\sigma)(2R_1+\sigma)\gamma}{((2R_1+\sigma)^2-\gamma^2)^2}\right)d\gamma d\sigma. \end{aligned} \tag{2.4.26}$$

Note that the first lines of this expression, which do not depend on G and are therefore the initial term in a successive approximation series for symbolically computing G, can be found in an explicit form:

$$\begin{aligned} G_0(\xi,\eta) &= -A_{12}\left[\frac{1}{6}(\xi^3-\eta^3-(\xi^2-\eta^2)^{3/2})+\frac{5}{2}\sqrt{\pi}R_1^3e^{1+\eta/R_1}\right.\\ &\quad\times\left(\operatorname{erf}(1)-\operatorname{erf}\left(\sqrt{1+\eta/R_1}\right)\right)+R_1^3\left(6e^{\eta/R_1}-34/3\right)-8R_1^2\eta\\ &\quad\left.-2R_1\eta^2+\frac{5}{3}\sqrt{R_1^2+R_1\eta}\left(5R_1^2+2R_1\eta\right)\right]. \end{aligned} \tag{2.4.27}$$

Using (2.4.26) and the same argument as in [101] the following result holds:

Theorem 2.1. *The equation (2.4.21) with boundary conditions (2.4.22)-(2.4.23) has a unique* $\mathcal{C}^2(\mathcal{T}_R)$ *solution.*

Therefore a smooth solution exists for equation (2.4.16) with boundary conditions (2.4.17)-(2.4.18).

2.4.3 Control law

Once the kernel is found, it is easy to derive the control law. Substituting the backstepping transformation into the outer boundary condition for the target system,

$$\begin{aligned} \tau_r(R_2,\theta) &= \int_0^{2\pi}\left(\int_{R_1}^{R_2}k_r(R_2,\theta,s,\phi)\tau(s,\phi)ds+k(R_2,\theta,R_2,\phi)\tau(R_2,\phi)\right)d\phi\\ &\quad+q\tau(R_2,\theta)-q\int_{R_1}^{R_2}\int_0^{2\pi}k(R_2,\theta,s,\phi)\tau(s,\phi)dsd\phi, \end{aligned} \tag{2.4.28}$$

and then the control law for the derivative of the temperature at the outer boundary becomes

$$\begin{aligned} \Gamma(t,\theta) &= q\tau(R_2,\theta)-\cos\theta\int_{R_1}^{R_2}\int_0^{2\pi}\frac{\sqrt{s}\cos\phi}{\sqrt{R_2}}\left(\left(q+\frac{1}{2R_2}\right)\hat{k}(R_2,s)\right.\\ &\quad\left.-\hat{k}_r(R_2,s)\right)\tau(t,s,\phi)dsd\phi. \end{aligned} \tag{2.4.29}$$

Note that q is a design parameter that does not enter the kernel equations at any point; it is set externally and enhances stability.

As we shall see in Section 2.6, $\hat{k}(R_2,s)$ is very close to $G_0(R_2+s,R_2-s)$ and $\hat{k}_r(R_2,s)$ is very close to $\frac{\partial G_0}{\partial\xi}(R_2+s,R_2-s)+\frac{\partial G_0}{\partial\eta}(R_2+s,R_2-s)$, where

$G_0(\xi,\eta)$ is defined in (2.4.27). This means that, introducing these approximations, we get explicit control laws (2.4.29), (2.3.10), using

$$\begin{aligned}\hat{k} \approx & -A_{12}\left[\frac{1}{3}(s^3+3r^2s-4(rs)^{3/2})-2R_1(r-s)^2+\frac{5}{2}\sqrt{\pi}R_1^3\mathrm{e}^{1+\frac{r-s}{R_1}}\right. \\ & \times\left(\mathrm{erf}(1)-\mathrm{erf}(\sqrt{1+\frac{r-s}{R_1}})\right)+\frac{5}{3}\sqrt{R_1^2+R_1(r-s)}\left(5R_1^2+2R_1(r-s)\right) \\ & \left.+R_1^3\left(3\mathrm{e}^{\frac{r-s}{R_1}}-34/3\right)-8R_1^2(r-s)\right]. \qquad (2.4.30)\end{aligned}$$

2.4.4 Inverse transformation

Having found the backstepping change of variables, we also look for the inverse of it. Postulating it as

$$\tau(r,\theta)=w(r,\theta)-\int_{R_1}^{r}\int_0^{2\pi}l(r,\theta,s,\phi)w(s,\phi)dsd\phi, \qquad (2.4.31)$$

then, introducing the expression for w in terms of τ an integral equation is found for this inverse kernel; introducing, as it was done for the direct transformation,

$$l(r,\theta,s,\phi) = \cos\theta\cos\phi\bar{l}(r,s), \qquad (2.4.32)$$

the equation for the inverse transformation is

$$\bar{l}(r,s)=-\bar{k}(r,s)+\pi\int_s^r\bar{l}(r,\rho)\bar{k}(\rho,s)d\rho. \qquad (2.4.33)$$

Using this integral equation a similar result to Theorem 2.1 holds for the inverse kernel.

2.5 Singular Pertubation Analysis for the Entire System

Now that we have derived a control law for the reduced system, we can drop the assumption that $\epsilon=0$ and instead consider it a small but nonzero parameter, and analyze the stability of the closed loop system. Now the quasi-steady-state solution is no longer the exact solution of the v PDE, but still plays an important role. Calling this previously calculated fast solution v_{ss},

$$v_{ss}=-\frac{A_1}{2}\int_{R_1}^{r}\int_0^{2\pi}\frac{r^2-s^2}{r}\cos\phi\tau(s,\phi)dsd\phi, \qquad (2.5.34)$$

an error variable z that measures the deviation of the velocity from the fast solution can be introduced:

$$z(t,r) = v(t,r) - v_{ss}(t,r). \tag{2.5.35}$$

We start by deriving the PDE that is verified by z:

$$\epsilon z_t = -\frac{z}{r^2} + \frac{z_r}{r} + z_{rr} + \epsilon \frac{A_1}{2} \int_{R_1}^{r} \int_0^{2\pi} \frac{r^2 - s^2}{r} \cos\phi \tau_t(s,\phi) ds d\phi, \tag{2.5.36}$$

where we have used the fact that v_{ss} verifies equation (2.3.9). This PDE without the last term is usually referred to as the Boundary Layer model; note that it is exponentially stable. The last term of (2.5.36) can be expressed in terms of τ introducing its differential equation and applying integration by parts and the τ boundary conditions, and then in terms w by using the inverse kernel.

The overall plant written in (z,w) variables has the form

$$\begin{aligned}
\epsilon z_t &= -\frac{z}{r^2} + \frac{z_r}{r} + z_{rr} + \epsilon \Bigg(\int_{R_1}^{r} Q_{zz}(r,s) z(s) ds \\
&\quad + \int_{R_1}^{r} \int_0^{2\pi} Q_{zw}^1(r,s,\phi) w(s,\phi) ds d\phi + \int_0^{2\pi} Q_{zw}^2(r,\phi) w(r,\phi) d\phi \\
&\quad + \int_0^{2\pi} Q_{zw_0}(r,\phi) w(R_1,\phi) d\phi \Bigg), & (2.5.37) \\
w_t &= \frac{w_{\theta\theta}}{r^2} + \frac{w_r}{r} + w_{rr} + Q_{wz}^2(r,\theta) z(r) + \int_{R_1}^{r} Q_{wz}^1(r,s,\theta) z(s) ds, & (2.5.38)
\end{aligned}$$

together with boundary conditions $z(R_1) = z(R_2) = 0$, $w_r(R_1,\theta) = 0$, $w_r(R_2,\theta) = qw(R_2,\theta)$, and periodic angular boundary conditions for w. For simplicity, we have denoted the following kernels:

$$\begin{aligned}
Q_{zz} &= A_{12}\pi \frac{r^2 - s^2}{r}, & (2.5.39) \\
Q_{zw}^1 &= -\frac{A_1}{2} \cos\phi \left(2\pi \bar{l}(r,s) + A_{12} \cos\phi \frac{r^4 - s^4 - 4r^2 s^2 \ln \frac{r}{s}}{4r} \right), & (2.5.40) \\
Q_{zw}^2 &= A_1 \cos\phi, & (2.5.41) \\
Q_{wz}^1 &= -A_2 \pi \cos\theta \bar{k}(r,s), & (2.5.42) \\
Q_{wz}^2 &= A_2 \cos\theta, & (2.5.43) \\
Q_{zw_0} &= \frac{A_1}{2} \frac{r^2 + R_1^2}{r R_1} \cos\phi. & (2.5.44)
\end{aligned}$$

For the stability proof we are going to use the following energy Lyapunov functionals:

$$E_w(t) = \frac{1}{2}\int_0^{2\pi}\int_{R_1}^{R_2} w^2(t,s,\phi)sdsd\phi, \tag{2.5.45}$$

$$E_z(t) = \frac{1}{2}\int_{R_1}^{R_2} z^2(t,s)sds. \tag{2.5.46}$$

The time derivative of E_w can be bounded in the following way:

$$\begin{aligned}\frac{dE_w}{dt} \le & -\int_0^{2\pi}\int_{R_1}^{R_2}\frac{w_\theta^2}{s^2}sdsd\phi - \frac{1}{2}\int_0^{2\pi}\int_{R_1}^{R_2} w_r^2 sdsd\phi + \left(q + \frac{R_2}{4(R_2-R_1)}\right) \\ & \times \int_0^{2\pi} R_2 w(R_2,\phi)^2 d\phi - \frac{1}{8(R_2-R_1)^2}\int_0^{2\pi}\int_{R_1}^{R_2} w^2 sdsd\phi \\ & + \beta_1\left(\int_0^{2\pi}\int_{R_1}^{R_2} w^2(s,\phi)sdsd\phi\right)^{\frac{1}{2}}\left(\int_{R_1}^{R_2} z^2(s)sds\right)^{\frac{1}{2}},\end{aligned} \tag{2.5.47}$$

where

$$\beta_1 = \sqrt{2\pi}\left(\|Q_{wz}^2\|_\infty + \sqrt{(R_2^2-R_1^2)\ln\frac{R_2}{R_1}}\|Q_{wz}^1\|_\infty\right). \tag{2.5.48}$$

The time derivative of E_z has the following bound:

$$\begin{aligned}\frac{dE_z}{dt} \le & -\left(\frac{1}{\epsilon R_2^2} - \gamma\right)\int_{R_1}^{R_2} z^2 sds + \beta_2\left(\int_0^{2\pi}\int_{R_1}^{R_2} w^2(s,\phi)sdsd\phi\right)^{\frac{1}{2}} \\ & \times \left(\int_{R_1}^{R_2} z^2(s)sds\right)^{\frac{1}{2}} + \beta_3\int_0^{2\pi} w^2(t,R_2,\phi)d\phi \\ & + \frac{1}{2}\int_{R_1}^{R_2}\int_0^{2\pi} w_r^2(t,r,\phi)sdsd\phi,\end{aligned} \tag{2.5.49}$$

where

$$\beta_2 = \sqrt{2\pi}\left(\|Q_{zw}^2\|_\infty + \sqrt{(R_2^2-R_1^2)\ln\frac{R_2}{R_1}}\|Q_{zw}^1\|_\infty\right), \tag{2.5.50}$$

$$\beta_3 = -\frac{R_2}{2}\left(q + \frac{R_2}{4(R_2-R_1)}\right), \tag{2.5.51}$$

$$\gamma = \gamma_1 + 2\gamma_2 + \frac{\gamma_3}{\beta_3}, \tag{2.5.52}$$

$$\gamma_1 = \sqrt{(R_2^2-R_1^2)\ln\frac{R_2}{R_1}}\|Q_{zz}\|_\infty, \tag{2.5.53}$$

$$\gamma_2 = \pi^2(R_2-R_1)^2\|Q_{zw_0}\|_\infty^2 R_2, \tag{2.5.54}$$

$$\gamma_3 = \frac{\pi^2}{2}(R_2-R_1)\|Q_{zw_0}\|_\infty^2. \tag{2.5.55}$$

In both of the previous calculations repeated use of Cauchy-Schwartz's and Young's inequality has been made, and the following Lemma (a version of Poincare's inequality) has been employed.

Lemma 2.2. *For any $\tau \in H^1(R_1, R_2)$ the following inequality holds:*

$$\begin{aligned} &\int_0^{2\pi}\int_{R_1}^{R_2} \tau^2(r,\theta) r dr d\theta \\ \leq\ & 2R_2(R_2 - R_1)\int_0^{2\pi} \tau^2(R_2,\theta)d\theta \\ &+4(R_2-R_1)^2\int_0^{2\pi}\int_{R_1}^{R_2} \tau_r^2(r,\theta) r dr d\theta. \end{aligned} \tag{2.5.56}$$

We skip the proof which is standard, see, e.g., [72].

Selecting the following Lyapunov function,

$$E(t) = E_w(t) + E_z(t), \tag{2.5.57}$$

we find its time derivative to be:

$$\begin{aligned} \frac{dE(t)}{dt} \leq\ & -\int_0^{2\pi}\int_{R_1}^{R_2} \frac{w_\theta^2}{s^2} s ds d\phi + \frac{R_2}{2}\left(q + \frac{R_2}{4(R_2-R_1)}\right) \\ & \times \int_0^{2\pi} w(t,R_2,\phi)^2 d\phi - \frac{1}{8(R_2-R_1)^2}\int_0^{2\pi}\int_{R_1}^{R_2} w^2 s ds d\phi \\ & +(\beta_1+\beta_2)\left(\int_{R_1}^{R_2} z^2(s) s ds\right)^{\frac{1}{2}}\left(\int_0^{2\pi}\int_{R_1}^{R_2} w^2(s,\phi) s ds d\phi\right)^{\frac{1}{2}} \\ & -\left(\frac{1}{\epsilon R_2^2} - \gamma\right)\int_{R_1}^{R_2} z^2 s ds. \end{aligned} \tag{2.5.58}$$

In this equation we have to choose q and ϵ so the final expression is negative definite. We set the first as:

$$q = -1 - \frac{R_2}{4(R_2 - R_1)}. \tag{2.5.59}$$

For finding a value for ϵ, we identify the quadratic form which appears in (2.5.58) and call its matrix A:

$$A = \begin{pmatrix} \frac{1}{8(R_2-R_1)^2} & -\frac{\beta_1+\beta_2}{2} \\ -\frac{\beta_1+\beta_2}{2} & \frac{1}{\epsilon R_2^2} - \gamma \end{pmatrix}. \tag{2.5.60}$$

Our interest is to find the maximum possible value of ϵ so $A > 0$. From Sylvester's criterion we get the condition for A to be positive definite:

$$0 < \left(\frac{1}{\epsilon R_2^2} - \gamma\right) - 2(R_2 - R_1)^2(\beta_1 + \beta_2)^2. \tag{2.5.61}$$

Solving for $1/\epsilon$,

$$\frac{1}{\epsilon} \;>\; 2R_2^2(R_2 - R_1)^2\left(\beta_1 + \beta_2\right)^2 + R_2^2\gamma. \tag{2.5.62}$$

Substituting γ, we can define an upper bound for ϵ:

$$\frac{1}{\epsilon*} \;=\; 2R_2^2(R_2 - R_1)^2\left(\beta_1 + \beta_2\right)^2 + R_2^2\left(\gamma_1 + 2\gamma_2 + 2\frac{\gamma_3}{R_2}\right). \tag{2.5.63}$$

Note that this bound is a function which depends exclusively of the geometry and physical parameters of the plant.

This establishes asymptotic stability for the plant in the z, w coordinates, when $\epsilon \in (0, \epsilon^*)$. Stability in the original coordinates follows from the following inequalities:

$$\|\tau\|_2^2 \;\leq\; \|w\|_2^2\left(1 + \|\bar{l}\|_\infty\sqrt{\frac{\pi(R_2 - R_1)(R_2^2 - R_1^2)}{R_1}}\right)^2 \tag{2.5.64}$$

and

$$\begin{aligned}\|v\|_2^2 \;&\leq\; 2\|z\|_2^2 + 2\|w\|_2^2\left(\frac{(R_2 - R_1)(R_2^2 - R_1^2)^2}{R_1^3}\right)\\ &\times\left(1 + \|\bar{l}\|_\infty\sqrt{\frac{\pi(R_2 - R_1)(R_2^2 - R_1^2)}{R_1}}\right)^2\end{aligned} \tag{2.5.65}$$

which are derived taking norm in the respective definitions. We have just proved the following theorem:

Theorem 2.3. *For a sufficiently small ϵ, the system (2.2.7)-(2.2.8) with boundary conditions (2.2.5)–(2.2.6) and control laws (2.3.10) and (2.4.29) is exponentially stable at the origin in the L^2 sense, that is, there exist positive constants M and*

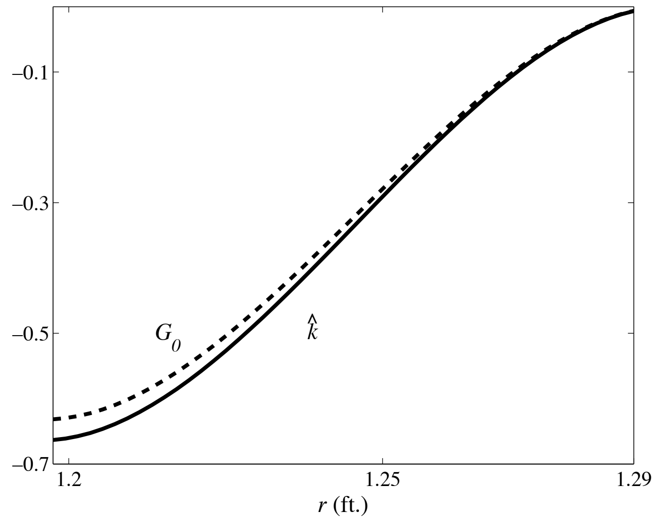

Figure 2.2: Exact (solid) and approximate (dashed) control kernels at R_2.

α, independent of the initial conditions, such that

$$\begin{aligned} & \int_{R_1}^{R_2} \left(v^2(t,s) + \int_0^{2\pi} \tau^2(t,s,\phi) d\phi \right) s ds \\ \leq \quad & M \mathrm{e}^{-\alpha t} \int_{R_1}^{R_2} \left(v^2(0,s) + \int_0^{2\pi} \tau^2(0,s,\phi) d\phi \right) s ds \end{aligned} \tag{2.5.66}$$

The proof of existence and uniqueness of classical solutions has been skipped, but follows from standard arguments due to linearity of (2.2.7)-(2.2.8) and due to the form of the boundary conditions.

2.6 Simulation Study

We show a prototypical simulation case. For numerical computations, a spectral method combined with the well-known Crank-Nicholson method (see, for example, [59]) has been used, using the following numerical values: $R_1 = 0.369$ m., $R_2 = 0.39$ m., $P = 8.06$, $Ra = 50$, $C = 7.8962 \times 10^3$, $K = 9.11$ °C/m. Note that the Prandtl number has a value greater than unity, but not too large; that value is typical, for instance, of water.

Interestingly, it can be shown that a discretized version of our plant approximates the ordinary differential equations of Lorenz's simplified model of con-

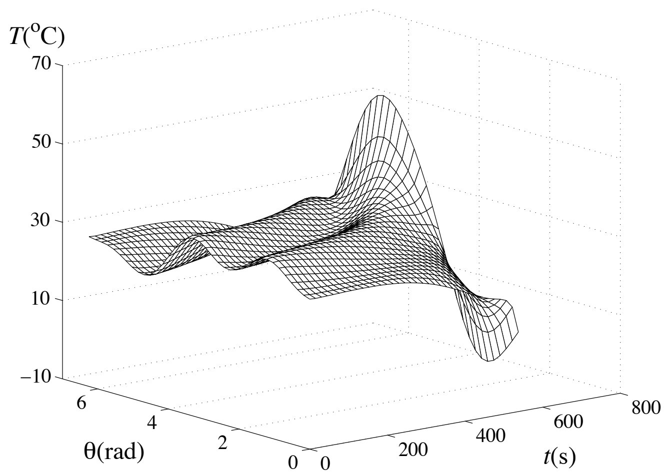

Figure 2.3: Open loop evolution of temperature at radius $r = 0.37$ m.

vection [83]. However, with the chosen plant parameters, the plant does not show chaotic behavior. On the other hand it is well known that the parameter values that lead to chaos in Lorenz's equations are not physical [56].

In Fig. 2.2 the shape of the control kernel, $\hat{k}(R_2, s)$ is plotted, showing that information near the inner boundary is given more weight in the control law, which makes sense as the boundary controller is on the opposite side and therefore has to react more agressively to compensate fluctuations of temperature in the interior part of the domain. The approximate kernel given by $G_0(R_2 + s, R_2 - s)$, which is (2.4.30) is also shown, and it can be seen that it is an excellent approximation. Fig. 2.3 is an open loop simulation of temperature, which grows very positive or very negative, depending on the angle, eventually becoming too large for further computations. In Fig. 2.4 closed loop simulations of the plant are shown in physical variables (velocity and temperature) showing how they reach the equilibrium state quickly, staying there afterwards. The magnitude of heat flux control is also shown, while the velocity actuation can be seen just looking at the $r = R_2$ section in the velocity plot, which is the outer cylinder rotation imposed by the control law. There is an initial, apparently instantaneous change in the velocity, which happens in a faster time scale than the evolution of the other variable, a typical behavior of singularly perturbed systems; since the boundary layer system is exponentially stable, once the control is set, the velocity goes very fast to the quasi-steady state and remains there for the rest of time. Fig. 2.5 provides a detail of this initial evolution. As can be seen, the only jump in velocity is located in the outer boundary, since the (closed loop) boundary conditions are not verified by the initial conditions and we do not consider actuator dynamics, but this is not particularly unrealistic—the velocities considered are of the order of milimeters per second.

This chapter is a partial reprint of the material as it appears in
R. Vazquez and M. Krstic, "Explicit integral operator feedback for local stabilization of nonlinear thermal convection loop PDEs," *Systems and Control Letters*, vol. 55, pp. 624–632, 2006.
The dissertation author was the primary author and the coauthor listed in this publication directed and supervised the research, which is the basis for this chapter.

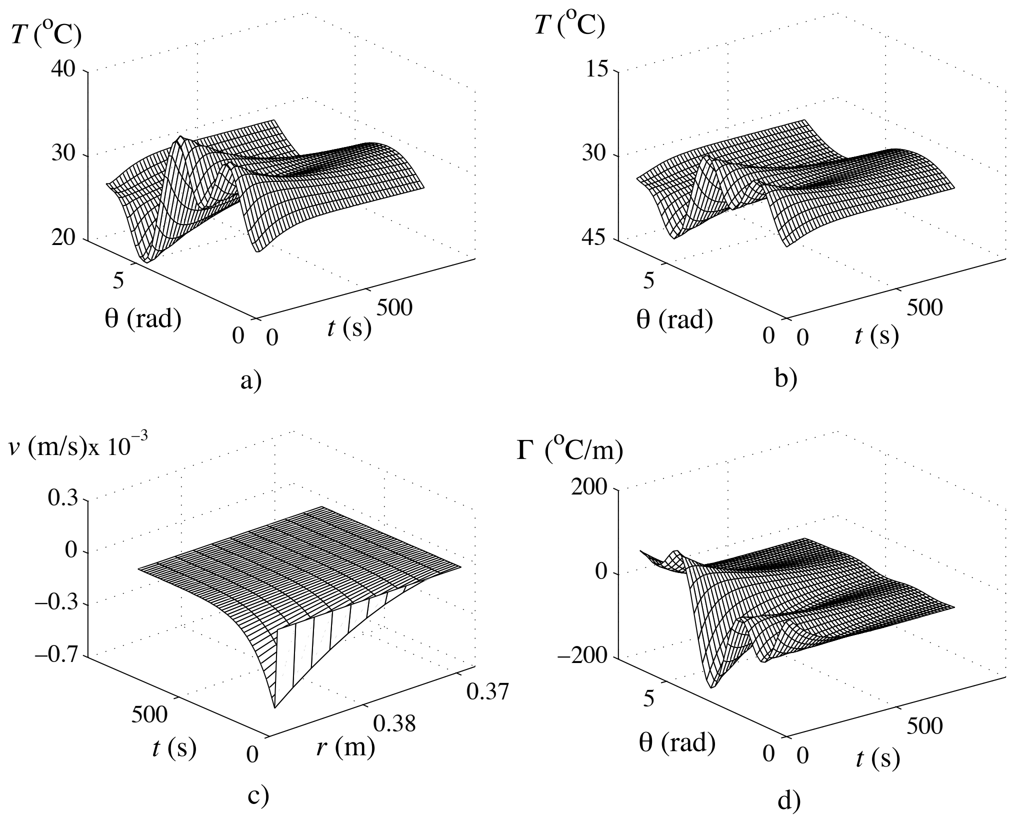

Figure 2.4: Closed-loop simulation. a) temperature at radius $r = 0.37$ m. b) temperature at radius $r = 0.38$ m. c) velocity d) temperature control effort.

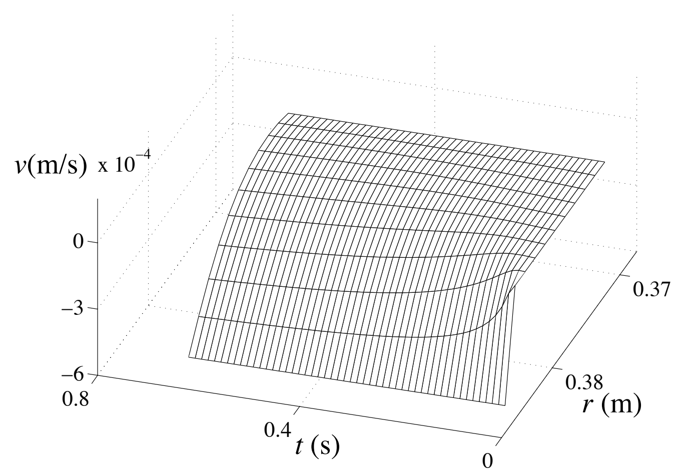

Figure 2.5: Detail of the initial evolution of velocity.

Chapter 3

Boundary Estimation for Output-Feedback Stabilization of a Thermal-Fluid Convection Loop

3.1 Introduction

In this chapter we consider the problem of designing an output feedback controller for the thermal fluid convection loop presented in Chapter 2.

Instead of using the direct approach of Chapter 2 (which will make the design problem technically difficult), we first reduce the complexity of the plant by showing that the temperature can be decomposed into two new independent variables. This allows us to express the system as the combination of two separate subsystem, which are stabilized separately. One of the subsystems is easily tractable and a Lyapunov method is used for obtaining an explicit output feedback stabilizing law. For the other subsystem we design a full state control law and an observer using singular perturbations and the dual PDE backstepping control/observer design methods [101, 102]. The observer is then used to obtain estimates for the control law. The design method is as in Chapter 2 and allows us to obtain explicit control and output injection gains.

Thus we obtain an output feedback control law, which is shown to stabilize the linearized closed loop system. As in Chapter 2, this is proved for a large enough Prandtl number and the theoretical result is supported by a numerical study.

3.2 Problem Statement

We start from the nondimensional linearized model of Section 2.2, which is given by (2.2.7)–(2.2.8) with boundary conditions (2.2.5)–(2.2.6). Our objective is to design stabilizing output feedback laws for V and Γ, the nondimensional velocity and temperature control, assuming that measurements of $v_r(r)$ (proportional to skin friction) and $\tau(r,\theta)$ are available only for $r = R_2$.

3.3 System Decomposition

Defining new variables

$$u(t,r) = \frac{1}{\pi}\int_0^{2\pi} \tau(t,r,\theta)\cos\theta d\theta, \tag{3.3.1}$$

$$U(t) = \frac{1}{\pi}\int_0^{2\pi} \Gamma(t,\theta)\cos\theta d\theta, \tag{3.3.2}$$

and letting $\zeta = \tau - u\cos\theta$ and $\Upsilon = \Gamma - U\cos\theta$, we can write the plant in (v,u,ζ) variables as

$$\epsilon v_t = \pi A_1 u - \frac{v}{r^2} + \frac{v_r}{r} + v_{rr}, \tag{3.3.3}$$

$$u_t = A_2 v - \frac{u}{r^2} + \frac{u_r}{r} + u_{rr}, \tag{3.3.4}$$

$$\zeta_t = \frac{\zeta_{\theta\theta}}{r^2} + \frac{\zeta_r}{r} + \zeta_{rr}, \tag{3.3.5}$$

with boundary conditions

$$\begin{aligned} v(t, R_1) &= 0, \quad v(t, R_2) = V(t), && (3.3.6) \\ u_r(t, R_1) &= 0, \quad u_r(t, R_2) = U(t), && (3.3.7) \\ \zeta_r(t, R_1, \theta) &= 0, \quad \zeta_r(t, R_2, \theta) = \Upsilon(t). && (3.3.8) \end{aligned}$$

Remark 3.1. The variable u is the first cosine coefficient of the Fourier series of the periodic variable τ whereas ζ contains the remaining periodic components. The variable ζ verifies

$$\int_0^{2\pi} \zeta \cos\theta d\theta = \int_0^{2\pi} \tau \cos\theta d\theta - \pi u = 0, \qquad (3.3.9)$$

and therefore is orthogonal (in the $L^2(0, 2\pi)$ sense) to $u \cos\theta$. Hence, both u and ζ are independent and needed to recover τ.

Our design task is to find output feedback control laws Υ, V and U such that the equilibrium profile $\zeta \equiv v \equiv u \equiv 0$ is exponentially stable. For the statement of stability, we define the norms

$$\begin{aligned} \|f\|_{L^2_\theta}^2 &= \int_0^{2\pi} \int_{R_1}^{R_2} f(r,\theta)^2 r dr d\theta, && (3.3.10) \\ \|f\|_{H^1_\theta}^2 &= \|f\|_{L^2_\theta}^2 + \|f_r\|_{L^2_\theta}^2 + \|\frac{f_\theta}{r}\|_{L^2_\theta}^2, && (3.3.11) \end{aligned}$$

for functions f that depend both on angle θ and radius r, and

$$\begin{aligned} \|f\|_{L^2}^2 &= \int_{R_1}^{R_2} f(r)^2 r dr d\theta, && (3.3.12) \\ \|f\|_{H^1}^2 &= \|f\|_{L^2}^2 + \|f_r\|_{L^2}^2, && (3.3.13) \end{aligned}$$

for functions f only depending on the radius.

Remark 3.2. Lemma 3.7 (see Section 3.8) shows that the L^2 and H^1 norms of τ can be written as a combination of the same norms of u and ζ. Hence, exponential stability in the L^2 norm (resp. H^1 norm) of the origin for both ζ and u is equivalent to exponential stability of the origin in the L^2 norm (resp. H^1 norm) of τ.

Thus, we study stability in the (v, u, ζ) system of equations (3.3.3)–(3.3.5). This system can be decomposed in two subsystem, the ζ subsystem with control law Υ, and the (v, u) subsystem with control laws V, U. Both subsystem are not coupled so we analyze and control them independently.

3.4 Stabilization of ζ Subsystem

For Υ we set the following output feedback law

$$\Upsilon = -q_0 \zeta(R2, \theta), \tag{3.4.14}$$

where $q_0 = \frac{1}{2(R_2 - R_1)}$. Then, we get the following stability property (see Section 3.8 for the proof).

Proposition 3.3. *Consider (3.3.5) with boundary conditions (3.3.8) and control law (3.4.14). Then, the equilibrium $\zeta \equiv 0$ is exponentially stable in the H^1 norm, i.e., there exists $C_1, c_1 > 0$ s.t.*

$$\|\zeta(t)\|_{H^1_\theta} \leq C_1 \mathrm{e}^{-c_1 t} \|\zeta(0)\|_{H^1_\theta}. \tag{3.4.15}$$

3.5 Stabilization of (v, u) Subsystem

In dealing with the (v, u) subsystem we follow a similar strategy to Chapter 2, but also adding an observer for state estimation.

First, we eliminate the convective term (v_r for (3.3.3) and u_r for (3.3.4). Define $\check{v} = v\sqrt{r}$, $\check{u} = u\sqrt{r}$. Then $\check{v}$ and $\check{u}$ verify

$$\epsilon \check{v}_t = \pi A_1 \check{u} - \lambda(r)\check{v} + \check{v}_{rr}, \tag{3.5.16}$$

$$\check{u}_t = A_2 \check{v} - \lambda(r)\check{u} + \check{u}_{rr}, \tag{3.5.17}$$

and boundary conditions

$$\check{v}(R_1) = 0, \quad \check{v}(R_2) = \check{V}, \tag{3.5.18}$$

$$\check{u}_r(R_1) = \frac{\check{u}(R_1)}{2R_1}, \quad \check{u}_r(R_2) = \check{U}, \tag{3.5.19}$$

where $\lambda(r) = \frac{3}{4r^2}$, $\check{V} = \sqrt{R_2}V$, $\check{U} = \frac{\check{u}(R_2)}{2R_2} + \sqrt{R_2}U$. We drop checks in the sequel for simplicity.

3.5.1 Control Design

First we design full state feedback laws V and U. As in Chapter 2 we assume that the parameter ϵ is small enough so we can use singular perturbation theory [70].

Quasi-steady-state

The first step is to compute the quasi-steady-state (QSS) by setting $\epsilon = 0$ in Equation (3.5.16). Then, the QSS is the solution of the linear ODE

$$v_{rr} - \lambda(r)v + \pi A_1 u(r) = 0, \tag{3.5.20}$$

with boundary conditions $v(R_1) = 0, v(R_2) = V$. The solution is

$$v = \int_{R_1}^{r} f(r,s)u(s)ds - f_R(r)\left(\int_{R_1}^{R_2} f(R_2,s)u(s)ds - V(r)\right), \tag{3.5.21}$$

where

$$f(r,s) = -\frac{\pi A_1}{2}\frac{r^2 - s^2}{\sqrt{rs}}, \tag{3.5.22}$$

$$f_R(r) = \frac{r^2 - R_1^2}{R_2^2 - R_1^2}\sqrt{\frac{R_2}{r}}. \tag{3.5.23}$$

The velocity control V appears inside (3.5.21). We use it to put the QSS in strict-feedback form [71], by eliminating the non-strict-feedback integral in the second line of (3.5.21), so we can use the backstepping method for strict-feedback parabolic PDE's [101]. For that, set

$$V = \int_{R_1}^{R_2} f(R_2,s)u(s)ds, \tag{3.5.24}$$

then the QSS is

$$v = \int_{R_1}^{r} f(r,s)u(s)ds. \tag{3.5.25}$$

Reduced model

The reduced model is obtained by plugging the QSS into Equation (3.5.16). We get

$$u_t = u_{rr} - \lambda(r)u + A_2 \int_{R_1}^{r} f(r,s)u(s)ds, \tag{3.5.26}$$

$$u_r(R_1) = \frac{u(R_1)}{2R_1}, \quad u_r(R_2) = U, \tag{3.5.27}$$

an strict-feedback parabolic PIDE with reaction and integral terms. We apply backstepping [101] to map (3.5.26)–(3.5.27) into the target system

$$w_t = w_{rr} - \lambda(r)w, \tag{3.5.28}$$

$$w_r(R_1) = \frac{w(R_1)}{2R_1}, w_r(R_2) = 0, \tag{3.5.29}$$

where the reaction term λ has been kept since it helps stability. The backstepping transformation is defined as follows

$$w = u - \int_{R_1}^{r} k^*(r,s)u(s)ds. \tag{3.5.30}$$

We use k^* to avoid confusions with the kernel k of Chapter 2. The kernel $k^*(r,s)$ is found to verify the following hyperbolic partial integro-differential equation in the domain $\mathcal{T}_R$

$$\begin{aligned} k^*_{rr} - k^*_{ss} &= (\lambda(r) - \lambda(s))k^*(r,s) - A_2 f(r,s) \\ &\quad + A_2 \int_{s}^{r} f(\sigma,s)k^*(r,\sigma)d\sigma, \end{aligned} \tag{3.5.31}$$

$$k^*(r,r) = 0, \quad k^*_s(r,R_1) = \frac{k^*(r,R_1)}{2R_1}. \tag{3.5.32}$$

If we substitute $k^* = \pi\hat{k}$ in (3.5.31)–(3.5.32), we obtain exactly (2.4.21)–(2.4.23). Hence, $k^* = \pi\hat{k}$ and the approximate expression (2.4.30) gives also a explicit formula for k^*. Using the kernel k, the control law U is found to be

$$U = \int_{R_1}^{R_2} k^*_r(R_2,s)u(s)ds. \tag{3.5.33}$$

The same argument as in Section 2.5 proves that for sufficiently small ϵ, the control laws V and U stabilize the system.

3.5.2 Observer Design

Since control laws (3.5.24) and (3.5.33) require knowledge of the full state of the system, we design an observer to estimate the state from the measurements $v_r(R_2)$ and $u(R_2)$. We postulate our observer as a copy of the plant with output injection of measurement error, as follows

$$\begin{aligned} \epsilon\hat{v}_t &= \hat{v}_{rr} - \lambda(r)\hat{v} + \pi A_1\hat{u}, && (3.5.34) \\ \hat{u}_t &= \hat{u}_{rr} - \lambda(r)\hat{u} + A_2\hat{v} + p_1(r)\left(u(R_2) - \hat{u}(R_2)\right) \\ &\quad + p_2(r)\left(v_r(R_2) - \hat{v}_r(R_2)\right), && (3.5.35) \\ \hat{v}(R_1) &= 0, \quad \hat{v}(R_2) = V, && (3.5.36) \\ \hat{u}_r(R_1) &= \frac{\hat{u}(R_1)}{2R_1}, && (3.5.37) \\ \hat{u}_r(R_2) &= U - p_{10}\left(u(R_2) - \hat{u}(R_2)\right), && (3.5.38) \end{aligned}$$

where hats denote estimated variables, and p_1, p_2 and p_{10} are output injection gains, to be found. Defining the observer error variables as $\tilde{v} = v - \hat{v}$, $\tilde{u} = u - \hat{u}$, the observer error equations are

$$\begin{aligned} \epsilon\tilde{v}_t &= \tilde{v}_{rr} - \lambda(r)\tilde{v} + \pi A_1\tilde{u}, && (3.5.39) \\ \tilde{u}_t &= \tilde{u}_{rr} - \lambda(r)\tilde{u} + A_2\tilde{v} - p_1(r)\tilde{u}(R_2) - p_2(r)\tilde{v}_r(R_2), && (3.5.40) \\ \tilde{v}(R_1) &= \tilde{v}(R_2) = 0, && (3.5.41) \\ \tilde{u}_r(R_1) &= \frac{\tilde{u}(R_1)}{2R_1}, \quad \tilde{u}_r(R_2) = p_{10}\tilde{u}(R_2). && (3.5.42) \end{aligned}$$

As in Section 3.5.1, we apply singular perturbation theory to design output injection gains p_1, p_2 and p_{10}.

Quasi-steady-state

Setting $\epsilon = 0$ in (3.5.39), the QSS is the solution of

$$\tilde{v}_{rr} - \lambda(r)\tilde{v} + \pi A_1\tilde{u} = 0, \tag{3.5.43}$$

with $\tilde{v}(R_1) = \tilde{v}(R_2) = 0$. The solution is

$$\tilde{v} = -\int_r^{R_2} f(r,s)\tilde{u}(s)ds + \int_{R_1}^{R_2} h(r,s)\tilde{u}(s)ds, \tag{3.5.44}$$

where

$$h(r,s) \quad = \quad f_R(R_2+R_1-r)f(R_1,s). \tag{3.5.45}$$

Using the measurement $v_r(R_2)$ to write the solution, the QSS is

$$\tilde{v} = -\int_r^{R_2} f(r,s)\tilde{u}(s)ds + h_R(r)v_r(R_2), \tag{3.5.46}$$

where

$$h_R(r) = \frac{r^2-R_2^2}{2\sqrt{R_2 r}}. \tag{3.5.47}$$

Note that we have written the QSS in terms of an "upper-triangular" rather than a strict-feedback ("lower-triangular") integral of the state $\tilde{u}$. This is necessary for applying the backstepping observer design method for collocated systems [102], which makes use of an upper-triangular transformation.

Reduced Model

Plugging (3.5.46) into (3.5.39) we get the reduced model for the observer error, which is

$$\begin{aligned}\tilde{u}_t \quad &= \quad \tilde{u}_{rr} - \lambda(r)\tilde{u} - A_2\left(\int_r^{R_2} f(r,s)\tilde{u}(s)ds - h_R(r)v_r(R_2)\right)\\ &\quad -p_1(r)\tilde{u}(R_2) - p_2(r)\tilde{v}_r(R_2),\end{aligned} \tag{3.5.48}$$

Set $p_2(r) = A_2 h_R(r)$. Then,

$$\tilde{u}_t \quad = \quad \tilde{u}_{rr} - \lambda(r)\tilde{u} - A_2\int_r^{R_2} f(r,s)\tilde{u}(s)ds - p_1(r)\tilde{u}(R_2), \tag{3.5.49}$$

is a parabolic PDE equation in u with an upper-triangular integral term, and boundary conditions

$$\tilde{u}_r(R_1) \quad = \quad \frac{\tilde{u}(R_1)}{2R_1}, \tilde{u}_r(R_2) = p_{10}\tilde{u}(R_2). \tag{3.5.50}$$

Following the backstepping observer design method for collocated systems [102], we apply an upper-triangular transformation,

$$\tilde{u} = \tilde{w} - \int_r^{R_2} p(r,s)\tilde{w}(s)ds, \tag{3.5.51}$$

where $\tilde{w}$ verifies

$$\begin{aligned}
\tilde{w}_t &= \tilde{w}_{rr} - \lambda(r)\tilde{w}, && (3.5.52)\\
\tilde{w}_r(R_1) &= \frac{\tilde{w}(R_1)}{2R_1}, \quad \tilde{w}_r(R_2) = 0. && (3.5.53)
\end{aligned}$$

The kernel $p(r,s)$ is found to verify the following equation in the domain $\mathcal{T}_R$

$$\begin{aligned}
p_{ss} - p_{rr} &= (\lambda(s) - \lambda(r))\, p + A_2 f(r,s) - A_2 \int_r^s f(r,\sigma)p(\sigma,s)d\sigma && (3.5.54)\\
p_r(R_1,s) &= \frac{p(R_1,s)}{2R_1}, \quad p(r,r) = 0. && (3.5.55)
\end{aligned}$$

From the kernel p the output injection gains in (3.5.49) and (3.5.50) are found to be $p_1 = -p_r(r,R_2)$ and $p_{10} = 0$.

Defining $\check{s} = r$, $\check{r} = s$ and $\check{p}(\check{r},\check{s}) = p(r,s)$, the kernel $\check{p}$ verifies

$$\begin{aligned}
\check{p}_{\check{r}\check{r}} - \check{p}_{ss} &= (\lambda(\check{r}) - \lambda(\check{s}))\, \check{p} + A_2 f(\check{s},\check{r}) - A_2 \int_{\check{s}}^{\check{r}} f(\check{s},\sigma)\check{p}(\check{r},\sigma)d\sigma, && (3.5.56)\\
\check{p}_{\check{s}}(\check{r},R_1) &= \frac{\check{p}(\check{r},R_1)}{2R_1}, \quad \check{p}(\check{r},\check{r}) = 0. && (3.5.57)
\end{aligned}$$

Since $f(r,s) = -f(s,r)$, equations (3.5.56)–(3.5.57) are the same as equations (3.5.31)–(3.5.32), verified by k. Hence, it follows that (3.5.56)–(3.5.57) is well-posed and $p(r,s) = k^*(s,r)$, so that $p_1(r) = -k_s^*(R_2,r)$. Equation (2.4.30) gives then an explicit expression for the output injection gain p_1.

3.5.3 Output feedback controller

Combining the results of Sections 3.5.1 and 3.5.2, we get the following output feedback controller:

$$\begin{aligned}
V &= \int_{R_1}^{R_2} f(R_2,s)\hat{u}(s)ds, && (3.5.58)\\
U &= \int_{R_1}^{R_2} k_r^*(R_2,s)\hat{u}(s)ds, && (3.5.59)
\end{aligned}$$

where the estimate $\hat{u}(r)$ is obtained from

$$\begin{aligned}
\epsilon\hat{v}_t &= \hat{v}_{rr} - \lambda(r)\hat{v} + \pi A_1 \hat{u}, && (3.5.60)\\
\hat{u}_t &= \hat{u}_{rr} - \lambda(r)\hat{u} + A_2\hat{v} - k_s^*(R_2,r)\left(u(R_2) - \hat{u}(R_2)\right) \\
&\quad + A_2 h_R(r)\left(v_r(R_2) - \hat{v}_r(R_2)\right), && (3.5.61)\\
\hat{v}(R_1) &= 0, \quad \hat{v}(R_2) = V, && (3.5.62)\\
\hat{u}_r(R_1) &= \frac{\hat{u}(R_1)}{2R_1}, \quad \hat{u}_r(R_2) = U. && (3.5.63)
\end{aligned}$$

The backstepping method [101, 102] guarantees that the output feedback control laws stabilize the reduced model (3.5.26), thus stabilizing the system when $\epsilon = 0$.

3.5.4 Singular perturbation analysis for small ϵ

Assume that ϵ is small but nonzero. Since $u = \hat{u} + \tilde{u}$ and $v = \hat{v} + \tilde{v}$, we show stability of the (u, v) system by proving stability in the $(\hat{v}, \tilde{v}, \hat{u}, \tilde{u})$ coordinates. We begin stating the following proposition regarding $(\tilde{v}, \tilde{u})$ (see Section 3.8 for the proof).

Proposition 3.4. *Consider equations (3.5.39)–(3.5.40) with boundary conditions (3.5.41)–(3.5.42). Then, there exists ϵ^* such that if $\epsilon \in (0, \epsilon^*)$, the equilibrium $\tilde{u} \equiv \tilde{v} \equiv 0$ is exponentially stable in the H^1 norm, i.e., there exists $C_2, c_2 > 0$ s.t.*

$$\|\tilde{v}(t)\|_{H^1} + \|\tilde{u}(t)\|_{H^1} \leq C_2 \mathrm{e}^{-c_2 t}\left(\|\tilde{v}(0)\|_{H^1} + \|\tilde{u}(0)\|_{H^1}\right). \qquad (3.5.64)$$

Now we study the $(\hat{v}, \hat{u})$ subsystem, which verifies (3.5.34)–(3.5.35). Since $\tilde{v}_r(R_2)$ and $\tilde{u}(R_2)$ feed into (3.5.35), it is not possible to obtain stability for $(\hat{v}, \hat{u})$ alone; rather, the whole $(\hat{v}, \tilde{v}, \hat{u}, \tilde{u})$ subsystem has to be considered. We get the following result.

Proposition 3.5. *Consider equations (3.5.34)–(3.5.35) and (3.5.39)–(3.5.40), with boundary conditions (3.5.36)–(3.5.38) and (3.5.41)–(3.5.42), and control laws (3.5.58)–(3.5.59). Then, there exists ϵ^* such that if $\epsilon \in (0, \epsilon^*)$, the equilibrium*

$\hat{u} \equiv \hat{v} \equiv \tilde{u} \equiv \tilde{v} \equiv 0$ *is exponentially stable in the* H^1 *norm, i.e., there exists* $C_3, c_3 > 0$ *s.t.*

$$\begin{aligned} & \|\hat{v}(t)\|_{H^1} + \|\hat{u}(t)\|_{H^1} + \|\tilde{v}(t)\|_{H^1} + \|\tilde{u}(t)\|_{H^1} \\ \leq \; & C_3 \mathrm{e}^{-c_3 t} \left(\|\hat{v}(0)\|_{H^1} + \|\hat{u}(0)\|_{H^1} \|\tilde{v}(0)\|_{H^1} + \|\tilde{u}(0)\|_{H^1} \right). \end{aligned} \tag{3.5.65}$$

We skip the proof of Proposition 3.5, since it follows exactly the same lines as the proof of Proposition 3.4 (see Section 3.8); using the same argument, the $(\hat{v}, \hat{u})$ system can be proven exponentially stable in the H^1 norm when $\tilde{v} \equiv \tilde{u} \equiv 0$. Since the $(\hat{v}, \hat{u})$ system is driven by $\tilde{v}_r(R_2)$ and $\tilde{u}(R_2)$, using the estimates in the proof of Proposition 3.4 the whole system is shown to be exponentially stable.

3.6 Main Result

Using the definition of Γ in terms of U and Υ, and writing the observer equations in terms of the original measurements $v_r(R_2)$ and $\tau(R_2, \theta)$, we get the output feedback control laws for the entire system

$$V = \int_{R_1}^{R_2} \frac{f(R_2, s)}{\sqrt{R_2}} \hat{u}(s) ds, \tag{3.6.66}$$

$$\begin{aligned} \Gamma = \; & \frac{\cos\theta}{\pi} \left(q_0 + \frac{1}{2\sqrt{R_2^3}} \right) \int_0^{2\pi} \tau(t, R_2, \phi) \cos\phi d\phi - q_0 \tau(t, R_2, \theta) \\ & + \cos\theta \int_{R_1}^{R_2} \frac{k_r^*(R_2, s)}{\sqrt{R_2}} \hat{u}(s) ds, \end{aligned} \tag{3.6.67}$$

where

$$\epsilon \hat{v}_t = \hat{v}_{rr} - \lambda(r)\hat{v} + \pi A_1 \hat{u}, \tag{3.6.68}$$

$$\begin{aligned} \hat{u}_t = \; & \hat{u}_{rr} - \lambda(r)\hat{u} + A_2 \hat{v} - k_s^*(R_2, r) \left(\frac{\sqrt{R_2}}{\pi} \int_0^{2\pi} \tau(t, R_2, \phi) \cos\phi d\phi - \hat{u}(R_2) \right) \\ & + A_2 h_R(r) \left(\sqrt{R_2} v_r(R_2) - \hat{v}_r(R_2) \right), \end{aligned} \tag{3.6.69}$$

$$\hat{v}(R_1) = 0, \hat{v}(R_2) = \int_{R_1}^{R_2} f(R_2, s) \hat{u}(s) ds, \tag{3.6.70}$$

$$\hat{u}_r(R_1) = \frac{\hat{u}(R_1)}{2R_1}, \quad \hat{u}_r(R_2) = \int_{R_1}^{R_2} k_r^*(R_2, s) \hat{u}(s) ds. \tag{3.6.71}$$

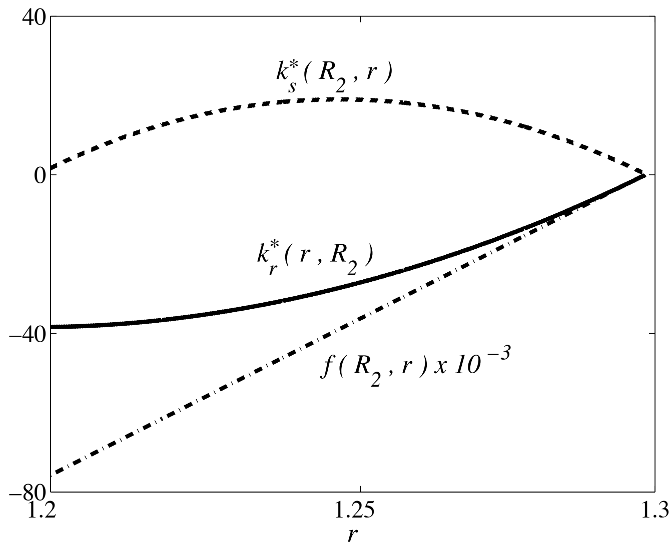

Figure 3.1: Control kernel $k_r^*(R_2, r)$ (solid), observer output injection kernel $k_s^*(R_2, r)$ (dashed), and velocity control kernel $f(R_2, r)$ (dash-dotted).

From Propositions 3.3 and 3.5, Lemma 3.7 and Remark 3.2, we get the following result.

Theorem 3.6. *Consider system (2.2.7)–(2.2.8) with boundary conditions (2.2.5)–(2.2.6) and output feedback control laws (3.6.66)–(3.6.71). Then, there exists* $\epsilon^* > 0$ *such that for* $\epsilon \in (0, \epsilon^*)$*, the equilibrium* $v \equiv \tau \equiv \tilde{v} \equiv \tilde{u} \equiv 0$ *is exponentially stable in the* H^1 *norm, i.e., there exists* $C_4, c_4 > 0$ *s.t.*

$$\begin{aligned} & \|v(t)\|_{H^1} + \|\tau(t)\|_{H^1_\theta} + \|\tilde{v}(t)\|_{H^1} + \|\tilde{u}(t)\|_{H^1} \\ \leq \ & C_4 \mathrm{e}^{-c_4 t} \left(\|v(0)\|_{H^1} + \|\tau(0)\|_{H^1_\theta} + \|\tilde{v}(0)\|_{H^1} + \|\tilde{u}(0)\|_{H^1} \right). \end{aligned} \quad (3.6.72)$$

3.7 Simulation Study

We use for simulation the same prototypical case that was shown open-loop unstable in Chapter 2. Numerical computations are carried out using a spectral method combined with the Crank-Nicholson method.

In Fig. 3.1 we show the shape of the kernels appearing in our control law. Note that the temperature control kernel $k_r^*(R_2, s)$ gives more weight in the control law to information near the inner boundary—as the boundary controller is on the opposite side, it has to react more agressively to compensate fluctuations of temperature in the interior part of the domain. This is also true for the velocity control kernel $f(R_2, r)$ and velocity output injection gain $h_R(r)$ (which is not explicitly shown as $h_R(r) = f(R_2, r)/\pi A_1$). The temperature output injection gain $k_s^*(R_2, s)$ is larger in the middle of the loop, where the states are somewhat more difficult to estimate (near the boundaries some information is known a priori).

In Fig. 3.2 closed loop simulations of the plant perturbation variables show how the states converge exponentially towards the equilibrium profile fairly quickly. We also plot the observer error, that converges to zero. In Fig. 3.3 we show the magnitude of the control law Γ.

3.8 Auxiliary Technical Results

In this section we prove some technical results that were used in the chapter.

Lemma 3.7. *For u and ζ defined as in Section 3.3, we have that*

$$\|\tau\|^2_{L^2_\theta} = \pi\|u\|^2_{L^2} + \|\zeta\|^2_{L^2_\theta}, \tag{3.8.73}$$

$$\|\tau\|^2_{H^1_\theta} = \pi\|u\|^2_{H^1} + \pi\int_{R_1}^{R_2} \frac{u^2(t,r)}{r^2} r dr + \|\zeta\|^2_{H^1_\theta}, \tag{3.8.74}$$

and the $\|\tau\|_{H^1_\theta}$ norm is equivalent to the norm

$$\|u\|_{H^1} + \|\zeta\|_{H^1_\theta}. \tag{3.8.75}$$

Proof. Using (3.3.9), we get

$$\begin{aligned}\int_0^{2\pi}\int_{R_1}^{R_2} \tau^2 r dr d\theta &= \pi\int_{R_1}^{R_2} u^2(t,r) r dr + \int_0^{2\pi}\int_{R_1}^{R_2} \zeta^2 r dr d\theta \\ &\quad + \int_{R_1}^{R_2} u(t,r)\int_0^{2\pi} \zeta\cos\theta d\theta r dr \\ &= \pi\int_{R_1}^{R_2} u^2(t,r) r dr + \int_0^{2\pi}\int_{R_1}^{R_2} \zeta^2 r dr d\theta, \end{aligned} \tag{3.8.76}$$

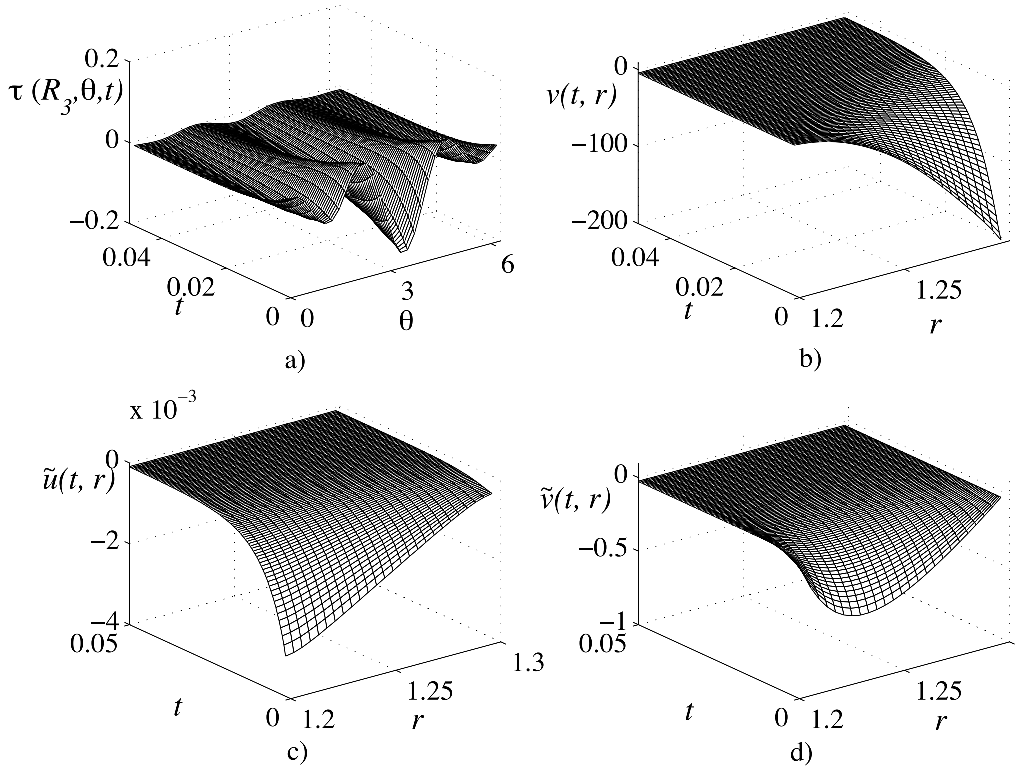

Figure 3.2: Closed loop simulation for the output feedback controller. a) temperature perturbation $\tau(t, r, \theta)$ at radius $R_3 = \frac{R_1+R_2}{2}$, b) velocity $v(t, r)$, c) observer error $\tilde{u}(t, r)$, d) observer error $\tilde{v}(t, r)$.

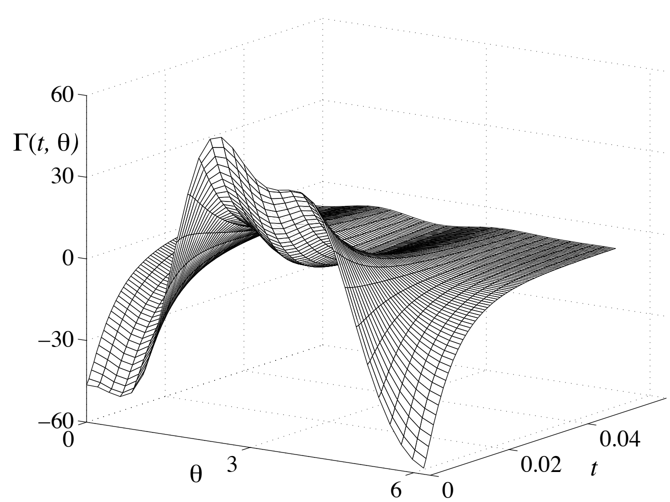

Figure 3.3: Magnitude of temperature control law Γ.

so (3.8.73) follows. Similarly, we have that

$$\begin{aligned}\int_0^{2\pi}\int_{R_1}^{R_2}\tau_r^2 r dr d\theta &= \pi\int_{R_1}^{R_2} u_r^2(t,r) r dr + \int_0^{2\pi}\int_{R_1}^{R_2}\zeta_r^2 r dr d\theta \\ &\quad + \int_{R_1}^{R_2} u_r(t,r)\int_0^{2\pi}\zeta_r\cos\theta d\theta r dr \\ &= \pi\int_{R_1}^{R_2} u_r^2(t,r) r dr + \int_0^{2\pi}\int_{R_1}^{R_2}\zeta_r^2 r dr d\theta, \qquad (3.8.77)\end{aligned}$$

and we also have that

$$\begin{aligned}\int_0^{2\pi}\int_{R_1}^{R_2}\frac{\tau_\theta^2}{r^2} r dr d\theta &= \pi\int_{R_1}^{R_2}\frac{u^2(t,r)}{r^2} r dr + \int_0^{2\pi}\int_{R_1}^{R_2}\frac{\zeta_\theta^2}{r^2} r dr d\theta \\ &\quad - \int_{R_1}^{R_2} u(t,r)\int_0^{2\pi}\zeta_\theta\sin\theta d\theta r dr \\ &= \pi\int_{R_1}^{R_2}\frac{u^2(t,r)}{r^2} r dr + \int_0^{2\pi}\int_{R_1}^{R_2}\frac{\zeta_\theta^2}{r^2} r dr d\theta \\ &\quad + \int_{R_1}^{R_2} u(t,r)\int_0^{2\pi}\zeta\cos\theta d\theta r dr \\ &= \pi\int_{R_1}^{R_2} u_r^2(t,r) r dr + \int_0^{2\pi}\int_{R_1}^{R_2}\zeta_r^2 r dr d\theta, \qquad (3.8.78)\end{aligned}$$

so (3.8.74) follows. The norm equivalence follows from (3.8.74) and Poincare's inequality for u. $\square$

Proof of Proposition 3.3. Define

$$\begin{aligned}L &= \frac{1}{2}\int_0^{2\pi}\int_{R_1}^{R_2}\left(\frac{\zeta_\theta^2(r,\theta)}{r^2} + \zeta_r^2(r,\theta) + \zeta^2(r,\theta)\right) r d\theta dr \\ &\quad + \frac{q_0 R_2}{2}\int_0^{2\pi}\zeta^2(R_2,\theta) d\theta, \qquad (3.8.79)\end{aligned}$$

then

$$\begin{aligned}\frac{dL}{dt} &= -\int_0^{2\pi}\int_{R_1}^{R_2}\left(\frac{\zeta_{\theta\theta}}{r^2} + \zeta_{rr} + \frac{\zeta_r}{r}\right)^2 r d\theta dr \\ &\quad - \int_0^{2\pi}\int_{R_1}^{R_2}\left(\frac{\zeta_\theta^2}{r^2} + \zeta_r^2\right) r d\theta dr \\ &\quad + \int_0^{2\pi} R_2\zeta_r(R_2,\theta)\zeta(R_2,\theta) d\theta \\ &\leq -DL \qquad (3.8.80)\end{aligned}$$

for some $D > 0$, where we have used (3.4.14), Poincare's inequality as in Lemma 2.2 and the fact that $R_2 - R_1 < 1$. As L is equivalent to the H^1_θ norm of ζ, H^1 exponential stability follows. $\square$

Proof of Proposition 3.4. Define $\tilde{z} = \tilde{v} - \tilde{v}_{ss}$, where

$$\tilde{v}_{ss} = -\int_r^{R_2} f(r,s)\tilde{u}(\xi)d\xi + \int_{R_1}^{R_2} h(r,s)\tilde{u}(\xi)d\xi, \tag{3.8.81}$$

and define $\tilde{w}$ by the backstepping transformation (3.5.51). From $(\tilde{z}, \tilde{w})$ definitions and the fact that the kernel of the transformation is $\mathcal{C}^2$, exponential stability in $(\tilde{z}, \tilde{w})$ coordinates implies exponential stability for $(\tilde{v}, \tilde{u})$. The observer error plant in $(\tilde{z}, \tilde{w})$ coordinates is

$$\begin{aligned}
\epsilon \tilde{z}_t &= \tilde{z}_{rr} - \lambda(r)\tilde{z} - \epsilon(\tilde{v}_{ss})_t, &(3.8.82)\\
\tilde{w}_t &= \tilde{w}_{rr} - \lambda(r)\tilde{w} + A_2\tilde{z} - A_2 p_2(r)\tilde{z}_r(R_2), &(3.8.83)\\
\tilde{z}(R_1) &= \tilde{z}(R_2) = 0, &(3.8.84)\\
\tilde{w}_r(R_1) &= \frac{\tilde{w}(R_1)}{2R_1}, \tilde{w}_r(R_2) = 0. &(3.8.85)
\end{aligned}$$

In (3.8.82) we need to express $(\tilde{v}_{ss})_t$ in terms of z and w. First, we write

$$\tilde{v}_{ss} = \int_r^{R_2} \tilde{f}(r,s)\tilde{w}(s)ds + \int_{R_1}^{R_2} \tilde{h}(r,s)\tilde{w}(s)ds, \tag{3.8.86}$$

where

$$\begin{aligned}
\tilde{f}(r,s) &= -f(r,s) + \int_r^{R_2} f(r,\sigma)p(\sigma,s)d\sigma, &(3.8.87)\\
\tilde{h}(r,s) &= h(r,s) - \int_{R_1}^{R_2} h(r,\sigma)p(\sigma,s)d\sigma. &(3.8.88)
\end{aligned}$$

Then, using (3.8.83),

$$\begin{aligned}
(\tilde{v}_{ss})_t = &\int_r^{R_2} \left(\tilde{f}_{ss}(r,s) - \tilde{f}(r,s)\lambda(s)\right) w(s)ds + \int_{R_1}^{R_2} \left(\tilde{h}_{ss}(r,s) - \tilde{h}(r,s)\lambda(s)\right)\\
&\times w(s)ds - (\tilde{f}_s(r,R_2) + \tilde{h}_s(r,R_2))w(R_2) - A_2 z_r(R_2)\left(\int_r^{R_2} \tilde{f}(r,s)p_2(s)ds\right.\\
&\left.+\int_{R_1}^{R_2} \tilde{h}(r,s)p_2(s)ds\right) + \left(\tilde{h}_s(r,R_1) - q\tilde{h}(r,R_1)\right) w(R_1) + \tilde{f}_s(r,r)w(r)\\
&+A_2\int_r^{R_2} \tilde{f}(r,s)z(s)ds + A_2\int_{R_1}^{R_2} \tilde{h}(r,s)z(s)ds. \qquad (3.8.89)
\end{aligned}$$

Define the Lyapunov functions

$$L_1 = \frac{1}{2}\int_{R_1}^{R_2}\left(\tilde{z}_r^2 + 3\frac{\tilde{z}^2}{R_1^2}\right)dr, \tag{3.8.90}$$

$$L_2 = \frac{1}{2}\int_{R_1}^{R_2}\left(\tilde{w}_r^2 + 3\frac{\tilde{w}^2}{R_1^2}\right)dr + \frac{\tilde{w}(R_1)^2}{4R_1}, \tag{3.8.91}$$

which are equivalent, using Poincare's inequality, to the H^1 norms of $\tilde{z}$ and $\tilde{w}$, respectively. Then

$$\begin{aligned}
\frac{dL_1}{dt} &= -\frac{1}{\epsilon}\int_{R_1}^{R_2}\left(\hat{z}_{rr}^2 + \left(\lambda + \frac{3}{R_1^2}\right)\hat{z}_r^2 + 3\frac{\lambda\hat{z}^2}{R_1^2}\right)dr \\
&\quad + \frac{1}{\epsilon}\int_{R_1}^{R_2}\frac{\lambda''(r)}{2}\hat{z}^2 dr + \int_{R_1}^{R_2}\left(-\hat{z}_{rr} + 3\frac{\hat{z}}{R_1^2}\right)(\tilde{v}_{ss})_t dr \\
&\leq -\frac{D_1}{\epsilon}\int_{R_1}^{R_2}\left(\hat{z}_{rr}^2 + \hat{z}_r^2 + 3\frac{\tilde{z}^2}{R_1^2}\right)dr \\
&\quad + D_2\int_{R_1}^{R_2}\left(\hat{z}_{rr}^2 + \hat{z}_r^2 + w_r^2 + w^2\right)dr,
\end{aligned} \tag{3.8.92}$$

where D_1 and D_2 are positive, and where we have used that $\lambda''(r) \leq 3\lambda(r)/R_1^2$, and Poincare's and Young's inequality to bound all the terms from $(v_{ss})_t$. Similarly,

$$\begin{aligned}
\frac{dL_2}{dt} &= -\int_{R_1}^{R_2}\left(\hat{w}_{rr}^2 + \left(\lambda + \frac{3}{R_1^2}\right)\hat{w}_r^2 + 3\frac{\lambda\hat{w}^2}{R_1^2}\right)dr + \int_{R_1}^{R_2}\frac{\lambda''(r)}{2}\hat{w}^2 dr \\
&\quad + \frac{\hat{w}(R_1)\hat{w}_t(R_1)}{2R_1} - \hat{w}_r(R_1)\hat{w}_t(R_1) - \left(\lambda(R_1) + \frac{3}{R_1^2}\right) \times \hat{w}_r(R_1)\hat{w}(R_1) \\
&\quad + \frac{\lambda'(R_1)}{2}\hat{w}(R_1)^2 + \int_{R_1}^{R_2}\left(-\hat{w}_{rr} + 3\frac{\hat{w}}{R_1^2}\right)A_2\left(\tilde{z} - p_2(r)\tilde{z}_r(R_2)\right)dr \\
&\leq -D_3\left(\int_{R_1}^{R_2}\left(\hat{w}_{rr}^2 + \hat{w}_r^2 + 3\frac{\tilde{w}^2}{R_1^2}\right)dr + \frac{\hat{w}(R_1)^2}{4R_1}\right) \\
&\quad + D_4\int_{R_1}^{R_2}\left(\hat{z}_{rr}^2 + \hat{z}_r^2\right)dr.
\end{aligned} \tag{3.8.93}$$

Setting $L_3 = L_1 + D_5 L_2$, and using Poincare's inequality, it follows that for some positive (and possibly large) D_5, there exists ϵ^* such that for $\epsilon \in (0, \epsilon^*)$, one has that

$$\frac{dL_3}{dt} \leq -D_6 L_3, \tag{3.8.94}$$

from which exponential stability is obtained. □

This chapter is a partial reprint of the material as it appears in
R. Vazquez and M. Krstic, "Explicit output feedback stabilization of a thermal convection loop by continuous backstepping and singular perturbations," submitted, *2007 American Control Conference*, New York, 2007.
The dissertation author was the primary author and the coauthor listed in this publication directed and supervised the research, which is the basis for this chapter.

Chapter 4

Boundary Stabilization of 2-D Navier-Stokes Channel Flow

4.1 Introduction

We present an explicit boundary control law which stabilizes the benchmark 2-D linearized Navier-Stokes channel flow. Despite the deceptive simplicity of the geometry, there is a number of complex issues underlying this problem [63, 66, 89, 95], making it extremely hard to solve. The fact that the channel is unbounded further complicates the problem [105].

Optimal control has so far been the most successful technique for addressing channel flow stabilization [63], in a periodic setting, by using a discretized version of the equations and employing high-dimensional algebraic Riccati equations for computation of gains. The computational complexity of this approach is formidable if a very fine grid is necessary in the discretizations, for example if the Reynolds number is very large. Using a Lyapunov/passivity approach, another control design [1, 10] was developed for stabilization of the (periodic) channel flow; the design was simple and explicit and did not rely on discretization or linearization, but its theory was restricted to low Reynolds numbers though in simulations the approach was successful at high Reynolds numbers, above the linear instability threshold. Other works make use of nonlinear model reduction techniques to solve the problem, though they employ in-domain actuation [6, 7, 9]. Boundary controllers using spectral decomposition and pole-placement methods have been developed, using normal actuation [15] or tangential actuation in an arbitrarily small subset of the walls [110].

The approach we present in this chapter is the first result that provides an explicit control law (with symbolically computed gains) for stabilization at an arbitrarily high Reynolds number in non-discretized linearized Navier-Stokes equations. Thanks to the explicitness of the controller, we are able to obtain approximate analytical solutions for the linearized Navier-Stokes equations. Exponential stability in the L^2, H^1 and H^2 norms is proved for the linearized system. We also justify the well-posedness of the system.

The main idea of our design is to use a Fourier transform, which allows separate analysis for each wave number. For certain wave numbers, a normal velocity controller puts the system into a form where a backstepping transforms the original normal velocity PDE into a stable heat equation. The rest of wave numbers are proved to be open loop exponentially stable, and left uncontrolled. These two results are combined to prove stability of the closed loop system for all wave numbers and in physical space.

4.2 Model

We consider a 2-D channel flow, also called Poiseuille flow [18]. This flow consists of an incompressible fluid between two parallel infinite plates separated from each other by a distance L_p and subject to a pressure gradient ∇P parallel to the plates. Denote U_c as the maximum centerline velocity of the Poiseuille flow (determined by ∇P), ρ and ν respectively as the density and the kinematic viscosity of the fluid, and the Reynolds number $Re = U_c L_p/\nu$. Define U_c, L_p, L_p/U_c and $\rho\nu U_c/L_p$ as velocity, length, time and pressure scales respectively, and set nondimensional spatial coordinates (x, y) where x is the streamwise direction (parallel and opposite to the pressure gradient) and y the wall normal direction, so that (x, y) are in a semi-infinite rectangle, $(x, y) \in \Omega = (-\infty, \infty) \times [0, 1]$ as shown in Figure 4.1. Assuming that the flow is two dimensional, the velocity field is determined by the dimensionless incompressible 2-D Navier-Stokes equations which are the following:

$$U_t = \frac{1}{Re}(U_{xx} + U_{yy}) - UU_x - VU_y - P_x\,, \tag{4.2.1}$$

$$V_t = \frac{1}{Re}(V_{xx} + V_{yy}) - UV_x - VV_y - P_y\,, \tag{4.2.2}$$

and the continuity equation

$$U_x + V_y = 0, \tag{4.2.3}$$

where U, V and P denote respectively the nondimensional streamwise velocity, wall-normal velocity, and pressure. The boundary conditions for the velocity field are the no-penetration, no-slip boundary conditions for the uncontrolled case, i.e.,

$$V(x, 0) = V(x, 1) = U(x, 0) = U(x, 1) = 0. \tag{4.2.4}$$

Instead of using (4.2.3) we can derive a Poisson for P, by combining (4.2.1), (4.2.2) and (4.2.3),

$$P_{xx} + P_{yy} = -2(V_y)^2 - 2V_xU_y, \tag{4.2.5}$$

with boundary conditions

$$P_y(x, 0) = \frac{V_{yy}(x, 0)}{Re}, \quad P_y(x, 1) = \frac{V_{yy}(x, 1)}{Re}, \tag{4.2.6}$$

which are obtained evaluating (4.2.2) at $y = 0, 1$.

The equilibrium solution of (4.2.1)–(4.2.4) with unity centerline velocity is the parabolic Poiseuille profile

$$U^e = 4y(1 - y), \tag{4.2.7}$$

$$V^e = 0, \tag{4.2.8}$$

$$P^e = P_0 - \frac{8}{Re}x, \tag{4.2.9}$$

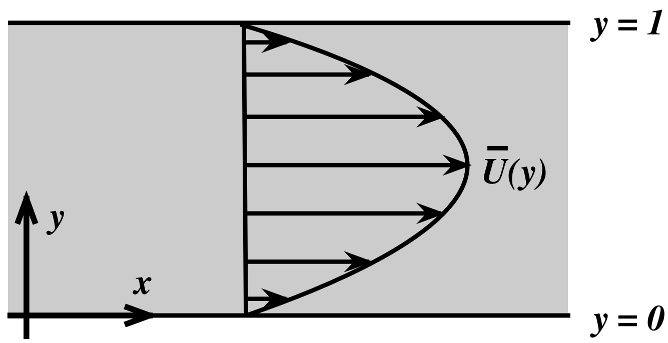

Figure 4.1: 2-D channel flow and equilibrium profile. Actuation is on the top wall.

shown in Figure 4.1. This equilibrium is unstable for high Reynolds numbers [95], even though the non-normality of the problem [89] may lead to large transient growth and enable a transition to turbulence at substantially smaller Reynolds number. Defining the fluctuation variables $u = U - U^e$ and $p = P - P^e$, and linearizing around the equilibrium profile (4.2.7)–(4.2.9), the plant equations are

$$
\begin{aligned}
u_t &= \frac{1}{Re}(u_{xx} + u_{yy}) + 4y(y-1)u_x + 4(2y-1)V - p_x, && (4.2.10)\\
V_t &= \frac{1}{Re}(V_{xx} + V_{yy}) + 4y(y-1)V_x - p_y, && (4.2.11)\\
p_{xx} + p_{yy} &= 8(2y-1)V_x, && (4.2.12)
\end{aligned}
$$

with boundary conditions

$$
\begin{aligned}
u(x,0) &= 0, && (4.2.13)\\
u(x,1) &= U_c(x), && (4.2.14)\\
V(x,0) &= 0, && (4.2.15)\\
V(x,1) &= V_c(x), && (4.2.16)\\
p_y(x,0) &= \frac{V_{yy}(x,0)}{Re}, && (4.2.17)\\
p_y(x,1) &= \frac{V_{yy}(x,1) + (V_c)_{xx}(x)}{Re} - (V_c)_t(x). && (4.2.18)
\end{aligned}
$$

The continuity equation is still verified

$$u_x + V_y = 0. \qquad (4.2.19)$$

We have added in (4.2.14) and (4.2.16) the actuation variables $U_c(x)$ and $V_c(x)$, respectively for streamwise and normal velocity boundary control. The actuators are placed along the top wall, $y = 1$, and we assume they can be independently actuated for all $x \in \mathbb{R}$. No actuation is done inside the channel or at the bottom wall.

Taking Laplacian in equation (4.2.11) and using (4.2.12), we get an autonomous equation for the normal velocity, the well-known Orr-Sommerfeld equation,

$$\triangle V_t = \frac{1}{Re}\triangle^2 V + 4y(y-1)\triangle V_x - 8V_x, \qquad (4.2.20)$$

with boundary conditions (4.2.15)–(4.2.16), as well as $V_y(x,0) = 0$, $V_y(x,1) = -(U_c)_x$, derived from (4.2.13)–(4.2.14) and (4.2.19). This equation is numerically studied in hydrodynamic theory to determine stability of the channel flow [89].

Defining $Y = -V_y$ and using the Fourier transform, it is possible to partially solve (4.2.20) and obtain an evolution equation for Y,

$$\begin{aligned} Y_t = {} & \frac{1}{Re}\left(Y_{xx} + Y_{yy}\right) + 4y(y-1)Y_x + \int_0^y \int_{-\infty}^{\infty} Y(\xi,\eta) \int_{-\infty}^{\infty} 16\pi k \mathrm{e}^{2\pi i k(x-\xi)} \\ & \times \left[\pi k(2y-1) - 2\sinh\left(2\pi k(y-\eta)\right) 2\pi k(2\eta-1)\cosh\left(2\pi k(y-\eta)\right)\right] dk d\xi d\eta \\ & + \int_0^1 \int_{-\infty}^{\infty} Y(\xi,\eta) \int_{-\infty}^{\infty} 32\pi k \mathrm{e}^{2\pi i k(x-\xi)} \frac{\cosh\left(2\pi k y\right)}{\sinh\left(2\pi k\right)} \left[\cosh\left(2\pi k(1-\eta)\right)\right. \\ & \left. + \pi k(2\eta-1)\sinh\left(2\pi k(1-\eta)\right)\right] dk d\xi d\eta \\ & + \int_{-\infty}^{\infty} \int_{-\infty}^{\infty} \left(\frac{Y_y(\xi,1) - (V_c)_{xx}(\xi)}{Re} + (V_c)_t(\xi)\right) 2\pi k \mathrm{e}^{2\pi i k(x-\xi)} \frac{\cosh\left(2\pi k y\right)}{\sinh\left(2\pi k\right)} dk d\xi \\ & - \int_{-\infty}^{\infty} \int_{-\infty}^{\infty} \frac{Y_y(\xi,0)}{Re} 2\pi k \mathrm{e}^{2\pi i k(x-\xi)} \frac{\cosh\left(2\pi k(1-y)\right)}{\sinh\left(2\pi k\right)} dk d\xi, \end{aligned} \qquad (4.2.21)$$

with boundary conditions $Y_y(x,0) = 0$ and $Y(x,1) = (U_c)_x$. Equation (4.2.21) governs the channel flow, since from Y and using (4.2.19), we recover both components of the velocity field:

$$V(x,y) = -\int_0^y Y(x,\eta) d\eta, \qquad (4.2.22)$$

$$u(x,y) = \int_{-\infty}^x Y(\xi,y) d\xi. \qquad (4.2.23)$$

Equation (4.2.21) displays the full complexity of the Navier-Stokes dynamics, which the PDE system (4.2.10)–(4.2.12) conceals through the presence of the pressure equation (4.2.12), and the Orr-Sommerfeld equation (4.2.20) conceals through the use of fourth order derivatives. Besides being unstable (for high Reynolds numbers), the Y system incorporates (on its right-hand side) the components of $Y(x,y)$ from everywhere in the domain. This is the main source of difficulty for both controlling and solving the Navier-Stokes equations. A perturbation somewhere in the flow is instantaneously felt everywhere—a consequence of the incompressible nature of the flow. Our approach to overcoming this obstacle is to use one of the two control variables (normal velocity $V_c(x)$, which is incorporated explicitly inside the equation) to prevent perturbations from propagating in the direction from the controlled boundary towards the uncontrolled boundary. This is a sort of "spatial causality" on y, which in the nonlinear control literature is referred to as the 'strict-feedback structure' [71].

4.3 Controller

The explicit control law consists of two parts—the normal velocity controller $V_c(x)$ and the streamwise velocity controller $U_c(x)$. $V_c(x)$ makes the integral operator in the third to fifth lines of (4.2.21) spatially causal in y,[1] which is a necessary structure for the application of a "backstepping" boundary controller for stabilization of spatially causal partial integro-differential equations [101]. $U_c(x)$ is a backstepping controller which stabilizes the spatially causal structure imposed by $V_c(x)$. The expressions for the control laws are

$$U_c(t,x) = \int_0^1 \int_{-\infty}^{\infty} Q_u(x-\xi,\eta)u(t,\xi,\eta)d\xi d\eta, \tag{4.3.24}$$

$$V_c(t,x) = h(t,x), \tag{4.3.25}$$

where h verifies the equation

$$h_t = h_{xx} + g(t,x), \tag{4.3.26}$$

[1] The first, second and sixth lines are already spatially causal in y.

where

$$g = \int_0^1 \int_{-\infty}^{\infty} Q_V(x-\xi,\eta)V(t,\xi,\eta)d\xi d\eta + \int_{-\infty}^{\infty} Q_0(x-\xi)\left(u_y(t,\xi,0) - u_y(t,\xi,1)\right)d\xi, \quad (4.3.27)$$

and the kernels Q_u, Q_V and Q_0 are defined as

$$Q_u = \int_{-\infty}^{\infty} \chi(k)K(k,1,\eta)\mathrm{e}^{2\pi ik(x-\xi)}dk, \quad (4.3.28)$$

$$Q_V = \int_{-\infty}^{\infty} \chi(k)16\pi ki(2\eta-1)\cosh\left(2\pi k(1-\eta)\right)\mathrm{e}^{2\pi ik(x-\xi)}dk, \quad (4.3.29)$$

$$Q_0 = \int_{-\infty}^{\infty} \chi(k)\frac{2\pi ki}{Re}\mathrm{e}^{2\pi ik(x-\xi)}dk. \quad (4.3.30)$$

In expressions (4.3.28)–(4.3.30), $\chi(k)$ is a truncating function in the wave number space whose definition is

$$\chi(k) = \begin{cases} 1, & m < |k| < M \\ 0, & \text{otherwise} \end{cases} \quad (4.3.31)$$

where m and M are respectively the low and high cut-off wave numbers, two design parameters which can be conservatively chosen as $m \leq \frac{1}{32\pi Re}$ and $M \geq \frac{1}{\pi}\sqrt{\frac{Re}{2}}$. The function $K(k,y,\eta)$ appearing in (4.3.28) is a (complex valued) gain kernel defined as

$$K(k,y,\eta) = \lim_{n\to\infty} K_n(k,y,\eta), \quad (4.3.32)$$

where K_n is recursively defined as [2]

$$\begin{aligned} K_0 = & -2\pi k\frac{\cosh\left(2\pi k(1-y+\eta)\right) - \cosh\left(2\pi k(y-\eta)\right)}{\sinh\left(2\pi k\right)} \\ & +4iRe\eta(\eta-1)\sinh\left(2\pi k(y-\eta)\right) \\ & -\frac{Re}{3}\pi ik\eta\left(21y^2 - 6y(3+4\eta) + \eta(12+7\eta)\right) \\ & -6\eta i\frac{Re}{\pi k}\left(1-\cosh\left(2\pi k(y-\eta)\right)\right) \end{aligned} \quad (4.3.33)$$

$$K_n = K_{n-1} - 4\pi kiRe\int_{y-\eta}^{y+\eta}\int_0^{y-\eta}\int_{-\delta}^{\delta}\left\{\frac{\sinh\left(\pi k(\xi+\delta)\right)}{\pi k} - (2\xi-1)\right.$$

[2] This infinite sequence is convergent, smooth, and uniformly bounded over $(y,\eta)\in[0,1]^2$, and analytic in k. See Proposition 4.8 for details.

$$
\begin{aligned}
&+2(\gamma-\delta-1)\cosh\left(\pi k(\xi+\delta)\right)\Big\}K_{n-1}\left(k,\frac{\gamma+\delta}{2},\frac{\gamma+\xi}{2}\right)d\xi d\delta d\gamma \\
&+\frac{Re}{2}\pi ik\int_{y-\eta}^{y+\eta}\int_{0}^{y-\eta}(\gamma-\delta)(\gamma-\delta-2)K_{n-1}\left(k,\frac{\gamma+\delta}{2},\frac{\gamma-\delta}{2}\right)d\delta d\gamma \\
&+2\pi k\int_{0}^{y-\eta}\frac{\cosh\left(2\pi k(1-\delta)\right)-\cosh\left(2\pi k\delta\right)}{\sinh\left(2\pi k\right)} \\
&\times K_{n-1}\left(k,y-\eta,\delta\right)d\delta. \qquad (4.3.34)
\end{aligned}
$$

The terms of this series can be computed symbolically as they only involve integration of polynomials and exponentials. In implementation, a few terms are sufficient to obtain a highly accurate approximation because the series is rapidly convergent [101].

Formulas (4.3.24)–(4.3.34) constitute the complet statement of our feedback law. Their mathematical validity is established in Theorem 4.4 and Proposition 4.8.

Remark 4.1. (4.3.25) is a dynamic controller whose magnitude is determined by the variable $h(t,x)$, which evolves according to (4.3.26). The initial condition $h(0,x)$ must verify the compatibility condition for the plant to be well-posed. This amounts to setting $h(0,x)\equiv V(0,1,x)$.

Remark 4.2. *Control kernels (4.3.29) and (4.3.30) can be explicitly expressed as*

$$
\begin{aligned}
Q_V(\xi,\eta) &= 8(2\eta-1)\frac{R_V(\xi,\eta,M)-R_V(\xi,\eta,m)}{\xi^2+(1-\eta)^2} \qquad (4.3.35)\\
Q_0(\xi,\eta) &= \frac{R_0(\xi,\eta,M)-R_0(\xi,\eta,m)}{Re\,\xi}, \qquad (4.3.36)
\end{aligned}
$$

where $R_V(\xi,\eta,k)$ and $R_0(\xi,\eta,k)$ are defined

$$
\begin{aligned}
R_V &= \frac{((1-\eta)^2-\xi^2)\sin(2\pi k\xi)\cosh(2\pi k(1-\eta))}{\pi(\xi^2+(1-\eta)^2)} \\
&\quad +2k\xi\cos\left(2\pi k\xi\right)\cosh\left(2\pi k(1-\eta)\right) \\
&\quad -\frac{2\xi(1-\eta)\cos\left(2\pi k\xi\right)\sinh\left(2\pi k(1-\eta)\right)}{\pi(\xi^2+(1-\eta)^2)} \\
&\quad -2k(1-\eta)\sin(2\pi k\xi)\sinh(2\pi k(1-\eta)) \qquad (4.3.37)\\
R_0 &= 2k\cos\left(2\pi k\xi\right)-\frac{\sin\left(\pi k\xi\right)}{2\pi\xi}. \qquad (4.3.38)
\end{aligned}
$$

Using the explicit formulae in (4.3.35)–(4.3.38) and approximating the kernel K by K_0 from (4.3.33), we compute the kernels Q_u, Q_V and Q_0 in (4.3.29)–(4.3.30) and show them in Fig. 4.2. The kernels are computed for the case of low Reynolds numbers, for which it holds that $K \approx K_0$; for large Reynolds numbers, the kernel Q_V does not change (since it does not depend on Re), while Q_0 will be smaller and Q_u larger, with a qualitatively similar *shape*. The most visible feature of the kernels is their *spatial decay* for increasing values of the argument $|x-\xi|$; this property, which we formalize in Theorem 4.4, allows to truncate the integrals with respect to ξ to the vicinity of x, which allows sensing to be restricted just to a neighborhood (in the x direction) of the actuator. Note also that, for Q_u and especially for Q_V, information about the states close to the uncontrolled end (and thus far away from the actuators and harder to stabilize) is given more weight in the control law, as one would expect from common sense.

4.4 Main Results

Due to the explicit form of the controller, the solution of the closed loop system is also obtained in the explicit form,

$$u(t,x,y) = u^*(t,x,y) + \epsilon_u(t,x,y), \tag{4.4.39}$$

$$V(t,x,y) = V^*(t,x,y) + \epsilon_V(t,x,y), \tag{4.4.40}$$

where

$$\begin{aligned} u^* &= 2\sum_{j=1}^{\infty}\int_{-\infty}^{\infty}\int_{-\infty}^{\infty}\chi(k)\mathrm{e}^{-t\frac{4k^2\pi^2+\pi^2j^2}{Re}+2\pi ik(x-\xi)} \\ &\quad\times\left[\sin(\pi jy)+\int_0^y L(k,y,\eta)\sin(\pi j\eta)\,d\eta\right] \\ &\quad\times\int_0^1\left[\sin(\pi j\eta)-\int_\eta^1 K(k,\sigma,\eta)\sin(\pi j\sigma)\,d\sigma\right] \\ &\quad\times u(0,\xi,\eta)d\eta d\xi dk\,, \qquad (4.4.41) \\ V^* &= -2\sum_{j=1}^{\infty}\int_{-\infty}^{\infty}\int_{-\infty}^{\infty}\chi(k)\mathrm{e}^{-t\frac{4k^2\pi^2+\pi^2j^2}{Re}+2\pi ik(x-\xi)} \end{aligned}$$

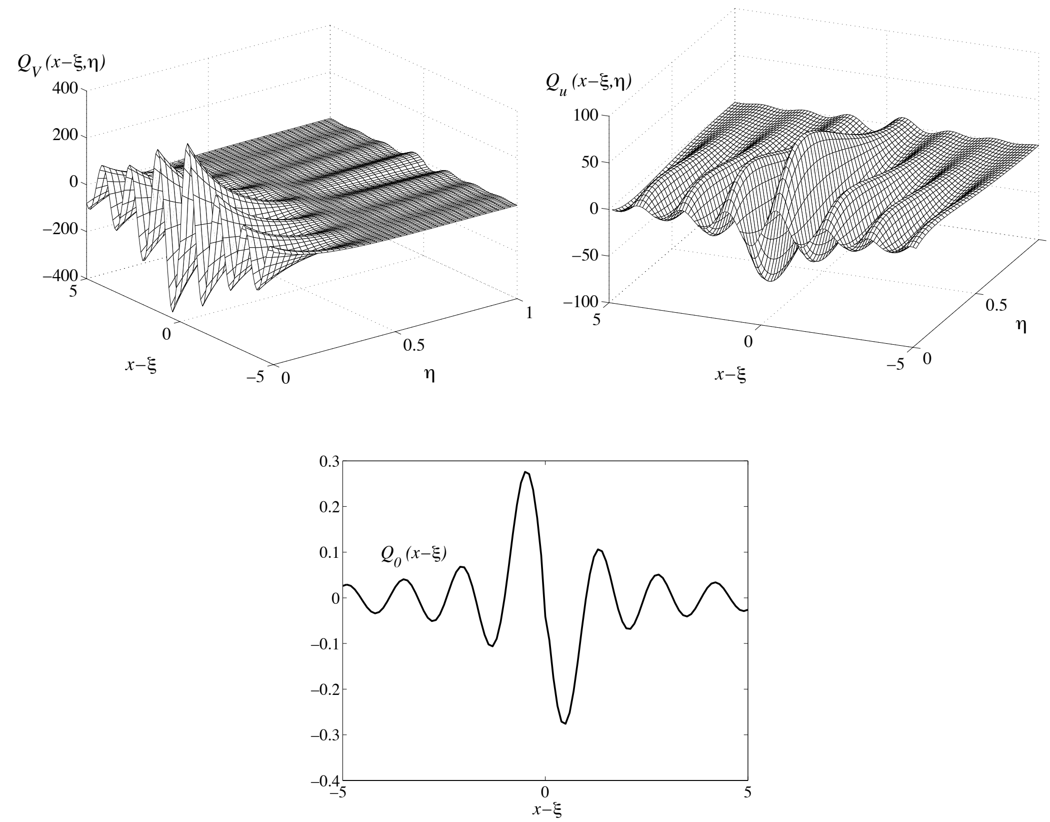

Figure 4.2: Feedback control kernels $Q_v(x-\xi,\eta)$ (upper left), $Q_u(x-\xi,\eta)$ (upper right) and $Q_0(x-\xi)$ (bottom).

$$\times\left[\int_0^y\left(\int_\eta^y L(k,\sigma,\eta)d\sigma\right)\sin(\pi j\eta)\,d\eta\right.$$
$$\left.+\frac{1-\cos(\pi j y)}{\pi j}\right]\int_0^1\left[\pi j\cos(\pi j\eta)\right.$$
$$+K(k,\eta,\eta)\sin(\pi j\eta)-\int_\eta^1 K_\eta(k,\sigma,\eta)$$
$$\left.\times\sin(\pi j\sigma)\,d\sigma\right]V(0,\xi,\eta)d\eta d\xi dk. \qquad (4.4.42)$$

The variables $\epsilon_u(t,x,y)$ and $\epsilon_V(t,x,y)$ represent the error of approximation of the velocity field and are bounded in the following way

$$||\epsilon_u(t)||_{L^2}^2+||\epsilon_V(t)||_{L^2}^2 \;\leq\; \mathrm{e}^{-\frac{1}{4Re}t}\left(||\epsilon_u(0)||_{L^2}^2+||\epsilon_V(0)||_{L^2}^2\right), \qquad (4.4.43)$$

where both $\epsilon_u(0,x,y)$ and $\epsilon_V(0,x,y)$ can be written in terms of the initial conditions of the velocity field as

$$\begin{aligned}\epsilon_u(0,x,y) &= u(0,x,y)-\int_{-\infty}^{\infty}\frac{\sin(2\pi M\xi)-\sin(2\pi m\xi)}{\pi\xi}\\ &\quad\times u(0,x-\xi,y)d\xi, \qquad (4.4.44)\\ \epsilon_V(0,x,y) &= V(0,x,y)-\int_{-\infty}^{\infty}\frac{\sin(2\pi M\xi)-\sin(2\pi m\xi)}{\pi\xi}\\ &\quad\times V(0,x-\xi,y)d\xi, \qquad (4.4.45)\end{aligned}$$

The bound on the errors is proportional to the initial kinetic energy of ϵ_u and ϵ_V, which, as made explicit in the expressions (4.4.44)–(4.4.45), is in turn proportional to the kinetic energy of u and V at very small and very large length scales (the integral that we are substacting from the initial conditions represents the intermediate length scale content), and decays exponentially. Therefore, this initial energy will typically be a very small fraction of the overall kinetic energy, making the errors ϵ_u and ϵ_V very small in comparison with u^* and V^* respectively.

The kernel L in (4.4.42) is defined as a convergent, smooth sequence of fuctions

$$L(k,y,\eta)=\lim_{n\to\infty}L_n(k,y,\eta), \qquad (4.4.46)$$

whose terms are recursively defined as

$$L_0 = K_0, \tag{4.4.47}$$

$$\begin{aligned} L_n &= L_{n-1} + 4iRe \int_{y-\eta}^{y+\eta} \int_0^{y-\eta} \int_{-\delta}^{\delta} \{2\pi k(\gamma+\xi-1)\cosh(\pi k(\xi-\delta)) \\ &\quad + \sinh(\pi k(\xi-\delta)) - \pi k(2\delta-1)\} L_{n-1}\left(k, \frac{\gamma+\xi}{2}, \frac{\gamma-\delta}{2}\right) d\xi d\delta d\gamma \\ &\quad - \frac{Re}{2}\pi ik \int_{y-\eta}^{y+\eta} \int_0^{y-\eta} (\gamma+\delta)(\gamma+\delta-2) \\ &\quad \times L_{n-1}\left(k, \frac{\gamma+\delta}{2}, \frac{\gamma-\delta}{2}\right) d\delta d\gamma \,. \end{aligned} \tag{4.4.48}$$

Control laws (4.3.24)–(4.3.34) guarantee the following results.

Theorem 4.3. *Assume $u_0(x,y)$ and $V_0(x,y)$, initial conditions for u and V, belong to $H^2(\Omega)$ and that the following compatibility conditions[3] are verified*

$$\frac{\partial}{\partial x}u_0(x,y) + \frac{\partial}{\partial y}V_0(x,y) = 0, \tag{4.4.49}$$

$$u_0(x,1) = \int_0^1 \int_{-\infty}^{\infty} Q_u(x-\xi,\eta)u_0(\xi,\eta)d\xi d\eta, \tag{4.4.50}$$

Then, the equilibrium $u(x,y) \equiv V(x,y) \equiv 0$ of system (4.2.10)–(4.2.18), with feedback law (4.3.24)–(4.3.34) where the function $h(t,x)$ in (4.3.26) verifies the initial condition $h(0,x) = V_0(x,1)$, is exponentially stable in the L^2, H^1 and H^2 norms. Moreover, the solutions for $u(t,x,y)$ and $V(t,x,y)$ belong to $L^2((0,\infty), H^2(\Omega))$ and are given explicitly by (4.4.39)–(4.4.48).

Theorem 4.4. *Under the same assumptions of Theorem 4.3, control laws U_c, V_c and kernels Q_u, Q_V, Q_0, as defined by (4.3.24)–(4.3.34), have the following properties:*

i. U_c and V_c are spatially invariant in x.

ii. $\int_{-\infty}^{\infty} V_c(t,\xi)d\xi = 0$ (zero net flux).

iii. $|Q| \leq C/|x-\xi|$, for $Q = Q_u, Q_V, Q_0$.

[3] *The compatibility condition $\int_{-\infty}^{\infty} V_c(t,x)dx = 0$ is automatically verified, see Theorem 4.4.*

iv. U_c *and* V_c *are smooth functions of* x.

v. Q_u, Q_V, Q_0 *are real valued.*

vi. Q_u, Q_V, Q_0 *are smooth in their arguments.*

vii. U_c *and* V_c *are* L^2 *functions of* x.

viii. All spatial derivatives of U_c *and* V_c *are* L^2 *function of* x.

Remark 4.5. By Sobolev's Embedding Theorem [107], H^2 stability suffices to establish continuity of the velocity field when the domain is bounded. The argument is not applicable to the infinite channel, but it holds if the channel is periodic, a setting for which our design extends trivially.

Remark 4.6. Theorem 4.4 ensures that the control laws are well behaved and their formal definition makes sense. Property i, spatial invariance, means that the feedback operators commute with translations in the x direction [12], which is crucial for implementation. Property ii ensures that we do not violate the physical restriction of zero net flux, which is derived from mass conservation. Property iii allows to truncate the integrals with respect to ξ to the vicinity of x, which allows sensing to be restricted just to a neighborhood (in the x direction) of the actuator. Properties iv to vi ensure that the control laws are well defined. Properties vii and viii prove finiteness of energy of the controllers and their spatial derivatives. These properties are illustrated in Fig. 4.2, which show the decay and smoothness of the kernels.

The next sections are devoted to proving these theorems. We first derive a priori estimates; then we prove well-posedness in a direct way using explicit closed-loop solutions.

4.5 L^2 stability

As common for infinite channels, we use a Fourier transform in x. The transform pair (direct and inverse transform) has the following definition:

$$f(k,y) = \int_{-\infty}^{\infty} f(x,y)\mathrm{e}^{-2\pi ikx}dx, \quad (4.5.51)$$

$$f(x,y) = \int_{-\infty}^{\infty} f(k,y)\mathrm{e}^{2\pi ikx}dk. \quad (4.5.52)$$

Note that we use the same symbol f for both the original $f(x,y)$ and the image $f(k,y)$. In hydrodynamics, k is referred to as the "wave number."

One property of the Fourier transform is that the L^2 norm is the same in Fourier space as in physical space, i.e.,

$$||f||_{L^2}^2 = \int_0^1\int_{-\infty}^{\infty} f^2(k,y)dkdy = \int_0^1\int_{-\infty}^{\infty} f^2(x,y)dxdy, \quad (4.5.53)$$

allowing us to derive L^2 exponential stability in physical space from the same property in Fourier space. This result is called Parseval's formula in the literature [28].

Remark 4.7. Given a state f, we define feedback operators that act on the state for each wave number k. Calling the result of the operator $Kf(k)$,

$$Kf(k) = \int_0^1 K(k,y)f(k,y)dy, \quad (4.5.54)$$

where K is a kernel that is itself a function of k. Applying the inverse transform we can write (4.5.54) in physical space

$$Kf(x) = \int_0^1\int_{-\infty}^{\infty} K(k,y)f(k,y)\mathrm{e}^{2\pi ikx}dkdy, \quad (4.5.55)$$

or in terms of f in physical space

$$Kf(x) = \int_{-\infty}^{\infty}\int_0^1\left(\int_{-\infty}^{\infty} K(k,y)\mathrm{e}^{2\pi ik(x-\xi)}dk\right) f(\xi,y)dyd\xi. \quad (4.5.56)$$

This is known as the Convolution Theorem. Supposing that f is an L^2 function of space, and that K is bounded and has finite support in k, it follows that Expression (4.5.56) makes sense and defines an L^2 function in space.

We also define the L^2 norm of $f(k,y)$ with respect to y:

$$||f(k)||^2_{\hat{L}^2} = \int_0^1 |f(k,y)|^2 dy. \tag{4.5.57}$$

The $\hat{L}^2$ norm as a function of k is related to the L^2 norm as

$$||f||^2_{L^2} = \int_{-\infty}^{\infty} ||f(k)||^2_{\hat{L}^2} dk \tag{4.5.58}$$

Equations (4.2.10)–(4.2.12) written in the Fourier domain are

$$\begin{aligned} u_t &= \frac{-4\pi^2 k^2 u + u_{yy}}{Re} + 8k\pi i y(y-1)u \\ &\quad +4(2y-1)V - 2\pi i k p, && (4.5.59) \\ V_t &= \frac{-4\pi^2 k^2 V + V_{yy}}{Re} + 8\pi k i y(y-1)V - p_y, && (4.5.60) \\ -4\pi^2 k^2 p + p_{yy} &= 16\pi k i(2y-1)V, && (4.5.61) \end{aligned}$$

with boundary conditions

$$\begin{aligned} u(k,0) &= 0, && (4.5.62) \\ u(k,1) &= U_c(k), && (4.5.63) \\ V(k,0) &= 0, && (4.5.64) \\ V(k,1) &= V_c(k), && (4.5.65) \\ p_y(k,0) &= \frac{V_{yy}(k,0)}{Re}, && (4.5.66) \\ p_y(k,1) &= \frac{V_{yy}(k,1) - 4\pi^2 k^2 V_c(k)}{Re} - (V_c)_t(k), && (4.5.67) \end{aligned}$$

and the continuity equation (4.2.19) is now

$$2\pi k i u(k,y) + V_y(k,y) = 0. \tag{4.5.68}$$

Thanks to linearity and spatial invariance, there is no coupling between different wave numbers. This allows us to consider the equations for each wave number independently. Then, the main idea behind the design of the controller is to consider two different cases depending on the wave number k. For wave numbers $m < |k| < M$, which we will refer to as *controlled* wave numbers, we will design a backstepping controller that achieves stabilization, whereas for wave numbers in the range $|k| \geq M$ or in the range $|k| \leq m$, which we will call *uncontrolled* wave numbers, the system is left without control but is exponentially stable. This is a well-known fact from hydrodynamic stability theory [95].

Estimates of m and M are found in the Section 4.5.2 based on Lyapunov analysis and allow us to use feedback for only the wave numbers $m < |k| < M$. This is crucial because feedback over the entire infinite range of k's would not be convergent. The truncations at $k = m, M$ are truncations in Fourier space which do not result in a discontinuity in x.

We now analyze equations (4.5.59)–(4.5.61) in detail, for both controlled and uncontrolled wave numbers.

4.5.1 Controlled wave numbers

For $m < |k| < M$ we first solve (4.5.61) in order to eliminate the pressure. The equation can be easily solved since it is just an ODE in y, for each k. Introducing its solution into (4.5.59), we are left with

$$\begin{aligned} u_t \;=\; & \frac{1}{Re}\left(-4\pi^2k^2u + u_{yy}\right) + 8\pi kiy(y-1)u + 4(2y-1)V \\ & +16\pi k\int_0^y V(k,\eta)(2\eta-1)\sinh\left(2\pi k(y-\eta)\right)d\eta + i\frac{\cosh\left(2\pi k(1-y)\right)}{\sinh\left(2\pi k\right)} \\ & \times\frac{V_{yy}(k,0)}{Re} - 16\pi k\frac{\cosh\left(2\pi ky\right)}{\sinh\left(2\pi k\right)}\int_0^1 V(k,\eta)(2\eta-1)\cosh\left(2\pi k(1-\eta)\right)d\eta \\ & -i\frac{\cosh\left(2\pi ky\right)}{\sinh\left(2\pi k\right)}\left(\frac{V_{yy}(k,1)-4\pi^2k^2V_c(k)}{Re} - (V_c)_t(k)\right). \end{aligned} \tag{4.5.69}$$

We don't need to separately write and control the V equation because, by the continuity equation (4.5.68) and using the fact that $V(k,0)=0$, we can write V in terms of u

$$V(k,y) = \int_0^y V_y(k,\eta)d\eta = -2\pi ki\int_0^y u(k,\eta)d\eta. \tag{4.5.70}$$

Introducing (4.5.70) in (4.5.69), and simplifying the resulting double integral by changing the order of integration, we reduce (4.5.69) to an autonomous equation that governs the whole velocity field. This equation is

$$
\begin{aligned}
u_t \;=\; & \frac{1}{Re}\left(-4\pi^2k^2u + u_{yy}\right) + 8\pi kiy(y-1)u + \frac{2\pi k\cosh\left(2\pi k(1-y)\right)}{\sinh\left(2\pi k\right)}\frac{u_y(k,0)}{Re} \\
& +8i\int_0^y \left\{\pi k(2y-1) - 2\sinh\left(2\pi k(y-\eta)\right) - 2\pi k(2\eta-1)\cosh\left(2\pi k(y-\eta)\right)\right\} \\
& \times u(k,\eta)d\eta + 16i\frac{\cosh\left(2\pi ky\right)}{\sinh\left(2\pi k\right)}\int_0^1 \left\{\pi k(2\eta-1)\cosh\left(2\pi k(1-\eta)\right)\right. \\
& \left.+\sinh\left(2\pi k(1-\eta)\right)\right\} u(k,\eta)d\eta \\
& +i\frac{\cosh\left(2\pi ky\right)}{\sinh\left(2\pi k\right)}\left(\frac{2\pi kiu_y(k,1) + 4\pi^2k^2V_c(k)}{Re} + (V_c)_t(k)\right), \qquad (4.5.71)
\end{aligned}
$$

with boundary conditions

$$
\begin{aligned}
u(k,0) &= 0, & (4.5.72)\\
u(k,1) &= U_c(k). & (4.5.73)
\end{aligned}
$$

Note that the relation between Y in (4.2.21) and u in (4.5.71) is that $Y(k,y) = 2\pi kiu(k,y)$.

Now, we design the controller in two steps. First, we set V_c so that (4.5.71) has a strict-feedback form in the sense previously defined:

$$
\begin{aligned}
(V_c)_t \;=\; & \frac{2\pi ki\left(u_y(k,0) - u_y(k,1)\right) - 4\pi^2k^2V_c}{Re} \\
& -16\pi ki\int_0^1 (2\eta-1)V(k,\eta)\cosh\left(2\pi k(1-\eta)\right)d\eta. \qquad (4.5.74)
\end{aligned}
$$

This can be integrated and explicitly stated as a dynamic controller in the Laplace domain:

$$
\begin{aligned}
V_c \;=\; & \frac{2\pi ki}{s + \frac{4\pi^2k^2}{Re}}\left[\frac{u_y(s,k,0) - u_y(s,k,1)}{Re}\right. \\
& \left. -8\int_0^1 (2\eta-1)V(s,k,\eta)\cosh\left(2\pi k(1-\eta)\right)d\eta\right]. \qquad (4.5.75)
\end{aligned}
$$

Control law (4.5.74) can be expressed in the time domain and physical space as (4.3.25)–(4.3.27) and (4.3.29), (4.3.30), by use of the convolution theorem of the Fourier transform.

Introducing V_c in (4.5.71) yields

$$\begin{aligned} u_t &= \frac{1}{Re}\left(-4\pi^2k^2u + u_{yy}\right) + 8\pi kiy(y-1)u + 8i\int_0^y \{\pi k(2y-1) \\ &\quad -2\sinh\left(2\pi k(y-\eta)\right) - 2\pi k(2\eta-1)\cosh\left(2\pi k(y-\eta)\right)\} u(k,\eta)d\eta \\ &\quad -2\pi k\frac{\cosh\left(2\pi ky\right) - \cosh\left(2\pi k(1-y)\right)}{\sinh\left(2\pi k\right)}\frac{u_y(k,0)}{Re}. \end{aligned} \tag{4.5.76}$$

Equation (4.5.76) can be stabilized using the backstepping technique for parabolic partial integro-differential equations [101]. This method consists in finding an invertible Volterra transformation that maps the original unstable equation into a target system with the desired stability properties.

Using backstepping, we map u, for each wave number $m < |k| < M$, into the family of heat equations

$$\alpha_t = \frac{1}{Re}\left(-4\pi^2k^2\alpha + \alpha_{yy}\right), \tag{4.5.77}$$

$$\alpha(k,0) = 0, \tag{4.5.78}$$

$$\alpha(k,1) = 0, \tag{4.5.79}$$

where

$$\alpha = u - \int_0^y K(k,y,\eta)u(t,k,\eta)d\eta, \tag{4.5.80}$$

$$u = \alpha + \int_0^y L(k,y,\eta)\alpha(t,k,\eta)d\eta, \tag{4.5.81}$$

are respectively the direct and inverse transformation. The kernel K is found by substituting (4.5.76) and (4.5.80) into (4.5.77)–(4.5.79). Then integration by parts, following exactly the same steps as in [101], leads to the following equation that K must verify.

$$\begin{aligned} \frac{1}{Re}K_{yy} &= \frac{1}{Re}K_{\eta\eta} + 8\pi ik\eta(\eta-1)K - 8i\left\{\pi k(2y-1) - \sinh\left(2\pi k(y-\eta)\right)\right. \\ &\quad \left. -2\pi k(2\eta-1)\cosh\left(2\pi k(y-\eta)\right)\right\} \\ &\quad +8i\int_\eta^y \{\pi k(2\xi-1) - 2\sinh\left(2\pi k(\xi-\eta)\right) \\ &\quad -2\pi k(2\eta-1)\cosh\left(2\pi k(\xi-\eta)\right)\} K(k,y,\xi)d\xi, \end{aligned} \tag{4.5.82}$$

a hyperbolic partial integro-differential equation (PIDE) in the region $\mathcal{T} = \{(y, \eta) : 0 \leq \eta \leq y \leq 1\}$ with boundary conditions:

$$\begin{aligned} K(y,y) &= -\frac{2Re}{3}\pi i k y^2(2y-3) - 2\pi k \frac{\cosh(2\pi k) - 1}{\sinh(2\pi k)}, & (4.5.83) \\ K(y,0) &= \frac{2\pi k}{\sinh(2\pi k)}\Big\{ \cosh(2\pi k y) - \cosh(2\pi k(1-y)) \\ &\quad + \int_0^y K(k,y,\xi)\left[\cosh(2\pi k(1-\xi)) - \cosh(2\pi k \xi)\right] d\xi \Big\}. & (4.5.84) \end{aligned}$$

Regarding (4.5.82)–(4.5.84) we have the following result.

Proposition 4.8. *Consider equation (4.5.82) in the domain* $(k, y, \eta) \in \mathbb{C} \times \mathcal{T}$ *with boundary conditions (4.5.83)–(4.5.84). There is a solution* K*, given by (4.3.32)–(4.3.34), such that* K *belongs to* $\mathcal{C}^2(\mathcal{T})$*. Moreover* K *as a complex-valued function of* k *is analytic in the annulus* $m < |k| < M$*.*

Sketch of Proof. We transform (4.5.82)–(4.5.84) into an integral equation. This is done following the same steps as in [101], by defining new variables $a = y + \eta$, $b = y - \eta$. Then one obtains a PIDE in a and b and parameterized by k, that can be partially solved by integration, finally reaching an integral equation of Volterra type in two variables. The integral equation can be solved explicitly for each k via a successive approximation series; this explicit solution is given by (4.3.32)–(4.3.34). For each $k \in \mathbb{C}$, the same method of [101] proves convergence of the series and hence the existence of a solution. One gets the following estimate when k is in the annulus $m < |k| < M$,

$$|K| \leq N e^{2N}, \tag{4.5.85}$$

where $N = Re\,(12\pi M + 2\sinh(2\pi M) + 2\pi M \cosh(2\pi M))$. Moreover using the estimate and the fact that the terms in the series definition (4.3.33)–(4.3.34) of K are analytic in k, it is shown that the kernel itself is also analytic as a complex function of k, for compact subsets of the annulus $m < |k| < M$. This implies analyticity in the given annulus [91]. $\mathcal{C}^1$ smoothness in y and η is shown by differentiating the integral equation, which yields the same type of equation for

K_y and K_η; then the argument for K holds for K_y and K_η (with a different but similarly looking exponent). Since the coefficients in the integral equation are smooth, this procedure can be iterated for K_{yy}, $K_{y\eta}$ and $K_{\eta\eta}$ (and even for higher derivatives, getting more smoothness, but we don't pursue that result). Thus $\mathcal{C}^2$ smoothness follows. □

Remark 4.9. Proposition 4.8 implies that the kernel and its first and second order derivatives in y and η are bounded for $m < |k| < M$ and $(y, \eta) \in \mathcal{T}$.

Remark 4.10. Using Proposition 4.8, Equations (4.5.80)–(4.5.81) and Remark 4.9, it is shown that the backstepping transformation (4.5.80) maps the spaces L^2, H^1 and H^2 back to themselves.

Remark 4.11. See also Theorem 8.25 for the statement and more detailed proof of a result that includes Proposition 4.8 as a particular case, since it considers equations of the kind of (4.5.82)–(4.5.84) with *time-varying* coefficients.

From the transformation (4.5.80) and the boundary condition (4.5.72) the control law is

$$U_c = \int_0^1 K(k,1,\eta)u(t,k,\eta)d\eta. \tag{4.5.86}$$

Using the convolution theorem of the Fourier transform (see Remark 4.7) we write the control law (4.5.86) back in physical space. The resulting expressions is (4.3.24).

The equation for the inverse kernel L in (4.5.81) is similar to the one of K and enjoys similar properties

$$\begin{aligned} \frac{1}{Re}L_{yy} \quad = \quad & \frac{1}{Re}L_{\eta\eta} - 8\pi i k y(y-1)L - 8i\left\{\pi k(2y-1) - 2\sinh\left(2\pi k(y-\eta)\right)\right. \\ & \left. -2\pi k(2\eta-1)\cosh\left(2\pi k(y-\eta)\right)\right\} \\ & -8i\int_\eta^y \left\{\pi k(2y-1) - \sinh\left(2\pi k(y-\xi)\right)\right. \\ & \left. +2\pi k(2\xi-1)\cosh\left(2\pi k(y-\xi)\right)\right\} L(k,\xi,\eta)d\xi, \end{aligned} \tag{4.5.87}$$

again a hyperbolic partial integro-differential equation in the region $\mathcal{T}$ with boundary conditions

$$
\begin{aligned}
L(y,y) &= -\frac{2Re}{3}\pi i k y^2(2y-3) - 2\pi k \frac{\cosh(2\pi k)-1}{\sinh(2\pi k)}, && (4.5.88)\\
L(y,0) &= \frac{2\pi k}{\sinh(2\pi k)}\Big\{\cosh(2\pi k y) - \cosh(2\pi k(1-y))\Big\}. && (4.5.89)
\end{aligned}
$$

The equation can be transformed into an integral equation and calculated via the successive approximation series (4.4.47)–(4.4.48). A similar result to Proposition 4.8 holds for L.

By using (4.5.70) and (4.5.80)–(4.5.81), V can also be expressed in terms of α

$$
\begin{aligned}
\alpha &= i\frac{V_y - \int_0^y K(k,y,\eta)V_y(t,k,\eta)d\eta}{2\pi k} && (4.5.90)\\
V &= -2\pi k i \int_0^y \left[1 + \int_\eta^y L(k,\eta,\sigma)d\sigma\right]\alpha(t,k,\eta)d\eta\,. && (4.5.91)
\end{aligned}
$$

Since (4.5.80)–(4.5.81) map (4.5.76) into (4.5.77), stability properties of the velocity field follows from those of the α system.

Proposition 4.12. *For any k in the range $m < |k| < M$, the equilibrium profile $u(t,k,y) \equiv V(t,k,y) \equiv 0$ of system (4.5.59)–(4.5.67) with control laws (4.5.74), (4.5.86) is exponentially stable in the L^2 norm, i.e.,*

$$
||V(t,k)||^2_{\hat{L}^2} + ||u(t,k)||^2_{\hat{L}^2} \;\leq\; D_0 \mathrm{e}^{\frac{-1}{2Re}t}\left(||V(0,k)||^2_{\hat{L}^2} + ||u(0,k)||^2_{\hat{L}^2}\right), \quad (4.5.92)
$$

where D_0 is defined as:

$$
D_0 \;=\; (1+4\pi^2M^2)\max_{m<|k|<M}\{(1+||L||_\infty)^2(1+||K||_\infty)^2\}. \quad (4.5.93)
$$

Proof. First, from the α equation (4.5.77) it is possible to get an L^2 estimate

$$
||\alpha(t,k)||^2_{\hat{L}^2} \leq \mathrm{e}^{-\frac{1}{2Re}t}||\alpha(0,k)||^2_{\hat{L}^2}, \quad (4.5.94)
$$

then employing the direct and inverse transformations (4.5.80)–(4.5.81) and (4.5.91) we get (4.5.92)–(4.5.93). □

Now, if we apply the feedback laws (4.5.74), (4.5.86) for *all* wave numbers $m < |k| < M$, then the control laws in physical space are given by expressions (4.3.24)–(4.3.30), where the inverse transform integrals are truncated at $k = m, M$ in (4.3.28)–(4.3.30). If we define

$$V^*(t,x,y) = \int_{-\infty}^{\infty} \chi(k) V(t,k,y) \mathrm{e}^{2\pi i k x} dk, \tag{4.5.95}$$

$$u^*(t,x,y) = \int_{-\infty}^{\infty} \chi(k) u(t,k,y) \mathrm{e}^{2\pi i k x} dk, \tag{4.5.96}$$

which are variables that contain all velocity field information for wave numbers $m < |k| < M$, the following result holds.

Proposition 4.13. *Consider equations (4.2.10)–(4.2.18) with control laws (4.3.24)–(4.3.25). Then the variables* $u^*(t,x,y)$ *and* $V^*(t,x,y)$ *defined in (4.5.95)–(4.5.96) decay exponentially:*

$$||V^*(t)||_{L^2}^2 + ||u^*(t)||_{L^2}^2 \leq D_0 \mathrm{e}^{\frac{-1}{2Re}t} \left(||V^*(0)||_{L^2}^2 + ||u^*(0)||_{L^2}^2 \right). \tag{4.5.97}$$

Proof. The Fourier transform of the star variables is, by definition, the same as the Fourier transform of the original variables for $m < |k| < M$, and zero otherwise. Therefore, applying Parseval's formula and Proposition 4.12,

$$\begin{aligned} ||V^*(t)||_{L^2}^2 + ||u^*(t)||_{L^2}^2 &= \int_{-\infty}^{\infty} \left(||V^*(t,k)||_{\hat{L}^2}^2 + ||u^*(t,k)||_{\hat{L}^2}^2 \right) dk \\ &= \int_{-\infty}^{\infty} \chi(k) \left(||V(t,k)||_{\hat{L}^2}^2 + ||u(t,k)||_{\hat{L}^2}^2 \right) dk \\ &\leq D_0 \mathrm{e}^{\frac{-1}{2Re}t} \int_{-\infty}^{\infty} \chi(k) \left(||V(0,k)||_{\hat{L}^2}^2 + ||u(0,k)||_{\hat{L}^2}^2 \right) dk \\ &= D_0 \mathrm{e}^{-\frac{1}{2Re}t} \left(||V^*(0)||_{L^2}^2 + ||u^*(0)||_{L^2}^2 \right), \end{aligned} \tag{4.5.98}$$

proving (4.5.97). □

4.5.2 Uncontrolled wave number analysis

For the uncontrolled system (4.5.59)–(4.5.60), we define, for each k, the Lyapunov functional

$$\Lambda(k,t) = \frac{1}{2} \left(||V(t,k)||_{\hat{L}^2}^2 + ||u(t,k)||_{\hat{L}^2}^2 \right) \tag{4.5.99}$$

The time derivative of Λ is

$$\begin{aligned}\dot{\Lambda} &= -\frac{8\pi^2k^2}{Re}\Lambda - \frac{1}{Re}\left(||u_y(k)||^2_{\hat{L}^2} + ||V_y(k)||^2_{\hat{L}^2}\right) \\ &\quad +4\int_0^1 (2y-1)\frac{u\bar{V}+\bar{u}V}{2}dy, \end{aligned} \tag{4.5.100}$$

where the bar denotes the complex conjugate, and the pressure term cancels out using integration by parts and the continuity equation (4.5.68). The second term in the first line of (4.5.100) can be bounded using the Poincare inequality, thanks to the Dirichlet boundary condition at $y = 0$:

$$-||u_y(k)||^2_{\hat{L}^2} - ||V_y(k)||^2_{\hat{L}^2} \leq -\frac{\Lambda}{2}. \tag{4.5.101}$$

Consider now separately the two cases $|k| \leq m$ and $|k| \geq M$. In the first case, we can bound the second line of (4.5.100) as

$$\dot{\Lambda} \leq -\frac{8\pi^2k^2}{Re}\Lambda - \frac{1}{2Re}\Lambda + 4\Lambda, \tag{4.5.102}$$

so, if $|k| \geq \frac{1}{\pi}\sqrt{\frac{Re}{2}}$, then

$$\dot{\Lambda} \leq -\frac{1}{2Re}\Lambda. \tag{4.5.103}$$

Now, consider the case of small wave numbers. We bound the second line of (4.5.100) using the continuity equation (4.5.68)

$$\dot{\Lambda} \leq -\frac{8\pi^2k^2}{Re}\Lambda - \frac{1}{2Re}\Lambda + 8\pi|k|\Lambda, \tag{4.5.104}$$

so, if $|k| \leq \frac{1}{32\pi Re}$, then

$$\dot{\Lambda} \leq -\frac{1}{4Re}\Lambda. \tag{4.5.105}$$

We have just proved the following result:

Proposition 4.14. *If* $m = \frac{1}{32\pi Re}$ *and* $M = \frac{1}{\pi}\sqrt{\frac{Re}{2}}$, *then for both* $|k| \leq m$ *and* $|k| \geq M$ *the equilibrium* $u(t,k,y) \equiv V(t,k,y) \equiv 0$ *of the uncontrolled system (4.5.59)–(4.5.67) is exponentially stable in the* L^2 *sense:*

$$||V(t,k)||^2_{\hat{L}^2} + ||u(t,k)||^2_{\hat{L}^2} \leq \mathrm{e}^{\frac{-1}{4Re}t}\left(||V(0,k)||^2_{\hat{L}^2} + ||u(0,k)||^2_{\hat{L}^2}\right). \tag{4.5.106}$$

Since the decay rate in (4.5.106) is independent of k, that allows us to claim the following result for *all* uncontrolled wave numbers.

Proposition 4.15. *The variables $\epsilon_u(t,x,y)$ and $\epsilon_V(t,x,y)$ defined as*

$$\epsilon_u(t,x,y) = \int_{-\infty}^{\infty} (1-\chi(k))\, u(t,k,y)\mathrm{e}^{2\pi ikx}dk, \tag{4.5.107}$$

$$\epsilon_V(t,x,y) = \int_{-\infty}^{\infty} (1-\chi(k))\, V(t,k,y)\mathrm{e}^{2\pi ikx}dk, \tag{4.5.108}$$

decay exponentially as

$$||\epsilon_V(t)||_{L^2}^2 + ||\epsilon_u(t)||_{L^2}^2 \;\; \leq \;\; \mathrm{e}^{\frac{-1}{4Re}t}\left(||\epsilon_V(0)||_{L^2}^2 + ||\epsilon_u(0)||_{L^2}^2\right). \tag{4.5.109}$$

Proof. As in Proposition 4.13. □

4.5.3 Analysis for the entire wave number range

Using (4.4.39)–(4.4.40),

$$\begin{aligned} ||V(t)||_{L^2}^2 &= \int_{-\infty}^{\infty} ||V(t,k)||_{\hat{L}^2}^2 dk \\ &= \int_0^1\int_{-\infty}^{\infty} \left(V^*(t,k,y)+\epsilon_V(t,k,y)\right)^2 dkdy \\ &= \int_0^1\int_{-\infty}^{\infty} \left((V^*)^2+\epsilon_V^2+2V^*\epsilon_V\right) dkdy \\ &= ||V^*(t)||_{L^2}^2 + ||\epsilon_V(t)||_{L^2}^2, \end{aligned} \tag{4.5.110}$$

where we have used the fact that $V^*(t,k,y)\epsilon_V(t,k,y) = \chi(k)(1-\chi(k))V(t,k,y)$ and $\chi(k)(1-\chi(k))$ is zero for all k by its definition (4.3.31).

This shows that the L^2 norm of V is the sum of the L^2 norms of $V^*(t,k,y)$ and $\epsilon_V(t,k,y)$. The same holds for u. Therefore, Theorem 4.3 follows from Propositions 4.13 and 4.15. Noting that D_0 as defined in (4.5.93) is greater than unity, we obtain the following estimate of the decay:

$$||V(t)||_{L^2}^2 + ||u(t)||_{L^2}^2 \;\; \leq \;\; D_0\mathrm{e}^{\frac{-1}{4Re}t}\left(||V(0)||_{L^2}^2 + ||u(0)||_{L^2}^2\right). \tag{4.5.111}$$

4.6 H^1 stability

We define the H^1 norm of $f(x,y)$ as

$$||f||^2_{H^1} \quad = \quad ||f||^2_{L^2} + ||f_x||^2_{L^2} + ||f_y||^2_{L^2}. \qquad (4.6.112)$$

We also define the H^1 norm of $f(k,y)$ with respect to y as

$$||f(k)||^2_{\hat{H}^1} = (1+4\pi^2k^2)||f(k)||^2_{\hat{L}^2} + ||f_y(k)||^2_{\hat{L}^2}. \qquad (4.6.113)$$

The $\hat{H}^1$ norm as a function of k is related to the H^1 norm as

$$||f||^2_{H^1} = \int_{-\infty}^{\infty} ||f(k)||^2_{\hat{H}^1} dk. \qquad (4.6.114)$$

4.6.1 H^1 stability for controlled wave numbers

For each k, one has that

$$||f(k)||^2_{\hat{H}^1} \quad \leq \quad (5+16\pi^2M^2)||f_y(k)||^2_{\hat{H}^1}, \qquad (4.6.115)$$

where we have used (4.6.113) and Poincare's inequality. This proves the equivalence, for any k, of the $\hat{H}^1$ norm of $f(k,y)$ and the $\hat{L}^2$ norm of just $f_y(k,y)$. Therefore, we only have to show exponential decay for u_y and V_y.

Due to the backstepping transformations (4.5.80), (4.5.81) and (4.5.90) (4.5.91),

$$\alpha_y \quad = \quad u_y - K(k,y,y)u - \int_0^y K_y(k,y,\eta)u(t,k,\eta)d\eta\,, \qquad (4.6.116)$$

$$u_y \quad = \quad \alpha_y + L(k,y,y)\alpha + \int_0^y L_y(k,y,\eta)\alpha(t,k,\eta)d\eta\,, \qquad (4.6.117)$$

$$\alpha \quad = \quad \frac{-1}{2\pi ki}\left(V_y - \int_0^y K(k,y,\eta)V_y(t,k,\eta)d\eta\right), \qquad (4.6.118)$$

$$V_y \quad = \quad -2\pi ki\left(\alpha + \int_0^y L(k,y,\eta)\alpha(t,k,\eta)d\eta\right), \qquad (4.6.119)$$

and then it is possible to write the following estimates, which are derived from simple estimates on α and α_y from (4.5.77)

$$||u_y(t,k)||^2_{\hat{L}^2} \quad \leq \quad D_1 \mathrm{e}^{-\frac{2}{5Re}t}||u_y(0,k)||^2_{\hat{L}^2}, \qquad (4.6.120)$$

$$||V_y(t,k)||^2_{\hat{L}^2} \quad \leq \quad D_0 \mathrm{e}^{-\frac{1}{2Re}t}||V_y(0,k)||^2_{\hat{L}^2}, \qquad (4.6.121)$$

where

$$D_1 \quad = \quad 5 \max_{m<|k|<M} \left\{(1+4||L||_\infty + 4||L_y||_\infty)^2(1+4||K||_\infty + 4||K_y||_\infty)^2\right\}. \quad (4.6.122)$$

Using these estimates the following proposition can be stated regarding the velocity field at each k in the controlled range.

Proposition 4.16. *For any k in the range $m < |k| < M$, the equilibrium profile $u(t,k,y) \equiv V(t,k,y) \equiv 0$ of the system (4.5.59)–(4.5.67) with control laws (4.5.74), (4.5.86) is exponentially stable in the H^1 sense*

$$||V(t,k)||^2_{\hat{H}^1} + ||u(t,k)||^2_{\hat{H}^1} \quad \leq \quad D_2 \mathrm{e}^{\frac{-2}{5Re}t} \left(||V(0,k)||^2_{\hat{H}^1} + ||u(0,k)||^2_{\hat{H}^1}\right), \quad (4.6.123)$$

where D_2 is defined as:

$$D_2 \quad = \quad (5 + 16\pi^2 M^2) \max\{D_0, D_1\}. \quad (4.6.124)$$

Thanks to the same argument as in Proposition 4.13, for *all* wave numbers $m < |k| < M$, the following result holds.

Proposition 4.17. *Consider equations (4.2.10)–(4.2.18) with feedback control laws (4.3.24)–(4.3.25). Then the variables $u^*(t,x,y)$ and $V^*(t,x,y)$ defined in (4.5.95)–(4.5.96) decay exponentially in the H^1 norm:*

$$||u^*(t)||^2_{H^1} + ||V^*(t)||^2_{H^1} \quad \leq \quad D_2 \mathrm{e}^{\frac{-2}{5Re}t} \left(||u^*(0)||^2_{H^1} + ||V^*(0)||^2_{H^1}\right). \quad (4.6.125)$$

4.6.2 H^1 stability for uncontrolled wave numbers

Following the same argument as in (4.5.99)–(4.5.105), a slightly different bound can be derived that keeps some of the $\hat{H}^1$ norm in (4.5.104)

$$\dot{\Lambda} \leq -\frac{\Lambda}{8Re} - \frac{\Lambda_H}{2Re}, \quad (4.6.126)$$

where

$$\Lambda_H(k,t) = \frac{1}{2}\left(||u_y(t,k)||^2_{\hat{L}^2} + ||V_y(t,k)||^2_{\hat{L}^2}\right). \quad (4.6.127)$$

The time derivative of Λ_H can be bounded as

$$\begin{aligned}
\frac{d\Lambda_H}{dt} &= \int_0^1 \frac{u_y\bar{u}_{yt}+\bar{u}_y u_{yt}+\bar{V}_y V_{yt}+V_y\bar{V}_{yt}}{2}dy \\
&= -\int_0^1 \frac{u_{yy}\bar{u}_t+\bar{u}_{yy}u_t+\bar{V}_{yy}V_t+V_{yy}\bar{V}_t}{2}dy \\
&= -\frac{1}{Re}\left(||u_{yy}||^2_{\hat{L}^2}+||V_{yy}||^2_{\hat{L}^2}\right)+4k^2\pi^2\int_0^1 \frac{u_{yy}\bar{u}+\bar{u}_{yy}u+\bar{V}_{yy}V+V_{yy}\bar{V}}{2Re}dy \\
&\quad +2\pi ki\int_0^1 \frac{u_{yy}\bar{p}-\bar{u}_{yy}p}{2}dy-\int_0^1 \frac{\bar{V}_{yy}p_y+V_{yy}\bar{p}_y}{2}dy \\
&\quad -4\int_0^1 (2y-1)\frac{u_{yy}\bar{V}+\bar{u}_{yy}V}{2}dy \\
&\quad +8\pi ki\int_0^1 y(y-1)\frac{u_{yy}\bar{u}-\bar{u}_{yy}u-\bar{V}_{yy}V+V_{yy}\bar{V}}{2}dy,
\end{aligned} \tag{4.6.128}$$

where we have used integration by parts and the Dirichlet boundary conditions of the uncontrolled wave number range. Doing further integration by parts and using the divergence free condition, we can simplify a little the previous expression:

$$\begin{aligned}
\frac{d\Lambda_H}{dt} &= -\frac{1}{Re}\left(||u_{yy}||^2_{\hat{L}^2}+||V_{yy}||^2_{\hat{L}^2}\right)-\frac{8k^2\pi^2}{Re}\Lambda_h \\
&\quad -16\pi^2k^2\int_0^1 (2y-1)\frac{\bar{u}V-u\bar{V}}{2}dy-\left.\frac{\bar{V}_{yy}p+V_{yy}\bar{p}}{2}\right|_0^1 .
\end{aligned} \tag{4.6.129}$$

Only the last term remains to be estimated. Using (4.5.66)–(4.5.67) with V_c being zero for uncontrolled wave number, the last term in (4.6.129) can be expresssed as

$$\left.\frac{\bar{V}_{yy}p+V_{yy}\bar{p}}{2}\right|_0^1 = Re\left.\frac{\bar{p}_y p+p_y\bar{p}}{2}\right|_0^1 . \tag{4.6.130}$$

This quantity can be estimated using the following lemma.

Lemma 4.18. *If the pressure p verifies the Poisson equation (4.5.61) with boundary conditions (4.5.66)–(4.5.67), then*

$$-\left.\frac{\bar{p}_y p+p_y\bar{p}}{2}\right|_0^1 \leq 16||V(t,k)||^2_{\hat{L}^2}. \tag{4.6.131}$$

Proof. Multiplying equation (4.5.61) by $\bar{p}$ and integrating from zero to one, one gets:

$$-4\pi^2k^2||p(t,k)||^2_{\hat{L}^2}+\int_0^1 \bar{p}p_{yy}dy = \int_0^1 16\pi ki(2y-1)\bar{p}V\,dy, \tag{4.6.132}$$

which integrated by parts, becomes

$$-\bar{p}p_y\Big|_0^1 = -4\pi^2k^2||p(t,k)||^2_{\hat{L}^2} - ||p_y(t,k)||^2_{\hat{L}^2} - \int_0^1 16\pi ki(2y-1)\bar{p}V\,dy. \quad (4.6.133)$$

Now using Young's inequality one finally arrives at

$$-\bar{p}p_y\Big|_0^1 \leq 16||V(t,k)||^2_{\hat{L}^2}. \quad (4.6.134)$$

For the other conjugate pair one proceeds analogously, thus completing the proof.

□

Using the lemma, the time derivative of Λ_H can be estimated as follows:

$$\frac{d\Lambda_H}{dt} \leq -\frac{8k^2\pi^2}{Re}\Lambda_H + 16\pi^2k^2\Lambda + 16Re\Lambda. \quad (4.6.135)$$

We take the following Lyapunov functional

$$\Lambda_T = \Lambda_H + (1 + 64Re^2 + 4\pi^2k^2 + 64Re\pi^2k^2)\Lambda, \quad (4.6.136)$$

which is *equivalent* to the H^1 norm, whose definition in terms of Λ and Λ_H is

$$||u(t,k)||^2_{\hat{H}^1} + ||V(t,k)||^2_{\hat{H}^1} = 2(1 + 4\pi^2k^2)\Lambda + 2\Lambda_H. \quad (4.6.137)$$

Computing the derivative of (4.6.136)

$$\frac{d\Lambda_T}{dt} \leq -\frac{\Lambda_H}{2Re} - \frac{1 + 4\pi^2k^2}{8Re}\Lambda \leq -d_1\Lambda_T, \quad (4.6.138)$$

where d_1 is a (possible very conservative) positive constant, which depends on the Reynolds number (but *not* on k)

$$d_1 = \frac{1}{8D_3Re}, \quad (4.6.139)$$

and where

$$D_3 = \max\{1 + 64Re^2, 1 + 16Re\}. \quad (4.6.140)$$

Deriving an estimate of the H^1 norm from this estimate for Λ_T, one reaches the following result.

Proposition 4.19. *If $m = \frac{1}{32\pi Re}$ and $M = \frac{1}{\pi}\sqrt{\frac{Re}{2}}$, then for both $|k| \leq m$ and $|k| \geq M$ the equilibrium $u(t,k,y) \equiv V(t,k,y) \equiv 0$ of the uncontrolled system (4.5.59)–(4.5.67) is exponentially stable in the H^1 sense:*

$$||V(t,k)||^2_{\hat{H}^1} + ||u(t,k)||^2_{\hat{H}^1} \leq D_3 \mathrm{e}^{-d_1 t}\left(||V(0,k)||^2_{\hat{H}^1} + ||u(0,k)||^2_{\hat{H}^1}\right). \quad (4.6.141)$$

Since the decay rate in (4.6.141) is independent of k, that allows us to claim the following result for *all* uncontrolled wave numbers.

Proposition 4.20. *The variables $\epsilon_u(t,x,y)$ and $\epsilon_V(t,x,y)$ defined as in (4.5.107)–(4.5.108) decay exponentially in the H^1 norm as*

$$||\epsilon_u(t)||^2_{H^1} + ||\epsilon_V(t)||^2_{H^1} \leq D_3 \mathrm{e}^{-d_1 t}\left(||\epsilon_u(0)||^2_{H^1} + ||\epsilon_V(0)||^2_{H^1}\right). \quad (4.6.142)$$

4.6.3 Analysis for all wave numbers

From Propositions 4.17 and 4.20, and using the same argument as in Section 4.5.3, the H^1 stability part of Theorem 4.3 is proved. One gets that

$$||u(t)||^2_{H^1} + ||V(t)||^2_{H^1} \leq D_4 \mathrm{e}^{-d_1 t}\left(||u(0)||^2_{H^1} + ||V(0)||^2_{H^1}\right), \quad (4.6.143)$$

where $D_4 = \max\{D_2, D_3\}$.

4.7 H^2 stability

The H^2 norm of $f(x,y)$ is defined as

$$||f||^2_{H^2} = ||f||^2_{H^1} + ||f_{xx}||^2_{L^2} + ||f_{xy}||^2_{L^2} + ||f_{yy}||^2_{L^2}. \quad (4.7.144)$$

We also define the $\hat{H}^2$ norm of $f(k,y)$ with respect to y as

$$\begin{aligned} ||f(k)||^2_{\hat{H}^2} &= ||f(k)||^2_{\hat{H}^1} + 16\pi^4 k^4 ||f(k)||^2_{\hat{L}^2} \\ &\quad + 4\pi^2 k^2 ||f_y(k)||^2_{\hat{L}^2} + ||f_{yy}(k)||^2_{\hat{L}^2}. \end{aligned} \quad (4.7.145)$$

The $\hat{H}^2$ norm as a function of k is related to the H^2 norm as

$$||f||^2_{H^2} = \int_{-\infty}^{\infty} ||f(k)||^2_{\hat{H}^2} dk. \quad (4.7.146)$$

4.7.1 H^2 stability for controlled wave numbers

Thanks to the backstepping transformations (4.5.80), (4.5.81) and (4.5.90), (4.5.91), one calculates the second order derivative of both u and V from α and its derivatives,

$$\begin{aligned}\alpha_{yy} &= u_{yy} - K(k,y,y)u_y - (2K_y(k,y,y) + K_\eta(k,y,y))u \\ &\quad - \int_0^y K_{yy}(k,y,\eta)u(t,k,\eta)d\eta\,, \qquad (4.7.147)\\ u_{yy} &= \alpha_{yy} + L(k,y,y)\alpha_y + (2L_y(k,y,y) + L_\eta(k,y,y))\alpha \\ &\quad + \int_0^y L_{yy}(k,y,\eta)\alpha(t,k,\eta)d\eta\,, \qquad (4.7.148)\\ \alpha_y &= \frac{-1}{2\pi ki}\left(V_{yy} - K(k,y,y)V_y - \int_0^y K_y(k,y,\eta)V_y(t,k,\eta)d\eta\right), \qquad (4.7.149)\\ V_{yy} &= -2\pi ki\left(\alpha_y + L(k,y,y)\alpha + \int_0^y L_y(k,y,\eta)\alpha(t,k,\eta)d\eta\right). \qquad (4.7.150)\end{aligned}$$

It is possible then to write the following estimates, which are derived from simple estimates on α, α_y and α_{yy} from (4.5.77):

$$\begin{aligned}||u(t,k)||^2_{\hat{H}^2} &\leq D_5 \mathrm{e}^{-\frac{2}{5Re}t}||u(0,k)||^2_{\hat{H}^2}, \qquad (4.7.151)\\ ||V(t,k)||^2_{\hat{H}^2} &\leq D_6 \mathrm{e}^{-\frac{2}{5Re}t}||V(0,k)||^2_{\hat{H}^2}. \qquad (4.7.152)\end{aligned}$$

The positive constants D_5 and D_6 are defined as in (4.6.122) and depend only on K and L.

Using these estimates the following proposition can be stated regarding the velocity field at each k in the controlled range.

Proposition 4.21. *For any k in the range $m < |k| < M$, the equilibrium profile $u(t,k,y) \equiv V(t,k,y) \equiv 0$ of the system (4.5.59)–(4.5.67) with control laws (4.5.74), (4.5.86) is exponentially stable in the H^2 sense*

$$||V(t,k)||^2_{\hat{H}^2} + ||u(t,k)||^2_{\hat{H}^2} \leq D_7 \mathrm{e}^{\frac{-2}{5Re}t}\left(||V(0,k)||^2_{\hat{H}^2} + ||u(0,k)||^2_{\hat{H}^2}\right), \qquad (4.7.153)$$

where D_7 is defined as:

$$D_7 = \max\{D_5, D_6\}. \qquad (4.7.154)$$

Thanks to the same argument as in Proposition 4.13, the following result holds for *all* wave numbers $m < |k| < M$.

Proposition 4.22. *Consider equations (4.2.10)–(4.2.18) with feedback control laws (4.3.25)–(4.3.24). Then the variables $u^*(t,x,y)$ and $V^*(t,x,y)$ defined in (4.5.95)–(4.5.96) decay exponentially in the H^2 norm:*

$$||u^*(t)||_{H^2}^2 + ||V^*(t)||_{H^2}^2 \leq D_8 e^{\frac{-2}{5Re}t}\left(||u^*(0)||_{H^2}^2 + ||V^*(0)||_{H^2}^2\right). \tag{4.7.155}$$

4.7.2 H^2 stability for uncontrolled wave numbers

For the uncontrolled wave number range, thanks to the Dirichlet boundary conditions, the $\hat{H}^2$ norm $||u(t,k)||_{\hat{H}^2}$ is equivalent to the norm

$$||u(t,k)||_{\hat{H}^1}^2 + \int_0^1 \left|u_{yy}(t,k,y) - 4\pi^2 k^2 u(t,k,y)\right|^2 dy, \tag{4.7.156}$$

i.e., to the $\hat{H}^1$ norm plus the $\hat{L}^2$ norm of the Laplacian, which we denote for short $||\triangle_k u(k)||_{\hat{L}^2}^2$. The proof of the norm equivalence is obtained integrating by parts,

$$\begin{aligned} ||\triangle_k u(k)||_{\hat{L}^2}^2 &= \int_0^1 \left|-4\pi^2 k^2 u(y,k) + u_{yy}(y,k)\right|^2 dy \\ &= \int_0^1 \left[16\pi^4 k^4 |u|^2(y,k) + |u_{yy}|^2(y,k) - 4\pi^2 k^2\left(u\bar{u}_{yy} + \bar{u}u_{yy}\right)\right] dy \\ &= 16\pi^4 k^4 ||u(k)||_{\hat{L}^2}^2 + ||u_{yy}(k)||_{\hat{L}^2}^2 + 8\pi^2 k^2 ||u_y(k)||_{\hat{L}^2}^2. \end{aligned} \tag{4.7.157}$$

The next norm equivalence property is less obvious and we state it in the following lemma:

Lemma 4.23. *Consider u and V verifying equations (4.5.59)–(4.5.60). Then, for the uncontrolled wave number range, the norm $||u||_{\hat{H}^2}^2 + ||V||_{\hat{H}^2}^2$ is equivalent to the norm*

$$||u||_{\hat{H}^1}^2 + ||V||_{\hat{H}^1}^2 + ||u_t||_{\hat{L}^2}^2 + ||V_t||_{\hat{L}^2}^2. \tag{4.7.158}$$

This means the Laplacian operator in norm (4.7.156) can be replaced by a time derivative, when considering the H^2 norm of u and V together.

Proof. Let us call

$$\begin{aligned}\Lambda_1 &= ||u_t(t,k)||^2_{\hat{L}^2} + ||V_t(t,k)||^2_{\hat{L}^2}, &(4.7.159)\\ \Lambda_2 &= \frac{||\triangle_k u(t,k)||^2_{\hat{L}^2} + ||\triangle_k V(t,k)||^2_{\hat{L}^2}}{Re^2}. &(4.7.160)\end{aligned}$$

Substituting in (4.7.159) equations (4.5.59)–(4.5.60),

$$\Lambda_1 = \Lambda_2 + \Lambda_3, \tag{4.7.161}$$

where Λ_3 contains the following terms

$$\begin{aligned}\Lambda_3 &= -\int_0^1 \frac{-2\pi ki\triangle_k u\bar{p} + \triangle_k V\bar{p}_y}{Re}dy - 2\pi ki\int_0^1 4y(1-y)\\ &\quad \times\frac{\triangle_k u\bar{u} + \triangle_k V\bar{V}}{Re}dy + \int_0^1 4(1-2y)\frac{\triangle_k u\bar{V}}{Re}dy - \int_0^1 \left(2\pi kip\bar{u}_t + p_y\bar{V}_t\right)dy\\ &\quad +2\pi ki\int_0^1 4y(1-y)\left(u\bar{u}_t + v\bar{V}_t\right)dy + \int_0^1 4(1-2y)\left(V\bar{u}_t\right)dy. &(4.7.162)\end{aligned}$$

Now one can estimate this quantity:

$$|\Lambda_3| \le 48(||u(k)||^2_{\hat{H}^1} + ||V(k)||^2_{\hat{H}^1}) + \frac{1}{2}\left(\Lambda_1 + \Lambda_2\right), \tag{4.7.163}$$

in which we have used integration by parts, Young's inequality, and Lemma 4.18. Therefore:

$$||u||^2_{\hat{H}^2} + ||V||^2_{\hat{H}^2} \le D_8\bigg(||u||^2_{\hat{H}^1} + ||V||^2_{\hat{H}^1} + \Lambda_1\bigg), \tag{4.7.164}$$

and

$$||u||^2_{\hat{H}^1} + ||V||^2_{\hat{H}^1} + \Lambda_1 \le D_8\bigg(||u||^2_{\hat{H}^2} + ||V||^2_{\hat{H}^2}\bigg), \tag{4.7.165}$$

where $D_8 = 97\max\{Re^2, 1/Re^2\}$. □

From Lemma 4.23 one gets $\hat{H}^2$ stability for the uncontrolled wave numbers. This is obtained by considering the norm $||u_t||^2_{\hat{L}^2} + ||V_t||^2_{\hat{L}^2}$ as a Lyapunov functional whose derivative can be bounded as

$$\frac{d}{dt}\frac{||u_t||^2_{\hat{L}^2} + ||V_t||^2_{\hat{L}^2}}{2} \le -\frac{1}{4Re}\left(||u_t||^2_{\hat{L}^2} + ||V_t||^2_{\hat{L}^2}\right), \tag{4.7.166}$$

which follows by taking the time derivative of (4.5.59)–(4.5.60) and applying the same argument as for L^2 stability. Thus,

$$||u_t(t,k)||^2_{\hat{L}^2} + ||V_t(t,k)||^2_{\hat{L}^2} \leq \mathrm{e}^{-\frac{1}{2Re}t}\left(||u_t(0,k)||^2_{\hat{L}^2} + ||V_t(0,k)||^2_{\hat{L}^2}\right). \quad (4.7.167)$$

Noting that $d_1 \leq 1/2Re$ and $D_3 \geq 1$, adding (4.7.167) to (4.6.141) and employing (4.7.164), (4.7.164) we obtain the following result.

Proposition 4.24. *If $m = \frac{1}{32\pi Re}$ and $M = \frac{1}{\pi}\sqrt{\frac{Re}{2}}$, then for both $|k| \leq m$ and $|k| \geq M$ the equilibrium $u(t,k,y) \equiv V(t,k,y) \equiv 0$ of the uncontrolled system (4.5.59)–(4.5.67) is exponentially stable in the H^2 sense:*

$$||V(t,k)||^2_{\hat{H}^2} + ||u(t,k)||^2_{\hat{H}^2} \leq D_8^2 D_3 \mathrm{e}^{-d_1 t}\left(||V(0,k)||^2_{\hat{H}^2} + ||u(0,k)||^2_{\hat{H}^2}\right). \quad (4.7.168)$$

Since the decay rate in (4.7.168) is independent of k, that allows us to claim the following result for *all* uncontrolled wave numbers.

Proposition 4.25. *The variables $\epsilon_u(t,x,y)$ and $\epsilon_V(t,x,y)$ defined as in (4.5.107)–(4.5.108) decay exponentially in the H^2 norm as*

$$||\epsilon_u(t)||^2_{H^2} + ||\epsilon_V(t)||^2_{H^2} \leq D_8^2 D_3 \mathrm{e}^{-d_1 t}\left(||\epsilon_u(0)||^2_{H^2} + ||\epsilon_V(0)||^2_{H^2}\right). \quad (4.7.169)$$

4.7.3 Analysis for all wave numbers

From Propositions 4.22 and 4.25, and again by the same argument as in Section 4.5.3, the H^2 stability part of Theorem 4.3 is proved. One gets that

$$||u(t)||^2_{H^2} + ||V(t)||^2_{H^2} \leq D_9 \mathrm{e}^{-d_1 t}\left(||u(0)||^2_{H^2} + ||V(0)||^2_{H^2}\right), \quad (4.7.170)$$

where $D_9 = \max\{D_7, D_8^2 D_3\}$.

4.8 Proof of well-posedness and explicit solutions

For showing well-posedness and derive the explicit solutions we decompose the system in two parts in the wave number space, using (4.4.39)–(4.4.40).

The star variables represent the controlled wave numbers in physical space and are defined in (4.5.95)–(4.5.96). The epsilon variables represent the uncontrolled wave number content in physical space and are defined in (4.5.107)–(4.5.107). Consider then the initial conditions u_0 and V_0 in Fourier space. Define

$$V_0^*(x,y) = \int_{-\infty}^{\infty} \chi(k) V_0(k,y) \mathrm{e}^{2\pi i k x} dk, \tag{4.8.171}$$

$$u_0^*(x,y) = \int_{-\infty}^{\infty} \chi(k) u_0(k,y) \mathrm{e}^{2\pi i k x} dk, \tag{4.8.172}$$

and similarly,

$$\epsilon_{V0}(x,y) = \int_{-\infty}^{\infty} (1-\chi(k))\, V_0(k,y) \mathrm{e}^{2\pi i k x} dk, \tag{4.8.173}$$

$$\epsilon_{u0}(x,y) = \int_{-\infty}^{\infty} (1-\chi(k))\, u_0(k,y) \mathrm{e}^{2\pi i k x} dk. \tag{4.8.174}$$

Note that $V_0^*, u_0^*, \epsilon_{V0}, \epsilon_{u0} \in H^2(\Omega)$ and also verify the required compatibility conditions. Define the following initial-boundary value problems for the star and epsilon variables.

$$P_1 \equiv \begin{cases} (u^*, V^*) \text{ verify (4.2.10)–(4.2.11) and (4.2.19)}, \\ u^*(t,x,0) = V^*(t,x,0) = 0, \\ u^*(t,x,1) = (4.3.24), \\ V^*(t,x,1) = (4.3.25), \\ u^*(0,x,y) = u_0^*(x,y), V^*(0,x,y) = V_0^*(x,y). \end{cases} \tag{4.8.175}$$

and

$$P_2 \equiv \begin{cases} (\epsilon_u, \epsilon_V) \text{ verify (4.2.10)–(4.2.11) and (4.2.19)}, \\ \epsilon_u(t,x,0) = \epsilon_V(t,x,0) = 0, \\ \epsilon_u(t,x,1) = \epsilon_V(t,x,1) = 0 \\ \epsilon_u(0,x,y) = \epsilon_{u0}(x,y), \epsilon_V(0,x,y) = \epsilon_{V0}(x,y). \end{cases} \tag{4.8.176}$$

By linearity and spatial invariance (implying that different wave numbers are independent of each other) the solution of the linearized Navier-Stokes equations is the sum of the solutions of P_1 and P_2. Hence if both systems are well-posed then the original problem is well-posed too.

System P_2 is the (uncontrolled) channel flow with no-slip, no-penetration boundary conditions. See [108, Proposition 1.2, pages 265–269], for an analysis of the linear Navier-Stokes equations and their regularity that allows for unbounded domains. It is shown that with the given degree of regularity of the initial conditions, the problem is well posed in the space $L^2((0,T),H^2(\Omega))$. Combining this fact with the a priori bounds of Section 4.7, it follows that P_2 is well-posed in $L^2((0,\infty),H^2(\Omega))$. Moreover the decay rate of the epsilon variables is given in Proposition 4.15.

We prove now that P_1 is well-posed using a direct method, taking advantage of the possibility of writing the exact solution of the problem. This is a classical way of showing well-posedness, see for example [29], where existence of solutions is shown by solving explicitly the problems with Fourier transform and series methods, and uniqueness is proved by energy methods.

Explicit solutions (4.4.41)–(4.4.42) are obtained in the following way. Equation (4.5.77) is a heat equation in $\alpha(t,k,y)$ and can be solved explicitly. The initial condition for this equation is

$$\alpha_0(k,y) = u_0^*(k,y) - \int_0^y K(k,y,\eta)u_0^*(k,\eta)d\eta, \tag{4.8.177}$$

and, since $u_0^* \in H^2(\Omega)$, then $\alpha_0 \in H^2(\Omega)$, moreover the compatibility condition $\alpha_0(k,0) = \alpha_0(k,1) = 0$ is verified from (4.8.177) and (4.4.50). Hence the solution of (4.5.77), a stable heat equation, is $L^2((0,\infty),H^2(\Omega))$. Using then (4.5.81) and (4.5.91), and applying the inverse Fourier transform, the solution for u^* and V^* is recovered in physical space, as given by (4.4.41)–(4.4.42). Both the inverse backstepping transformation and the inverse Fourier transform map $L^2((0,\infty),H^2(\Omega))$ back into itself, hence the existence of a solution with the desired regularity properties follows. Explicit formulas can be written for the control laws; in particular $V_c(t)$ is well-defined as the traces $u_y(0,k)$ and $u_y(1,k)$ appearing in Equation (4.3.27) can be computed due to the regularity of u.

Remark 4.26. Note that in fact a higher regularity can be proved for P_1, due to the smoothing properties of the heat equation. We don't pursue more than H^2 regularity in this work. Note also that regularity in x, which is determined in Fourier space by the behavior of the solution for large values of k, is guaranteed for P_1 because the solution is nonzero only for a finite subset of wave numbers. Hence the solution of P_1 is smooth in x.

Uniqueness follows from the a priori bounds shown in Sections 4.5–4.7. Given two solutions in the same space, their difference verifies as well the a priori bounds with zero initial conditions, hence its norm is zero for all times and both solutions must be the same.

4.9 Proof of Theorem 4.4

Consider expressions (4.3.24)–(4.3.34).

Points i and iv are deduced trivially from the fact that (4.3.24) and (4.3.27) are defined as convolutions, and properties of the heat equation (4.3.26).

Point ii is verified if

$$\int_{-\infty}^{\infty} V_c(t,x)dx = 0. \tag{4.9.178}$$

From the definition of the Fourier transform of V_c,

$$V_c(t,k=0) = \int_{-\infty}^{\infty} V_c(t,x)dx. \tag{4.9.179}$$

Therefore, as $k = 0$ lies on the uncontrolled wave number range $-m < k < m$, then $V_c(t,k=0) = 0$ and the property is verified.

Point iii bounds the decay rate of kernels (4.3.28)–(4.3.30). Kernel definitions are of the form

$$Q(x-\xi,y) = \int_{-\infty}^{\infty} \chi(k) f(k,y) \mathrm{e}^{2\pi i k(x-\xi)} dk, \tag{4.9.180}$$

for some f analytic in k and smooth in y. Then, integrating by parts, we find that

$$\begin{aligned} |Q(x-\xi,y)| &\leq \frac{(M-m)}{\pi|x-\xi|} \max_{m<|k|<M} \left|\frac{df}{dk}(k,y)\right| + \frac{2}{\pi|x-\xi|} \max_{m<|k|<M} |f(k,y)| \\ &= \frac{C}{|x-\xi|}, \end{aligned} \tag{4.9.181}$$

showing that the kernels decay at least like $1/|x-\xi|$. This bound is made explicit in Remark 4.2.

From the definition of the inverse Fourier transform (4.5.52), it is straightforward to show that if the real part of $f(k,y)$ is even and the imaginary part of $f(k,y)$ is odd, then the resulting $f(x,y)$ will always be real. Then, Point v can be proved showing that the functions under the integrals in (4.3.28)–(4.3.30), which are inverse Fourier transforms, have this property. This is immediate for (4.3.29) and (4.3.30). For (4.3.28), the property must be shown for the kernel K, defined by the sequence (4.3.33)–(4.3.34). Since K is the limit of the sequence, it will have the property if all K_n share the property. This can be proved by induction. For K_0, the property is evident from its definition (4.3.33) and can be immediately verified. For K_n, if the property is assumed for K_{n-1}, then from expression (4.3.34) and taking into account that the product of even or odd functions is even and the product of an even function times an odd function is odd, then follows that K_n also shares the property. Therefore, the limit K has a real inverse transform, and kernel Q_u is real.

Point vi is deduced from the definition of the kernels (4.3.28)–(4.3.30) as truncated Fourier inverse integrals, which makes the kernels smooth in $x-\xi$. Smoothness in η is deduced from smoothness of the functions under the integrals.

For Point vii, consider expression (4.3.24) and (4.3.28). Then,

$$\begin{aligned}
||U_c||_{L^2}^2 &= \int_{-\infty}^{\infty} U_c(t,x)^2 dx \\
&= \int_{-\infty}^{\infty} |U_c|(t,k)^2 dk \\
&= \int_{-\infty}^{\infty} \chi(k)\left|\int_0^1 K(k,1,\eta)u(t,y,k)d\eta\right|^2 dk \\
&\leq 2(M-m)\max_{m\leq|k|\leq M}\{||K||_\infty\}||u(t)||_{L^2}^2,
\end{aligned} \tag{4.9.182}$$

and the result follows from Theorem 4.3.

On the other hand, for V_c one has to use its dynamic equation (4.3.26)–(4.3.27), and a Lyapunov functional consisting in half its L^2 norm. One then has, using Young's inequality

$$\frac{d}{dt}\frac{|V_c(k)|^2}{2} \leq \frac{-\pi^2 k^2}{Re}|V_c(k)|^2 + \frac{|u_y|^2(t,k,0)+|u_y|^2(t,k,1)}{Re} \\ +64\cosh\left(2\pi M\right)||V(t,k)||^2_{\hat{L}^2}, \qquad (4.9.183)$$

and supposing the control law is initialized at zero (see Remark 4.1), and using the H^2 norm to bound the second line of (4.9.183) one gets

$$|V_c(t,k)|^2 \leq \int_0^t \mathrm{e}^{-\frac{\pi^2 m^2}{Re}(t-\tau)} \left[10\frac{||u(\tau,k)||^2_{\hat{H}^2}}{Re} \right. \\ \left. +64\cosh\left(2\pi M\right)||V(\tau,k)||^2_{\hat{L}^2}\right] d\tau. \qquad (4.9.184)$$

Integrating in k

$$||V_c(t)||^2_{L^2} \leq \int_0^t \mathrm{e}^{-\frac{\pi^2 m^2}{Re}(t-\tau)} \left[10\frac{||u(\tau)||^2_{H^2}}{Re} \right. \\ \left. +64\cosh\left(2\pi M\right)||V(\tau)||^2_{L^2}\right] d\tau, \qquad (4.9.185)$$

and then the result follows from Theorem 4.3.

For Point viii, consider the jth spatial derivative of U_c and calculate its L_2 spatial norm

$$\left|\left|\frac{d^j}{dx^j}U_c\right|\right|^2_{L^2} = \int_{-\infty}^{\infty}\left(\frac{d^j}{dx^j}U_c(t,x)\right)^2 dx \\ = \int_{-\infty}^{\infty}|2\pi k|^{2j}|U_c|(t,k)^2 dk \\ \leq (2\pi M)^{2j}||U_c||^2_{L^2}, \qquad (4.9.186)$$

so the result for U_c follows from Point vii. We proceed similarly for V_c, thus proving Point viii.

This chapter is a partial reprint of the material as it appears in R. Vazquez and M. Krstic, "A closed-form feedback controller for stabilization of linearized Navier-Stokes equations: the 2D Poiseuille flow," *Proc. of the 2005 CDC*, Sevilla, Spain, 2005.

R. Vazquez and M. Krstic, “Higher order stability properties of a 2D Navier-Stokes system with an explicit boundary controller,” *Proc. of the 2006 ACC*, Minneapolis, 2006.

The dissertation author was the primary author and the coauthor listed in these publications directed and supervised the research, which is the basis for this chapter.

Chapter 5

Boundary Estimation for 2-D Navier-Stokes Channel Flow

5.1 Introduction

The absence of effective state estimators for Navier-Stokes equations modeling turbulent fluid flows is considered one of the key obstacles to reliable, model-based weather forecasting. We present a nonlinear observer for the channel flow, a benchmark problem in turbulence. The observer measures pressure and skin friction at one of the walls of the channel (which have been called the "footprints" of turbulence [22], in the sense that they completely determine the flow inside the domain) and estimates velocities and pressure throughout the channel. Previous observer designs for the channel flow were in the form of an Extended Kalman Filter for the spatially discretized Navier-Stokes equations and employed high-dimensional algebraic Riccati equations for computation of observer gains [32, 62]. Our obsever consists of a copy of the *nonlinear* plant with output injection of measurement errors, with output injection gains designed for the linearized error system. Thus, in structure our observer is also similar to an Extended Kalman Filter, however it is designed for the continuum Navier-Stokes model and the output injection gains are are given explicitly, by a symbolically computable formula.

As done for the control design in Chapter 4, we use a Fourier transform approach allowing separate analysis for different wave numbers. For a range of wave numbers, we design output injection gains to guarantee observer convergence, while for the very large and small wave numbers the system is known to be exponentially stable, and simply a copy of the plant is used. These two results are combined to prove observer error convergence for all wave numbers.

5.2 Observer

The observer consists of a copy of (4.2.1)–(4.2.2), to which we add output injection of the pressure P and the streamwise velocity gradient U_y (proportional to friction) at the wall

$$\begin{aligned} \hat{U}_t &= \frac{1}{Re}\left(\hat{U}_{xx}+\hat{U}_{yy}\right)-\hat{P}_x-\hat{U}\hat{U}_x-\hat{V}\hat{U}_y \\ &\quad+\int_{-\infty}^{\infty} Q_1(x-\xi,y)\Big(U_y(\xi,0)-\hat{U}_y(\xi,0)\Big)d\xi \\ &\quad+\int_{-\infty}^{\infty} Q_2(x-\xi,y)\left(P(\xi,0)-\hat{P}(\xi,0)\right)d\xi, \end{aligned} \tag{5.2.1}$$

$$\begin{aligned} \hat{V}_t &= \frac{1}{Re}\left(\hat{V}_{xx}+\hat{V}_{yy}\right)-\hat{P}_y-\hat{U}\hat{V}_x-\hat{V}\hat{V}_y \\ &\quad+\int_{-\infty}^{\infty} Q_3(x-\xi,y)\left(U_y(\xi,0)-\hat{U}_y(\xi,0)\right)d\xi \\ &\quad+\int_{-\infty}^{\infty} Q_4(x-\xi,y)\left(P(\xi,0)-\hat{P}(\xi,0)\right)d\xi, \end{aligned} \tag{5.2.2}$$

where as usual the observer (estimated) variables are denoted by a hat. In addition the observer verifies the continuity equation

$$\hat{U}_x+\hat{V}_y=0, \tag{5.2.3}$$

and boundary conditions

$$\hat{U}(t,x,0)=\hat{U}(t,x,1)=\hat{V}(t,x,0)=\hat{V}(t,x,1)=0. \tag{5.2.4}$$

The observer employs four output injection kernels defined as follows.

$$\begin{aligned}
Q_1(x,y) &= \int_{-\infty}^{\infty} \chi(k) l(k,y,0) \mathrm{e}^{2\pi i k x} dk + \frac{R_1(x,y,M) - R_1(x,y,m)}{Re}, && (5.2.5)\\
Q_2(x,y) &= R_2(x,y,M) - R_2(x,y,m), && (5.2.6)\\
Q_3(x,y) &= -\int_{-\infty}^{\infty} \int_0^y \chi(k) 2\pi k i l(k,\eta,0) \mathrm{e}^{2\pi i k x} d\eta dk \\
&\quad -\frac{R_2(x,y,M) - R_2(x,y,m)}{Re}, && (5.2.7)\\
Q_4(x,y) &= R_1(x,y,M) - R_1(x,y,m), && (5.2.8)
\end{aligned}$$

where

$$\begin{aligned}
R_1(x,y,k) &= \frac{2x}{\pi(x^2+y^2)^2}\left[y\cosh(2\pi k y)\sin(2\pi k x) - x\sinh(2\pi k y)\cos(2\pi k x)\right] \\
&\quad -\frac{2k}{(x^2+y^2)}\left[y\cosh(2\pi k y)\cos(2\pi k x) + x\sinh(2\pi k y)\sin(2\pi k x)\right] \\
&\quad +\frac{\sinh(2\pi k y)\cos(2\pi k x)}{\pi(x^2+y^2)}, && (5.2.9)\\
R_2(x,y,k) &= \frac{2x}{\pi(x^2+y^2)^2}\left[x\cosh(2\pi k y)\sin(2\pi k x) + y\sinh(2\pi k y)\cos(2\pi k x)\right] \\
&\quad -\frac{2k}{(x^2+y^2)}\left[x\cosh(2\pi k y)\cos(2\pi k x) - y\sinh(2\pi k y)\sin(2\pi k x)\right] \\
&\quad -\frac{\cosh(2\pi k y)\sin(2\pi k x)}{\pi(x^2+y^2)}, && (5.2.10)
\end{aligned}$$

$\chi(k)$ is defined as in (4.3.31), and

$$l(k,y,\eta) = \lim_{n\to\infty} l_n(k,y,\eta), \qquad (5.2.11)$$

where l_n is recursively defined as [1]

$$\begin{aligned}
l_0 &= -i\pi k Re(1-y)\Bigg((1-\eta^2) + \frac{(1-y)^2}{3} - 2(1-\eta) + 2(y-\eta)(2-y+\eta) \\
&\quad -4(y-\eta)(1-\eta)\Bigg) - 4iRe(1-y)(y-2\eta)\sinh(2\pi k(y-\eta)), && (5.2.12)\\
l_n &= l_{n-1} + \frac{Re}{4}\int_{y-\eta}^{2-(y+\eta)} \int_0^{y-\eta} \int_{\gamma}^{\gamma-\delta+y-\eta} f\left(k, 1-\gamma-\frac{\xi+\delta}{2}, 1-\frac{\xi-\delta}{2}\right) \\
&\quad \times l_{n-1}\left(k, 1-\frac{\gamma-\delta}{2}, 1-\frac{\gamma+\delta}{2}\right) d\xi d\delta d\gamma + \frac{Re}{2}\int_{y-\eta}^{2-(y+\eta)} \int_0^{y-\eta} (\gamma-\delta-2)
\end{aligned}$$

[1] This recursion is proved convergent, smooth, and uniformly bounded over $(y,\eta) \in [0,1]^2$, with a bound continuously dependent on k, as stated in Proposition 5.3

$$\times(\gamma-\delta)\pi ikl_{n-1}\left(k,1-\frac{\gamma-\delta}{2},1-\frac{\gamma+\delta}{2}\right)d\delta d\gamma, \tag{5.2.13}$$

where f is defined as

$$\begin{aligned} f(k,y,\eta) &= 8i\left\{\pi k(2y-1)-\sinh\left(2\pi k(y-\eta)\right)\right. \\ &\quad \left.-2\pi k(2\eta-1)\cosh\left(2\pi k(y-\eta)\right)\right\}. \end{aligned} \tag{5.2.14}$$

The terms of this recursion can be computed symbolically as they only involve integration of polynomials and exponentials. In implementation, only a few steps will be sufficient to obtain a highly accurate approximation because the recursion is rapidly convergent [101].

Remark 5.1. Note that the observer equations (5.2.1)–(5.2.2) can be regarded as forced Navier-Stokes equations, with the output injection acting as a body force. This means that any standard DNS solver for the forced Navier-Stokes equations can be used to implement the observer without needing major modifications.

As we did in Section 4.3, we illustrate the properties of the output injection kernels Q_1, Q_2, Q_3 and Q_4 in Fig. 5.1. In the plot, we have used the explicit formulae in (5.2.5)–(5.2.8) and approximated the kernel l by l_0 from (5.2.12). The kernel are computed for the case of low Reynolds numbers, for which it holds that $l \approx l_0$; for large Reynolds numbers, Q_2 and Q_4 remain the same (as they do not depend on Re), while Q_1 and Q_3 will have a similar *shape* with increased gains due to the contribution of the l kernel, which grows with Re. Note that in all cases, the gains are larger when closer to the $y = 1$ wall (and thus far away from the measurements).

Remark 5.2. The output injection terms in (5.2.1)–(5.2.2) and output injection operators defined in (5.2.5)-(5.2.8) share the properties of the feedback operators that were stated in Theorem 4.4. In particular, they are spatially invariant, well-defined, smooth, have a finite energy, i.e., finite L^2 norm, and, as illustrated in Fig. 5.1, are decaying in the x direction—a property that allows to truncate the

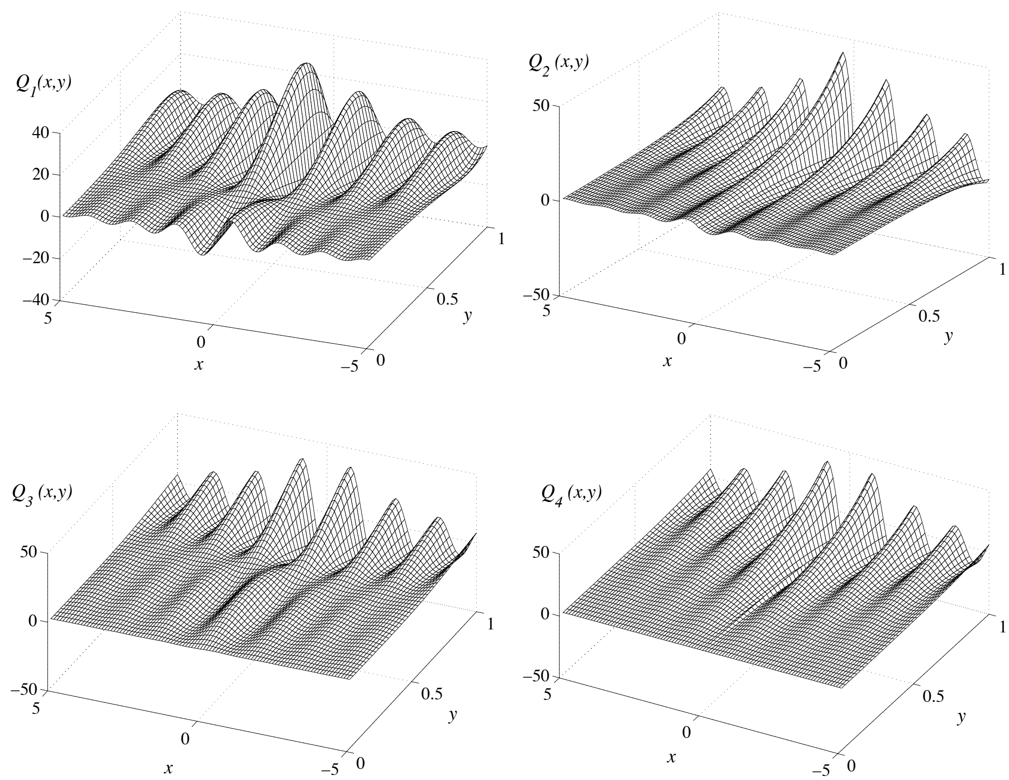

Figure 5.1: Output injection kernels $Q_1(x, y)$ (upper left), $Q_2(x, y)$ (upper right), $Q_3(x, y)$ (lower left) and $Q_4(x, y)$ (lower right).

integrals in (5.2.1)–(5.2.2) with respect to ξ to the vicinity of x, which allows sensing to be restricted just to a neighborhood (in the x direction) of the portion of the channel whose velocity one wants to estimate.

5.3 Observer Convergence Proof

Substracting the observer equations from the plant equations we obtain the error equations, with states $\tilde{U} = U - \hat{U}, \tilde{V} = V - \hat{V}, \tilde{P} = P - \hat{P}$.

$$\begin{aligned} \tilde{U}_t &= \frac{1}{Re}\left(\tilde{U}_{xx} + \tilde{U}_{yy}\right) - \tilde{P}_x + \tilde{U}\tilde{U}_x + \tilde{V}\tilde{U}_y - U\tilde{U}_x - V\tilde{U}_y - \tilde{U}U_x - \tilde{V}U_y \\ &\quad + \int_{-\infty}^{\infty} Q_1(x-\xi, y)\tilde{U}_y(\xi, 0)d\xi + \int_{-\infty}^{\infty} Q_2(x-\xi, y)\tilde{P}(\xi, 0)d\xi, \qquad (5.3.15) \\ \tilde{V}_t &= \frac{1}{Re}\left(\tilde{V}_{xx} + \tilde{V}_{yy}\right) - \tilde{P}_y + \tilde{U}\tilde{V}_x + \tilde{V}\tilde{V}_y - U\tilde{V}_x - V\tilde{V}_y - \tilde{U}V_x - \tilde{V}V_y \\ &\quad + \int_{-\infty}^{\infty} Q_3(x-\xi, y)\tilde{U}_y(\xi, 0)d\xi + \int_{-\infty}^{\infty} Q_4(x-\xi, y)\tilde{P}(\xi, 0)d\xi, \qquad (5.3.16) \end{aligned}$$

the continuity equation

$$\tilde{U}_x + \tilde{U}_y = 0, \qquad (5.3.17)$$

and boundary conditions

$$\begin{aligned} \tilde{U}(t, x, 0) &= \tilde{U}(t, x, 1) = 0, \qquad (5.3.18) \\ \tilde{V}(t, x, 0) &= \tilde{V}(t, x, 1) = 0. \qquad (5.3.19) \end{aligned}$$

We define the fluctuation variable as in Chapter 4,

$$u(t, x, y) = U(t, x, y) - U^e(y), \qquad (5.3.20)$$

where $U^e(y)$ was defined in (4.2.7). Using this variable we can write the equations as

$$\begin{aligned} \tilde{U}_t &= \frac{1}{Re}\left(\tilde{U}_{xx} + \tilde{U}_{yy}\right) - \tilde{P}_x + \mathcal{N}_U\left(\tilde{V}, \tilde{U}, u, V\right) - U^e\tilde{U}_x - U^e_y\tilde{V} \\ &\quad + \int_{-\infty}^{\infty} Q_1(x-\xi, y)\tilde{U}_y(\xi, 0)d\xi + \int_{-\infty}^{\infty} Q_2(x-\xi, y)\tilde{P}(\xi, 0)d\xi, \qquad (5.3.21) \\ \tilde{V}_t &= \frac{1}{Re}\left(\tilde{V}_{xx} + \tilde{V}_{yy}\right) - \tilde{P}_y + \mathcal{N}_V\left(\tilde{V}, \tilde{U}, u, V\right) + U^e\tilde{V}_x \\ &\quad + \int_{-\infty}^{\infty} Q_3(x-\xi, y)\tilde{U}_y(\xi, 0)d\xi + \int_{-\infty}^{\infty} Q_4(x-\xi, y)\tilde{P}(\xi, 0)d\xi, \qquad (5.3.22) \end{aligned}$$

and higher order terms

$$\mathcal{N}_U = \tilde{U}\tilde{U}_x + \tilde{V}\tilde{U}_y - u\tilde{U}_x - V\tilde{U}_y - \tilde{U}u_x - \tilde{V}u_y, \tag{5.3.23}$$

$$\mathcal{N}_V = \tilde{U}\tilde{V}_x + \tilde{V}\tilde{V}_y - u\tilde{V}_x - V\tilde{V}_y - \tilde{U}V_x - \tilde{V}V_y, \tag{5.3.24}$$

which are quadratic in $\tilde{V}, \tilde{U}, u, V$.

When the observer state $(\hat{U}, \hat{V})$ is close to the actual state (U, V), and when the fluctuation (u, V) around the equilibrium state is small, then the nonlinear terms $\mathcal{N}_U(\tilde{U}, \tilde{V}, u, V)$, $\mathcal{N}_V(\tilde{U}, \tilde{V}, u, V)$ are small and dominated by the linear terms in the equations.

We use the Fourier transform defined in (4.5.51)–(4.5.52). The output injection kernels defined in (5.2.5) and (5.2.6) written in Fourier space are

$$Q_1(k,y) = \chi(k)l(k,y,0) + \chi(k)\frac{2\pi k \sinh(2\pi k y)}{Re}, \tag{5.3.25}$$

$$Q_2(k,y) = \chi(k)2\pi k i \cosh(2\pi k y), \tag{5.3.26}$$

$$Q_3(k,y) = -\chi(k)2\pi k i \int_0^y l(k,\eta,0)d\eta - \chi(k)\frac{2\pi k i \cosh(2\pi k y)}{Re}, \tag{5.3.27}$$

$$Q_4(k,y) = \chi(k)2\pi k \sinh(2\pi k y), \tag{5.3.28}$$

where we have used the truncating function $\chi(k)$.

Equations (5.3.21)–(5.3.22) in Fourier space are

$$\begin{aligned}\tilde{U}_t &= \frac{1}{Re}\left(-4\pi^2k^2\tilde{U} + \tilde{U}_{yy}\right) - 2\pi k i\tilde{P} - 2\pi k i U^e\tilde{U} - U^e_y\tilde{V} \\ &\quad + Q_1(k,y)\tilde{U}_y(k,0) + Q_2(k,y)\tilde{P}(k,0),\end{aligned} \tag{5.3.29}$$

$$\begin{aligned}\tilde{V}_t &= \frac{1}{Re}\left(-4\pi^2k^2\tilde{V} + \tilde{V}_{yy}\right) - \tilde{P}_y - 2\pi k i U^e\tilde{V} \\ &\quad + Q_3(k,y)\tilde{U}_y(k,0) + Q_4(k,y)\tilde{P}(k,0),\end{aligned} \tag{5.3.30}$$

with boundary conditions

$$\tilde{U}(t,k,0) = \tilde{U}(t,k,1) = 0, \tag{5.3.31}$$

$$\tilde{V}(t,k,0) = \tilde{V}(t,k,1) = 0. \tag{5.3.32}$$

and the continuity equation, whose expression in Fourier space is

$$2\pi k i\tilde{U}(k,y) + \tilde{V}_y(k,y) = 0. \tag{5.3.33}$$

Equations (5.3.29)–(5.3.33) are uncoupled for each wave number, and therefore, as in Chapter 4, can be studied separately for $m \leq |k| \leq M$, which we will refer as the *observed* wave number range, and $|k| > M$, $|k| < m$, the *unobserved* wave number range, where m and M are parameters that ensure stability for the unobserved wave number equations.

5.3.1 Observed wave number analysis

First we use (5.3.29)–(5.3.33) to derive an equation for the pressure error, in order to eliminate it from (5.3.29)–(5.3.30). This is done as in Chapter 4, taking divergence of equations (5.3.29)–(5.3.30) and using (5.3.33). Note that, from (5.3.25)–(5.3.28),

$$2\pi i k Q_1 + Q_{3y} = 0, \quad 2\pi i k Q_2 + Q_{4y} = 0, \tag{5.3.34}$$

hence the output injection terms are cancelled when obtaining the pressure equation, which is

$$-4\pi^2 k^2 \tilde{P} + \tilde{P}_{yy} \;\; = \;\; -4\pi k i U_y^e \tilde{V}. \tag{5.3.35}$$

We solve (5.3.35) in terms of the boundary values at $y = 0$, which are $\tilde{P}(k, 0)$, a measured state, and

$$\tilde{P}_y(k, 0) = -2\pi k i \frac{\tilde{U}_y(k, 0)}{Re}, \tag{5.3.36}$$

which has been obtained from (5.3.30) at $y = 0$ using that in (5.3.27)–(5.3.28), $Q_3(k, 0) = Q_4(k, 0) = 0$, and from (5.3.33) $\tilde{V}_{yy}(k, 0) = -2\pi k i \tilde{U}_y(k, 0)$. The solution to (5.3.35) is

$$\begin{aligned} \tilde{P} \;\; = \;\; & 4i \int_0^y \sinh\left(2\pi k (y - \eta)\right) U^e(\eta) \tilde{V}(k, \eta) d\eta \\ & + \cosh\left(2\pi k y\right) \tilde{P}(k, 0) - i \frac{\sinh\left(2\pi k y\right)}{Re} U_y(k, 0). \end{aligned} \tag{5.3.37}$$

Inserting (5.3.37) into (5.3.29)–(5.3.30), and using (4.2.7), we see that the output injection kernels eliminate the terms with $\tilde{P}(k,0)$, yielding

$$\begin{aligned}\tilde{U}_t &= \frac{1}{Re}\left(-4\pi^2k^2\tilde{U}+\tilde{U}_{yy}\right)+8i\pi ky(y-1)\tilde{U}+(2y-1)\tilde{V}+l(k,y,0)\tilde{U}_y(k,0)\\ &\quad +16\pi k\int_0^y \sinh\left(2\pi k(y-\eta)\right)(2\eta-1)\tilde{V}(k,\eta)d\eta, && (5.3.38)\\ \tilde{V}_t &= \frac{1}{Re}\left(-4\pi^2k^2\tilde{V}+\tilde{V}_{yy}\right)+8i\pi ky(y-1)\tilde{V}-2\pi ki\int_0^y l(k,\eta,0)d\eta\tilde{U}_y(k,0)\\ &\quad -16\pi ki\int_0^y \cosh\left(2\pi k(y-\eta)\right)(2\eta-1)\tilde{V}(k,\eta)d\eta, && (5.3.39)\end{aligned}$$

with boundary conditions (5.3.31)–(5.3.31).

We don't need to separately control the $\tilde{V}$ equation because, by the continuity equation (5.3.33) and using the fact that $\tilde{V}(k,0)=0$, we can write $\tilde{V}$ in terms of $\tilde{U}$

$$\tilde{V}(k,y)=\int_0^y \tilde{V}_y(k,\eta)d\eta=-2\pi ki\int_0^y \tilde{U}(k,\eta)d\eta. \quad (5.3.40)$$

Introducing (5.3.40) in (5.3.38), and simplifying the resulting double integral by changing the order of integration, we reduce (5.3.38) to the following autonomous equation that governs the observer error system

$$\begin{aligned}\tilde{U}_t &= \frac{1}{Re}\left(-4\pi^2k^2\tilde{U}+\tilde{U}_{yy}\right)+8i\pi ky(y-1)\tilde{U}\\ &\quad +8i\int_0^y \{\pi k(2y-1)-2\sinh\left(2\pi k(y-\eta)\right)\\ &\quad -2\pi k(2\eta-1)\cosh\left(2\pi k(y-\eta)\right)\}u(k,\eta)d\eta+l(k,y,0)\tilde{U}_y(k,0). && (5.3.41)\end{aligned}$$

Defining for notational convenience

$$\begin{aligned}\epsilon &= \frac{1}{Re}, && (5.3.42)\\ \phi(k,y) &= 8\pi iky(y-1), && (5.3.43)\end{aligned}$$

we can write (5.3.41) as

$$\begin{aligned}\tilde{U}_t &= \epsilon\left(-4\pi^2k^2\tilde{U}+\tilde{U}_{yy}\right)+\phi(k,y)\tilde{U}+\int_0^y f(k,y,\eta)u(k,\eta)d\eta\\ &\quad +l(k,y,0)\tilde{U}_y(k,0), && (5.3.44)\end{aligned}$$

where f was defined in (5.2.14). For showing error convergence, we need to prove convegence of $\tilde{U}$ to the origin. We design the gain $l(k, y, 0)$, using the backstepping observer design technique for parabolic PDEs [102]. The idea of the method is to transform (5.3.44), for $m \leq |k| \leq M$, into the family of heat equations (parametrized by k)

$$\alpha_t = \epsilon\left(-4\pi^2 k^2 \alpha + \alpha_{yy}\right) \tag{5.3.45}$$

$$\alpha(k,0) = 0 \tag{5.3.46}$$

$$\alpha(k,1) = 0\,, \tag{5.3.47}$$

where

$$\tilde{U} = \alpha - \int_0^y l(k,y,\eta)\alpha(t,k,\eta)d\eta \tag{5.3.48}$$

is the backstepping transformation as defined in [102]. The kernel l is found to verify the following equation

$$\epsilon l_{\eta\eta} = \epsilon l_{yy} + \phi(k,y)l(k,y,\eta) - f(k,y,\eta) + \int_\eta^y f(k,y,\xi)l(k,\xi,\eta)d\xi, \tag{5.3.49}$$

a hyperbolic partial integro-differential equation in the region $\mathcal{T}$ with boundary conditions

$$l(k,y,y) = \frac{2}{\epsilon}\int_y^1 \phi(k,\eta)d\eta, \tag{5.3.50}$$

$$l(k,1,\eta) = 0. \tag{5.3.51}$$

We have the following result regarding (5.3.49)–(5.3.51).

Proposition 5.3. *Consider equation (5.3.49) in the domain $(k, y, \eta) \in \mathbb{C} \times \mathcal{T}$ with boundary conditions (5.3.50)–(5.3.51). There is a solution l, given by (5.2.11)–(5.2.13), such that l belongs to $\mathcal{C}^2(\mathcal{T})$. Moreover l as a complex-valued function of k is analytic in the annulus $m < |k| < M$.*

Proof. Following [102], (5.3.49)–(5.3.51) can be transformed into an equation analogous to (4.5.82)–(4.5.84). Then, applying Proposition 4.8, the result follows. □

Once the kernel l is found, the gain that appears in (5.3.39) is explicitly known. Since (5.3.45)–(5.3.48) is analogous to (4.5.77)–(4.5.80), by the same arguments of Sections 4.5–4.7, exponential stability in L^2, H^1 and H^2 norms of $\tilde{U}$ and $\tilde{V}$ follow for all $m \leq |k| \leq M$.

5.3.2 Unobserved wave number analysis

When $|k| < m$ or $|k| > M$, the observer error linearization verifies the following equations

$$\tilde{U}_t = \frac{1}{Re}\left(-4\pi^2k^2\tilde{U} + \tilde{U}_{yy}\right) - 2\pi k i\tilde{P} + 8i\pi ky(y-1)\tilde{U} + (2y-1)\tilde{V}, \quad (5.3.52)$$

$$\tilde{V}_t = \frac{1}{Re}\left(-4\pi^2k^2\tilde{V} + \tilde{V}_{yy}\right) - \tilde{P}_y + 8i\pi ky(y-1)\tilde{V}, \quad (5.3.53)$$

the continuity equation (5.3.33) and boundary conditions (5.3.31)–(5.3.31). These are just the linearized, uncontrolled Navier-Stokes equations that were studied in Section 4.5.2. Then, following exactly the same arguments of Sections 4.5–4.7 for the uncontrolled Navier-Stokes equations, it follows that for $m = \frac{1}{32\pi Re}$ and $M = \frac{1}{\pi}\sqrt{\frac{Re}{2}}$ we get exponential stability of the unobserved wave number range in the L^2, H^1 and H^2 norms.

5.3.3 Analysis for the entire wave number range

The analysis sketched in the previous section can be combined for all wave numbers, to prove the following result.

Theorem 5.4. *Consider the (U, V) system (4.2.1)–(4.2.3), with boundary conditions (4.2.4), and the $(\hat{U}, \hat{V})$ system (5.2.1)–(5.2.3) with boundary conditions (5.2.4), and suppose that both are well posed in $L^2((0,\infty), H^2(\Omega))$. Consider now the observer error system $(\tilde{U}, \tilde{V})$. There exists positive constants C_1 and C_2 such that, if the L^2 norms of the initial conditions for $\tilde{U}$ and $\tilde{V}$ are less than C_1, i.e.*

$$\int_0^1 \int_{-\infty}^{\infty} \left(\tilde{U}^2(0,x,y) + \tilde{V}^2(0,x,y)\right) dxdy < C_1, \quad (5.3.54)$$

and if the turbulent kinetic energy of U and V (defined as the L^2 norm of the fluctuation with respect to the Pouisseuille equilibrium profile) is less than C_2 for all time, i.e. $\forall t \geq 0$,

$$\int_0^1 \int_{-\infty}^{\infty} \left(u^2(t,x,y) + V^2(t,x,y)\right) dxdy < C_2, \tag{5.3.55}$$

then the L^2 norms of $\tilde{U}$, $\tilde{V}$ converge to zero:

$$\lim_{t\to\infty} \int_0^1 \int_{-\infty}^{\infty} \left(\tilde{U}^2(t,x,y) + \tilde{V}^2(t,x,y)\right) dxdy = 0. \tag{5.3.56}$$

Proof. Exponential stability in the L^2 norm follows for the linearized $(\tilde{U}, \tilde{V})$ system from the analysis of Sections 5.3.1–5.3.2. Hence local L^2 exponential stability follows for the nonlinear system (5.3.21)–(5.3.22). We set C_1 and C_2 in conditions (5.3.54)–(5.3.55) small enough to guarantee that the nonlinear system is "close" enough to the linearized system (in the L^2 sense) so that the local exponential stability property holds for all times. $\square$

Remark 5.5. Following [32], we may consider the *mean turbulent profile* instead of considering the exact *laminar* equilibrium profile. This amounts to changing U^e in (5.3.21)–(5.3.22) and following the same steps as in Sections 5.3.1–5.3.2 for the new observer error system. Hence, the observer gains and cutoff wave number M and m will change (but only quantitatively) for the turbulent mean profile. Then Theorem 5.4 still holds and guarantees convergence of estimates under the same assumptions, meaning now that the state has to stay close enough to the mean turbulent profile at all times.

Remark 5.6. The meaning of this theorem is that, for a fully developed channel flow (whether laminar or turbulent), with a Reynolds number possibly above the critical value (the boundary of linear stability) but not too far above it, the observer is guaranteed to be convergent to the real velocity and pressure field, provided its initial estimates are not too far from the actual initial profile.

Remark 5.7. We have assumed the well-posedness of the nonlinear Navier-Stokes system for Theorem 5.4, as a proof is beyond the scope of this dissertation. For the linearized case, assumptions (5.3.54)–(5.3.55) can be dropped and, under certain compatibility conditions on the initial conditions of both the observer and the plant, well-posedness follows as in Section 4.8.

5.4 An Output Feedback Stabilizing Controller

We combine the result of Chapter 4 and the observer of Section 5.2 to obtain an output feedback controller for the linearized Navier-Stokes controlled system (4.2.10)–(4.2.18). The expression of the control laws are as follows

$$\begin{aligned} U_c(t,x) &= \int_0^1 \int_{-\infty}^{\infty} Q_u(x-\xi,\eta)\hat{u}(t,\xi,\eta)d\xi d\eta, && (5.4.57) \\ V_c(t,x) &= h(t,x), && (5.4.58) \end{aligned}$$

where h verifies the equation

$$h_t = h_{xx} + g(t,x), \tag{5.4.59}$$

where

$$\begin{aligned} g \;=\; & \int_0^1 \int_{-\infty}^{\infty} Q_V(x-\xi,\eta)\hat{V}(t,\xi,\eta)d\xi d\eta \\ & + \int_{-\infty}^{\infty} Q_0(x-\xi)\left(\hat{u}_y(t,\xi,0) - \hat{u}_y(t,\xi,1)\right)d\xi, \qquad (5.4.60) \end{aligned}$$

with Q_u, Q_V and Q_0 as in (4.3.28)–(4.3.30) and where $(\hat{V},\hat{u})$ in (5.4.57)–(5.4.60) are obtained from

$$\begin{aligned} \hat{u}_t \;=\; & \frac{1}{Re}\left(\hat{u}_{xx} + \hat{u}_{yy}\right) - \hat{p}_x + 4y(y-1)\hat{u}_x + 4(2y-1)\hat{V} \\ & + \int_{-\infty}^{\infty} Q_1(x-\xi,y)(u_y(\xi,0) - \hat{u}_y(\xi,0))d\xi \\ & + \int_{-\infty}^{\infty} Q_2(x-\xi,y)\left(p(\xi,0) - \hat{p}(\xi,0)\right)d\xi, \qquad (5.4.61) \\ \hat{V}_t \;=\; & \frac{1}{Re}\left(\hat{V}_{xx} + \hat{V}_{yy}\right) - \hat{p}_y + 4y(y-1)\hat{V}_x \\ & + \int_{-\infty}^{\infty} Q_3(x-\xi,y)\left(u_y(\xi,0) - \hat{u}_y(\xi,0)\right)d\xi \\ & + \int_{-\infty}^{\infty} Q_4(x-\xi,y)\left(p(\xi,0) - \hat{p}(\xi,0)\right)d\xi, \qquad (5.4.62) \end{aligned}$$

with Q_1, Q_2, Q_3 and Q_4 as in (5.2.5)–(5.2.8), equation

$$\hat{u}_x + \hat{V}_y = 0, \tag{5.4.63}$$

and boundary conditions

$$\hat{u}(t,x,0) = \hat{V}(t,x,0) = 0, \tag{5.4.64}$$

$$\hat{u}(t,x,1) = U_c, \tag{5.4.65}$$

$$\hat{V}(t,x,1) = V_c. \tag{5.4.66}$$

Equations (5.4.66)–(5.4.57) are the complete statement of a dynamic controller that guarantees the following result.

Theorem 5.8. *Consider the (u,V) system (4.2.10)–(4.2.18) and the $(\hat{u},\hat{V})$ system (5.4.61)–(5.4.66), with feedback laws (5.4.57)–(5.4.60), and assume both are well-posed in the $L^2\left((0,\infty),H^2(\Omega)\right)$ space. Then, the equilibrium $u(x,y) \equiv V(x,y) \equiv \hat{u}(x,y) \equiv \hat{V}(x,y) \equiv 0$ is exponentially stable in the L^2, H^1 and H^2 norms.*

Proof. Since the plant is linearized, the proof is standard and follows from the stabilizing properties of the full state controller and the observer convergence result. We sketch the details. First, we express the plant in $(\tilde{U},\tilde{V},\hat{u},\hat{V})$ coordinates; since the $(\tilde{U},\tilde{V})$ verifies (5.3.29)–(5.3.33), the proof of Section 5.3 applies and we get exponential stability for $(\tilde{U},\tilde{V})$ in the L^2, H^1 and H^2 norms (without the additional conditions of Theorem 5.4, because the $(\tilde{U},\tilde{V})$ is already linearized in this case). Then, the $(\hat{u},\hat{V})$ system is like the (u,V) system in (4.2.10)–(4.2.18) but with additional, smooth (see Remark 5.2) forcing terms, as stated in Remark 5.1, that exponentially decay. Hence from the proof of Theorem 4.3, we get exponential stability for $(\hat{u},\hat{V})$. $\square$

Remark 5.9. For simplicity we have skipped the statement of explicit solutions and the proof of well-posedness, which would follow as in Section 4.8. For the uncontrolled/unobserved wave numbers the system $(\tilde{U},\tilde{V},\hat{u},\hat{V})$ is decomposed into two well-posed, uncoupled Navier-Stokes channel flow systems, while for controlled/observed wave numbers the system $(\tilde{U}, \tilde{V}, \hat{u}, \hat{V})$ is mapped to two heat equations which are well-posed, given certain compatibility conditions (which are rather involved for this case and whose statement we skip). Hence, well-posedness and explicit solutions follows.

This chapter is a partial reprint of the material as it appears in
R. Vazquez and M. Krstic, "A closed-form observer for the channel flow Navier-Stokes system," *Proc. of the 2005 CDC*, Sevilla, Spain, 2005.
The dissertation author was the primary author and the coauthor listed in this publication directed and supervised the research, which is the basis for this chapter.

Chapter 6

Boundary Stabilization of 3-D Magnetohydrodynamic Channel Flow

6.1 Introduction

In this chapter we consider an incompressible 3-D magnetohydrodynamic (MHD) channel flow, also known as the Hartmann flow, a benchmark model for applications such as cooling systems (computer systems, fusion reactors), hypersonic flight and propulsion. In this flow, an electrically conducting fluid moves between parallel plates and is affected by an imposed transverse magnetic field. When a conducting fluid moves in the presence of a magnetic field, it produces an electric field due to charge separation and subsequently an electric current. The interaction between this created electric current and the imposed magnetic field originates a body force, called the Lorentz force, which acts on the fluid itself. The velocity and electromagnetic fields are mathematically described by the MHD equations [85], which are the Navier-Stokes equation coupled with the Maxwell equations.

The area of conducting fluids moving in magnetic fields, even though rich in applications, has only been recently considered and is under development. There are some recent results in stabilization of magnetohydrodynamic flows, for instance using nonlinear model reduction [8], open-loop control [20] and optimal control [42]. Applications include, for instance, drag reduction [86], or mixing enhancement for cooling systems [94]. Some experimental results are available as well, showing that control of such flows is technologically feasible; actuators consist of magnets and electrodes [23, 86, 109]. Mathematical studies of controllability of magnetohydrodynamic flows have been done, though they do not provide explicit controllers [14, 106].

Our controller is designed for the continuum MHD model and is designed similarly to the 2-D channel flow controller of Chapter 4. Following Chapter 4, control synthesis is done in the wave number space after application of a Fourier transform in the spatially invariant directions (x and z). Large wave numbers are found to be stable and left uncontrolled whereas for small wave numbers control is used. Writing the velocity field in some appropriate coordinates, the resulting system is very similar to the Orr-Sommerfeld-Squire system of PDE's for non-conducting fluids and presents the same difficulties (non-normality leading to a large transient growth mechanism [66, 95]). Thus, applying the same ideas as in [34], we use backstepping not only to guarantee stability but also to decouple the system in order to prevent transients. The control gains are computed solving linear hyperbolic PDEs—a much simpler task than, for instance, solving nonlinear Riccati equations. Actuation of velocity and electric potential is done at only one of the channel walls. Full state knowledge is assumed, but the controller can be combined with the dual observer for 3-D MHD channel flow that we present in Chapter 7 to obtain an output feedback controller. For zero magnetic field or non-conducting fluids, the problem reduces to the 3-D Navier-Stokes Channel flow and the control design still holds.

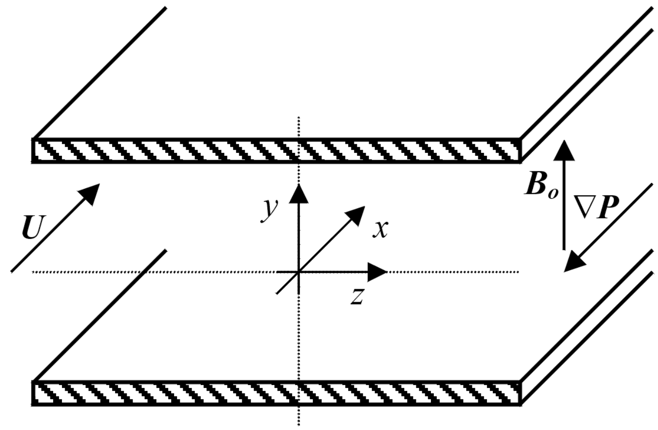

Figure 6.1: Hartmann Flow.

6.2 Model

We consider a 3-D MHD channel flow, also called Hartmann flow [60]. This flow consists of an incompressible conducting fluid enclosed between two parallel plates, separated by a distance L_p, under the influence of a pressure gradient ∇P parallel to the walls and a magnetic field B_0 normal to the walls, as shown in Figure 6.1. Under the assumption of a very small magnetic Reynolds number

$$Re_M = \mu_m \sigma U_c L_p \ll 1, \tag{6.2.1}$$

where μ_m is the magnetic permeability of the fluid, σ the conductivity of the fluid, and U_c the reference velocity (maximum velocity of the Hartmann equilibrium profile), the dynamics of the magnetic field can be neglected and the dimensionless velocity and electric potential field is governed by the inductionless MHD equations [79].

We set nondimensional coordinates (x, y, z), where x is the streamwise direction (parallel to the pressure gradient), y the wall normal direction (parallel to the magnetic field) and z the spanwise direction, so that $(x, y, z) \in (-\infty, \infty) \times [0, 1] \times (-\infty, \infty)$. The governing equations are

$$U_t = \frac{\triangle U}{Re} - UU_x - VU_y - WU_z - P_x + N\phi_z$$

$$
\begin{aligned}
& -NU\,, && (6.2.2)\\
V_t &= \frac{\triangle V}{Re} - UV_x - VV_y - WV_z - P_y\,, && (6.2.3)\\
W_t &= \frac{\triangle W}{Re} - UW_x - VW_y - WW_z - P_z - N\phi_x \\
& -NW\,, && (6.2.4)\\
\triangle\phi &= U_z - W_x\,, && (6.2.5)
\end{aligned}
$$

where U, V and W denote, respectively, the streamwise, wall-normal and spanwise velocities, P the pressure, ϕ the electric potential, $Re = \frac{U_c L_p}{\nu}$ is the Reynolds number and $N = \frac{\sigma L_p B_0^2}{\rho U_c}$ the Stuart number. Since the fluid is incompressible, the continuity equation is verified

$$U_x + V_y + W_z = 0\,. \tag{6.2.6}$$

The boundary conditions for the velocity field are

$$
\begin{aligned}
U(t,x,0,z) &= U(t,x,1,z) = U_c(t,x,z), && (6.2.7)\\
V(t,x,0,z) &= V(t,x,1,z) = V_c(t,x,z), && (6.2.8)\\
W(t,x,0,z) &= W(t,x,1,z) = W_c(t,x,z), && (6.2.9)
\end{aligned}
$$

where $U_c(t,x,z)$, $V_c(t,x,z)$ and $W_c(t,x,z)$ denote, respectively, the actuators for streamwise, wall-normal and spanwise velocity in the upper wall. Assuming perfectly conducting walls, the electric potential must verify

$$\phi(t,x,0,z) = 0,\ \phi(t,x,1,z) = \Phi_c(t,x,z), \tag{6.2.10}$$

where $\Phi_c(t,x,z)$ is the imposed potential (electromagnetic actuation) in the upper wall. The nondimensional electric current, $j(t,x,y,z)$, is a vector field that can be computed from the electric potential and velocity fields as follows:

$$
\begin{aligned}
j^x(t,x,y,z) &= -\phi_x - W, && (6.2.11)\\
j^y(t,x,y,z) &= -\phi_y, && (6.2.12)\\
j^z(t,x,y,z) &= -\phi_z + U, && (6.2.13)
\end{aligned}
$$

where j^x, j^y, and j^z denote the components of j.

We assume that all actuators can be independently actuated for every $(x, z) \in \mathbb{R}^2$. Note that no actuation is done inside the channel or at the bottom wall.

6.3 Equilibrium profile

The equilibrium profile for system (6.2.2)–(6.2.5) with no control can be calculated following the same steps that yield the Poiseuille solution for Navier-Stokes channel flow. Thus, we assume a steady solution with only one nonzero nondimensional velocity component, U^e, that depends only on the y coordinate. Substituting U^e in equation (6.2.2), one finds that it verifies the following equation,

$$0 = \frac{U^e_{yy}(y)}{Re} - P^e_x - NU^e(y)\,, \tag{6.3.14}$$

whose nondimensional solution is, setting P^e such that the maximum velocity (centerline velocity) is unity,

$$\begin{aligned}
U^e(y) &= \frac{\sinh(H(1-y)) - \sinh H + \sinh(Hy)}{2\sinh H/2 - \sinh H}, && (6.3.15)\\
V^e &= W^e = \phi^e = 0, && (6.3.16)\\
P^e &= \frac{N \sinh H}{2\sinh H/2 - \sinh H} x, && (6.3.17)\\
j^{xe} &= j^{ye} = 0, j^{ze} = U^e(y). && (6.3.18)
\end{aligned}$$

where $H = \sqrt{ReN} = B_0 L_p \sqrt{\frac{\sigma}{\rho\nu}}$ is the Hartmann number. In Fig. 6.3(left) we show $U^e(y)$ for different values of H. Since the equilibrium profile is nondimensional the centerline velocity is always 1. For $H = 0$ the classic parabolic Poiseuille profile is recovered. In Fig. 6.3(right) we show $U^e_y(y)$, proportional to shear stress, whose maximum is reached at the boundaries and grows with H.

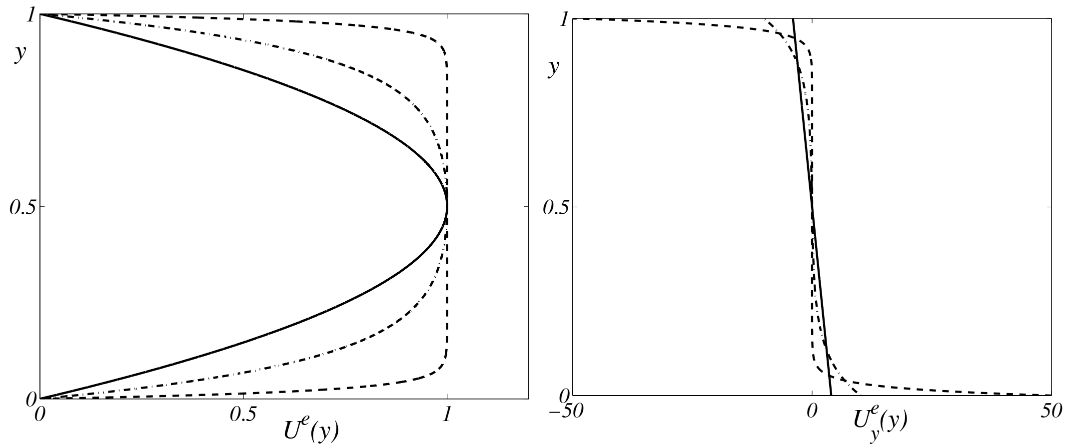

Figure 6.2: Streamwise equilibrium velocity $U^e(y)$ (left) and $U^e_y(y)$ (right), for different values of H. Solid, $H = 0$; dash-dotted, $H = 10$; dashed, $H = 50$.

6.4 The Plant in Wave Number Space

Define the fluctuation variables

$$\begin{aligned} u(t,x,y) &= U(t,x,y) - U^e(y), && (6.4.19) \\ p(t,x,y) &= P(t,x,y) - P^e(y), && (6.4.20) \end{aligned}$$

where $U^e(y)$ and $P^e(y)$ are, respectively, the equilibrium velocity and pressure given in (6.3.15) and (6.3.17). The linearization of (6.2.2)–(6.2.4) around the Hartmann equilibrium profile, written in the fluctuation variables (u, V, W, p, ϕ), is

$$\begin{aligned} u_t &= \frac{\triangle u}{Re} - U^e(y)u_x - U^e_y(y)V - p_x + N\phi_z - Nu\,, && (6.4.21) \\ V_t &= \frac{\triangle V}{Re} - U^e(y)V_x - p_y\,, && (6.4.22) \\ W_t &= \frac{\triangle W}{Re} - U^e(y)W_x - p_z - N\phi_x - NW\,. && (6.4.23) \end{aligned}$$

The equation for the potential is

$$\triangle\phi = u_z - W_x\,, \tag{6.4.24}$$

and the fluctuation velocity field verifies the continuity equation,

$$u_x + V_y + W_z = 0\,, \tag{6.4.25}$$

and the following boundary conditions

$$\begin{aligned} u(t,x,0,z) &= W(t,x,0,z) = V(t,x,0,z) = 0, && (6.4.26)\\ u(t,x,1,z) &= U_c(t,x,z), && (6.4.27)\\ V(t,x,1,z) &= V_c(t,x,z), && (6.4.28)\\ W(t,x,1,z) &= W_c(t,x,z), && (6.4.29)\\ \phi(t,x,0,z) &= 0,\ \phi(t,x,1,z) = \Phi_c(t,x,z). && (6.4.30)\end{aligned}$$

To guarantee stability, our design task is to design feedback laws U_c, V_c, W_c and Φ_c, so that the origin of the velocity fluctuation system is exponentially stable. Full state knowledge is assumed.

Since the plant is linear and spatially invariant [12], we use a Fourier transform in the x and z coordinates (the spatially invariant directions). The transform pair (direct and inverse transform) is defined as

$$f(k_x,y,k_z)=\int_{-\infty}^{\infty}\int_{-\infty}^{\infty} f(x,y,z)\mathrm{e}^{-2\pi i(k_x x+k_z z)}dzdx, \qquad (6.4.31)$$

$$f(x,y,z)=\int_{-\infty}^{\infty}\int_{-\infty}^{\infty} f(k_x,y,k_z)\mathrm{e}^{2\pi i(k_x x+k_z z)}dk_zdk_x. \qquad (6.4.32)$$

As in Chapter 4, we use the same symbol f for both the original $f(x,y,z)$ and the image $f(k_x,y,k_z)$. As k in Chapter 4, k_x and k_z are referred to as the "wave numbers."

The plant equations in wave number space are

$$\begin{aligned} u_t &= \frac{-\alpha^2 u + u_{yy}}{Re} - \beta u - U_y^e V - 2\pi k_x ip + 2\pi k_z iN\phi - Nu, && (6.4.33)\\ V_t &= \frac{-\alpha^2 V + V_{yy}}{Re} - \beta V - p_y, && (6.4.34)\\ W_t &= \frac{-\alpha^2 W + W_{yy}}{Re} - \beta W - 2\pi k_z ip - 2\pi k_x iN\phi - NW && (6.4.35)\end{aligned}$$

where $\alpha^2 = 4\pi^2(k_x^2 + k_z^2)$ and $\beta = 2\pi i k_x U^e$.

The continuity equation in wave number space is expressed as

$$2\pi i k_x u + V_y + 2\pi k_z W = 0, \qquad (6.4.36)$$

and the equation for the potential is

$$-\alpha^2\phi + \phi_{yy} = 2\pi i\left(k_z u - k_x W\right). \tag{6.4.37}$$

The boundary conditions are

$$u(t,k_x,0,k_z) = W(t,k_x,0,k_z) = V(t,k_x,0,k_z) = 0, \tag{6.4.38}$$

$$u(t,k_x,1,k_z) = U_c(t,k_x,k_z), \tag{6.4.39}$$

$$V(t,k_x,1,k_z) = V_c(t,k_x,k_z), \tag{6.4.40}$$

$$W(t,k_x,1,k_z) = W_c(t,k_x,k_z), \tag{6.4.41}$$

$$\phi(t,k_x,0,k_z) = 0,\ \phi(t,k_x,1,k_z) = \Phi_c(t,k_x,k_z). \tag{6.4.42}$$

6.5 Control Design

We design the controller in wave number space. Note that (6.4.33)–(6.4.42) are uncoupled for each wave number. Therefore, as in Chapter 4 and [34], the range $k_x^2 + k_z^2 \leq M^2$, which we refer to as the *controlled* wave number range, and the range $k_x^2 + k_z^2 > M^2$, the *uncontrolled* wave number range, can be studied separately. If stability for all wave numbers is established, stability in physical space follows as in Section 4.6.3. The number M, which will be computed in Section 6.5.2, is a parameter that ensures stability for uncontrolled wave numbers.

As in (4.3.31), we define χ, a *truncating* function, as

$$\chi(k_x,k_z) = \begin{cases} 1, & k_x^2 + k_z^2 \leq M^2, \\ 0, & \text{otherwise}. \end{cases} \tag{6.5.43}$$

Then, we reflect that we don't use control for large wave numbers by setting

$$\begin{pmatrix} U_c(t,x,z) \\ V_c(t,x,z) \\ W_c(t,x,z) \\ \Phi_c(t,x,z) \end{pmatrix} = \int_{-\infty}^{\infty}\int_{-\infty}^{\infty} \chi(k_x,k_z) \begin{pmatrix} U_c(t,k_x,k_z) \\ V_c(t,k_x,k_z) \\ W_c(t,k_x,k_z) \\ \Phi_c(t,k_x,k_z) \end{pmatrix} \times \mathrm{e}^{2\pi i(k_x x + k_z z)} dk_z dk_x. \tag{6.5.44}$$

Next we design stabilizing control laws for small wave numbers and analyze uncontrolled wave numbers.

6.5.1 Controlled wave number analysis

Consider $k_x^2 + k_z^2 \leq M^2$. Then $\chi = 1$, so there is control. Using the continuity equation (6.4.36) and taking divergence of (6.4.33)–(6.4.35), a Poisson equation for the pressure is derived,

$$-\alpha^2 p + p_{yy} = -4\pi k_x i U_y^e(y) V + N V_y. \tag{6.5.45}$$

Evaluating equation (6.4.34) at $y = 0$ one finds that

$$\begin{aligned} p_y(k_x, 0, k_z) &= \frac{V_{yy}(k_x, 0, k_z)}{Re} \\ &= -2\pi i \frac{k_x u_{y0} + k_z W_{y0}}{Re}, \end{aligned} \tag{6.5.46}$$

where we use (6.4.36) for expressing V_{yy} at the bottom in terms of $u_{y0} = u_y(k_x, 0, k_z)$ and $W_{y0} = W_y(k_x, 0, k_z)$. Similarly, evaluating equation (6.4.34) at $y = 1$ we get

$$\begin{aligned} p_y(k_x, 1, k_z) &= \frac{V_{yy}(k_x, 1, k_z)}{Re} - (V_c)_t - \alpha^2 \frac{V_c}{Re} \\ &= -2\pi i \frac{k_x u_{y1} + k_z W_{y1}}{Re} - (V_c)_t - \alpha^2 \frac{V_c}{Re}, \end{aligned} \tag{6.5.47}$$

where we use (6.4.36) for expressing V_{yy} at the top wall in terms of $u_{y1} = u_y(k_x, 1, k_z)$ and $W_{y1} = W_y(k_x, 1, k_z)$ and the controller V_c.

Equation (6.5.45) can be solved in terms of integrals of the state and the boundary terms appearing in (6.5.46) and (6.5.47).

$$\begin{aligned} p \;=\; & -\frac{4\pi k_x i}{\alpha} \int_0^y U_y^e(\eta) \sinh(\alpha(y-\eta)) V(k_x, \eta, k_z) d\eta \\ & + N \int_0^y \frac{\sinh(\alpha(y-\eta))}{\alpha} V_y(k_x, \eta, k_z) d\eta + 2\pi i \frac{\cosh(\alpha(1-y))}{\alpha \sinh \alpha} \frac{k_x u_{y0} + k_z W_{y0}}{Re} \\ & + \frac{4\pi k_x i \cosh(\alpha y)}{\alpha \sinh \alpha} \int_0^1 U_y^e(\eta) \cosh(\alpha(1-\eta)) V(k_x, \eta, k_z) d\eta \\ & - N \frac{\cosh(\alpha y)}{\alpha \sinh \alpha} \int_0^1 \cosh(\alpha(1-\eta)) V_y(k_x, \eta, k_z) d\eta \\ & - 2\pi i \frac{\cosh(\alpha y)}{\alpha \sinh \alpha} \frac{k_x u_{y1} + k_z W_{y1}}{Re} - \frac{\cosh(\alpha y)}{\alpha \sinh \alpha} \left((V_c)_t + \alpha^2 \frac{V_c}{Re} \right). \end{aligned} \tag{6.5.48}$$

We proceed as in Section 4.5.1 and use the controller V_c, which appears *inside* the pressure solution (6.5.48), to make the pressure strict-feedback (spatially causal in y), which is a necessary structure for the application of a backstepping boundary controller [101]. Since the first two lines in (6.5.48) are already spatially causal, we need to cancel the third, fourth, and fifth lines of (6.5.48). Set

$$\begin{aligned}(V_c)_t &= \alpha^2\frac{V_c}{Re} + 2\pi i\frac{k_x(u_{y0}-u_{y1}) + k_z(W_{y0}-W_{y1})}{Re}\\ &\quad +4\pi k_x i\int_0^1 U_y^e(\eta)\cosh\left(\alpha(1-\eta)\right)V(k_x,\eta,k_z)d\eta\\ &\quad -N\int_0^1 \cosh\left(\alpha(1-\eta)\right)V_y(k_x,\eta,k_z)d\eta, \end{aligned} \tag{6.5.49}$$

which can be written as

$$\begin{aligned}(V_c)_t &= \alpha^2\frac{V_c}{Re} + 2\pi i\frac{k_x(u_{y0}-u_{y1}) + k_z(W_{y0}-W_{y1})}{Re}\\ &\quad -NV_c + \int_0^1 \cosh\left(\alpha(1-\eta)\right)V(k_x,\eta,k_z)\left(N+4\pi k_x i U_y^e(\eta)\right)d\eta. \end{aligned} \tag{6.5.50}$$

Then, the pressure is written in terms of a strict-feedback integral of the state V and the boundary terms u_{y0}, W_{y0} (proportional to the skin friction at the bottom) as follows

$$\begin{aligned} p &= -\frac{4\pi k_x i}{\alpha}\int_0^y U_y^e(\eta)\sinh\left(\alpha(y-\eta)\right)V(k_x,\eta,k_z)d\eta\\ &\quad -2\pi i\frac{\cosh(\alpha y)-\cosh\left(\alpha(1-y)\right)}{Re\alpha\sinh\alpha}\left(k_x u_{y0}+k_z W_{y0}\right)\\ &\quad +N\int_0^y\frac{\sinh\left(\alpha(y-\eta)\right)}{\alpha}V_y(k_x,\eta,k_z)d\eta. \end{aligned} \tag{6.5.51}$$

Similarly, solving for ϕ in terms of the control Φ_c and the right hand side of its Poisson equation (6.4.37),

$$\begin{aligned} \phi &= \frac{2\pi i}{\alpha}\int_0^y \sinh\left(\alpha(y-\eta)\right)\left(k_z u(k_x,\eta,k_z) - k_x W(k_x,\eta,k_z)\right)d\eta\\ &\quad -\frac{2\pi i\sinh(\alpha y)}{\alpha\sinh\alpha}\int_0^1 \sinh\left(\alpha(1-\eta)\right)\left(k_z u(k_x,\eta,k_z) - k_x W(k_x,\eta,k_z)\right)d\eta\\ &\quad +\frac{\sinh(\alpha y)}{\sinh\alpha}\Phi_c(k_x,k_y). \end{aligned} \tag{6.5.52}$$

As in the pressure equation (6.5.48), an actuator (Φ_c in this case) appears inside the solution for the potential. The second line of (6.5.52) is a non-strict-feedback integral and needs to be cancelled to apply the backstepping method. For this we use Φ_c by setting

$$\Phi_c(k_x, k_y) = \frac{2\pi i}{\alpha} \int_0^1 \sinh\left(\alpha(1-\eta)\right)\left(k_z u(k_x,\eta,k_z) - k_x W(k_x,\eta,k_z)\right) d\eta. \quad (6.5.53)$$

Then the potential can be expressed as a strict-feedback integral of the states u and W as follows

$$\phi = \frac{2\pi i}{\alpha} \int_0^y \sinh\left(\alpha(y-\eta)\right)\left(k_z u(k_x,\eta,k_z) - k_x W(k_x,\eta,k_z)\right) d\eta. \quad (6.5.54)$$

Introducing the expressions (6.5.51) and (6.5.54) in (6.4.33) and (6.4.35), we get

$$\begin{aligned}
u_t &= \frac{-\alpha^2 u + u_{yy}}{Re} - \beta u - U_y^e(y)V - Nu - 4\pi^2 k_x \\
&\quad \times \frac{\cosh(\alpha y) - \cosh(\alpha(1-y))}{Re\alpha \sinh\alpha}\left(k_x u_{y0} + k_z W_{y0}\right) \\
&\quad - \frac{8\pi k_x^2}{\alpha}\int_0^y U_y^e(\eta)\sinh\left(\alpha(y-\eta)\right)V(k_x,\eta,k_z)d\eta \\
&\quad - 2\pi i k_x N \int_0^y \frac{\sinh\left(\alpha(y-\eta)\right)}{\alpha} V_y(k_x,\eta,k_z)d\eta \\
&\quad - \frac{4\pi^2 k_z N}{\alpha}\int_0^y \sinh\left(\alpha(y-\eta)\right)\left(k_z U(k_x,\eta,k_z) - k_x W(k_x,\eta,k_z)\right) d\eta, \quad (6.5.55) \\
W_t &= \frac{-\alpha^2 W + W_{yy}}{Re} - \beta W - NW - 4\pi^2 k_z \\
&\quad \times \frac{\cosh(\alpha y) - \cosh(\alpha(1-y))}{Re\alpha \sinh\alpha}\left(k_x u_{y0} + k_z W_{y0}\right) \\
&\quad - \frac{8\pi k_x k_z}{\alpha}\int_0^y U_y^e(\eta)\sinh\left(\alpha(y-\eta)\right)V(k_x,\eta,k_z)d\eta \\
&\quad - 2\pi i k_z N \int_0^y \frac{\sinh\left(\alpha(y-\eta)\right)}{\alpha} V_y(k_x,\eta,k_z)d\eta \\
&\quad + \frac{4\pi^2 k_x N}{\alpha}\int_0^y \sinh\left(\alpha(y-\eta)\right)\left(k_z U(k_x,\eta,k_z) - k_x W(k_x,\eta,k_z)\right) d\eta. \quad (6.5.56)
\end{aligned}$$

We have omitted the equation for V since, from (6.4.36) and using the fact that $V(k_x, 0, k_z) = 0$, V is computed as

$$V = -2\pi i \int_0^y \left(k_x U(k_x,\eta,k_z) + k_z W(k_x,\eta,k_z)\right) d\eta. \quad (6.5.57)$$

Now we use the following change of variables and its inverse,

$$Y = 2\pi i \left(k_x u + k_z W\right), \; \omega = 2\pi i \left(k_z u - k_x W\right), \tag{6.5.58}$$

$$u = \frac{2\pi i}{\alpha^2}\left(k_x Y + k_z \omega\right), \; W = \frac{2\pi i}{\alpha^2}\left(k_z Y - k_x \omega\right). \tag{6.5.59}$$

Defining $\epsilon = \frac{1}{Re}$ and the following functions

$$f = 4\pi i k_x \left\{ \frac{U_y^e}{2} + \int_\eta^y U_y^e(\sigma) \frac{\sinh\left(\alpha(y-\sigma)\right)}{\alpha} d\sigma \right\} + N\alpha \sinh\left(\alpha(y-\sigma)\right), \tag{6.5.60}$$

$$g = -\alpha \frac{\cosh\left(\alpha y\right) - \cosh\left(\alpha(1-y)\right)}{Re \sinh \alpha}, \tag{6.5.61}$$

$$h_1 = 2\pi i k_z U_y^e, \tag{6.5.62}$$

$$h_2 = -N\alpha \sinh\left(\alpha(y-\eta)\right), \tag{6.5.63}$$

equations (6.5.55)–(6.5.56) expressed in terms of Y and ω are

$$\begin{aligned} Y_t &= \epsilon\left(-\alpha^2 Y + Y_{yy}\right) - \beta Y - NY + gY_{y0} \\ &\quad + \int_0^y f(k_x, y, \eta, k_z) Y(k_x, \eta, k_z) d\eta, \end{aligned} \tag{6.5.64}$$

$$\begin{aligned} \omega_t &= \epsilon\left(-\alpha^2 \omega + \omega_{yy}\right) - \beta\omega - N\omega + h_1(y) \int_0^y Y(k_x, \eta, k_z) d\eta \\ &\quad + \int_0^y h_2(y, \eta) \omega(k_x, \eta, k_z) d\eta, \end{aligned} \tag{6.5.65}$$

where we have used the inverse change of variables (6.5.59) to express u_{y0} and W_{y0} in terms of $Y_{y0} = Y_y(k_x, 0, k_z)$ as follows

$$Y_{y0} = 2\pi i \left(k_x u_{y0} + k_z W_{y0}\right), \tag{6.5.66}$$

with boundary conditions

$$Y(t, k_x, 0, k_z) = \omega(t, k_x, 0, k_z) = 0, \tag{6.5.67}$$

$$Y(t, k_x, 1, k_z) = Y_c(t, k_x, k_z) \tag{6.5.68}$$

$$\omega(t, k_x, 1, k_z) = \omega_c(t, k_x, k_z), \tag{6.5.69}$$

where

$$Y_c = 2\pi i \left(k_x U_c + k_z W_c\right), \tag{6.5.70}$$

$$\omega_c = 2\pi i \left(k_z U_c - k_x W_c\right). \tag{6.5.71}$$

Equations (6.5.64)–(6.5.65) are a coupled, strict-feedback plant, with integral and reaction terms. As in [34], a variant of the design presented in [101] can be used to stabilize the system using a double backstepping transformation. The transformation maps, for each k_x and k_z, the variables (Y, ω) into the variables (Ψ, Ω), that verify the following family of heat equations (parameterized in k_x, k_z)

$$\Psi_t = \epsilon\left(-\alpha^2\Psi + \Psi_{yy}\right) - \beta\Psi - N\psi, \qquad (6.5.72)$$

$$\Omega_t = \epsilon\left(-\alpha^2\Omega + \Omega_{yy}\right) - \beta\Omega - N\Omega, \qquad (6.5.73)$$

with boundary conditions

$$\Psi(k_x, 0, k_z) = \Psi(k_x, 1, k_z) = 0, \qquad (6.5.74)$$

$$\Omega(k_x, 0, k_z) = \Omega(k_x, 1, k_z) = 0. \qquad (6.5.75)$$

The transformation is defined as follows,

$$\Psi = Y - \int_0^y K(k_x, y, \eta, k_z) Y(k_x, \eta, k_z) d\eta, \qquad (6.5.76)$$

$$\begin{aligned} \Omega = {} & \omega - \int_0^y \Gamma_1(k_x, y, \eta, k_z) Y(k_x, \eta, k_z) d\eta \\ & - \int_0^y \Gamma_2(k_x, y, \eta, k_z) \omega(k_x, \eta, k_z) d\eta. \end{aligned} \qquad (6.5.77)$$

As in Section 4.5.1 and following [34, 101], the functions $K(k_x, y, \eta, k_z)$, $\Gamma_1(k_x, y, \eta, k_z)$, and $\Gamma_2(k_x, y, \eta, k_z)$ are found as the solution of the following partial integro-differential equations,

$$\epsilon K_{yy} = \epsilon K_{\eta\eta} + (\beta(y) - \beta(\eta)) K - f + \int_\eta^y f(\eta, \xi) K(y, \xi) d\xi, \qquad (6.5.78)$$

$$\begin{aligned} \epsilon\Gamma_{1yy} = {} & \epsilon\Gamma_{1\eta\eta} + (\beta(y) - \beta(\eta)) \Gamma_1 - h_1 + \int_\eta^y \Gamma_2(y, \xi) h_1(\xi) d\xi \\ & + \int_\eta^y f(\eta, \xi) \Gamma_1(y, \xi) d\xi, \end{aligned} \qquad (6.5.79)$$

$$\epsilon\Gamma_{2yy} = \epsilon\Gamma_{2\eta\eta} + (\beta(y) - \beta(\eta)) \Gamma_2 - h_2 + \int_\eta^y h_2(\xi, \eta) \Gamma_2(y, \xi) d\xi. \qquad (6.5.80)$$

Equations (6.5.78)–(6.5.80) are hyperbolic partial integro-differential equation in the region $\mathcal{T} = \{(y,\eta) : 0 \leq y \leq 1, 0 \leq \eta \leq y\}$. Their boundary conditions are

$$
\begin{aligned}
K(y,y) &= -\frac{g(0)}{\epsilon}, && (6.5.81)\\
K(y,0) &= \frac{\int_0^y K(y,\eta)g(\eta)d\eta - g(y)}{\epsilon}, && (6.5.82)\\
\Gamma_1(y,y) &= 0, && (6.5.83)\\
\Gamma_1(y,0) &= \frac{\int_0^y \Gamma_1(y,\eta)g(\eta)d\eta}{\epsilon}, && (6.5.84)\\
\Gamma_2(y,y) &= 0,\ \Gamma_2(y,0) = 0. && (6.5.85)
\end{aligned}
$$

Remark 6.1. Equations (6.5.78)–(6.5.85) are well-posed and can be solved symbolically, by means of a successive approximation series, or numerically [34, 101]. Note that (6.5.78) and (6.5.80) are autonomous. Hence, one must solve first for $K(k_x, y, \eta, k_z)$ and $\Gamma_2(k_x, y, \eta, k_z)$. Then the solution for Γ_2 is plugged in Equation 6.5.79 which then can be solved for $\Gamma_1(k_x, y, \eta, k_z)$.

Control laws Y_c and W_c are found evaluating (6.5.76)–(6.5.77) at $y = 1$ and using (6.5.68)–(6.5.69) and (6.5.74)–(6.5.75), which yields

$$
\begin{aligned}
Y_c(t,k_x,k_z) &= \int_0^1 K(k_x,1,\eta,k_z)Y(k_x,\eta,k_z)d\eta, && (6.5.86)\\
\omega_c(t,k_x,k_z) &= \int_0^1 \Gamma_1(k_x,1,\eta,k_z)Y(k_x,\eta,k_z)d\eta \\
&\quad + \int_0^1 \Gamma_2(k_x,1,\eta,k_z)\omega(k_x,\eta,k_z)d\eta. && (6.5.87)
\end{aligned}
$$

Using (6.5.58)–(6.5.59) to write (6.5.86)–(6.5.87) in (u, W), we get

$$
\begin{aligned}
U_c &= \int_0^1 K^{Uu}(k_x,1,\eta,k_z)u(k_x,\eta,k_z)d\eta \\
&\quad + \int_0^1 K^{UW}(k_x,1,\eta,k_z)W(k_x,\eta,k_z)d\eta, && (6.5.88)\\
W_c &= \int_0^1 K^{Wu}(k_x,1,\eta,k_z)u(k_x,\eta,k_z)d\eta \\
&\quad + \int_0^1 K^{WW}(k_x,1,\eta,k_z)W(k_x,\eta,k_z)d\eta, && (6.5.89)
\end{aligned}
$$

where

$$\begin{pmatrix} K^{Uu} \\ K^{UW} \\ K^{Wu} \\ K^{WW} \end{pmatrix} = \mathbf{A} \begin{pmatrix} K(k_x, y, \eta, k_z) \\ \Gamma_1(k_x, y, \eta, k_z) \\ 0 \\ \Gamma_2(k_x, y, \eta, k_z) \end{pmatrix}, \tag{6.5.90}$$

and where the matrix $\mathbf{A}$ is defined as

$$\mathbf{A} = -\frac{4\pi^2}{\alpha^2} \begin{pmatrix} k_x^2 & k_x k_z & k_x k_z & k_z^2 \\ k_x k_z & k_z^2 & -k_x^2 & -k_x k_z \\ k_x k_z & -k_x^2 & k_z^2 & -k_x k_z \\ k_z^2 & -k_x k_z & -k_x k_z & k_x^2 \end{pmatrix}. \tag{6.5.91}$$

Using the same argument as in Section 4.5.1, stability in the controlled wave number range follows from stability of (6.5.72)–(6.5.73) and the invertibility of the transformation (6.5.76)–(6.5.77). We get the following result, whose proof we sketch (see [34] for more details).

Proposition 6.2. *For $k_x^2 + k_z^2 \leq M^2$, the equilibrium $u \equiv V \equiv W \equiv 0$ of system (6.4.33)–(6.4.42) with control laws (6.5.50), (6.5.53), (6.5.88)–(6.5.89) is exponentially stable in the L^2 norm, i.e.,*

$$\begin{aligned} &\int_0^1 \left(|u|^2 + |V|^2 + |W|^2\right)(t, k_x, y, k_z)dy \\ \leq\ & C_1 \mathrm{e}^{-2\epsilon t} \int_0^1 \left(|u|^2 + |V|^2 + |W|^2\right)(0, k_x, y, k_z)dy, \end{aligned} \tag{6.5.92}$$

where $C_1 \geq 0$.

Proof. From equations (6.5.72)–(6.5.73) we get, using a standard Lyapunov argument,

$$\begin{aligned} &\int_0^1 \left(|\Psi|^2 + |\Omega|^2\right)(t, k_x, y, k_z)dy \\ \leq\ & \mathrm{e}^{-2\epsilon t} \int_0^1 \left(|\Psi|^2 + |\Omega|^2\right)(0, k_x, y, k_z)dy, \end{aligned} \tag{6.5.93}$$

and then from the transformation (6.5.76)–(6.5.77) and its inverse (which is guaranteed to exist [101]), we get that

$$\begin{aligned} & \int_0^1 \left(|Y|^2 + |\omega|^2\right)(t, k_x, y, k_z)dy \\ \leq \; & C_0 \mathrm{e}^{-2\epsilon t} \int_0^1 \left(|Y|^2 + |\omega|^2\right)(0, k_x, y, k_z)dy, \end{aligned} \tag{6.5.94}$$

where $C_0 > 0$ is a constant depending on the kernels K, Γ_1 and Γ_2 and their inverses. Then writing (u, W) in terms of (Y, ω) and bounding the norm of V by the norm of Y (using $Y = -V_y$ and Poincare's inequality), the result follows. $\square$

6.5.2 Uncontrolled wave number analysis

When $k_x^2 + k_z^2 > M$, the plant verifies the following equations

$$u_t = \frac{-\alpha^2 u + u_{yy}}{Re} - \beta u - U_y^e(y)V - 2\pi k_x i p + 2\pi k_z i N\phi - Nu\,, \tag{6.5.95}$$

$$V_t = \frac{-\alpha^2 V + V_{yy}}{Re} - \beta V - p_y\,, \tag{6.5.96}$$

$$W_t = \frac{-\alpha^2 W + W_{yy}}{Re} - \beta W - 2\pi k_z i p - 2\pi k_x i N\phi - NW\,, \tag{6.5.97}$$

the Poisson equation for the potential

$$-\alpha^2 \phi + \phi_{yy} = 2\pi i \left(k_z u - k_x W\right) \tag{6.5.98}$$

the continuity equation

$$2\pi i k_x u + V_y + 2\pi k_z W = 0, \tag{6.5.99}$$

and Dirichlet boundary conditions

$$u(t, k_x, 0, k_y) = V(t, k_x, 0, k_y) = W(t, k_x, 0, k_y) = 0, \tag{6.5.100}$$

$$u(t, k_x, 1, k_y) = V(t, k_x, 1, k_y) = W(t, k_x, 1, k_y) = 0, \tag{6.5.101}$$

$$\phi(t, k_x, 0, k_y) = \phi(t, k_x, 1, k_y) = 0. \tag{6.5.102}$$

Using the transformation (6.5.58) to write the system in (Y, ω) coordinates, one gets the following equations for Y and ω.

$$Y_t = \epsilon\left(-\alpha^2 Y + Y_{yy}\right) - \beta Y - 2\pi k_x i U_y^e V + \alpha^2 p - NY, \tag{6.5.103}$$

$$\omega_t = \epsilon\left(-\alpha^2 \omega + \omega_{yy}\right) - \beta \omega - 2\pi k_z i U_y^e V - \alpha^2 N\phi - N\omega. \tag{6.5.104}$$

The Poisson equation for the potential is, in terms of ω,

$$-\alpha^2\phi + \phi_{yy} = \omega. \tag{6.5.105}$$

Consider the Lyapunov function

$$\Lambda = \int_0^1 \frac{|u|^2 + |V|^2 + |W|^2}{2} dy, \tag{6.5.106}$$

where we write $\int_0^1 f = \int_0^1 f(k_x, y, k_z)dy$. The function Λ is the L^2 norm (kinematic energy) of the velocity field.

Substituting Y and ω from (6.5.59) into (6.5.106), we get

$$\begin{aligned}
\Lambda &= \int_0^1 4\pi^2 \left[\frac{k_x^2|Y|^2 + k_z^2|\omega|^2 + k_xk_z(\bar{Y}\omega + Y\bar{\omega})}{2\alpha^4}\right. \\
&\quad \left. + \frac{k_z^2|Y|^2 + k_x^2|\omega|^2 - k_xk_z(\bar{Y}\omega + Y\bar{\omega})}{2\alpha^4}\right] dy + \int_0^1 \frac{|V|^2}{2} dy \\
&= \int_0^1 \frac{|Y|^2 + |\omega|^2 + \alpha^2|V|^2}{2\alpha^2} dy.
\end{aligned} \tag{6.5.107}$$

Define then a new Lyapunov function,

$$\Lambda_1 = \alpha^2\Lambda = \int_0^1 \frac{|Y|^2 + |\omega|^2 + \alpha^2|V|^2}{2} dy. \tag{6.5.108}$$

The time derivative of Λ_1 can be estimated as follows,

$$\begin{aligned}
\dot{\Lambda}_1 &= -2\epsilon\alpha^2\Lambda_1 - \epsilon\int_0^1 \left(|Y_y|^2 + |\omega_y|^2 + \alpha^2|V_y|^2\right) - N\int_0^1 \left(|Y|^2 + |\omega|^2\right) \\
&\quad - \int_0^1 \pi i U_y^e(y) V(2k_x\bar{Y} + k_z\bar{\omega}) + \int_0^1 \pi i U_y^e(y)\bar{V}(2k_xY + k_z\omega) \\
&\quad -\alpha^2 N \int_0^1 \frac{\bar{\phi}\omega + \phi\bar{\omega}}{2} + \alpha^2\int_0^1 \frac{\bar{P}Y + P\bar{Y} - \bar{P}_yV - P_y\bar{V}}{2}.
\end{aligned} \tag{6.5.109}$$

For bounding (6.5.109), we use the following two lemmas.

Lemma 6.3.

$$-\alpha^2\int_0^1 \frac{\bar{\phi}\omega + \phi\bar{\omega}}{2} \le \int_0^1 |\omega|^2. \tag{6.5.110}$$

Proof. Note that substituting $\alpha^2\phi$ from (6.5.105), we can write

$$-\alpha^2\int_0^1 \frac{\bar{\phi}\omega+\phi\bar{\omega}}{2} = -\int_0^1 \frac{\bar{\phi}_{yy}\omega+\phi_{yy}\bar{\omega}}{2} + \int_0^1 |\omega|^2. \tag{6.5.111}$$

Therefore, we need to prove that

$$\int_0^1 \left(\bar{\phi}_{yy}\omega+\phi_{yy}\bar{\omega}\right) \geq 0. \tag{6.5.112}$$

Substituting ω from equation (6.5.105) into (6.5.112), we get

$$\begin{aligned} &\int_0^1 \left(\bar{\phi}_{yy}\omega+\phi_{yy}\bar{\omega}\right) \\ = \ &\int_0^1 |\phi_{yy}|^2 - \alpha^2\int_0^1 \left(\bar{\phi}_{yy}\phi+\phi_{yy}\bar{\phi}\right) \\ = \ &\int_0^1 |\phi_{yy}|^2 + \alpha^2\int_0^1 |\phi_y|^2, \end{aligned} \tag{6.5.113}$$

which is nonnegative. ∎

Lemma 6.4.

$$|U^e_y(y)| \leq 4+H. \tag{6.5.114}$$

Proof. Computing $U^e_y(y)$ from (6.3.15),

$$U^e_y(y) = H\frac{\cosh(Hy)-\cosh(H(1-y))}{2\sinh H/2-\sinh H}. \tag{6.5.115}$$

Calling $g_1(y)=\cosh(Hy)-\cosh(H(1-y))$, we get

$$g_1'(y) = H\left(\sinh(Hy)+\sinh(H(1-y))\right). \tag{6.5.116}$$

Since $g_1'(t)$ is always positive for $y\in(0,1)$, the maximum of g_1 must be in the boundaries. Therefore $g_1 \leq \cosh H - 1$. Call

$$g_2(H) = H\frac{\cosh H-1}{\sinh H-2\sinh H/2}. \tag{6.5.117}$$

We have that $|U^e_y(y)| \leq g_2(H)$. One can rewrite g_2 as

$$g_2 = H\frac{\sinh H/2}{\cosh H/2-1}. \tag{6.5.118}$$

Since, by L'Hôpital's rule, $g_2(0) = 4$, it suffices to verify that $g_2'(H) \leq 1$. Computing g', we get

$$g_2'(H) = \frac{g_3}{g_4}, \tag{6.5.119}$$

where $g_3 = \sinh H/2 - H/2$ and $g_4 = \cosh H/2 - 1$. We need to show that $g_3 \leq g_4$. Since $g_3(0) = g_4(0) = 0$, it is enough that $g_3' \leq g_4'$, which follows from

$$g_3' = 1/2\left(\cosh H/2 - 1\right) \leq 1/2(\sinh H/2) = g_4', \tag{6.5.120}$$

because $\cosh x - 1 \leq \sinh x$ for $x \geq 0$. □

Integrating by parts and applying Lemma 6.3,

$$\begin{aligned}\dot{\Lambda}_1 \leq\ & -2\epsilon\alpha^2\Lambda_1 - \epsilon\int_0^1 \left(|Y_y|^2 + |\omega_y|^2 + \alpha^2|V_y|^2\right) \\ & + \int_0^1 \pi i U_y^e(y)\bar{V}(k_x Y + k_z\omega) \\ & - \int_0^1 \pi i U_y^e(y) V(k_x\bar{Y} + k_z\bar{\omega}) - N\int_0^1 |Y|^2. \end{aligned} \tag{6.5.121}$$

Using Lemma 6.4 to bound U_y^e in (6.5.121),

$$\begin{aligned}\dot{\Lambda}_1 &\leq -2\epsilon\left(1+\alpha^2\right)\Lambda_1 - N\int_0^1 |Y|^2 dy \\ &\quad +2\pi\left(4+H\right)\int_0^1 \left(|V|(|k_x||Y| + |k_z||\omega|\right) dy \\ &\leq \left(4 + H - 2\epsilon\left(1+\alpha^2\right)\right)\Lambda_1 \end{aligned} \tag{6.5.122}$$

where we have applied Young's and Poincare's inequalities. Hence, if $\alpha^2 \geq \frac{4+H}{2\epsilon}$,

$$\dot{\Lambda}_1 \leq -2\epsilon\Lambda_1. \tag{6.5.123}$$

Dividing (6.5.123) by α^2 and using (6.5.108), we get that

$$\dot{\Lambda} \leq -2\epsilon\Lambda, \tag{6.5.124}$$

and stability in the uncontrolled wave number range follows when $k_x^2 + k_z^2 \geq M^2$ for M (conservatively) chosen as

$$M \geq \frac{1}{2\pi}\sqrt{\frac{(H+4)Re}{2}}. \tag{6.5.125}$$

We summarize the result in the following proposition.

Proposition 6.5. *For $k_x^2 + k_z^2 \geq M^2$ where $M \geq \frac{1}{2\pi}\sqrt{\frac{(H+4)Re}{2}}$, the equilibrium $u \equiv V \equiv W \equiv 0$ of the uncontrolled system (6.5.95)–(6.5.102) is exponentially stable in the L^2 sense, i.e.,*

$$\begin{aligned} &\int_0^1 \left(|u|^2 + |V|^2 + |W|^2\right)(t, k_x, y, k_z)dy \\ \leq \quad & \mathrm{e}^{-2\epsilon t} \int_0^1 \left(|u|^2 + |V|^2 + |W|^2\right)(0, k_x, y, k_z)dy. \end{aligned} \tag{6.5.126}$$

6.5.3 Main result

Substituting (6.5.50), (6.5.53) and (6.5.88)–(6.5.89) in (6.5.44), and using the Fourier convolution theorem, we get the control laws in physical space, which can be expressed compactly as

$$\begin{aligned} \begin{pmatrix} U_c \\ W_c \\ \Phi_c \end{pmatrix} = & \int_{-\infty}^{\infty} \int_0^1 \int_{-\infty}^{\infty} \mathbf{\Sigma}(x - \xi, \eta, z - \zeta) \\ & \times \begin{pmatrix} u(\xi, \eta, \zeta) \\ W(\xi, \eta, \zeta) \end{pmatrix} d\xi d\eta d\zeta, \end{aligned} \tag{6.5.127}$$

where

$$\begin{aligned} \mathbf{\Sigma}(\xi, \eta, \zeta) \quad = \quad & \int_{-\infty}^{\infty} \int_{-\infty}^{\infty} \mathbf{\Sigma}(k_x, \eta, k_z) \\ & \times \chi(k_x, k_z) \mathrm{e}^{2\pi i(k_x\xi + k_z\zeta)} dk_z dk_x, \end{aligned} \tag{6.5.128}$$

and

$$\mathbf{\Sigma} = \begin{pmatrix} K^{Uu}(k_x, 1, \eta, k_z) & K^{UW}(k_x, 1, \eta, k_z) \\ K^{Wu}(k_x, 1, \eta, k_z) & K^{WW}(k_x, 1, \eta, k_z) \\ \frac{2\pi i k_z \sinh(\alpha(1-\eta))}{\alpha} & -\frac{2\pi i k_k \sinh(\alpha(1-\eta))}{\alpha} \end{pmatrix}, \tag{6.5.129}$$

where the kernels appearing in (6.5.129) were defined in (6.5.90). Control law V_c is a dynamic feedback law computed as the solution of the following forced parabolic equation

$$(V_c)_t = \frac{(V_c)_{xx} + (V_c)_{zz}}{Re} - NV_c + g(t, x, z), \tag{6.5.130}$$

where $g(t, x, z)$ is defined as

$$
\begin{aligned}
g = \int_{-\infty}^{\infty} \int_{-\infty}^{\infty} \Bigg[\int_0^1 & g_V(x-\xi, \eta, z-\zeta) V(\xi, \eta, \zeta) d\eta \\
& + g_W(x-\xi, z-\zeta) \left(W_y(\xi, 0, \zeta) - W_y(\xi, 1, \zeta) \right) \\
& + g_u(x-\xi, z-\zeta) \left(u_y(\xi, 0, \zeta) - u_y(\xi, 1, \zeta) \right) \Bigg] d\xi d\zeta,
\end{aligned} \tag{6.5.131}
$$

and

$$
g_u = \int_{-\infty}^{\infty} \int_{-\infty}^{\infty} 2\pi i \frac{k_x}{Re} \chi(k_x, k_z) \mathrm{e}^{2\pi i (k_x \xi + k_z \zeta)} dk_z dk_x, \tag{6.5.132}
$$

$$
\begin{aligned}
g_V = \int_{-\infty}^{\infty} \int_{-\infty}^{\infty} & \cosh\left(\alpha(1-\eta)\right) \left(N + 4\pi k_x i U_y^e(\eta) \right) \\
& \times \chi(k_x, k_z) \mathrm{e}^{2\pi i (k_x \xi + k_z \zeta)} dk_z dk_x,
\end{aligned} \tag{6.5.133}
$$

$$
g_W = \int_{-\infty}^{\infty} \int_{-\infty}^{\infty} 2\pi i \frac{k_z}{Re} \chi(k_x, k_z) \mathrm{e}^{2\pi i (k_x \xi + k_z \zeta)} dk_z dk_x. \tag{6.5.134}
$$

As in Section 4.6.3, considering all wave numbers and using Proposition 6.2 and Proposition 6.5, the following result holds regarding the convergence of the closed-loop system.

Theorem 6.6. *Consider the system (6.4.21)–(6.4.30) with control laws (6.5.127)–(6.5.134). Then the equilibrium profile $u \equiv V \equiv W \equiv 0$ is asymptotically stable in the L^2 norm, i.e.,*

$$
\begin{aligned}
& \int_{-\infty}^{\infty} \int_0^1 \int_{-\infty}^{\infty} \left(u^2 + V^2 + W^2 \right) (t, x, y, z) dx dy dz \\
& C_2 \mathrm{e}^{-2\epsilon t} \int_{-\infty}^{\infty} \int_0^1 \int_{-\infty}^{\infty} \left(u^2 + V^2 + W^2 \right) (0, x, y, z) dx dy dz.
\end{aligned} \tag{6.5.135}
$$

where $C_2 = \max\{C_1, 1\} \geq 0$.

Remark 6.7. We have assumed in the above result that the closed-loop linearized system is well-posed and that the velocity and electromagnetic field equations have at least L^2 solutions. See [99] for a statement of well-posedness of MHD equations in bounded domains. However, there are no results about well-posedness of 3-D MHD equations in unbounded domains and such an study is beyond the scope of this dissertation. Hence we assume that the solutions for the velocity field, pressure and electric field, and their estimates, exist, are unique and regular enough for all statements and a priori estimates to make sense.

Remark 6.8. In case that $N = 0$, meaning that either there is no imposed magnetic field or the fluid is nonconducting, Equations (6.2.2)–(6.2.4) are the Navier-Stokes equations and our controller solves the stabilization problem for a 3-D channel flow. The solution is the same as obtained beginning with the 3-D problem and using the same tools [34] . Some physical insight can be gained analyzing this case. In the context of hydrodynamic stability theory, the linearized system written in (Y, ω) variables verify equations analogous to the classical Orr-Sommerfeld-Squire equations. These are Equations (6.5.64)–(6.5.65) for controlled wave numbers and Equations (6.5.103)–(6.5.104) for uncontrolled wave numbers. As in [34], we use the backstepping transformations (6.5.76)–(6.5.77) not only to stabilize (using gain K) but also to decouple the system (using gains Γ_1, Γ_2) in the small wave number range, where non-normality effects are more severe. Even if the linearized system is stable, non-normality produces large transient growths [89, 95], which enhanced by nonlinear effects may allow the velocity field to wander far away from the origin. This warrants the use of extra gains to map the system into two uncoupled heat equations (6.5.72)–(6.5.73).

This chapter is a partial reprint of the material as it appears in
R. Vazquez, E. Schuster and M. Krstic, "A closed-form feedback controller for stabilization of magnetohydrodynamic channel flow," submitted, *2007 European Control Conference*, Kos, Greece, 2007.
The dissertation author was the primary author and the coauthors listed in this publication directed and supervised the research, which is the basis for this chapter.

Chapter 7

Boundary Estimation for 3-D Magnetohydrodynamic Channel Flow

7.1 Introduction

In this chapter we design an observer for the MHD channel flow introduced in Chapter 6. Our observer obtains estimates of the velocity, pressure, electric potential and current fields in the whole domain, derived only from wall measurements. Obtaining such an estimate can be of interest in itself, depending on the application. For example, the absence of effective state estimators modeling turbulent fluid flows is considered one of the key obstacles to reliable, model-based weather forecasting. In other engineering applications in which active control is needed, such as drag reduction [86] or mixing enhancement for cooling systems, designs usually assume unrealistic full state knowledge, therefore a state estimator is necessary for effective implementation. If the fluid is not conductive, or there is no magnetic field, the result still holds and the observer reduces to an estimator for the 3-D channel flow, which is an important result on its own.

Our design for the MHD system extends the 2-D channel flow observer of Chapter 5 using similar ideas. The observer is designed for the continuum MHD model and consists of a copy of the plant together with output injection of measurement error. As happened with the MHD system in Chapter 6, the observer error system is similar to the Orr-Sommerfeld-Squire system of PDE's and presents the similar difficulties (non-normality leading to a large transient growth mechanism [66, 95]).

7.2 Observer

For simplicity, we first design an estimator for the linearized system. In Section 7.4, using the linear gains, we present a nonlinear observer following the procedure of Chapter 5.

We employ the fluctuation variables around the equilibrium of the Hartmann flow, u and p, which were defined in (6.4.19)–(6.4.20).

The linearization of the uncontrolled MHD equations (6.2.2)–(6.2.10) around the Hartmann equilibrium profile, written in the fluctuation variables (u, V, W), is

$$\begin{aligned} u_t &= \frac{\triangle u}{Re} - U^e(y)u_x - U^e_y(y)V - p_x + N\phi_z - NU, && (7.2.1)\\ V_t &= \frac{\triangle V}{Re} - U^e(y)V_x - p_y, && (7.2.2)\\ W_t &= \frac{\triangle W}{Re} - U^e(y)W_x - p_z - N\phi_x - NW\,. && (7.2.3) \end{aligned}$$

The potential verifies the equation

$$\triangle\phi = u_z - W_x\,, \qquad (7.2.4)$$

and the fluctuation velocity field verifies the continuity equation,

$$u_x + V_y + W_z = 0\,, \qquad (7.2.5)$$

and boundary conditions

$$
\begin{aligned}
u(t,x,0,z) &= W(t,x,0,z) = V(t,x,0,z) = 0, && (7.2.6)\\
u(t,x,1,z) &= W(t,x,1,z) = V(t,x,1,z) = 0, && (7.2.7)\\
\phi(t,x,0,z) &= 0,\ \phi(t,x,1,z) = 0. && (7.2.8)
\end{aligned}
$$

We design the observer for the linearized equations. It consists of a copy of (7.2.1)–(7.2.8), to which we add output injection of the pressure p, the potential flux ϕ_y (proportional to current), and both the streamwise and spanwise velocity gradients, u_y and W_y, (proportional to friction) at the bottom wall.

Denoting the observer (estimated) variables by a hat, the equations for the estimated velocity field are

$$
\begin{aligned}
\hat{u}_t &= \frac{\triangle \hat{u}}{Re} - U^e(y)\hat{u}_x - U^e_y(y)\hat{V} - \hat{p}_x + N\hat{\phi}_z - N\hat{u} - Q^U, && (7.2.9)\\
\hat{V}_t &= \frac{\triangle \hat{V}}{Re} - U^e(y)\hat{V}_x - \hat{p}_y - Q^V, && (7.2.10)\\
\hat{W}_t &= \frac{\triangle \hat{W}}{Re} - U^e(y)\hat{W}_x - \hat{p}_z - N\hat{\phi}_x - N\hat{W} - Q^W. && (7.2.11)
\end{aligned}
$$

The additional Q terms in the observer equation are related to output injection and defined as follows.

$$
\begin{pmatrix} Q^U \\ Q^V \\ Q^W \end{pmatrix} = \int_{-\infty}^{\infty}\int_{-\infty}^{\infty} \mathbf{L}(x-\xi, y, z-\zeta) \begin{pmatrix} p(\xi,0,\zeta) - \hat{p}(\xi,0,\zeta) \\ u_y(\xi,0,\zeta) - \hat{u}_y(\xi,0,\zeta) \\ W_y(\xi,0,\zeta) - \hat{W}_y(\xi,0,\zeta) \\ \phi_y(\xi,0,\zeta) - \hat{\phi}_y(\xi,0,\zeta) \end{pmatrix} d\xi d\zeta, \quad (7.2.12)
$$

where $\mathbf{L}$ is an output injection kernel matrix, defined as

$$
\mathbf{L} = \begin{pmatrix} L^{UP} & L^{UU} & L^{UW} & L^{U\phi} \\ L^{VP} & L^{VU} & L^{VW} & L^{V\phi} \\ L^{WP} & L^{WU} & L^{WW} & L^{W\phi} \end{pmatrix}, \quad (7.2.13)
$$

whose entries will be designed to ensure observer convergence. The estimated potential is computed from

$$
\triangle \hat{\phi} = \hat{u}_z - \hat{W}_x, \quad (7.2.14)
$$

and the observer verifies the continuity equation,

$$\hat{u}_x + \hat{V}_y + \hat{W}_z = 0, \tag{7.2.15}$$

and Dirichlet boundary conditions,

$$\hat{u}(t,x,0,z) = \hat{W}(t,x,0,z) = \hat{V}(t,x,0,z) = 0, \tag{7.2.16}$$

$$\hat{u}(t,x,1,z) = \hat{W}(t,x,1,z) = \hat{V}(t,x,1,z) = 0, \tag{7.2.17}$$

$$\hat{\phi}(t,x,0,z) = \hat{\phi}(t,x,1,z) = 0. \tag{7.2.18}$$

The estimated current field is computed from the other estimated variables using a copy of equations (6.2.11)–(6.2.13).

$$\hat{j}^x(t,x,y,z) = -\hat{\phi}_x - \hat{W}, \tag{7.2.19}$$

$$\hat{j}^y(t,x,y,z) = -\hat{\phi}_y, \tag{7.2.20}$$

$$\hat{j}^z(t,x,y,z) = -\hat{\phi}_z + \hat{u}. \tag{7.2.21}$$

Remark 7.1. Note that the observer equations (7.2.9)–(7.2.21) can be regarded as forced MHD equations, with the output injection acting as a body force. This means that any standard DNS solver for the forced MHD equations can be used to implement the observer without the need of major modifications.

As inputs to the observer, appearing in (7.2.12), one needs measurements of pressure, skin friction and current in the lower wall. For obtaining these measurements, pressure, skin friction and current sensors have to be embedded into one of the walls. Pressure and skin friction sensors are common in flow control, while for current measurement one could use an array of discrete current sensors, as depicted in Figure 7.1.

7.3 Observer design and convergence analysis

Substracting the observer equations from the linearized plant equations we obtain the error equations, with states $\tilde{U} = u - \hat{u} = U - \hat{U}, \tilde{V} = V - \hat{V}, \tilde{W} =$

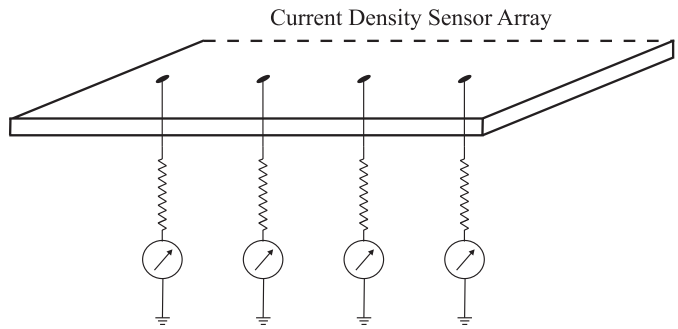

Figure 7.1: An array of current sensors in the lower wall.

$W - \hat{W}, \tilde{P} = p - \hat{p}, \tilde{\phi} = \phi - \hat{\phi}$,

$$\begin{aligned} \tilde{U}_t &= \frac{\triangle \tilde{U}}{Re} - U^e(y)\tilde{U}_x - U^e_y(y)\tilde{V} - \tilde{P}_x + N\tilde{\phi}_z \\ &\quad -N\tilde{U} + Q^U, \end{aligned} \tag{7.3.22}$$

$$\tilde{V}_t = \frac{\triangle \tilde{V}}{Re} - U^e(y)\tilde{V}_x - \tilde{P}_y + Q^V, \tag{7.3.23}$$

$$\tilde{W}_t = \frac{\triangle \tilde{W}}{Re} - U^e(y)\tilde{W}_x - \tilde{P}_z - N\tilde{\phi}_x - N\tilde{W} + Q^W. \tag{7.3.24}$$

The observer error verifies the continuity equation,

$$\tilde{U}_x + \tilde{V}_y + \tilde{W}_z = 0, \tag{7.3.25}$$

while the potential error is governed by

$$\triangle \tilde{\phi} = \tilde{U}_z - \tilde{W}_x. \tag{7.3.26}$$

The boundary conditions for the error states are

$$\tilde{U}(t,x,0,z) = \tilde{V}(t,x,0,z) = \tilde{W}(t,x,0,z) = 0, \tag{7.3.27}$$

$$\tilde{U}(t,x,1,z) = \tilde{V}(t,x,1,z) = \tilde{W}(t,x,1,z) = 0, \tag{7.3.28}$$

$$\tilde{\phi}(t,x,0,z) = \tilde{\phi}(t,x,1,z) = 0. \tag{7.3.29}$$

To guarantee observer convergence, our design task is to design the output injection gains $\mathbf{L}$ defined in (7.2.12) that appear in Q^U, Q^V and Q^W, so that the origin of the error system is exponentially stable.

Using the Fourier transform defined in (6.4.31)–(6.4.32), we get the observer error equations in Fourier space, which are

$$\begin{aligned}
\tilde{U}_t &= \frac{-\alpha^2\tilde{U}+\tilde{U}_{yy}}{Re} - \beta\tilde{U} - U_y^e\tilde{V} - 2\pi k_x i\tilde{P} + 2\pi k_z i N\tilde{\phi} - N\tilde{U} \\
&\quad + L^{UP}P_0 + L^{UU}U_{y0} + L^{UW}W_{y0} + L^{U\phi}\phi_{y0}, &(7.3.30)\\
\tilde{V}_t &= \frac{-\alpha^2\tilde{V}+\tilde{V}_{yy}}{Re} - \beta\tilde{V} - \tilde{P}_y \\
&\quad + L^{VP}P_0 + L^{VU}U_{y0} + L^{VW}W_{y0} + L^{V\phi}\phi_{y0}, &(7.3.31)\\
\tilde{W}_t &= \frac{-\alpha^2\tilde{W}+W_{yy}}{Re} - \beta\tilde{W} - 2\pi k_z i\tilde{P} - 2\pi k_x i N\tilde{\phi} - N\tilde{W} \\
&\quad + L^{WP}P_0 + L^{WU}U_{y0} + L^{WW}W_{y0} + L^{W\phi}\phi_{y0} &(7.3.32)
\end{aligned}$$

where $\alpha^2 = 4\pi^2(k_x^2 + k_z^2)$, the L's are the entries of $\mathbf{L}$ in Fourier space, and where we have used the definition (7.2.12) of the output injection terms as convolutions, which become products in Fourier space. We have written for short $P_0 = \tilde{P}(k_x, 0, k_z)$, $U_{y0} = \tilde{U}_y(k_x, 0, k_z)$, $W_{y0} = \tilde{W}_y(k_x, 0, k_z)$, $\phi_{y0} = \tilde{\phi}_y(k_x, 0, k_z)$.

The continuity equation in Fourier space is expressed as

$$2\pi i k_x\tilde{U} + \tilde{V}_y + 2\pi k_z\tilde{W} = 0, \tag{7.3.33}$$

and the equation for the potential is

$$-\alpha^2\tilde{\phi} + \hat{\phi}_{yy} = 2\pi i\left(k_z\tilde{U} - k_x\tilde{W}\right). \tag{7.3.34}$$

Note that (7.3.38)–(7.3.33) is uncoupled for each wave number. Therefore, as in Chapter 5, we define the range $k_x^2 + k_z^2 \leq M^2$ as the *observed* wave number range, and the range $k_x^2 + k_z^2 > M^2$ as the *unobserved* wave number range, and study them separately. If stability for all wave numbers is established, stability in physical space follows as in Section 4.6.3. The number M, which will be computed in Section 7.3.2, is a parameter that ensures stability for the unobserved wave number range.

We reflect that we don't use output injection for unobserved wave numbers by writing

$$\mathbf{L} = \chi(k_x, y, k_z)\mathbf{R}(k_x, y, k_x), \tag{7.3.35}$$

where χ was defined in (6.5.43). Then L can be written in physical space, using the definition of the Fourier transform and the convolution theorem, as

$$\mathbf{L}(x,y,z) \quad = \quad \int_{-\infty}^{\infty}\int_{-\infty}^{\infty}\chi(k_x,y,k_z)\mathbf{R}(k_x,y,k_z)\mathrm{e}^{2\pi i(k_x x+k_z z)}dk_z dk_x. \tag{7.3.36}$$

The matrix $\mathbf{R}$ is defined as

$$\mathbf{R} = \begin{pmatrix} R^{UP} & R^{UU} & R^{UW} & R^{U\phi} \\ R^{VP} & R^{VU} & R^{VW} & R^{V\phi} \\ R^{WP} & R^{WU} & R^{WW} & R^{W\phi} \end{pmatrix}, \tag{7.3.37}$$

and using $\mathbf{R}$ we can write the observer error equations as

$$\begin{aligned} \tilde{U}_t &= \frac{-\alpha^2\tilde{U}+\tilde{U}_{yy}}{Re} - \beta\tilde{U} - U_y^e\tilde{V} - 2\pi k_x i\tilde{P} + 2\pi k_z iN\tilde{\phi} - N\tilde{U} \\ &\quad +\chi(k_x,k_z)\left\{R^{UP}P_0 + R^{UU}U_{y0} + R^{UW}W_{y0} + R^{U\phi}\phi_{y0}\right\}, \qquad (7.3.38) \\ \tilde{V}_t &= \frac{-\alpha^2\tilde{V}+\tilde{V}_{yy}}{Re} - \beta\tilde{V} - \tilde{P}_y \\ &\quad +\chi(k_x,k_z)\left\{R^{VP}P_0 + R^{VU}U_{y0} + R^{VW}W_{y0}R^{V\phi}\phi_{y0}\right\}, \qquad (7.3.39) \\ \tilde{W}_t &= \frac{-\alpha^2\tilde{W}+W_{yy}}{Re} - \beta\tilde{W} - 2\pi k_z i\tilde{P} - 2\pi k_x iN\tilde{\phi} - N\tilde{W} \\ &\quad +\chi(k_x,k_z)\left\{R^{WP}P_0 + R^{WU}U_{y0} + R^{WW}W_{y0} + R^{W\phi}\phi_{y0}\right\}. \qquad (7.3.40) \end{aligned}$$

7.3.1 Observed wave number analysis

Consider $k_x^2 + k_z^2 \leq M^2$. Then $\chi = 1$, so output injection is present. Using the continuity equation (7.3.33) and equations (7.3.38)–(7.3.40), the following Poisson equation for the pressure is derived,

$$-\alpha^2\tilde{P} + \tilde{P}_{yy} = \Upsilon - 4\pi k_x iU_y^e(y)\tilde{V} + NV_y, \tag{7.3.41}$$

where Υ contains all the terms due to output injection,

$$\begin{aligned} \Upsilon \quad = \quad & P_0\left(2\pi ik_xR^{UP} + R_y^{VP} + 2\pi k_zR^{WP}\right) \\ & +U_{y0}\left(2\pi ik_xR^{UU} + R_y^{VU} + 2\pi k_zR^{WU}\right) \\ & +W_{y0}\left(2\pi ik_xR^{UW} + R_y^{VW} + 2\pi k_zR^{WW}\right) \\ & +\phi_{y0}\left(2\pi ik_xR^{U\phi} + R_y^{V\phi} + 2\pi k_zR^{W\phi}\right). \qquad (7.3.42) \end{aligned}$$

We want to make (7.3.41) independent of the output injection gains, for which we need $\Upsilon = 0$. Hence, we set

$$
\begin{aligned}
R^{VP}(k_x,y,k_z) &= R^{VP}(k_x,0,k_z) - 2\pi i \int_0^y \left(k_x R^{UP}\right. \\
&\quad \left.+ k_z R^{WP}\right)(k_x,\eta,k_z)d\eta, && (7.3.43)\\
R^{VU}(k_x,y,k_z) &= R^{VU}(k_x,0,k_z) - 2\pi i \int_0^y \left(k_x R^{UU}\right. \\
&\quad \left.+ k_z R^{WU}\right)(k_x,\eta,k_z)d\eta, && (7.3.44)\\
R^{VW}(k_x,y,k_z) &= R^{VW}(k_x,0,k_z) - 2\pi i \int_0^y \left(k_x R^{UW}\right. \\
&\quad \left.+ k_z R^{WW}\right)(k_x,\eta,k_z)d\eta, && (7.3.45)\\
R^{V\phi}(k_x,y,k_z) &= R^{V\phi}(k_x,0,k_z) - 2\pi i \int_0^y \left(k_x R^{U\phi}\right. \\
&\quad \left.+ k_z R^{W\phi}\right)(k_x,\eta,k_z)d\eta, && (7.3.46)
\end{aligned}
$$

which means that, in physical space, $\nabla \cdot \mathbf{L} = 0$. Hence, as Equation (7.3.41) is derived by taking divergence of (7.3.38)–(7.3.40), the output injection terms cancel away.

Expression (7.3.41) can be solved in terms of the values of the pressure at the bottom wall.

$$
\begin{aligned}
\tilde{P} &= -\frac{4\pi k_x i}{\alpha}\int_0^y U_y^e(\eta)\sinh\left(\alpha(y-\eta)\right)\tilde{V}(k_x,\eta,k_z)d\eta + \cosh\left(\alpha y\right)P_0 \\
&\quad + \frac{\sinh\left(\alpha y\right)}{\alpha}\tilde{P}_y(k_x,0,k_z) + N\int_0^y \frac{\sinh\left(\alpha(y-\eta)\right)}{\alpha}\tilde{V}_y(k_x,\eta,k_z)d\eta. && (7.3.47)
\end{aligned}
$$

Evaluating equation (7.3.39) at $y=0$ one finds that

$$
\begin{aligned}
\tilde{P}_y(k_x,0,k_z) &= \Upsilon_0 + \frac{\tilde{V}_{yy}(k_x,0,k_z)}{Re} \\
&= \Upsilon_0 - 2\pi i\frac{k_x U_{y0}(k_x,0,k_z) + k_z\tilde{W}_{y0}}{Re}, && (7.3.48)
\end{aligned}
$$

where we have used (7.3.33) for expressing $\tilde{V}_{yy}$ at the bottom in terms of measurements. In (7.3.48),

$$
\begin{aligned}
\Upsilon_0 &= P_0 R^{VP}(k_x,0,k_z) + U_{y0}R^{VU}(k_x,0,k_z) \\
&\quad + W_{y0}R^{VW}(k_x,0,k_z) + \phi_{y0}R^{V\phi}(k_x,0,k_z), && (7.3.49)
\end{aligned}
$$

and as before we need the pressure to be independent of any output injection gains. Hence, we set

$$R^{VP}(k_x,0,k_z) \;=\; R^{VU}(k_x,0,k_z) = R^{VW}(k_x,0,k_z) = R^{V\phi}(k_x,0,k_z) = 0. \quad (7.3.50)$$

Then, the pressure can be expressed independently of the output injection gains in terms of a strict-feedback [71] integral of the state $\tilde{V}$ and measurements,

$$\begin{aligned}\tilde{P} \;=\; & -\frac{4\pi k_x i}{\alpha}\int_0^y U_y^e(\eta)\sinh\left(\alpha(y-\eta)\right)\tilde{V}(k_x,\eta,k_z)d\eta + \cosh\left(\alpha y\right)P_0 \\ & -2\pi i\frac{\sinh\left(\alpha y\right)}{Re\alpha}\left(k_x U_{y0} + k_z W_{y0}\right) \\ & +N\int_0^y \frac{\sinh\left(\alpha(y-\eta)\right)}{\alpha}\tilde{V}_y(k_x,\eta,k_z)d\eta. \end{aligned} \quad (7.3.51)$$

Similarly, solving for ϕ in terms of the measurement ϕ_{y0} and the right hand side of its Poisson equation (7.3.34),

$$\begin{aligned}\tilde{\phi} \;=\; & \frac{2\pi i}{\alpha}\int_0^y \sinh\left(\alpha(y-\eta)\right)\left(k_z\tilde{U}(k_x,\eta,k_z) - k_x\tilde{W}(k_x,\eta,k_z)\right)d\eta \\ & +\frac{\sinh\left(\alpha y\right)}{\alpha}\phi_{y0}. \end{aligned} \quad (7.3.52)$$

Introducing the expressions (7.3.51) and (7.3.52) in (7.3.38) and (7.3.40), we get

$$\begin{aligned}\tilde{U}_t \;=\; & \frac{-\alpha^2\tilde{U} + \tilde{U}_{yy}}{Re} - \beta\tilde{U} - U_y^e(y)\tilde{V} - N\tilde{U} \\ & +P_0\left(R^{UP} - 2\pi k_x i\cosh\left(\alpha y\right)\right) + U_{y0}\left(R^{UU} - \frac{4\pi^2 k_x^2}{\alpha Re}\sinh\left(\alpha y\right)\right) \\ & +W_{y0}\left(R^{UW} - \frac{4\pi^2 k_x k_z}{\alpha Re}\sinh\left(\alpha y\right)\right) + \phi_{y0}\left(R^{U\phi} + N\frac{2\pi k_z i}{\alpha}\sinh\left(\alpha y\right)\right) \\ & -\frac{8\pi k_x^2}{\alpha}\int_0^y U_y^e(\eta)\sinh\left(\alpha(y-\eta)\right)\tilde{V}(k_x,\eta,k_z)d\eta \\ & -\frac{4\pi^2 k_z N}{\alpha}\int_0^y \sinh\left(\alpha(y-\eta)\right)\left(k_z\tilde{U}(k_x,\eta,k_z) - k_x\tilde{W}(k_x,\eta,k_z)\right)d\eta \\ & -2\pi i k_x N\int_0^y \frac{\sinh\left(\alpha(y-\eta)\right)}{\alpha}\tilde{V}_y(k_x,\eta,k_z)d\eta, \end{aligned} \quad (7.3.53)$$

$$\tilde{W}_t \;=\; \frac{-\alpha^2\tilde{W} + W_{yy}}{Re} - \beta\tilde{W} - N\tilde{W}$$

$$
\begin{aligned}
&+P_0\left(R^{WP}-2\pi k_z i\cosh(\alpha y)\right)+U_{y0}\left(R^{WU}-\frac{4\pi^2 k_x k_z}{\alpha Re}\sinh(\alpha y)\right)\\
&+W_{y0}\left(R^{WW}-\frac{4\pi^2 k_z^2}{\alpha Re}\sinh(\alpha y)\right)+\phi_{y0}\left(R^{W\phi}-N\frac{2\pi k_x i}{\alpha}\sinh(\alpha y)\right)\\
&-\frac{8\pi k_x k_z}{\alpha}\int_0^y U_y^e(\eta)\sinh(\alpha(y-\eta))\tilde{V}(k_x,\eta,k_z)d\eta\\
&+\frac{4\pi^2 k_x N}{\alpha}\int_0^y \sinh(\alpha(y-\eta))\left(k_z\tilde{U}(k_x,\eta,k_z)-k_x\tilde{W}(k_x,\eta,k_z)\right)d\eta\\
&-2\pi i k_z N\int_0^y \frac{\sinh(\alpha(y-\eta))}{\alpha}\tilde{V}_y(k_x,\eta,k_z)d\eta. \qquad (7.3.54)
\end{aligned}
$$

Note that we have omitted the equation for $\tilde{V}$ since, from (7.3.33) and using the fact that $\tilde{V}(k_x,0,k_z)=0$, $\tilde{V}$ is computed from $\tilde{U}$ and $\tilde{W}$:

$$
\tilde{V}=-2\pi i\int_0^y\left(k_x\tilde{U}(k_x,\eta,k_z)+k_z\tilde{W}(k_x,\eta,k_z)\right)d\eta. \qquad (7.3.55)
$$

We now set the output injection terms to directly cancel the boundary terms coming from (7.3.51) and (7.3.52), while still leaving some additional gains to stabilize the system. Thus, we define

$$
\begin{aligned}
R^{UP} &= 2\pi k_x i\cosh(\alpha y), && (7.3.56)\\
R^{WP} &= 2\pi k_z i\cosh(\alpha y), && (7.3.57)\\
R^{UU} &= \frac{4\pi^2 k_x^2}{\alpha Re}\sinh(\alpha y)+\Pi_1(k_x,y,k_z), && (7.3.58)\\
R^{WU} &= \frac{4\pi^2 k_x k_z}{\alpha Re}\sinh(\alpha y)+\Pi_2(k_x,y,k_z), && (7.3.59)\\
R^{UW} &= \frac{4\pi^2 k_x k_z}{\alpha Re}\sinh(\alpha y)+\Pi_3(k_x,y,k_z), && (7.3.60)\\
R^{WW} &= \frac{4\pi^2 k_z^2}{\alpha Re}\sinh(\alpha y)+\Pi_4(k_x,y,k_z), && (7.3.61)\\
R^{U\phi} &= -N\frac{2\pi k_z i}{\alpha}\sinh(\alpha y), && (7.3.62)\\
R^{W\phi} &= N\frac{2\pi k_x i}{\alpha}\sinh(\alpha y), && (7.3.63)
\end{aligned}
$$

where the gains Π_1, Π_2, Π_3 and Π_4 are to be defined later. From (7.3.43)–(7.3.46), (7.3.50) and (7.3.56)–(7.3.63), we get a explicit expression for the remaining entries of **R**,

$$R^{VP} = \alpha \sinh(\alpha y), \tag{7.3.64}$$

$$R^{VU} = 2\pi i(k_x + k_z)\frac{1-\cosh(\alpha y)}{Re} - 2\pi i \times \int_0^y (k_x \Pi_1(k_x,\eta,k_z) + k_z \Pi_2(k_x,\eta,k_z))\, d\eta, \tag{7.3.65}$$

$$R^{VW} = 2\pi i(k_x + k_z)\frac{1-\cosh(\alpha y)}{Re} - 2\pi i \times \int_0^y (k_x \Pi_3(k_x,\eta,k_z) + k_z \Pi_4(k_x,\eta,k_z))\, d\eta, \tag{7.3.66}$$

$$R^{V\phi} = 0. \tag{7.3.67}$$

Introducing (7.3.56)–(7.3.67) in equations (7.3.53)–(7.3.54) we get

$$\begin{aligned} \tilde{U}_t &= \frac{-\alpha^2\tilde{U} + \tilde{U}_{yy}}{Re} - \beta\tilde{U} - U_y^e(y)\tilde{V} - N\tilde{U} + \Pi_1 U_{y0} + \Pi_3 W_{y0} \\ &\quad -\frac{4\pi^2 k_z N}{\alpha}\int_0^y \sinh(\alpha(y-\eta))\left(k_z\tilde{U}(k_x,\eta,k_z) - k_x\tilde{W}(k_x,\eta,k_z)\right) d\eta \\ &\quad -\frac{8\pi k_x^2}{\alpha}\int_0^y U_y^e(\eta)\sinh(\alpha(y-\eta))\,\tilde{V}(k_x,\eta,k_z)d\eta \\ &\quad -2\pi i k_x N\int_0^y \frac{\sinh(\alpha(y-\eta))}{\alpha}\tilde{V}_y(k_x,\eta,k_z)d\eta, \end{aligned} \tag{7.3.68}$$

$$\begin{aligned} \tilde{W}_t &= \frac{-\alpha^2\tilde{W} + W_{yy}}{Re} - \beta\tilde{W} - N\tilde{W} + \Pi_2 U_{y0} + \Pi_4 W_{y0} \\ &\quad -\frac{8\pi k_x k_z}{\alpha}\int_0^y U_y^e(\eta)\sinh(\alpha(y-\eta))\,\tilde{V}(k_x,\eta,k_z)d\eta \\ &\quad +\frac{4\pi^2 k_x N}{\alpha}\int_0^y \sinh(\alpha(y-\eta))\left(k_z\tilde{U}(k_x,\eta,k_z) - k_x\tilde{W}(k_x,\eta,k_z)\right) d\eta \\ &\quad -2\pi i k_z N\int_0^y \frac{\sinh(\alpha(y-\eta))}{\alpha}\tilde{V}_y(k_x,\eta,k_z)d\eta. \end{aligned} \tag{7.3.69}$$

Now, we introduce the following change of variables and its inverses,

$$Y = 2\pi i\left(k_x\tilde{U} + k_z\tilde{W}\right),\ \omega = 2\pi i\left(k_z\tilde{U} - k_x\tilde{W}\right), \tag{7.3.70}$$

$$U = \frac{2\pi i}{\alpha^2}(k_x Y + k_z\omega),\ W = \frac{2\pi i}{\alpha^2}(k_z Y - k_x\omega). \tag{7.3.71}$$

Defining $\epsilon = \frac{1}{Re}$ and the following functions

$$\beta = 2\pi i k_x U^e, \tag{7.3.72}$$

$$
\begin{aligned}
f &= 4\pi i k_x \left\{ \frac{U^e_y}{2} + \int_\eta^y U^e_y(\sigma) \frac{\sinh\left(\alpha(y-\sigma)\right)}{\alpha} d\sigma \right\} \\
&\quad + N\alpha \sinh\left(\alpha(y-\sigma)\right), \qquad (7.3.73) \\
h_1 &= 2\pi i k_z U^e_y, \qquad (7.3.74) \\
h_2 &= -N\alpha \sinh\left(\alpha(y-\eta)\right), \qquad (7.3.75)
\end{aligned}
$$

equations (7.3.68)–(7.3.69) expressed in terms of Y and ω are

$$
\begin{aligned}
Y_t &= \epsilon\left(-\alpha^2 Y + Y_{yy}\right) - \beta Y - NY \\
&\quad - \frac{4\pi^2}{\alpha^2}\left(k_x^2\Pi_1 + k_x k_z \Pi_2 + k_x k_z \Pi_3 + k_z^2 \Pi_4\right) Y_{y0} \\
&\quad - \frac{4\pi^2}{\alpha^2}\left(k_x k_z \Pi_1 + k_z^2 \Pi_2 - k_x^2 \Pi_3 - k_x k_z \Pi_4\right) \omega_{y0} \\
&\quad + \int_0^y f(k_x, y, \eta, k_z) Y(k_x, \eta, k_z) d\eta, \qquad (7.3.76) \\
\omega_t &= \epsilon\left(-\alpha^2 \omega + \omega_{yy}\right) - \beta\omega - N\omega \\
&\quad - \frac{4\pi^2}{\alpha^2}\left(k_x k_z \Pi_1 - k_x^2 \Pi_2 + k_z^2 \Pi_3 - k_x k_z \Pi_4\right) Y_{y0} \\
&\quad - \frac{4\pi^2}{\alpha^2}\left(k_z^2 \Pi_1 - k_x k_z \Pi_2 - k_x k_z \Pi_3 + k_x^2 \Pi_4\right) \omega_{y0} \\
&\quad + h_1(y) \int_0^y Y(k_x, \eta, k_z) d\eta + \int_0^y h_2(y, \eta) \omega(k_x, \eta, k_z) d\eta, \qquad (7.3.77)
\end{aligned}
$$

where we have used the inverse change of variables (7.3.71) to express U_{y0} and W_{y0} in terms of $Y_{y0} = Y(k_x, 0, k_z)$ and $\omega_{y0} = \omega(k_x, 0, k_z)$. We define now the output injection gains Π_1, Π_2, Π_3 and Π_4 in the following way

$$
\begin{pmatrix} \Pi_1 \\ \Pi_2 \\ \Pi_3 \\ \Pi_4 \end{pmatrix} = \mathbf{A}^{-1} \begin{pmatrix} l(k_x, y, 0, k_z) \\ 0 \\ \theta_1(k_x, y, 0, k_z) \\ \theta_2(k_x, y, 0, k_z) \end{pmatrix}, \qquad (7.3.78)
$$

where the matrix $\mathbf{A}$ was defined in (6.5.91). Note that since $\det(A) = -1$ its inverse appearing in equation (7.3.78) is well-defined. The functions $l(k_x, y, \eta, k_z)$, $\theta_1(k_x, y, \eta, k_z)$, and $\theta_2(k_x, y, \eta, k_z)$ in (7.3.78) are to be found. Using (7.3.78), equations (7.3.76)–(7.3.77) become

$$
\begin{aligned}
Y_t &= \epsilon\left(-\alpha^2 Y + Y_{yy}\right) - \beta Y - NY + l(k_x, y, 0, k_z) Y_{y0} \\
&\quad + \int_0^y f(k_x, y, \eta, k_z) Y(k_x, \eta, k_z) d\eta, && (7.3.79) \\
\omega_t &= \epsilon\left(-\alpha^2 \omega + \omega_{yy}\right) - \beta\omega - N\omega + \theta_1(k_x, y, 0, k_z) Y_{y0} \\
&\quad + \theta_2(k_x, y, 0, k_z)\omega_{y0} + h_1 \int_0^y Y(k_x, \eta, k_z) d\eta \\
&\quad + \int_0^y h_2(y, \eta)\omega(k_x, \eta, k_z) d\eta. && (7.3.80)
\end{aligned}
$$

Equations (7.3.79)–(7.3.80) are a coupled, strict-feedback plant, with integral and reaction terms. A variant of the design presented in [102] can be used to design the gains $l(k_x, y, 0, k_z)$, $\theta_1(k_x, y, 0, k_z)$ and $\theta_2(k_x, y, 0, k_z)$ using a double backstepping transformation as in Section 6.5.1. The transformation maps, for each k_x and k_z, the variables (Y, ω) into the variables (Ψ, Ω), that verify the following family of heat equations (parameterized in k_x, k_z).

$$
\begin{aligned}
\Psi_t &= \epsilon\left(-\alpha^2 \Psi + \Psi_{yy}\right) - \beta\Psi - N\psi, && (7.3.81) \\
\Omega_t &= \epsilon\left(-\alpha^2 \Omega + \Omega_{yy}\right) - \beta\Omega - N\Omega, && (7.3.82)
\end{aligned}
$$

with boundary conditions

$$
\begin{aligned}
\Psi(k_x, 0, k_z) &= \Psi(k_x, 1, k_z) = 0, && (7.3.83) \\
\Omega(k_x, 0, k_z) &= \Omega(k_x, 1, k_z) = 0. && (7.3.84)
\end{aligned}
$$

The transformation is defined as follows,

$$
\begin{aligned}
Y &= \Psi - \int_0^y l(k_x, y, \eta, k_z)\Psi(k_x, \eta, k_z) d\eta, && (7.3.85) \\
\omega &= \Omega - \int_0^y \theta_1(k_x, y, \eta, k_z)\Psi(k_x, \eta, k_z) d\eta \\
&\quad - \int_0^y \theta_2(k_x, y, \eta, k_z)\Omega(k_x, \eta, k_z) d\eta. && (7.3.86)
\end{aligned}
$$

Following Section 6.5.1 and [101,102], we find the functions $l(k_x, y, \eta, k_z)$, $\theta_1(k_x, y, \eta, k_z)$, and $\theta_2(k_x, y, \eta, k_z)$ solving the following partial integro-differential equations,

$$
\begin{aligned}
\epsilon l_{\eta\eta} &= \epsilon l_{yy} - (\beta(y) - \beta(\eta))\, l - f + \int_\eta^y f(y,\xi) l(\xi,\eta) d\xi, && (7.3.87)\\
\epsilon \theta_{1\eta\eta} &= \epsilon \theta_{1yy} - (\beta(y) - \beta(\eta))\, \theta_1(y,\eta) - h_1 + h_1 \int_\eta^y l(\xi,\eta) d\xi \\
&\quad + \int_\eta^y h_2(y,\xi)\theta_1(\xi,\eta) d\xi, && (7.3.88)\\
\epsilon \theta_{2\eta\eta} &= \epsilon \theta_{2yy} - (\beta(y) - \beta(\eta))\, \theta_2 - h_2 + \int_\eta^y h_2(y,\xi)\theta_2(\xi,\eta) d\xi. && (7.3.89)
\end{aligned}
$$

Equations (7.3.87)–(7.3.89) are hyperbolic partial integro-differential equation in the region $\mathcal{T} = \{(y,\eta) : 0 \le y \le 1, 0 \le \eta \le y\}$. Their boundary conditions are

$$
\begin{aligned}
l(k_x, y, y, k_z) &= l(k_x, 1, \eta, k_z) = 0, && (7.3.90)\\
\theta_1(k_x, y, y, k_z) &= \theta_1(k_x, 1, \eta, k_z) = 0, && (7.3.91)\\
\theta_2(k_x, y, y, k_z) &= = \theta_2(k_x, 1, \eta, k_z) = 0. && (7.3.92)
\end{aligned}
$$

Remark 7.2. Equations (7.3.87)–(7.3.92) are well-posed and can be solved symbolically, by means of a successive approximation series, or numerically. See [101, 102] for techniques in solving similar equations. Note that both Equation 7.3.87 and Equation 7.3.89 are autonomous. Hence, one must solve first for $l(k_x, y, \eta, k_z)$ and $\theta_2(k_x, y, \eta, k_z)$. Then the solution for l is plugged in Equation 7.3.88 which then can be solved for $\theta_1(k_x, y, \eta, k_z)$. The observer gains are then found just by setting $\eta = 0$ in the kernels $l(k_x, y, \eta, k_z)$, $\theta_2(k_x, y, \eta, k_z)$ and $\theta_1(k_x, y, \eta, k_z)$.

Stability in the observed wave number range follows from stability of (7.3.81)–(7.3.82) and the invertibility of the transformation (7.3.85)–(7.3.86), as in Proposition 6.2.

7.3.2 Unobserved wave number analysis

When $k_x^2 + k_z^2 > M$, there is no output injection, as $\chi = 0$, and the linearized observer error verifies the following equations

$$
\tilde{U}_t = \frac{-\alpha^2 \tilde{U} + \tilde{U}_{yy}}{Re} - \beta \tilde{U} - U_y^e(y)\tilde{V} - 2\pi k_x i \tilde{P} + 2\pi k_z i N \tilde{\phi} - N\tilde{U}, \quad (7.3.93)
$$

$$\tilde{V}_t = \frac{-\alpha^2\tilde{V} + \tilde{V}_{yy}}{Re} - \beta\tilde{V} - \tilde{P}_y, \tag{7.3.94}$$

$$\tilde{W}_t = \frac{-\alpha^2\tilde{W} + W_{yy}}{Re} - \beta\tilde{W} - 2\pi k_z i\tilde{P} - 2\pi k_x iN\tilde{\phi} - N\tilde{W}, \tag{7.3.95}$$

the Poisson equation for the potential (7.3.34) and the continuity equation (7.3.33).

Note that (7.3.93)–(7.3.95) are the same equations as (6.5.95)–(6.5.97). Hence the analysis of Section 6.5.2 can be applied, obtaining a result similar to Proposition 6.5. Hence, stability in the unobserved wave number range follows when $k_x^2 + k_z^2 \geq M^2$ for M (conservatively) chosen as

$$M \geq \frac{1}{2\pi}\sqrt{\frac{(H+4)Re}{2}}. \tag{7.3.96}$$

7.3.3 Main result

As in Section 4.6.3, considering all wave numbers, the following result holds regarding the convergence of the observer.

Theorem 7.3. *Consider the system (7.2.1)–(7.2.8), and the system (7.2.9)–(7.2.18), and suppose that both have classical solutions. Then, the L^2 norms of $\tilde{U}$, $\tilde{V}$, $\tilde{W}$ converge to zero, i.e.,*

$$\lim_{t\to\infty}\int_{-\infty}^{\infty}\int_0^1\int_{-\infty}^{\infty}\left(\tilde{U}^2+\tilde{V}^2+\tilde{W}^2\right)(t,x,y,z)dxdydz=0. \tag{7.3.97}$$

Remark 7.4. The convergence result stated in Theorem 7.3 guarantees asymptotic convergence of the estimated states to the actual values of the *linearized* plant. For this to be true for the *nonlinear* plant, as in Theorem 5.4, we need additional conditions. Namely, the estimates have to be initialized close enough to the real initial values and the MHD system has to stay in a neighborhood of the equilibrium at all times.

Remark 7.5. In case that $N = 0$, meaning that either there is no imposed magnetic field or the fluid is nonconducting, Equations (7.2.1)–(7.2.3) are the linearized Navier-Stokes equations and the observer reduces to a velocity/pressure estimator for a 3D channel flow. This is a result of high interest on its own that can be seen as dual to the 3-D channel flow control problem. See Remark 6.8 for some physical insight for this case.

Remark 7.6. As in Section 5.4, we can combine the results of this chapter and Chapter 6 to obtain an output feedback law that stabilizes the plant (6.4.21)–(6.4.30) using only wall measurements. Such a control law would use the estimates $(\hat{u}, \hat{V}, \hat{W})$ from the observer (7.2.1)–(7.3.26) with boundary conditions for $(\hat{u}, \hat{V}, \hat{W})$ as in (6.4.26)–(6.4.30), replacing the real states (u, V, W) in the control laws (6.5.127)–(6.5.134). Then, using Theorems 6.6 and 7.3 and standard arguments for linear output feedback controllers, a similar result to Theorem 5.8 holds guaranteeing the L^2 stability of the closed-loop system.

7.4 A nonlinear estimator

As we did in Chapter 5, we postulate a nonlinear observer to improve the convergence result of the linear estimator. This observer has the same structure and gains as the linear observer, but the nonlinear terms are added. In this we follow the design technique of Chapter 5 which used an approach similar to an Extended Kalman Filter, in which gains are deduced for a linearized version of the plant and then used for a nonlinear observer.

The nonlinear observer equations are the following

$$\begin{aligned} \hat{U}_t &= \frac{\triangle \hat{U}}{Re} - \hat{U}\hat{U}_x - \hat{V}\hat{U}_y - \hat{W}\hat{U}_z - \hat{P}_x + N\hat{\phi}_z \\ &\quad -N\hat{U} - Q^U, && (7.4.98) \\ \hat{V}_t &= \frac{\triangle \hat{V}}{Re} - \hat{U}\hat{V}_x - \hat{V}\hat{V}_y - \hat{W}\hat{V}_z - \hat{P}_y - Q^V, && (7.4.99) \\ \hat{W}_t &= \frac{\triangle \hat{W}}{Re} - \hat{U}\hat{W}_x - \hat{V}\hat{W}_y - \hat{W}\hat{W}_z - \hat{P}_z - N\hat{\phi}_x \\ &\quad -N\hat{W} - Q^W. && (7.4.100) \end{aligned}$$

The estimated potential is computed from

$$\triangle \hat{\phi} = \hat{U}_z - \hat{W}_x, \qquad (7.4.101)$$

and the observer verifies the continuity equation,

$$\hat{U}_x + \hat{V}_y + \hat{W}_z = 0, \tag{7.4.102}$$

and Dirichlet boundary conditions,

$$\begin{aligned}
\hat{U}(t,x,0,z) &= \hat{W}(t,x,0,z) = \hat{V}(t,x,0,z) = 0, && (7.4.103)\\
\hat{U}(t,x,1,z) &= \hat{W}(t,x,1,z) = \hat{V}(t,x,1,z) = 0, && (7.4.104)\\
\hat{\phi}(t,x,0,z) &= \hat{\phi}(t,x,1,z) = 0. && (7.4.105)
\end{aligned}$$

The estimated current field is computed from the other estimated variables using a copy of equations (6.2.11)–(6.2.13).

$$\begin{aligned}
\hat{j}^x(t,x,y,z) &= -\hat{\phi}_x - \hat{W}, && (7.4.106)\\
\hat{j}^y(t,x,y,z) &= -\hat{\phi}_y, && (7.4.107)\\
\hat{j}^z(t,x,y,z) &= -\hat{\phi}_z + \hat{U}. && (7.4.108)
\end{aligned}$$

In (7.4.98)–(7.4.100), the Q terms are the same as for the linear observer. Hence, the observer is designed for the linearized plant and then the linear gains are used for the nonlinear observer. Such a nonlinear observer will produce closer estimates of the states in a larger range of initial conditions.

Using the fluctuation variable and the observer error varaibles, we can write the nonlinear observer velocity field error equations as follows.

$$\begin{aligned}
\tilde{U}_t &= \frac{\triangle \tilde{U}}{Re} - U^e(y)\tilde{U}_x + \mathcal{N}^U(\tilde{U},\tilde{V},\tilde{W},u,V,W)\\
&\quad -U^e_y(y)\tilde{V} - \tilde{P}_x + N\tilde{\phi}_z - N\tilde{U} + Q^U, && (7.4.109)\\
\tilde{V}_t &= \frac{\triangle \tilde{V}}{Re} - U^e(y)\tilde{V}_x + \mathcal{N}^V(\tilde{U},\tilde{V},\tilde{W},u,V,W) - \tilde{P}_y + Q^V, && (7.4.110)\\
\tilde{W}_t &= \frac{\triangle \tilde{W}}{Re} - U^e(y)\tilde{W}_x + \mathcal{N}^W(\tilde{U},\tilde{V},\tilde{W},u,V,W)\\
&\quad -\tilde{P}_z - N\tilde{\phi}_x - N\tilde{W} + Q^W, && (7.4.111)
\end{aligned}$$

where we have introduced

$$\begin{aligned}\mathcal{N}^U &= \tilde{U}\tilde{U}_x - u\tilde{U}_x - \tilde{U}u_x + \tilde{V}\tilde{U}_y - V\tilde{U}_y - \tilde{V}u_y \\ &\quad + \tilde{W}\tilde{U}_z - W\tilde{U}_z - \tilde{W}u_z, \qquad (7.4.112)\\ \mathcal{N}^V &= \tilde{U}\tilde{V}_x - u\tilde{V}_x - \tilde{U}V_x + \tilde{V}\tilde{V}_y - V\tilde{V}_y - \tilde{V}V_y \\ &\quad + \tilde{W}\tilde{V}_z - W\tilde{V}_z - \tilde{W}V_z, \qquad (7.4.113)\\ \mathcal{N}^W &= \tilde{U}\tilde{W}_x - u\tilde{W}_x - \tilde{U}W_x + \tilde{V}\tilde{W}_y - V\tilde{W}_y - \tilde{V}W_y \\ &\quad + \tilde{W}\tilde{W}_z - W\tilde{W}_z - \tilde{W}W_z, \qquad (7.4.114)\end{aligned}$$

Assuming, for the purposes of observer design and analysis, that the observer state $(\hat{U}, \hat{V}, \hat{W})$ is close to the actual state (U, V, W) (i.e., the error state is close to zero), and that the fluctuation (u, V, W) around the equilibrium state is small, then $\mathcal{N}_U(\tilde{U}, \tilde{V}, \tilde{W}, u, V, W)$, $\mathcal{N}_V(\tilde{U}, \tilde{V}, \tilde{W}, u, V, W)$ and $\mathcal{N}_W(\tilde{U}, \tilde{V}, \tilde{W}, u, V, W)$ are small and dominated by the linear terms in the equations, so they can be neglected. The linearized error equations are then

$$\begin{aligned}\tilde{U}_t &= \frac{\triangle\tilde{U}}{Re} - U^e(y)\tilde{U}_x - U^e_y(y)\tilde{V} - \tilde{P}_x + N\tilde{\phi}_z - N\tilde{U} + Q^U, \qquad (7.4.115)\\ \tilde{V}_t &= \frac{\triangle\tilde{V}}{Re} - U^e(y)\tilde{V}_x - \tilde{P}_y + Q^V, \qquad (7.4.116)\\ \tilde{W}_t &= \frac{\triangle\tilde{W}}{Re} - U^e(y)\tilde{W}_x - \tilde{P}_z - N\tilde{\phi}_x - N\tilde{W} + Q^W, \qquad (7.4.117)\end{aligned}$$

which are the same as (7.3.22)–(7.3.24). Thus, as expected, the error equations for the observer designed for the linearized plant, and the linearized error equations for the nonlinear observer are the same; this is the main reason why the same gains derived in Section 7.3 are used. A similar result to Theorem 5.4 holds for the nonlinear observer (7.4.98)–(7.4.100). We skip the details.

Remark 7.7. Following [32], we may consider the *mean turbulent profile* instead of considering the exact *laminar* equilibrium profile. This amounts to changing U^e in definition (6.3.15). Since U^e appears in Equations (7.3.72)–(7.3.75), which are used to compute output injection gains in Equations (7.3.87)–(7.3.89), the observer gains will change (quantitatively) for the turbulent mean profile. However Theorem 7.3 still holds and guarantees convergence of estimates, but for these estimates to be good enough we require the same assumptions, meaning now that the state has to stay close enough to the mean turbulent profile at all times. The use of the nonlinear observer of Section 7.4 will allow larger discrepancies between the state and the profile while still producing valid estimates.

This chapter is a partial reprint of the material as it appears in
R. Vazquez, E. Schuster and M. Krstic, "A closed-form observer for the 3D inductionless MHD and Navier-Stokes channel flow," *Proc. of the 2006 CDC*, San Diego, 2006.
The dissertation author was the primary author and the coauthors listed in this publication directed and supervised the research, which is the basis for this chapter.

Chapter 8

Stable Poiseuille Flow Transfer for 2-D Navier-Stokes Channel Flow

8.1 Introduction

In this chapter we consider a 2-D channel flow and solve the problem of *transferring* the velocity field from one steady state (Poiseuille equilibrium) to another. The transition has to be fast and stable, following a "nice" (in some adequate sense) pre-determined flow trajectory. For example, we may wish to smoothly accelerate fluid at rest up to a given Reynolds number, probably close or over the critical value (which may change due to unsteady pressure gradient effects [68]), avoiding transition to turbulence. The means at our disposal are the imposed pressure gradient and velocity actuation at one of the walls.

Most works in channel flow control in the literature consider a constant pressure gradient (fixed Reynolds number) and a developed flow which is already close to the desired solution. The problem of generating and tracking flow trajectories has not been considered so far for a channel flow. Velocity tracking problems have been considered, from the point of view of mathematical controllability, in the setting of an optimal control framework [57].

Steady-state transfer problems for wide classes of infinite dimensional systems have been solved in the past using quasi-static deformation theory. Examples include semilinear heat equations [37], semilinear wave equations [38], and Schrödinger's equation [19, 39]. Other applications are the shallow water problem [36] and the Couette-Taylor flow controllability problem [96]. For the channel flow, this approach would require to modify the pressure gradient very slowly, and simultaneously gain-schedule a fixed Reynold number boundary controller like the one designed in Chapter 4. However, we follow an alternative approach, finding analytically an *exact*, *fast* and well-behaved trajectory of the system which is then stabilized by means of boundary control. This approach allows for a fast transfer and requires less actuation—since the tracked trajectory is an exact solution, the boundary velocity control effort is only necessary for stabilization and will be zero in the absence of perturbations.

The stabilization part of the design follows a similar approach to Chapter 4, however since the problem is unsteady, it uses the backstepping method for time-varying infinite dimensional parabolic systems [103]. This method requires to solve a nonstandard partial integro-differential boundary value equation, and we provide a very general proof of its well-posedness. A similar looking equation was proved well-posed [40, 97], requiring analyticity in time of the unsteady coefficients. Later it was shown *ill-posed* [67] for $\mathcal{C}^\infty$ unsteady coefficients. We settle the issue identifying the most natural class of functions for which the equation is solvable, which is the Gevrey class [58] (consisting of functions whose Taylor series "almost" converge).

8.2 Trajectory generation and control objective

The stationary family of solutions of (4.2.1)–(4.2.4) is the (nondimensional) Poiseuille family of parabolic profiles, $\mathcal{P}^\delta$, which is described by a single parameter δ (the maximum centerline velocity, which is determined by the magnitude of the pressure gradient) in the following way

$$\mathcal{P}^\delta = (U^\delta, V^\delta, P^\delta) = \left(4\delta y(1-y), 0, -\frac{8\delta}{Re}x\right). \tag{8.2.1}$$

Note that the velocity actuation at the wall is zero for $\mathcal{P}^\delta$, since both U^δ and V^δ are zero at the boundaries. For $\delta = 1$ we obtain the fully developed profile at the given Reynolds number. The pressure gradient $P_x^\delta = -\frac{8\delta}{Re}$ must be externally sustained for (8.2.1) to be a stationary solution [18].

Our first task is, given δ_0 and δ_1, to generate an unsteady trajectory path $\Theta(t) = (U(t), V(t), P(t))$, where space dependence is omitted for clarity, connecting $\mathcal{P}^{\delta_0}$ to $\mathcal{P}^{\delta_1}$. We assume $\delta_0 = 0$ and $\delta_1 = 1$ (rest to fully developed flow) for simplicity. Other values (for instance for a deceleration problem) may be considered as well.

Consider the trajectory $\Theta^q(t)$ defined by

$$\Theta^q(t) = (U^q(t), V^q(t), P^q(t)) = (g(t,y), 0, -xq(t)), \tag{8.2.2}$$

where q is the *chosen* external pressure gradient. Then, by substitution we see that (8.2.2) verifies (4.2.1)–(4.2.4) whenever

$$g_t = \frac{g_{yy}}{Re} + q. \tag{8.2.3}$$

Since $\mathcal{P}^0 \equiv 0$, we set $\Theta^q(0) = 0$, which implies $g(0,y) = q(0) = 0$. We impose $g(t,0) = g(t,1) = 0$ so no velocity control effort is needed to steer the trajectory, only to stabilize it. Given these initial-boundary data, choosing q completely determines g from (8.2.3) and consequently $\Theta^q(t)$, so $q(t)$ parameterizes $\Theta^q(t)$.

Choosing $q(t)$ as

$$q(t) = \frac{8}{Re}\left(1 - \mathrm{e}^{-ct}\right), \tag{8.2.4}$$

with $c > 0$ a design parameter, then $q(0) = 0$ and $\lim_{t\to\infty} q(t) = 8/Re$. This selection of q, determines a value g in (8.2.3) that verifies the following result.

Proposition 8.1. *Let* $\kappa_m = \pi(2m+1)$*. Consider* $g(t,y)$ *defined by (8.2.3) where* q *is given by (8.2.4), boundary conditions* $g(t,0) = g(t,1) = 0$ *and initial conditions* $g(0,y) \equiv 0$*. Assume as well that* $cRe \neq \kappa_m^2$ *for any* $m \in \mathbb{N}$*. Then* g *has the following properties.*

i. The explicit expression for g *in* $(0,\infty)\times[0,1]$ *is given by*

$$g \; = \; 16\sum_{m=0}^{\infty}\frac{\sin(\kappa_m y)}{\kappa_m}\left[\frac{1-\mathrm{e}^{-\frac{\kappa_m^2}{Re}t}}{\kappa_m^2} - \frac{\mathrm{e}^{-ct}-\mathrm{e}^{-\frac{\kappa_m^2}{Re}t}}{\kappa_m^2 - cRe}\right]. \tag{8.2.5}$$

ii. The following limit holds.

$$\lim_{t\to\infty} g(t,y) = 4y(1-y). \tag{8.2.6}$$

iii. The function g *belongs to the space* $C^\omega(0,\infty)\times C^\infty[0,1]$*, i.e., it is analytic in time and smooth in space.*

iv. The following estimates are verified for every time $t \geq 0$*, and every* $y \in [0,1]$*.*

$$0 < g(t,y) \;\leq\; 1, \tag{8.2.7}$$

$$|g_y(t,y)| \;\leq\; 4, \tag{8.2.8}$$

$$-8 < g_{yy}(t,y) \;\leq\; 0. \tag{8.2.9}$$

Proof. In the proof we make use of many properties of the heat equation [45].

Point i is obtained by a Fourier expansion and application of Duhamel's Principle for solving (8.2.3). That yields the solution

$$g(t,y) = 2\sum_{m=0}^{\infty}\frac{\sin(\kappa_m y)}{\kappa_m}\int_0^t \mathrm{e}^{-\frac{\kappa_m^2}{Re}(t-\tau)}q(\tau)d\tau, \tag{8.2.10}$$

and plugging in the expression (8.2.4) for q and solving explicitly the integral (where the assumption on c is used), (8.2.5) is found.

Point ii can be obtained by taking limit in (8.2.5) as t goes to infinity. Then

$$\lim_{t\to\infty} g(t,y) = 16\sum_{m=0}^{\infty}\frac{\sin(\kappa_m y)}{\kappa_m^3} = 4y(1-y), \tag{8.2.11}$$

which can be verified by computing the Fourier series of $4y(1-y)$ and noting that it coincides with the infinite sum.

Point iii is a standard property of the solutions of the heat equation, taking into account that q itself is $C^{\omega}(0,\infty)\times C^{\infty}[0,1]$.

Point iv is proved using the maximum principle for the heat equation. Having proved smoothness in Point iii, we can first consider the equation that g_{yy} verifies by differentiation of (8.2.3)

$$(g_{yy})_t = \frac{1}{Re}(g_{yy})_{yy}. \tag{8.2.12}$$

The boundary conditions for (8.2.12) can be determined plugging (8.2.4) in (8.2.3), and taking limit as y goes to 0 and 1. Then, using the fact that $g(t,0)=g(t,1)=0$, it follows that $g_{yy}(t,0) = g_{yy}(t,0) = -8(1-\mathrm{e}^{-ct})$. The initial condition is $g_{yy}(0,y) = 0$, and it holds that $\lim_{t\to\infty} g_{yy}(t,y) = -8$. By the maximum and minimum principle, and since $-8 < g_{yy}(t,0) < 0$, it follows that $-8 < g_{yy} < 0$.

Consider now g_y. The fact that the boundary conditions of g are $g(t,0) = g(t,1) = 0$, the initial condition is zero, and (8.2.3) has constant coefficients in y, implies that g is symmetric around $y = 1/2$, i.e., $g(y) = g(1-y)$. Hence, it follows that $g_y(y) = -g_y(1-y)$, which implies $g_y(1/2) = 0$. Then,

$$g_y(t,y) = \int_{1/2}^{y} g_{yy}(t,\eta)d\eta,\ y\in(1/2,1), \tag{8.2.13}$$

$$g_y(t,y) = -\int_{y}^{1/2} g_{yy}(t,\eta)d\eta,\ y\in(0,1/2), \tag{8.2.14}$$

so taking absolute value and using the previous bound,

$$|g_y(t,y)| \le 8(y-1/2) \le 4,\ y\in(1/2,1), \tag{8.2.15}$$

$$|g_y(t,y)| \le 8(1/2-y) \le 4,\ y\in(0,1/2), \tag{8.2.16}$$

and the bound follows. For g, one has that

$$g(t,y) = -\int_{y}^{1} g_y(\eta)d\eta = -\int_{y}^{1}\int_{1/2}^{\eta} g_{yy}(t,\sigma)d\sigma d\eta,\ y\in(1/2,1), \tag{8.2.17}$$

$$g(t,y) = \int_{0}^{y} g_y(\eta)d\eta = -\int_{0}^{y}\int_{\eta}^{1/2} g_{yy}(t,\sigma)d\sigma d\eta,\ y\in(0,1/2), \tag{8.2.18}$$

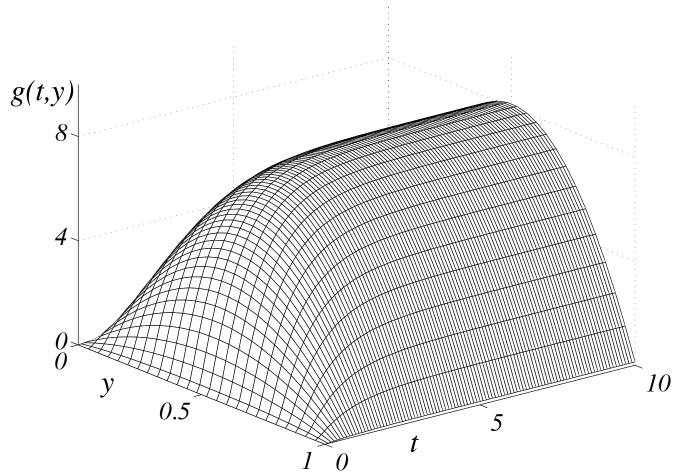

Figure 8.1: Evolution of $g(t, y)$ for $c = 1$, $Re = 1$.

so taking absolute value and using the bound on g_{yy}, we get from the integrals that

$$|g(t, y)| \leq 4y(1 - y) \leq 1,\ y \in (1/2, 1), \tag{8.2.19}$$

$$|g(t, y)| \leq 4y(1 - y) \leq 1,\ y \in (0, 1/2), \tag{8.2.20}$$

thus finishing the proof of Point iv. □

In Figure 8.1 we represent g, computed numerically from (8.2.3), for $c = 1, Re = 1$.

It follows from (8.2.4) and Proposition 8.1 that $\Theta^q(t)$ is a solution of the trajectory generation problem, since its components are smooth and solve (4.2.1)–(4.2.4), and additionally, we have that $\Theta^q(0) = \mathcal{P}^0$ and $\lim_{t\to\infty} \Theta^q(t) = \mathcal{P}^1$, so $\Theta^q(t)$ connects the chosen Poiseuille profiles[1].

Remark 8.2. The fact that an exact trajectory is obtained from a linear parabolic PDE, Equation (8.2.3), can be exploited to move between equilibria in *arbitrary finite time*, since it is known [47] that this kind of equations have finite-time zero

[1]Reaching $\mathcal{P}^1$ only after an infinitely long time, however by construction through rapidly decaying exponentials, Θ^q closely approaches $\mathcal{P}^1$ after a short time, as shown in Fig. 8.1. In this sense, we consider Θ^q a *fast* trajectory.

controllability for even initial data (i.e., $g(0,1-y)=g(0,y)$, for every $y\in[0,1]$). Motion planning theory for the heat equation [75] allows to define an *explicit* finite-time trajectory, in the framework of Gevrey functions. We do not pursue a finite-time result[2], however we present in Section 8.7 a proof guaranteeing that our method allows tracking of trajectories defined in Gevrey spaces.

Using (8.2.2) and following the notation of Chapter 4, we define the fluctuation variables as

$$\begin{aligned}(u,V,p) &= (U,V,P)-\Theta^q(t)\\ &= (U-g(t,y),V,P+xq(t)).\end{aligned}\tag{8.2.21}$$

The fluctuation variables verify the following equations,

$$u_t = \frac{\triangle u}{Re}-p_x-uu_x-Vu_y-g(t,y)u_x-g_y(t,y)V,\tag{8.2.22}$$
$$V_t = \frac{\triangle V}{Re}-p_y-uV_x-VV_y-g(t,y)V_x,\tag{8.2.23}$$

where we have used $\triangle=\partial_{xx}+\partial_{yy}$ for simplicity, and boundary conditions

$$u(t,x,0) = V(t,x,0)=0,\tag{8.2.24}$$
$$u(t,x,1) = U_c(t,x),\tag{8.2.25}$$
$$V(t,x,1) = V_c(t,x),\tag{8.2.26}$$

where U_c and V_c are respectively the streamwise and normal velocity actuators at the upper wall. Our new control objective is to stabilize the equilibrium at the origin in (8.2.22)–(8.2.23) using U_c and V_c. That will imply, considering (8.2.21), that the trajectory Θ^q is stabilized.

Linearizing (8.2.22)–(8.2.23), we obtain

$$u_t = \frac{\triangle u}{Re}-p_x-g(t,y)u_x-g_y(t,y)V,\tag{8.2.27}$$
$$V_t = \frac{\triangle V}{Re}-p_y-g(t,y)V_x,\tag{8.2.28}$$

[2]Exponential stability is enough for practical purposes.

with boundary conditions (8.2.24)–(8.2.26).

We consider the problem of stabilizing the origin of (8.2.27)–(8.2.28), and later show how its solution *locally*[3] stabilizes the origin of (8.2.22)–(8.2.23).

8.3 Mathematical preliminaries

In this section we present the framework that we use to solve the stabilization problem. We begin by stating our main work assumption.

Assumption 8.3. *Assume that the perturbation velocity field* (u, V) *and the pressure* p *are periodic in* x *with some period* $2h > 0$.

Remark 8.4. In Assumption 8.3 we follow [96, 108]. This assumption allows to derive existence and uniqueness results.

8.3.1 Periodic function spaces

Denote the boundaries of Ω as $\partial\Omega_0 = \{(x, y) : x \in \mathbb{R}, y = 0\}$ (the uncontrolled boundary) and $\partial\Omega_1 = \{(x, y) : x \in \mathbb{R}, y = 1\}$ (the controlled boundary). Under Assumption 8.3, we can identify Ω and its boundary with

$$\Omega_h = \{(x, y) \in \Omega : -h \leq x \leq h\}, \tag{8.3.29}$$

$$\partial\Omega_{hi} = \{(x, y) \in \partial\Omega_i : \leq x \leq h\},\ i = 0, 1. \tag{8.3.30}$$

Let $L^2(\Omega_h)$ be the usual Lebesgue space of square-integrable functions, endowed with the scalar product

$$(\phi, \psi)_{L^2(\Omega_h)} = \int_{-h}^{h} \int_{0}^{1} \phi(x, y)\psi(x, y)dydx. \tag{8.3.31}$$

Define then $L^2_h(\Omega) = L^2(\Omega_h)$, where now

$$(\phi, \psi)_{L^2_h(\Omega)} = (\phi|_{\Omega_h}, \psi|_{\Omega_h})_{L^2(\Omega_h)}. \tag{8.3.32}$$

[3]Local stabilization of the origin of (8.2.22)–(8.2.23) suffices, since we assume the initial data are zero, i.e. the velocity field starts at the origin itself.

8.3.2 Fourier series expansion

Given a function ϕ defined on Ω, we define the sequence of its complex Fourier coefficients $(\phi_n(y))_{n\in\mathbb{Z}}$ as

$$\phi_n(y) = \frac{1}{2h}\int_{-h}^{h} \phi(x,y)\mathrm{e}^{\frac{in\pi}{h}x}dx, \;\; n \in \mathbb{Z}. \tag{8.3.33}$$

We will write simply ϕ_n in the sequel. It is well known that if $\phi \in L_h^2(\Omega)$, then (8.3.33) is well defined and $(\phi_n(\cdot))_{n\in\mathbb{Z}}$ is in the (complex valued) $\ell^2\left(\mathbb{Z}, L^2(0,1)\right)$ space, i.e.,

$$\sum_{n\in\mathbb{Z}}\int_0^1 |\phi_n(y)|^2 dy < \infty. \tag{8.3.34}$$

One can recover ϕ from its Fourier series,

$$\phi(x,y) = \sum_{n\in\mathbb{Z}} \phi_n(y)\mathrm{e}^{-\frac{in\pi}{h}x}. \tag{8.3.35}$$

Equation (8.3.35) always yields a $L_h^2(\Omega)$ function, if $(\phi_n(\cdot))_{n\in\mathbb{Z}} \in \ell^2\left(\mathbb{Z}, L^2(0,1)\right)$. Actually it can be considered the "inverse" of (8.3.33) in the sense of L^2 functions, i.e., applying consecutively (8.3.33) and (8.3.35) or vice versa yields the same function almost everywhere.

One important result is Parseval's formula, which allows to compute scalar products in L^2 using Fourier coefficients. Consider $\phi, \psi \in L_h^2(\Omega)$. Then,

$$(\phi,\psi)_{L_h^2(\Omega)} = 2h\left((\phi_n), (\psi_n)\right)_{\ell^2(\mathbb{Z},L^2(0,1))} \tag{8.3.36}$$

where the $\ell^2\left(\mathbb{Z}, L^2(0,1)\right)$ scalar product is

$$\left((\phi_n), (\psi_n)\right)_{\ell^2(\mathbb{Z},L^2(0,1))} = \sum_{n\in\mathbb{Z}}\int_0^1 \phi_n(y)\overline{\psi}_n(y)dy, \tag{8.3.37}$$

and where the bar denotes the complex conjugate.

Using (8.3.36), and given ψ in $L^2(\Omega_h)$, we can compute its norm by computing its Fourier coefficients ψ_n. Then,

$$\|\psi\|^2_{L^2(\Omega_h)} = 2h\|\psi_n\|^2_{\ell^2(\mathbb{Z},L^2(0,1))} = 2h\sum_{n\in\mathbb{Z}}\|\psi_n\|^2_{L^2(0,1)}, \tag{8.3.38}$$

where

$$\|\psi_n\|^2_{L^2(0,1)} = \int_0^1 |\psi_n(y)|^2 dy. \tag{8.3.39}$$

In the sequel we omit the subindexes when clear from the context.

8.3.3 H^1 and H^2 spaces

We define the spaces

$$\begin{aligned} H^1_h(\Omega) &= \{f|_{\Omega_h} \in H^1(\Omega_h),\ f|_{x=-h} = f|_{x=h} \text{ a.e.}\}, & (8.3.40)\\ H^2_h(\Omega) &= \{f|_{\Omega_h} \in H^2(\Omega_h) \cap H^1_h(\Omega),\ \nabla f|_{x=-h} = \nabla f|_{x=h} \text{ a.e.}\}, & (8.3.41)\end{aligned}$$

where $H^1(\Omega_h)$ and $H^2(\Omega_h)$ are defined as usual. The norms of these spaces are

$$\begin{aligned} \|\phi\|^2_{H^1_h(\Omega)} &= \|\phi\|^2_{L^2_h(\Omega)} + \|\phi_y\|^2_{L^2_h(\Omega)} + \|\phi_x\|^2_{L^2_h(\Omega)}, & (8.3.42)\\ \|\phi\|^2_{H^2_h(\Omega)} &= \|\phi\|^2_{H^1_h(\Omega)} + \|\phi_{yy}\|^2_{L^2_h(\Omega)} + \|\phi_{xx}\|^2_{L^2_h(\Omega)} + \|\phi_{xy}\|^2_{L^2_h(\Omega)}, & (8.3.43)\end{aligned}$$

or, in terms of the Fourier coefficients, by

$$\begin{aligned} \|\phi\|^2_{H^1_h(\Omega)} &= 2h\sum\left[(1+\frac{\pi^2n^2}{h^2})\|\phi_n\|^2_{L^2(0,1)} + \|\phi_{ny}\|^2_{L^2(0,1)}\right]. & (8.3.44)\\ \|\phi\|^2_{H^2_h(\Omega)} &= 2h\sum(1+\frac{\pi^2n^2}{h^2}+\frac{\pi^4n^4}{h^4})\|\phi_n\|^2_{L^2(0,1)} + 2h\sum(1+\frac{\pi^2n^2}{h^2})\|\phi_{ny}\|^2_{L^2(0,1)} & \\ &\quad +2h\sum\|\phi_{nyy}\|^2_{L^2(0,1)}. & (8.3.45)\end{aligned}$$

The following lemmas hold in these spaces.

Lemma 8.5. *(Poincaré's inequality in $H^2(0,1)$). Suppose that f is a complex valued function belonging to $H^2(0,1)$, such that $f(0) = f(1) = 0$. Then $\|f_y\|^2_{L^2(0,1)} \leq \|f_{yy}\|^2_{L^2(0,1)}$.*

Proof. Set $f_1(y) = \Re(f)$ and $f_2 = \Im(f)$.

There exists $a \in (0,1)$ such that $f_{1y}(a) = 0$. Therefore,

$$\begin{aligned} f_{1y}(y) &= \int_a^y f_{1yy}(\eta)d\eta,\ y \in (a,1), & (8.3.46)\\ f_{1y}(y) &= -\int_y^a f_{1yy}(\eta)d\eta,\ y \in (1,a). & (8.3.47)\end{aligned}$$

Taking absolute value and bounding the integrals,

$$|f_{1y}(y)| \leq \int_a^1 |f_{1yy}(\eta)|d\eta \leq \int_0^1 |f_{1yy}(\eta)|d\eta,\ y \in (a,1), \tag{8.3.48}$$

$$|f_{1y}(y)| \leq \int_1^a |f_{1yy}(\eta)|d\eta \leq \int_0^1 |f_{1yy}(\eta)|d\eta,\ y \in (1,a), \tag{8.3.49}$$

which implies the bound for the whole interval. Then, by Cauchy-Schwarz inequality,

$$|f_{1y}(y)|^2 \leq \left(\int_0^1 |f_{1yy}(\eta)|d\eta\right)^2 \leq \int_0^1 f_{1yy}^2(\eta)d\eta, \tag{8.3.50}$$

and integrating,

$$\|f_{1y}\|^2_{L^2(0,1)} = \int_0^1 f_{1y}^2(y)dy \leq \int_0^1 f_{1yy}^2(\eta)d\eta = \|f_{1yy}\|^2_{L^2(0,1)}, \tag{8.3.51}$$

and analogously for f_2. Thus,

$$\begin{aligned} \|f_y\|^2_{L^2(0,1)} &= \|f_{1y} + if_{2y}\|^2_{L^2(0,1)} = \|f_{1y}\|^2_{L^2(0,1)} + \|f_{2y}\|^2_{L^2(0,1)} \\ &\leq \|f_{1yy}\|^2_{L^2(0,1)} + \|f_{2yy}\|^2_{L^2(0,1)} = \|f_{yy}\|^2_{L^2(0,1)}, \end{aligned} \tag{8.3.52}$$

thus proving the result. □

Lemma 8.6. *(Poincaré's inequalities in $H^1_h(\Omega)$ and $H^2_h(\Omega)$). Let $\phi \in H^1_h(\Omega)$ be such that $\phi|_{\partial\Omega_0} \equiv 0$, and $\psi \in H^2_h(\Omega)$ such that $\psi|_{\partial\Omega_i} \equiv 0$ for $i = 0, 1$. Then*

$$\|\phi\|^2_{L^2_h(\Omega)} \leq \|\phi_y\|^2_{L^2_h(\Omega)}, \tag{8.3.53}$$

$$\|\psi_y\|^2_{L^2_h(\Omega)} \leq \|\psi_{yy}\|^2_{L^2_h(\Omega)}. \tag{8.3.54}$$

Proof. Using Parseval's formula,

$$\begin{aligned} \|\phi\|^2_{L^2_h(\Omega)} &= \sum \|\phi_n\|^2_{L^2(0,1)} \\ &\leq \sum \|\phi_{ny}\|^2_{L^2(0,1)}, \end{aligned} \tag{8.3.55}$$

where we have used the classical Poincaré's formula for functions of $H^1(0,1)$ vanishing at 0, since $\phi \in H^1_h(\Omega)$ implies $\phi_n \in H^1(0,1)$, and $\phi|_{\partial\Omega_0} \equiv 0$ implies $\phi_n(0) = 0$.

By the same reasoning, $\psi \in H_h^2(\Omega)$ implies $\psi_n \in H^2(0,1)$, and $\psi|_{\partial\Omega_i} \equiv 0$ implies $\psi_n(i) = 0$, for $i = 0, 1$. Applying Lemma 8.5 for every n,

$$\begin{aligned} \|\psi_y\|^2_{L^2_h(\Omega)} &= \sum \|\psi_{ny}\|^2_{L^2(0,1)} \\ &\leq \sum \|\phi_{nyy}\|^2_{L^2(0,1)} = \|\psi_{yy}\|^2_{L^2_h(\Omega)}, \end{aligned} \tag{8.3.56}$$

thus proving the lemma. □

Remark 8.7. As in Lemma 8.6, let $\phi \in H_h^1(\Omega)$ be such that $\phi|_{\partial\Omega_0} \equiv 0$, and $\psi \in H_h^2(\Omega)$ such that $\psi|_{\partial\Omega_i} \equiv 0$ for $i = 0, 1$. Then we can redefine the H^1 norm of ϕ and H^2 norm of ψ as

$$\|\phi\|^2_{H^1_h(\Omega)} = \|\phi_y\|^2_{L^2_h(\Omega)} + \|\phi_x\|^2_{L^2_h(\Omega)}, \tag{8.3.57}$$

$$\|\psi\|^2_{H^2_h(\Omega)} = \|\psi_{yy}\|^2_{L^2_h(\Omega)} + \|\psi_{xx}\|^2_{L^2_h(\Omega)} + \|\psi_{xy}\|^2_{L^2_h(\Omega)}, \tag{8.3.58}$$

or, in terms of the Fourier coefficients,

$$\|\phi\|^2_{H^1_h(\Omega)} = \sum \left[\frac{\pi^2 n^2}{h^2} \|\phi_n\|^2_{L^2(0,1)} + \|\phi_{ny}\|^2_{L^2(0,1)} \right], \tag{8.3.59}$$

$$\|\psi\|^2_{H^2_h(\Omega)} = \sum \left[\frac{\pi^4 n^4}{h^4} \|\psi_n\|^2_{L^2(0,1)} + \frac{\pi^2 n^2}{h^2} \|\psi_{ny}\|^2_{L^2(0,1)} + \|\psi_{nyy}\|^2_{L^2(0,1)} \right]. \tag{8.3.60}$$

8.3.4 Spaces for the velocity field

Calling $\mathbf{w} = (u, V)$, we define

$$H_{0h}(\Omega) = \{\mathbf{w} \in [L^2_h(\Omega)]^2 : \nabla \cdot \mathbf{w} = 0, \mathbf{w}|_{\partial\Omega_0} = 0\}, \tag{8.3.61}$$

$$H^1_{0h}(\Omega) = H_{0h}(\Omega) \cap [H^1_h(\Omega)]^2, \tag{8.3.62}$$

$$H^2_{0h}(\Omega) = H_{0h}(\Omega) \cap [H^2_h(\Omega)]^2, \tag{8.3.63}$$

endowed with the scalar product of, respectively, $[L^2_h(\Omega)]^2$, $[H^1_h(\Omega)]^2$ and $[H^2_h(\Omega)]^2$. See [108, page 9] for the precise meaning of the terms in (8.3.61).

These are the spaces for the velocity field and where the main results have to be considered.

8.3.5 Transformations of L^2 functions

The following definitions establish facts and notations useful for our solution, based on the backstepping method [101]. This method consists in finding an invertible transformation of the original variables into others whose stability properties are easy to establish. We study the kind of transformations that appear in the method.

Definition 8.8. *Let* $\mathcal{T} = \{(y, \eta) \in \mathbb{R}^2 : 0 \leq \eta \leq y \leq 1\}$. *Given complex valued functions* $f \in L^2(0,1)$ *and* $K \in L^\infty(\mathcal{T})$, *we define the* transformed *variable* $g = (\mathrm{I} - K)f$, *where the operator* Kf *is defined by*

$$Kf(y) = \int_0^y K(y,\eta) f(\eta) d\eta, \tag{8.3.64}$$

i.e. a Volterra operator. We call $\mathrm{I} - K$ *the* direct *transformation with* kernel K. *Now, if there exists a function* $L \in L^\infty(\mathcal{T})$ *such that* $f = (\mathrm{I} + L)g$, *then we say that the transformation is invertible, and we call* $\mathrm{I} + L$ *the* inverse *transformation, and* L *the* inverse kernel *(or the inverse of* K*).*

The following result is immediate from the theory of Volterra integral equations [61].

Proposition 8.9. *For* $K \in L^\infty(\mathcal{T})$, *the transformation* $\mathrm{I} - K$ *is always invertible. Moreover,* L *is related to* K *by*

$$\begin{aligned} L(y,\eta) &= K(y,\eta) + \int_\eta^y K(y,\sigma) L(\sigma,\eta) d\sigma \\ &= K(y,\eta) + \int_\eta^y L(y,\sigma) K(\sigma,\eta) d\sigma. \end{aligned} \tag{8.3.65}$$

The following result holds.

Proposition 8.10. *If* $f \in L^2(0,1)$ *then* $g = (\mathrm{I} - K)f$ *is in* $L^2(0,1)$. *Similarly, if* $g \in L^2(0,1)$ *then* $f = (\mathrm{I} + L)g$ *is in* $L^2(0,1)$. *Moreover,*

$$\|g\|^2_{L^2(0,1)} \leq (1 + \|K\|_{L^\infty})^2 \|f\|^2_{L^2(0,1)}, \tag{8.3.66}$$

$$\|f\|^2_{L^2(0,1)} \leq (1 + \|L\|_{L^\infty})^2 \|g\|^2_{L^2(0,1)}. \tag{8.3.67}$$

Proof. Calculating the L^2 norm on the transformed variable in Definition 8.8, and then using Cauchy-Schwarz inequality repeatedly,

$$\begin{aligned}\int_0^1 |g(y)|^2 dy &= \int_0^1 \left| f(y) - \int_0^y K(y,\eta) f(\eta) d\eta \right|^2 dy \\ &= \int_0^1 \Bigg(|f(y)|^2 - f(y) \overline{\int_0^y K(y,\eta) f(\eta) d\eta} - \overline{f(y)} \int_0^y K(y,\eta) f(\eta) d\eta \\ &\quad + \left| \int_0^y K(y,\eta) f(\eta) d\eta \right|^2 d\eta \Bigg) dy \\ &\leq \int_0^1 \Bigg(|f(y)|^2 + 2\|K\|_{L^\infty} |f(y)| \int_0^y |f(\eta)| d\eta \\ &\quad + \|K\|_{L^\infty}^2 \int_0^y |f(\eta)|^2 \, d\eta \Bigg) dy, \end{aligned} \tag{8.3.68}$$

and now since

$$\int_0^1 |f(y)| \int_0^y |f(\eta)| d\eta dy \leq \left(\int_0^1 |f(y)| dy \right)^2 \leq \int_0^1 |f(y)|^2 dy, \tag{8.3.69}$$

then

$$\begin{aligned}\int_0^1 |g(y)|^2 dy &\leq \int_0^1 \left(1 + 2\|K\|_{L^\infty} + \|K\|_{L^\infty}^2\right) |f(y)|^2 dy \\ &= (1 + \|K\|_{L^\infty})^2 \int_0^1 |f(y)|^2 dy, \end{aligned} \tag{8.3.70}$$

so one has that

$$\|g\|_{L^2(0,1)}^2 \leq (1 + \|K\|_{L^\infty})^2 \|f\|_{L^2(0,1)}^2, \tag{8.3.71}$$

and similarly for the inverse transformation. □

Proposition 8.10 allows to define a norm equivalent to the L^2 norm,

$$\|f\|_{KL^2(0,1)}^2 = \|(\mathrm{I} - K) f\|_{L^2(0,1)}^2 = \|g\|_{L^2(0,1)}^2. \tag{8.3.72}$$

For $\mathcal{C}^1(\mathcal{T})$ and $\mathcal{C}^2(\mathcal{T})$ kernels K and L, one has an equivalent version of Proposition 8.9 and Proposition 8.10, allowing to define respectively a $KH^1(0,1)$ and $KH^2(0,1)$ norm, which are equivalent to the $H^1(0,1)$ and $H^2(0,1)$ norm.

$$\|f\|_{KH^1(0,1)}^2 = \|(I - K) f\|_{H^1(0,1)}^2 = \|g\|_{H^1(0,1)}^2, \tag{8.3.73}$$

$$\|f\|_{KH^2(0,1)}^2 = \|(I - K) f\|_{H^2(0,1)}^2 = \|g\|_{H^2(0,1)}^2. \tag{8.3.74}$$

where higher derivatives are calculated from the transformation in the following way

$$\begin{aligned} g_y &= f_y - K(y,y)f(y) - \int_0^y K_y(y,\eta)f(\eta)d\eta, & (8.3.75)\\ g_{yy} &= f_{yy} - K(y,y)f_y(y) - 2K_y(y,y)f(y) - K_\eta(y,y)f(y) \\ &\quad - \int_0^y K_{yy}(y,\eta)f(\eta)d\eta, & (8.3.76)\end{aligned}$$

and similarly for the inverse transformation. This implies that the following estimates hold

$$\begin{aligned} \|f\|^2_{KH^1(0,1)} &\leq (1+\|K\|_{L^\infty}+\|K_y\|_{L^\infty})^2\|f\|^2_{H^1(0,1)}, & (8.3.77)\\ \|f\|^2_{KH^1(0,1)} &\geq (1+\|L\|_{L^\infty}+\|L_y\|_{L^\infty})^{-2}\|f\|^2_{H^1(0,1)}, & (8.3.78)\end{aligned}$$

and other similar estimates for the H^2 norm.

8.3.6 Transformations of the velocity field

We define transformations of functions in $H_{0h}(\Omega)$.

Definition 8.11. *Consider a set of indices $A = \{a_1, \ldots, a_j\} \subset \mathbb{Z}$, and $\mathcal{K} = (K_n(y,\eta))_{n\in A}$ a family of $L^\infty(\mathcal{T})$ kernels. Then, for $\mathbf{w} = (u,v) \in H_{0h}(\Omega)$, one defines the* transformed *variable $\omega = (\alpha,\beta) = (\mathrm{I}-\mathcal{K})\mathbf{w}$, through its Fourier components,*

$$\omega_n = \begin{cases} ((\mathrm{I}-K_n)u_n, 0) & \text{for}\, n \in A, \\ \mathbf{w}_n, & \text{otherwise.}\end{cases} \qquad (8.3.79)$$

The inverse transformation, $\mathbf{w} = (I+\mathcal{L})\omega$, is defined by

$$\mathbf{w} = \begin{cases} ((\mathrm{I}+L_n)\alpha_n, \hat{L}_n\alpha_n) & \text{for}\, n \in A, \\ \omega_n, & \text{otherwise,}\end{cases} \qquad (8.3.80)$$

where the new operator $\hat{L}_n$ is defined by

$$\hat{L}_n f = -\pi i \frac{n}{h}\int_0^y \left(f(\eta) + \int_0^\eta L(\eta,\sigma)f(\sigma)d\sigma\right)d\eta. \qquad (8.3.81)$$

It is straightforward to show that $\mathbf{w}$ is well defined in (8.3.80). We only need to check the second component of $\mathbf{w}$ in (8.3.80) when $n \in A$, which is

$$\hat{L}_n \alpha_n = -\pi i \frac{n}{h} \int_0^y \left(\alpha_n(\eta) + \int_0^\eta L(\eta,\sigma)\alpha_n(\sigma) d\sigma \right) d\eta, \tag{8.3.82}$$

and then substituting the definition of α_n from the direct transformation, and after some manipulation,

$$\begin{aligned} \hat{L}_n \alpha_n &= -\pi i \frac{n}{h} \int_0^y \left(u_n(\eta) - \int_0^\eta \left[K_n(\eta,\sigma) - L_n(\eta,\sigma) \right.\right. \\ &\quad \left.\left. + \int_\sigma^\eta L_n(\eta,\delta) K_n(\delta,\sigma) d\delta \right] u_n(\delta) d\sigma \right) d\eta, \end{aligned} \tag{8.3.83}$$

where the expression in brackets is zero by Proposition 8.9. Then,

$$\hat{L}_n \alpha_n = -\pi i \frac{n}{h} \int_0^y u_n(\eta) d\eta, \tag{8.3.84}$$

and since the divergence-free condition in Fourier space is $\pi i \frac{n}{h} u_n + v_{ny} = 0$ and $v_n(0) = 0$ one gets that

$$\hat{L}_n \alpha_n = \int_0^y v_{ny}(\eta) d\eta = v_n(y) - v_n(0) = v_n(y). \tag{8.3.85}$$

This way, even though the second component of the velocity is apparently lost in the direct transformation, it can be recovered and the transformation is still invertible. Using a similar argument as in Proposition 8.10,

$$\|\omega\|^2_{H_{0h}(\Omega)} \leq (1 + \|\mathcal{K}\|_{L^\infty})^2 \|\mathbf{w}\|^2_{H_{0h}(\Omega)}, \tag{8.3.86}$$

$$\|\mathbf{w}\|^2_{H_{0h}(\Omega)} \leq (1 + N^2)(1 + \|\mathcal{L}\|_{L^\infty})^2 \|\omega\|^2_{H_{0h}(\Omega)}, \tag{8.3.87}$$

where $N = \max_{n \in A}\{\pi \frac{n}{h}\}$, and

$$\|\mathcal{K}\|_{L^\infty} = \max_{n \in A}\{\|K_n\|_{L^\infty}\}, \tag{8.3.88}$$

$$\|\mathcal{L}\|_{L^\infty} = \max_{n \in A}\{\|L_n\|_{L^\infty}\}. \tag{8.3.89}$$

This allows the definition of a norm, as in (8.3.72), equivalent to the $H_{0h}(\Omega)$, that we call $\mathcal{K}H_{0h}(\Omega)$,

$$\|\mathbf{w}\|^2_{\mathcal{K}H_{0h}(\Omega)} = \|\omega\|^2_{H_{0h}(\Omega)}. \tag{8.3.90}$$

For $\mathcal{C}^1(\mathcal{T})$ and $\mathcal{C}^2(\mathcal{T})$ kernel families one can define as well $\mathcal{K}H^1_{0h}(\Omega)$ and $\mathcal{K}H^2_{0h}(\Omega)$ norms, respectively equivalent to the regular $H^1_{0h}(\Omega)$ and $H^2_{0h}(\Omega)$ norms.

Remark 8.12. All previous results hold for transformation kernels depending on time, as long as they are uniformly bounded on the time interval (finite or infinite) considered (see Proposition 8.21 for such a statement).

8.4 Main result

First, we state the stabilizing control laws for the controllers V_c and U_c.

The controller $V_c(t,x)$ is a dynamic controller, found as the unique solution of the following forced parabolic equation

$$\begin{aligned} V_{ct} &= \frac{V_{cxx}}{Re} - \sum_{0<|n|<M} \int_{-h}^{h} \mathrm{e}^{i\gamma_n(\xi-x)} \left[2i \int_0^1 g_y(t,\eta) \cosh\left(\gamma_n(1-\eta)\right) v(t,\xi,\eta) d\eta \right. \\ & \quad \left. -i \frac{u_y(t,\xi,0) - u_y(t,\xi,1)}{Re} \right] d\xi, \end{aligned} \tag{8.4.91}$$

initialized at zero[4], with periodic boundary conditions, i.e., $V_c(t,-h) = V_c(t,h)$.

The control law U_c is given by

$$U_c(t,x) = \sum_{0<|n|<M} \int_{-h}^{h} \int_0^1 \mathrm{e}^{i\gamma_n(\xi-x)} K_n(t,1,\eta) u(t,\xi,\eta) d\eta d\xi, \tag{8.4.92}$$

where $M = \frac{2h\sqrt{Re}}{\pi}$, and $\gamma_n = \pi n/h$. For every integer n such that $0 < |n| < M$, K_n in (8.4.92) is the solution of the following kernel equation[5]

$$\begin{aligned} K_{nt} &= \frac{1}{Re}\left(K_{nyy} - K_{n\eta\eta}\right) - \lambda_n(t,\eta) K_n + f_n(y,\eta) \\ & \quad - \int_\eta^y f_n(\xi,\eta) K_n(t,y,\xi) d\xi, \end{aligned} \tag{8.4.93}$$

a linear partial integro-differential equation in the region $\Gamma = \{(t,y,\eta) \in (0,\infty) \times$

[4]If the velocity field initial conditions at the boundary were not zero, then it is required that $V_c(0,x) = V(0,x,1)$. We asume for simplicity $V(0,x,1) = 0$.

[5]See Proposition 8.21 in Section 8.5 regarding the solvability of (8.4.93)–(8.4.95).

$\mathcal{T}\}$, where $\mathcal{T} = \{(y,\eta) \in \mathbb{R}^2 : 0 \leq \eta \leq y \leq 1\}$, with boundary conditions

$$K_n(t,y,y) = -Re\left(\int_0^y \frac{\lambda_n(\sigma)}{2} d\sigma + \mu_n(0)\right), \tag{8.4.94}$$

$$K_n(t,y,0) = Re\left[\int_0^y \mu_n(\sigma) K_n(t,y,\sigma) d\sigma - \mu_n(y)\right], \tag{8.4.95}$$

and where the coefficients in (8.4.93)–(8.4.95) are

$$\lambda_n(t,y) = -i\gamma_n g(t,y), \tag{8.4.96}$$

$$f_n(t,y,\eta) = -\, i\gamma_n \left[g_y(t,y) + 2\gamma_n \int_\eta^y g_y(t,\sigma) \times \sinh\left(\gamma_n(y-\sigma)\right) d\sigma\right], \tag{8.4.97}$$

$$\mu_n(y) = \frac{\gamma_n}{Re} \frac{\cosh\left(\gamma_n(1-y)\right) - \cosh\left(\gamma_n y\right)}{\sinh \gamma_n}. \tag{8.4.98}$$

Remark 8.13. Averaging (in x) Equation (8.4.91) it can be seen that the mean component of V_c is zero (provided it is initialized at zero), thus the physical constraint of zero net flux is enforced. This can be written as

$$\int_{-h}^{h} V_c(t,\xi) d\xi = 0. \tag{8.4.99}$$

Verifying this condition is crucial, since its violation would imply not satisfying mass conservation in the channel. Also it is mathematically important to ensure the well-posedness of the closed-loop problem.

In the sequel, let the letter C with a subindex denote a positive constant. We now state our results.

Proposition 8.14. *Define $\mathbf{w}(t) = (u(t), V(t))$. Call $\mathbf{w}_0$ the initial condition of the velocity field. Suppose that $\mathbf{w}_0 \in H^2_{0h}(\Omega)$ and verifies the compatibility conditions $V_0(x,1) = 0$ and*

$$u_0(x,1) = \sum_{0<|n|<M} \int_{-h}^{h} \int_0^1 e^{i\gamma_n(\xi - x)} K_n(0,1,\eta) u_0(\xi,\eta) d\eta d\xi. \tag{8.4.100}$$

Then, for any Reynolds number, there exists a unique solution $\mathbf{w}(t)$ of (8.2.27)–(8.2.26) with control laws (8.4.91)–(8.4.92), with $\mathbf{w} \in L^2((0,\infty), H^2_{0h}(\Omega))$. Moreover, the equilibrium $\mathbf{w} \equiv 0$ is exponentially stable in the L^2, H^1 and H^2 norms, *i.e., there exist numbers $C_1(Re, h)$, $C_2(Re, h) > 0$ such that for $t \geq 0$, the solution* $\mathbf{w}$ *satisfies*

$$\|\mathbf{w}(t)\| \leq C_1 \mathrm{e}^{-C_2 t} \|\mathbf{w}_0\|, \tag{8.4.101}$$

where $\|\cdot\|$ represents the $H_{0h}(\Omega)$, $H^1_{0h}(\Omega)$ or $H^2_{0h}(\Omega)$ norm.

The result above is valid for any initial condition. If we consider the nonlinear terms, we obtain just local stability.

Proposition 8.15. *Suppose that $\mathbf{w}_0 \in H^2_{0h}(\Omega)$ verifying $V_0(x, 1) = 0$ and (8.4.100). Then, for every Reynolds number, there exists $\epsilon > 0$ such that if $\|\mathbf{w}_0\| < \epsilon$ then there is a unique solution $\mathbf{w}(t)$ of the Navier-Stokes system (8.2.22)–(8.2.23) with boundary conditions (8.2.24)–(8.2.26) and control laws (8.4.91)–(8.4.92), such that $\mathbf{w} \in L^2((0,\infty), H^2_{0h}(\Omega))$. Moreover the equilibrium $\mathbf{w} \equiv 0$ is locally exponentially stable in the L^2, H^1 and H^2 norms, i.e., there exist numbers $C_1(Re, h)$, $C_2(Re, h) > 0$ such that, for $t \geq 0$, the solution $\mathbf{w}$ satisfies*

$$\|\mathbf{w}(t)\| \leq C_1 \mathrm{e}^{-C_2 t} \|\mathbf{w}_0\|, \tag{8.4.102}$$

where $\|\cdot\|$ represents the $H_{0h}(\Omega)$, $H^1_{0h}(\Omega)$ or $H^2_{0h}(\Omega)$ norm.

Recall that the aim is to pass asymptotically and robustly from one Poiseuille flow (or from a point in a neighborhood) to another arbitrary Poiseuille flow (or a neighborhood), for the nonlinear Navier-Stokes equations. From the results of Section 8.2 and Proposition 8.15, we obtain our main result, which solves the problem.

Theorem 8.16. *Call $\mathbf{W} = (U, V, P)$. Consider two arbitrary Poiseuille flows $\mathcal{P}^{\delta_1}$ and $\mathcal{P}^{\delta_2}$, as in (8.2.1). Then for every Reynolds number there exist neighborhoods $\mathcal{V}_0$ of $\mathcal{P}^{\delta_0}$ and $\mathcal{V}_1$ of $\mathcal{P}^{\delta_1}$, in $H^2(\Omega)$, such that, for every $\mathbf{W}_0 \in \mathcal{V}_0$ such that $\mathbf{W}_0 - \mathcal{P}^{\delta_0}$ is periodic in x, there exists a unique solution $\mathbf{W}$ of (4.2.1)–(4.2.3), with imposed pressure gradient (8.2.4), and control laws (8.4.91)–(8.4.98), which writes $\mathbf{W}(t) = \Theta^q(t) + \mathbf{w}(t)$, where $\Theta^q(t)$ is given by (8.2.2), such that $\mathbf{W}(t) \in \mathcal{V}_2$*

for t large enough. Moreover, there exist numbers $C_1(Re,h)$, $C_2(Re,h) > 0$ such that, for $t \geq 0$, $\mathbf{w}$ satisfies

$$\|\mathbf{w}(t)\| \leq C_1 \mathrm{e}^{-C_2 t} \|\mathbf{w}_0\|, \tag{8.4.103}$$

where $\|\cdot\|$ represents the $H_{0h}(\Omega)$, $H^1_{0h}(\Omega)$ or $H^2_{0h}(\Omega)$ norm.

Remark 8.17. If in the previous results, the initial data is only in $H^1_{0h}(\Omega)$ (small enough for Proposition 8.15 in the $H^1_{0h}(\Omega)$-norm), even without the compatibility condition (8.4.100), we still have a unique solution $\mathbf{w}(t)$ in $L^2((0,\infty), H^1_{0h}(\Omega))$ and the exponential decay of the $H^1_{0h}(\Omega)$-norm.

Remark 8.18. To make a faster tranfer, the exponential decay rate C_2 in Propositions 8.14 and 8.15 and Theorem 8.16 can be made as large as desired, just increasing as much as necessary M and λ_n in (8.4.96), so that

$$M = \frac{2h\sqrt{Re}}{\pi} + \bar{M}, \tag{8.4.104}$$

$$\lambda_n = -i\gamma_n g(t,y) + \bar{\lambda}, \tag{8.4.105}$$

for large enough $\bar{M}, \bar{\lambda} > 0$. Increasing M means that more modes are controlled, whereas the modes left uncontrolled (see Section 8.5.1) are more damped. Increasing λ means that more damping is added in the target system (8.5.160), so that controlled modes (see Section 8.5.2) decay faster.

The next sections are devoted to proving the results, explaining the control design method, and studying the solvability of Equations (8.4.93)–(8.4.95).

8.5 Proof of Proposition 8.14

Equations (8.2.27)–(8.2.28) written in the periodic Fourier space are

$$u_{nt} = \frac{\triangle_n u_n}{Re} - i\gamma_n(p_n + g(t,y)u_n) - g_y(t,y)V_n, \tag{8.5.106}$$

$$V_{nt} = \frac{\triangle_n V_n}{Re} - p_{ny} - i\gamma_n g(t,y)V_n, \tag{8.5.107}$$

where $\triangle_n = \partial_{yy} - \gamma_n^2$ has been introduced for simplifying the expressions, and where $\gamma_n = \pi n/h$. The boundary conditions are

$$\begin{aligned} u_n(t,0) &= V_n(t,0) = 0, & (8.5.108)\\ u_n(t,1) &= U_{cn}(t), & (8.5.109)\\ V_n(t,1) &= V_{cn}(t), & (8.5.110)\end{aligned}$$

and the divergence-free condition is

$$\gamma_n u_n + V_{ny} = 0. \tag{8.5.111}$$

From (8.5.106)–(8.5.107) an equation for the pressure can be derived,

$$p_{nyy} - \gamma_n^2 p_n = -2i\gamma_n g_y(t,y) V_n, \tag{8.5.112}$$

with boundary conditions obtained from evaluating (8.5.107) at the boundaries and using (8.5.109)–(8.5.110),

$$\begin{aligned} p_{ny}(t,0) &= -i\gamma_n \frac{u_{ny}(t,0)}{Re}, & (8.5.113)\\ p_{ny}(t,1) &= -i\gamma_n \frac{u_{ny}(t,1)}{Re} - \dot{V}_{cn} - \gamma_n^2 \frac{V_{cn}}{Re}. & (8.5.114)\end{aligned}$$

As in Chapter 4 for the continuous-spectrum Fourier space, the equations for different n are uncoupled due to linearity and spatial invariance, allowing separate consideration for each mode n. As before, most modes, which we refer to as *uncontrolled*, are naturally stable and thus left without control. A finite set of modes, called *controlled*, are unstable and require control.

8.5.1 Uncontrolled modes

These are $n = 0$ and large modes that verify $|n| \geq M$, where $M > 0$ will be made precise.

$n = 0$ (mean velocity field)

From (8.5.111), $V_0 \equiv 0$. Then, u_0 verifies

$$u_{0t} = \frac{u_{0yy}}{Re}, \tag{8.5.115}$$

with $u_0(0) = u_0(1) = 0$. The following estimates hold by applying Lemma 8.5,

$$\begin{aligned}
\frac{d}{dt}\|u_0\|^2_{L^2(0,1)} &\leq -\frac{2}{Re}\|u_0\|^2_{L^2(0,1)}, && (8.5.116)\\
\frac{d}{dt}\|u_0\|^2_{H^1(0,1)} &\leq -\frac{2}{Re}\|u_0\|^2_{H^1(0,1)}, && (8.5.117)\\
\frac{d}{dt}\|u_0\|^2_{H^2(0,1)} &\leq -\frac{1}{Re}\|u_0\|^2_{H^2(0,1)}, && (8.5.118)
\end{aligned}$$

implying

$$\begin{aligned}
\|u_0(t)\|^2_{L^2(0,1)} &\leq \mathrm{e}^{-\frac{2}{Re}t}\|u_0(0)\|^2_{L^2(0,1)}, && (8.5.119)\\
\|u_0(t)\|^2_{H^1(0,1)} &\leq \mathrm{e}^{-\frac{2}{Re}t}\|u_0(0)\|^2_{H^1(0,1)}, && (8.5.120)\\
\|u_0(t)\|^2_{H^2(0,1)} &\leq \mathrm{e}^{-\frac{1}{Re}t}\|u_0(0)\|^2_{H^2(0,1)}. && (8.5.121)
\end{aligned}$$

Modes for large $|n|$

If $\mathbf{w}_n = (u_n, V_n)$, then, considering no control ($V_{cn} = U_{cn} = 0$),

$$\begin{aligned}
\frac{d}{dt}\|\mathbf{w}_n\|^2_{L^2(0,1)^2} &= -2\frac{\|\mathbf{w}_{ny}\|^2_{L^2(0,1)^2}}{Re} - 2\gamma_n^2\frac{\|\mathbf{w}_n\|^2_{L^2(0,1)^2}}{Re} - (g_y u_n, V_n)_{L^2(0,1)^2}\\
&\quad - (g_y V_n, u_n)_{L^2(0,1)^2} - (u_n, i\gamma_n p_n)_{L^2(0,1)^2} - (i\gamma_n p_n, u_n)_{L^2(0,1)^2}\\
&\quad - (V_n, p_{ny})_{L^2(0,1)^2} - (p_{ny}, V_n)_{L^2(0,1)^2}\,. && (8.5.122)
\end{aligned}$$

Consider the pressure terms like those in the last two lines of (8.5.122). Using the divergence- free condition $i\gamma_n u_n + V_{ny} = 0$, and integrating by parts,

$$-(u_n, i\gamma_n p_n)_{L^2(0,1)^2} = -(V_{ny}, p_n)_{L^2(0,1)^2} = (V_n, p_{ny})_{L^2(0,1)^2}\,. \qquad (8.5.123)$$

Therefore, the pressure terms in (8.5.122) cancel each other. Then, using Cauchy-Schwarz inequality and $ab \leq (a^2 + b^2)/2$,

$$\begin{aligned}
\frac{d}{dt}\|\mathbf{w}_n\|^2_{L^2(0,1)^2} &\leq -2\frac{\|\mathbf{w}_{ny}\|^2_{L^2(0,1)^2}}{Re} - 2\gamma_n^2\frac{\|\mathbf{w}_n\|^2_{L^2(0,1)^2}}{Re}\\
&\quad + \|g_y\|_{L^\infty(0,1)}\|\mathbf{w}_n\|^2_{L^2(0,1)^2}. && (8.5.124)
\end{aligned}$$

Since $|g_y(t, y)| \leq 4$, choosing $|\gamma_n| \geq \sqrt{2Re}$, i.e.,

$$|n| \geq M = \frac{2h\sqrt{Re}}{\pi}, \qquad (8.5.125)$$

yields

$$\frac{d}{dt}\|\mathbf{w}_n\|^2_{L^2(0,1)^2} \leq -2\frac{\|\mathbf{w}_{ny}\|^2_{L^2(0,1)^2}}{Re} - \gamma_n^2\frac{\|\mathbf{w}_n\|^2_{L^2(0,1)^2}}{Re} \leq -2\frac{\|\mathbf{w}_n\|^2_{L^2(0,1)^2}}{Re}, \quad (8.5.126)$$

by Poincaré's inequality, therefore achieving L^2 exponential stability for large modes ($|n| \geq M$).

H^1 exponential stability is proved for the same set of modes. For this, calculate first the time derivative of $\|\mathbf{w}_{ny}\|^2_{L^2(0,1)^2}$

$$\begin{aligned}
\frac{d}{dt}\|\mathbf{w}_{ny}\|^2_{L^2(0,1)^2}, \quad &= \quad (\mathbf{w}_{ny}, \mathbf{w}_{nyt})_{L^2(0,1)^2} + (\mathbf{w}_{nyt}, \mathbf{w}_{ny})_{L^2(0,1)^2} \\
&= \quad -(\mathbf{w}_{nyy}, \mathbf{w}_{nt})_{L^2(0,1)^2} - (\mathbf{w}_{nt}, \mathbf{w}_{nyy})_{L^2(0,1)^2} \\
&= \quad -2\frac{\|\mathbf{w}_{nyy}\|^2_{L^2(0,1)^2}}{Re} - 2\gamma_n^2\frac{\|\mathbf{w}_{ny}\|^2_{L^2(0,1)^2}}{Re} \\
&\quad\quad +i\gamma_n(\mathbf{w}_{nyy}, g\mathbf{w}_n)_{L^2(0,1)^2} - i\gamma_n(g\mathbf{w}_n, \mathbf{w}_{nyy})_{L^2(0,1)^2} \\
&\quad\quad +i\gamma_n(u_{nyy}, p_n)_{L^2(0,1)} - i\gamma_n(p_n, u_{nyy})_{L^2(0,1)} \\
&\quad\quad -(V_{nyy}, p_{ny})_{L^2(0,1)} - (p_{ny}, V_{nyy})_{L^2(0,1)} \\
&\quad\quad -(u_{nyy}, g_y V_n)_{L^2(0,1)} - (g_y V_n, u_{nyy})_{L^2(0,1)}. \quad (8.5.127)
\end{aligned}$$

Let us study first the terms without pressure. We have that

$$\begin{aligned}
&\quad i\gamma_n(\mathbf{w}_{nyy}, g\mathbf{w}_n)_{L^2(0,1)^2} - i\gamma_n(g\mathbf{w}_n, \mathbf{w}_{nyy})_{L^2(0,1)^2} \\
&\quad -(u_{nyy}, g_y V_n)_{L^2(0,1)} - (g_y V_n, u_{nyy})_{L^2(0,1)} \\
&= \quad -i\gamma_n(\mathbf{w}_{ny}, g\mathbf{w}_{ny} + g_y\mathbf{w}_n)_{L^2(0,1)^2} + i\gamma_n(g\mathbf{w}_{ny} + g_y\mathbf{w}_n, \mathbf{w}_{ny})_{L^2(0,1)^2} \\
&\quad +(u_{ny}, g_{yy}V_n + g_y V_{ny})_{L^2(0,1)} + (g_{yy}V_n + g_y V_{ny}, u_{ny})_{L^2(0,1)} \\
&= \quad -i\gamma_n(\mathbf{w}_{ny}, g_y\mathbf{w}_n)_{L^2(0,1)^2} + i\gamma_n(g_y\mathbf{w}_n, \mathbf{w}_{ny})_{L^2(0,1)^2} \\
&\quad +(u_{ny}, g_{yy}V_n)_{L^2(0,1)} + (g_{yy}V_n, u_{ny})_{L^2(0,1)} \\
&\quad +i\gamma_n(u_{ny}, g_y u_n)_{L^2(0,1)} - i\gamma_n(g_y u_n, u_{ny})_{L^2(0,1)} \\
&= \quad -i\gamma_n(\mathbf{w}_{ny}, g_y\mathbf{w}_n)_{L^2(0,1)^2} + i\gamma_n(g_y\mathbf{w}_n, \mathbf{w}_{ny})_{L^2(0,1)^2} \\
&\quad +(u_{ny}, g_{yy}V_n)_{L^2(0,1)} + (g_{yy}V_n, u_{ny})_{L^2(0,1)} \\
&\leq \quad \frac{\gamma_n^2+1}{Re}\|\mathbf{w}_{ny}\|^2_{L^2(0,1)^2} + Re\left(\|g_y\|^2_{L^\infty(0,1)} + \|g_{yy}\|^2_{L^\infty(0,1)}\right) \\
&\quad \times\|\mathbf{w}_n\|^2_{L^2(0,1)^2}, \quad (8.5.128)
\end{aligned}$$

where we have used repeatedly integration by parts, Cauchy-Schwarz inequality and the divergence-free condition.

Now for the pressure terms, proceeding as before,

$$
\begin{aligned}
& i\gamma_n(u_{nyy}, p_n)_{L^2(0,1)} - i\gamma_n(p_n, u_{nyy})_{L^2(0,1)} - (V_{nyy}, p_{ny})_{L^2(0,1)} - (p_{ny}, V_{nyy})_{L^2(0,1)} \\
= \quad & -\Big[V_{nyy}(t,y)\overline{p}_n(t,y) + \overline{V}_{nyy}(t,y)p_n(t,y)\Big]_{y=0}^{y=1} \\
= \quad & -Re\Big[p_{ny}(t,y)\overline{p}_n(t,y) + \overline{p}_{ny}(t,y)p_n(t,y)\Big]_{y=0}^{y=1}, \qquad (8.5.129)
\end{aligned}
$$

where the last equality is deduced from (8.5.107) evaluated at the boundaries.

Regarding (8.5.129) we have the following result.

Lemma 8.19.

$$
-\Big[p_{ny}(t,y)\overline{p}_n(t,y) + \overline{p}_{ny}(t,y)p_n(t,y)\Big]_{y=0}^{y=1} \leq 2\|g_y\|^2_{L^\infty(0,1)}\|V_n\|^2_{L^2(0,1)} \qquad (8.5.130)
$$

Proof. Multiplying the Poisson pressure equation (8.5.112) by $\overline{p}_n$ and integrating, one has

$$
(p_{nyy}, p_n)_{L^2(0,1)} - \gamma_n^2\|p_n\|^2_{L^2(0,1)} = -2i\gamma_n(g_y(t,y)V_n, p_n)_{L^2(0,1)} \qquad (8.5.131)
$$

integrating by parts, and using (8.5.113)–(8.5.114), it follows that

$$
\begin{aligned}
& \Big[p_{ny}(t,y)\overline{p}_n(t,y)\Big]_{y=0}^{y=1} - \|p_{ny}\|^2_{L^2(0,1)} - \gamma_n^2\|p_n\|^2_{L^2(0,1)} \\
= \quad & -2i\gamma_n(g_y(t,y)V_n, p_n)_{L^2(0,1)}, \qquad (8.5.132)
\end{aligned}
$$

and using Cauchy-Schwarz inequality,

$$
\begin{aligned}
-\Big[p_{ny}(t,y)\overline{p}_n(t,y)\Big]_{y=0}^{y=1} \quad = \quad & -\|p_{ny}\|^2_{L^2(0,1)} - \gamma_n^2\|p_n\|^2_{L^2(0,1)} \\
& +2i\gamma_n(g_y(t,y)V_n, p_n)_{L^2(0,1)} \\
\leq \quad & \|g_y\|^2_{L^\infty(0,1)}\|V_n\|^2_{L^2(0,1)}. \qquad (8.5.133)
\end{aligned}
$$

Adding (8.5.133) to its complex conjugate yields the result. □

By previous estimates we reach then

$$
\begin{aligned}
\frac{d}{dt}\|\mathbf{w}_{ny}\|^2_{L^2(0,1)^2} &\leq -2\frac{\|\mathbf{w}_{nyy}\|^2_{L^2(0,1)^2}}{Re} - 2\gamma_n^2\frac{\|\mathbf{w}_{ny}\|^2_{L^2(0,1)^2}}{Re} + \frac{\gamma_n^2+1}{Re}\|\mathbf{w}_{ny}\|^2_{L^2(0,1)^2} \\
&\quad + Re\left(3\|g_y\|^2_{L^\infty(0,1)} + \|g_{yy}\|^2_{L^\infty(0,1)}\right)\|\mathbf{w}_n\|^2_{L^2(0,1)^2}, \qquad (8.5.134)
\end{aligned}
$$

and using Lemma 8.5, and substituting the bounds on g, one gets that

$$
\begin{aligned}
\frac{d}{dt}\|\mathbf{w}_{ny}\|^2_{L^2(0,1)^2} &\leq -\frac{\|\mathbf{w}_{nyy}\|^2_{L^2(0,1)^2}}{Re} - \gamma_n^2\frac{\|\mathbf{w}_{ny}\|^2_{L^2(0,1)^2}}{Re} \\
&\quad + C_3\|\mathbf{w}_n\|^2_{L^2(0,1)^2}. \qquad (8.5.135)
\end{aligned}
$$

So then, setting

$$
L = \frac{1 + ReC_3 + \gamma_n^2}{2}\|\mathbf{w}_n\|^2_{L^2(0,1)^2} + \|\mathbf{w}_{ny}\|^2_{L^2(0,1)^2}, \qquad (8.5.136)
$$

which is obviously equivalent to the H^1 norm, one has

$$
\begin{aligned}
\frac{d}{dt}L &\leq -\frac{1+\gamma_n^2}{Re}\|\mathbf{w}_n\|^2_{L^2(0,1)^2} - \frac{1}{Re}\|\mathbf{w}_{ny}\|^2_{L^2(0,1)^2} \\
&\leq -C_4 L, \qquad (8.5.137)
\end{aligned}
$$

where $C_4 > 0$ depends on Re, but not on n, therefore achieving H^1 stability for $\mathbf{w}_n$ with decay rate independent of n.

We next prove H^2 stability. The definition of the H^2 norm for the modes $|n| \geq M$ is, using Remark 8.7,

$$
\begin{aligned}
\|\mathbf{w}_n\|^2_{H^2(0,1)^2} &= \|u_{nyy}\|^2_{L^2(0,1)} + \|V_{nyy}\|^2_{L^2(0,1)} + \gamma_n^2\left(\|u_{ny}\|^2_{L^2(0,1)} + \|V_{ny}\|^2_{L^2(0,1)}\right) \\
&\quad + \gamma_n^4\left(\|u_n\|^2_{L^2(0,1)} + \|V_n\|^2_{L^2(0,1)}\right). \qquad (8.5.138)
\end{aligned}
$$

Since

$$
\begin{aligned}
\|\triangle_n u_n\|^2_{L^2(0,1)} &= (\triangle_n u_n, \triangle_n \overline{u}_n)_{L^2(0,1)} \\
&= (u_{nyy} - \gamma_n^2 u_n, \overline{u}_{nyy} - \gamma_n^2\overline{u}_n)_{L^2(0,1)} \\
&= \|u_{nyy}\|^2_{L^2(0,1)} + \gamma_n^4\|u_n\|^2_{L^2(0,1)} - \gamma_n^2(u_{nyy}, \overline{u}_n)_{L^2(0,1)} \\
&\quad - \gamma_n^2(\overline{u}_{nyy}, u_n)_{L^2(0,1)}, \qquad (8.5.139)
\end{aligned}
$$

hence, integrating by parts,

$$\|\triangle_n u_n\|^2_{L^2(0,1)} = \|u_{nyy}\|^2_{L^2(0,1)} + \gamma_n^4\|u_n\|^2_{L^2(0,1)} + 2\gamma_n^2\|u_{ny}\|^2_{L^2(0,1)}. \quad (8.5.140)$$

This shows that $\|\triangle_n \mathbf{w}_n\|^2_{L^2(0,1)^2}$ is equivalent to $\|\mathbf{w}_n\|^2_{H^2(0,1)^2}$. The next norm equivalence is less obvious and we state it in a lemma.

Lemma 8.20. *For* $\mathbf{w}$ *verifying (8.5.106)–(8.5.107), the norms* $\|\triangle_n \mathbf{w}_n\|^2_{L^2(0,1)^2}$ *and therefore* $\|\mathbf{w}_n\|^2_{H^2(0,1)^2}$ *areequivalent to the norm* $\|\mathbf{w}_n\|^2_{H^1(0,1)^2} + \|\mathbf{w}_{nt}\|^2_{L^2(0,1)^2}$.

Proof. We compute $\|\mathbf{w}_{nt}\|^2_{L^2(0,1)^2}$ from (8.5.106)–(8.5.107).

$$\|\mathbf{w}_{nt}\|^2_{L^2(0,1)^2} = \frac{\|\triangle_n \mathbf{w}_n\|^2_{L^2(0,1)^2}}{Re^2} + \Lambda, \quad (8.5.141)$$

where Λ is defined as

$$\begin{aligned}
\Lambda = & -i\gamma_n(p_n, \overline{u}_{nt})_{L^2(0,1)} - i\gamma_n(g(t,y)u_n, \overline{u}_{nt})_{L^2(0,1)} \\
& -(g_y(t,y)V_n, \overline{u}_{nt})_{L^2(0,1)} - (p_{ny}, \overline{V}_{nt})_{L^2(0,1)} - i\gamma_n(g(t,y)V_n, \overline{V}_{nt})_{L^2(0,1)} \\
& +\frac{1}{Re}\left(i\gamma_n(\triangle_n u_n, \overline{p}_n)_{L^2(0,1)} + i\gamma_n(\triangle_n u_n, g(t,y)\overline{u}_n)_{L^2(0,1)}\right. \\
& -(\triangle_n u_n, g_y(t,y)\overline{V}_n)_{L^2(0,1)} - (\triangle_n V_n, \overline{p}_{ny})_{L^2(0,1)} \\
& \left. +i\gamma_n(\triangle_n V_n, g(t,y)\overline{V}_n)_{L^2(0,1)}\right). \quad (8.5.142)
\end{aligned}$$

Integrating by parts and using the divergence-free condition,

$$-i\gamma_n(p_n, \overline{u}_{nt}) - (p_{ny}, \overline{V}_{nt})_{L^2(0,1)} = (p_n, -i\gamma_n\overline{u}_{nt} + \overline{V}_{nt})_{L^2(0,1)} = 0. \quad (8.5.143)$$

Similarly,

$$\begin{aligned}
i\gamma_n(\triangle_n u_n, \overline{p}_n)_{L^2(0,1)} - (\triangle_n V_n, \overline{p}_{ny})_{L^2(0,1)} &= (\triangle_n u_n + i\gamma_n \triangle_n V_{ny}, \overline{p}_n)_{L^2(0,1)} \\
&\quad - \left[\triangle_n V_n(t,y)\overline{p}_n(t,y)\right]_{y=0}^{y=1} \\
&= - \left[\triangle_n V_n(t,y)\overline{p}_n(t,y)\right]_{y=0}^{y=1}, \quad (8.5.144)
\end{aligned}$$

and using Equation (8.5.129) and Lemma 8.19,

$$- \left[\triangle_n V_n(t,y)\overline{p}_n(t,y)\right]_{y=0}^{y=1} = -Re\left[p_n(t,y)\overline{p}_n(t,y)\right]_{y=0}^{y=1} \leq Re\|g_y\|^2_{L^\infty(0,1)}\|V_n\|^2_{L^2(0,1)}, \quad (8.5.145)$$

hence

$$\begin{aligned}
\Lambda \;\leq\; & \|g_y\|^2_{L^\infty(0,1)}\|V_n\|^2_{L^2(0,1)} - i\gamma_n(g(t,y)u_n, \overline{u}_{nt})_{L^2(0,1)} - (g_y(t,y)V_n, \overline{u}_{nt})_{L^2(0,1)} \\
& - i\gamma_n(g(t,y)V_n, \overline{V}_{nt})_{L^2(0,1)} + \frac{1}{Re}\left(i\gamma_n(\triangle_n u_n, g(t,y)\overline{u}_n)_{L^2(0,1)}\right. \\
& \left. -(\triangle_n u_n, g_y(t,y)\overline{V}_n)_{L^2(0,1)} + i\gamma_n(\triangle_n V_n, g(t,y)\overline{V}_n)_{L^2(0,1)}\right). \qquad (8.5.146)
\end{aligned}$$

Then,

$$|\Lambda| \;\leq\; C_1\|\mathbf{w}_n\|^2_{H^1(0,1)^2} + \frac{1}{2}\left(\|\mathbf{w}_{nt}\|^2_{L^2(0,1)^2} + \frac{\|\triangle_n \mathbf{w}_n\|^2_{L^2(0,1)^2}}{Re^2}\right), \quad (8.5.147)$$

for some $C_1 > 0$. It follows that

$$\begin{aligned}
\|\mathbf{w}_n\|^2_{H^1(0,1)^2} + \|\mathbf{w}_{nt}\|^2_{L^2(0,1)^2} \;&\leq\; C_2\|\triangle_n \mathbf{w}_n\|^2_{L^2(0,1)^2}, & (8.5.148)\\
\|\triangle_n \mathbf{w}_n\|^2_{L^2(0,1)^2} \;&\leq\; C_3\left(\|\mathbf{w}_n\|^2_{H^1(0,1)^2} + \|\mathbf{w}_{nt}\|^2_{L^2(0,1)^2}\right). & (8.5.149)
\end{aligned}$$

Since we get the result for $\|\triangle_n \mathbf{w}_n\|^2_{L^2(0,1)^2}$, we also get it for $\|\mathbf{w}_n\|^2_{H^2(0,1)^2}$, thus completing the proof. □

Now, taking a time derivative in equations (8.5.106)–(8.5.107), and repeating the same argument as in the L^2 proof of stability, the following estimate holds.

$$\frac{d}{dt}\|\mathbf{w}_{nt}\|^2_{L^2(0,1)^2} \leq -2\frac{\|\mathbf{w}_{nt}\|^2_{L^2(0,1)^2}}{Re} + C_4\|\mathbf{w}_{nt}\|_{L^2(0,1)^2}\|\mathbf{w}_n\|_{L^2(0,1)^2}, \qquad (8.5.150)$$

where the last term is due to the time-varying coefficients. Combining Equation (8.5.150), the previous estimates for the L^2 and H^1 norms and Lemma 8.20, H^2 stability follows.

8.5.2 Controlled modes. Construction of control laws

The remaining modes, $0 < |n| < M$, are open-loop unstable and must be controlled. We design the control in several steps.

Pressure shaping

Solving (8.5.112)–(8.5.114),

$$\begin{aligned}
p_n \;=\; & -2i\int_0^y g_y(t,\eta)\sinh\left(\gamma_n(y-\eta)\right)V_n(t,\eta)d\eta \\
& +2i\frac{\cosh\left(\gamma_n y\right)}{\sinh\gamma_n}\int_0^1 g_y(t,\eta)\cosh\left(\gamma_n(1-\eta)\right)V_n(t,\eta)d\eta \\
& +i\frac{\cosh\left(\gamma_n(1-y)\right)}{\sinh\gamma_n}\frac{u_{ny}(t,0)}{Re} \\
& -\frac{\cosh\left(\gamma_n y)\right)}{\sinh\gamma_n}\left(i\frac{u_{ny}(t,1)}{Re}+\frac{\dot{V}_{cn}}{\gamma_n}+\gamma_n\frac{V_{cn}}{Re}\right).
\end{aligned} \tag{8.5.151}$$

As in (4.5.69), V_{cn} appears "inside" (8.5.151), allowing to "shape" it. We follow Section 4.5.1 and design V_{cn} to enforce in (8.5.151) a strict-feedback structure [71] in y. Hence,

$$\begin{aligned}
\frac{\dot{V}_{cn}}{\gamma_n} \;=\; & -\gamma_n\frac{V_{cn}}{Re}-i\frac{u_{ny}(t,0)-u_{ny}(t,1)}{Re} \\
& -2i\int_0^1 g_y(t,\eta)\cosh\left(\gamma_n(1-\eta)\right)V_n(t,\eta)d\eta,
\end{aligned} \tag{8.5.152}$$

i.e.,

$$\begin{aligned}
V_{cn} \;=\; & -i\int_0^t \mathrm{e}^{-\gamma_n^2\tau}\left(\gamma_n\frac{u_{ny}(\tau,0)-u_{ny}(\tau,1)}{Re}\right. \\
& \left.+2\int_0^1 g_y(\tau,\eta)\cosh\left(\gamma_n(1-\eta)\right)V_n(\tau,\eta)d\eta\right)d\tau.
\end{aligned} \tag{8.5.153}$$

Plugging (8.5.152) into (8.5.151), the pressure reduces to

$$\begin{aligned}
p_n \;=\; & -2i\int_0^y g_y(t,\eta)\sinh\left(\gamma_n(y-\eta)\right)V_n(t,\eta)d\eta \\
& +i\frac{\cosh\left(\gamma_n(1-y)\right)-\cosh\left(\gamma_n y\right)}{\sinh\gamma_n}\frac{u_{ny}(t,0)}{Re}.
\end{aligned} \tag{8.5.154}$$

Substituting (8.5.154) into (8.5.106)–(8.5.107) yields

$$\begin{aligned}
u_{nt} \;=\; & \frac{u_{nyy}}{Re}-\frac{\gamma_n^2 u_n}{Re}-i\gamma_n g(t,y)u_n-g_y(t,y)V_n \\
& -2\gamma_n\int_0^y g_y(t,\eta)\sinh\left(\gamma_n(y-\eta)\right)V_n(t,\eta)d\eta
\end{aligned}$$

$$
\begin{aligned}
&+\gamma_n \frac{\cosh\left(\gamma_n(1-y)\right) - \cosh\left(\gamma_n y\right)}{Re \sinh \gamma_n} u_{ny}(t,0), && (8.5.155)\\
V_{nt} &= \frac{V_{nyy}}{Re} - \frac{\gamma_n^2 V_n}{Re} - i\gamma_n g(t,y) V_n \\
&+2i\gamma_n \int_0^y g_y(t,\eta) \cosh\left(\gamma_n(y-\eta)\right) V_n(t,\eta) d\eta \\
&+i\gamma_n \frac{\sinh\left(\gamma_n(1-y)\right) + \sinh\left(\gamma_n y\right)}{Re \sinh \gamma_n} u_{ny}(t,0). && (8.5.156)
\end{aligned}
$$

Control of velocity field

Our objective is now to control (8.5.155)–(8.5.156) by means of U_{cn}. By (8.5.111), V_n can be computed as $V_n(y,t) = -i\gamma_n \int_0^y u_n(t,\eta) d\eta$. Then, only (8.5.155) has to be considered. Using (8.5.111) to express (8.5.155) as an autonomous equation in u_n,

$$
\begin{aligned}
u_{nt} &= \frac{\triangle_n u_n}{Re} + \lambda_n(t,y) u_n + \int_0^y f_n(t,y,\eta) u_n(t,\eta) d\eta \\
&+\mu_n(y) u_{ny}(t,0), && (8.5.157)
\end{aligned}
$$

with boundary conditions

$$
\begin{aligned}
u_n(t,0) &= 0, && (8.5.158)\\
u_n(t,1) &= U_{cn}(t), && (8.5.159)
\end{aligned}
$$

where λ_n, f_n and μ_n were defined in (8.4.96)–(8.4.98). This is a boundary control problem for a parabolic PIDE with time-dependent coefficients, solvable by backstepping [103] thanks to the strict-feedback structure. Following [103] we map u_n, for each mode $0 < |n| < M$, into the family of heat equations

$$
\begin{aligned}
\alpha_{nt} &= \frac{1}{Re}\left(-\gamma_n^2 \alpha_n + \alpha_{nyy}\right) && (8.5.160)\\
\alpha_n(k,0) &= \alpha_n(k,1) = 0\,, && (8.5.161)
\end{aligned}
$$

where

$$
\begin{aligned}
\alpha_n &= (I - K_n) u_n && (8.5.162)\\
u_n &= (I + L_n) \alpha_n, && (8.5.163)
\end{aligned}
$$

are respectively the direct and inverse transformation. The kernel K_n is found to verify Equations (8.4.93)–(8.4.95), and L_n verifies a similar equation, or can be derived from K_n using Proposition 8.9. For (8.4.93)–(8.4.95), the following result holds.

Proposition 8.21. *For every $n \in A$, there exists a solution $K_n(t, y, \eta)$ of (8.4.93)–(8.4.95) defined in $\Gamma = \{(t, y, \eta) \in (0, \infty) \times \mathcal{T}\}$ and such that we have $K_n \in L^\infty((0, \infty), \mathcal{C}^\infty(\mathcal{T}))$, where $\mathcal{T} = \{(y, \eta) \in \mathbb{R}^2 : 0 \leq \eta \leq y \leq 1\}$.*

We prove this Proposition in Section 8.7.

The control law is, from (8.5.162), (8.5.161) and (8.5.159),

$$U_{cn} = \int_0^1 K_n(t, 1, \eta) u_n(t, k, \eta) d\eta, \tag{8.5.164}$$

Stability closed-loop properties follow from (8.5.160)–(8.5.163). Since from (8.5.160)–(8.5.161), one has that

$$\begin{aligned}
\|\alpha_n(t)\|^2_{L^2(0,1)} &\leq \mathrm{e}^{-\frac{2}{Re}t} \|\alpha_n(0)\|^2_{L^2(0,1)}, & (8.5.165)\\
\|\alpha_n(t)\|^2_{H^1(0,1)} &\leq \mathrm{e}^{-\frac{2}{Re}t} \|\alpha_n(0)\|^2_{H^1(0,1)}, & (8.5.166)\\
\|\alpha_n(t)\|^2_{H^2(0,1)} &\leq \mathrm{e}^{-\frac{1}{Re}t} \|\alpha_n(0)\|^2_{H^2(0,1)}. & (8.5.167)
\end{aligned}$$

Hence, from (8.5.162)–(8.5.163) and using the norms (8.3.71) and (8.3.73)–(8.3.74), we obtain

$$\begin{aligned}
\|u_n(t)\|^2_{K_n L^2(0,1)} &\leq \mathrm{e}^{-\frac{2}{Re}t} \|u_n(0)\|^2_{K_n L^2(0,1)}, & (8.5.168)\\
\|u_n(t)\|^2_{K_n H^1(0,1)} &\leq \mathrm{e}^{-\frac{2}{Re}t} \|u_n(0)\|^2_{K_n H^1(0,1)}, & (8.5.169)\\
\|u_n(t)\|^2_{K_n H^2(0,1)} &\leq \mathrm{e}^{-\frac{1}{Re}t} \|u_n(0)\|^2_{K_n H^2(0,1)}. & (8.5.170)
\end{aligned}$$

8.5.3 Stability for the whole system

If we call $A = \{n \in \mathbb{Z} : 0 < |n| < M\}$, and $\mathcal{K} = K_n(t, y, \eta)_{n \in A}$, and apply the control laws (8.5.164) and (8.5.153) in physical space, which yield (8.4.91)–(8.4.92), then we can prove stability for the $\mathcal{K}H_{0h}(\Omega)$ norm, defined by (8.3.90), as follows:

$$\begin{aligned}
\|\mathbf{w}\|^2_{\mathcal{K}H_{0h}(\Omega)} &= \sum_{n\notin A}\|\mathbf{w}_n\|^2_{L^2(0,1)^2} + \sum_{n\in A}\|u_n\|^2_{K_nL^2(0,1)} \\
&\leq \mathrm{e}^{-\frac{2}{Re}t}\left[\sum_{n\notin A}\|\mathbf{w}_n(0)\|^2_{L^2(0,1)^2} + \sum_{n\in A}\|u_n(0)\|^2_{K_nL^2(0,1)}\right] \\
&\leq \mathrm{e}^{-\frac{2}{Re}t}\|\mathbf{w}(0)\|^2_{\mathcal{K}H_{0h}(\Omega)}. \qquad (8.5.171)
\end{aligned}$$

By norm equivalence, this proves the L^2 part of Proposition 8.14. Similarly,

$$\begin{aligned}
\|\mathbf{w}\|^2_{\mathcal{K}H^1_{0h}(\Omega)} &= \|u_0\|^2_{H^1(0,1)} + \sum_{0<|n|<M}\|u_n\|^2_{K_nH^1(0,1)} + \sum_{|n|\geq M}\|\mathbf{w}_n\|^2_{H^1(0,1)^2} \\
&\leq \mathrm{e}^{-\frac{2}{Re}t}\|u_0(0)\|^2_{H^1(0,1)} + \sum_{0<|n|<M}\mathrm{e}^{-\frac{2}{Re}t}\|u_n(0)\|^2_{K_nH^1(0,1)} \\
&\quad + \sum_{|n|\geq M}C_1\mathrm{e}^{-C_2t}\|\mathbf{w}_n(0)\|^2_{H^1(0,1)^2} \\
&\leq C_3\mathrm{e}^{-C_4t}\|\mathbf{w}(0)\|^2_{\mathcal{K}H^1_{0h}(\Omega)}. \qquad (8.5.172)
\end{aligned}$$

The same argument shows H^2 stability.

$$\begin{aligned}
\|\mathbf{w}\|^2_{\mathcal{K}H^2_{0h}(\Omega)} &= \|u_0\|^2_{H^2(0,1)} + \sum_{0<|n|<M}\|u_n\|^2_{K_nH^2(0,1)} + \sum_{|n|\geq M}\|\mathbf{w}_n\|^2_{H^2(0,1)^2} \\
&\leq \mathrm{e}^{-\frac{1}{Re}t}\|u_0(0)\|^2_{H^2(0,1)} + \sum_{0<|n|<M}\mathrm{e}^{-\frac{1}{Re}t}\|u_n(0)\|^2_{K_nH^2(0,1)} \\
&\quad + \sum_{|n|\geq M}C_5\mathrm{e}^{-C_6t}\|\mathbf{w}_n(0)\|^2_{H^2(0,1)^2} \\
&\leq C_7\mathrm{e}^{-C_8t}\|\mathbf{w}(0)\|^2_{\mathcal{K}H^2_{0h}(\Omega)}. \qquad (8.5.173)
\end{aligned}$$

The first part of Proposition 8.14 is proved.

8.5.4 Well-posedness

It remains to prove the well-posedness of (8.2.27)–(8.2.26) with control laws (8.4.91)–(8.4.92).

Define the space $H^1_{\mathrm{per}}(-h,h) = \{\phi \in H^1(-h,h) : \phi(h) = \phi(-h)\}$. Define in a similar way $H^2_{\mathrm{per}}(-h,h) = \{\phi \in H^2(-h,h) : \phi(h) = \phi(-h), \phi_x(h) = \phi_x(-h)\}$. We first show the following result regarding the regularity of the control laws.

Proposition 8.22. *Given any $T > 0$, assume that the velocity field (u, V) verifies*

$$(u, V) \in L^2((0,T), H^2_{0h}(\Omega)). \tag{8.5.174}$$

Then, control laws $V_c(t,x)$ and $U_c(t,x)$ defined by (8.4.91) and (8.4.92) respectively verify

$$U_c, V_c \in L^2((0,T), H^2_{\text{per}}(-h,h)) \cap H^1((0,T), H^1_{\text{per}}(-h,h)). \tag{8.5.175}$$

Proof. We begin showing (8.5.175) for V_c. From (8.4.91) we can write

$$V_{ct} = \frac{V_{cxx}}{Re} - f(t,x), \tag{8.5.176}$$

where

$$\begin{aligned} f(t,x) \quad = \quad & \sum_{0<|n|<M} \int_{-h}^{h} \mathrm{e}^{i\gamma_n(\xi - x)} \left[2i \int_0^1 g_y(t,\eta) \cosh\left(\gamma_n(1-\eta)\right) C(t,\xi,\eta) d\eta \right. \\ & \left. -i \frac{u_y(t,\xi,0) - u_y(t,\xi,1)}{Re} \right] d\xi, \end{aligned} \tag{8.5.177}$$

with $V_c(t,h) = V_c(t,-h)$, and initial conditions $V_c(0,x) = 0$. Note that f in (8.5.177) is defined as a finite sum of convolutions in the periodic domain of certain functions with the smooth function $\mathrm{e}^{i\gamma_n x}$. Hence, even though there is a gradient and a trace in the definition of f, from the smoothing properties of convolution we have that $f \in L^2((0,T), \mathcal{C}^p_{\text{per}}([-h,h])$ for every integer p, where for any function ϕ, $\phi \in \mathcal{C}^p_{per}([-h,h])$ means that ϕ is of class $\mathcal{C}^p$ and $\phi^{(i)}(-h) = \phi^{(i)}(h)$ for every $i \in \{0,\dots,p\}$, and where $\mathcal{C}^p_{\text{per}}([-h,h]$ is equipped with the usual $\mathcal{C}^p$-topology. Therefore by standard properties of the heat equation (see for example [45, pg. 360, Theorem 5] for the non-periodic case), we get that $V_c \in H^1([0,T), \mathcal{C}^p_{\text{per}}([-h,h])$ for every integer p. Hence,

$$V_c \in L^2((0,T), H^2_{\text{per}}(-h,h)) \cap H^1((0,T), H^1_{\text{per}}(-h,h)). \tag{8.5.178}$$

Similarly, the definition of U_c is

$$U_c(t,x) = \sum_{0<|n|<M} \int_{-h}^{h} \int_0^1 \mathrm{e}^{i\gamma_n(\xi - x)} K_n(t,1,\eta) u(t,\xi,\eta) d\eta d\xi, \tag{8.5.179}$$

again a finite sum of convolutions with a smooth function. Hence, by the same argument it follows that

$$U_c \in L^2((0,T), H^2_{\text{per}}(-h,h)) \cap H^1((0,T), H^1_{\text{per}}(-h,h)), \tag{8.5.180}$$

proving the result. $\square$

We apply a slightly modified version of [57, Theorem 2.1]; see also [55, Theorem 4.4] for a similar argument. Note that from Remark 8.13 and the assumptions of Proposition 8.14, the following compatibility conditions are verified

$$u_0(x,1) = U_c(0,x), \quad V_0(x,1) = V_c(0,x), \quad \int_{-h}^{h} V_c(t,x)dx = 0. \tag{8.5.181}$$

Then, for U_c and V_c satisfying (8.5.175), we get that there exist a unique solution to the linearized Navier-Stokes equations such that $(u,V) \in L^2((0,T), H^2_{0h}(\Omega))$. But Proposition 8.22 guarantees that then (8.5.175) is true. Hence the result follows for any finite time T.

Estimates in Section 8.5.3 guarantee the decay of the $H^2_{0h}(\Omega)$ norm of the velocity field (this implies that the $H^2_{0h}(\Omega)$ norm does not blow up). Therefore the argument can be applied repeatedly any number of times, thus proving $(u,V) \in L^2((0,\infty), H^2_{0h}(\Omega))$.

8.6 Proof of Proposition 8.15

We now consider the fully nonlinear Navier-Stokes equations (8.2.22)–(8.2.23). Denote the nonlinear term as $\mathbf{N} = (N^u, N^v)$, where

$$N^u = -uu_x - Vu_y, \tag{8.6.182}$$

$$N^v = -uV_x - VV_y. \tag{8.6.183}$$

One has by using [108, Lemma 3.4 p. 292],

$$(\mathbf{w}, \mathbf{N})_{H_{0h}(\Omega)} \leq \|\mathbf{w}\|_{\mathcal{K}H_{0h}(\Omega)} \|\mathbf{w}\|^2_{\mathcal{K}H_{1h}(\Omega)}, \tag{8.6.184}$$

The bound above is valid not only for $(\mathbf{w}, \mathbf{N})_{H_{0h}(\Omega)}$ but for any partial sum of $(\mathbf{w}_n, \mathbf{N}_n)_{L^2(0,1)^2}$, by the same argument.

The application of pressure shaping and backstepping transformation to the nonlinear system results in a new term in the target system, which appears as

$$\alpha_{nt} = \frac{1}{Re}\left(-\gamma_n^2\alpha_n + \alpha_{nyy}\right) + N_n^\alpha, \tag{8.6.185}$$

where N_n^α is defined by

$$N_n^\alpha = (I - K_n)N_n^u + (I - K_n)N_n^p. \tag{8.6.186}$$

The term N_n^p is due to pressure shaping and is defined by

$$\begin{aligned} N_n^p \; = \; & 2\sum_{j\in\mathbb{Z}}\left[\frac{\cosh(\gamma_n y)}{\sinh\gamma_n}\int_0^1 N_{nj}^q\cosh(\gamma_n(1-\eta))\,d\eta\right. \\ & \left. + \int_0^y N_{nj}^q\sinh(\gamma_n(y-\eta))\,d\eta\right], \end{aligned} \tag{8.6.187}$$

where

$$N_{nj}^q = -\gamma_j\gamma_{n-j}u_j u_{n-j} - i\gamma_{n-j}u_{jy}V_{n-j}. \tag{8.6.188}$$

Then, for $n \in A$,

$$\begin{aligned} (\alpha_n, N_n^\alpha)_{L^2(0,1)} \; \leq \; & C_2\left[(|\alpha_n|, |N_n^u|)_{L^2(0,1)} + (|\alpha_n|, |N_n^p|)_{L^2(0,1)}\right] \\ \leq \; & C_2\|\alpha_n\|_{L^2(0,1)}\sum_{j\in\mathbb{Z}}\left\{\left[|\gamma_j|\|u_j u_{n-j}\|_{L^2(0,1)} + \|u_{jy}V_{n-j}\|_{L^2(0,1)}\right]\right. \\ & \left.\times\left[1 + C_3|\gamma_{n-j}|\right]\right\}, \end{aligned} \tag{8.6.189}$$

where $C_2 = 1 + \|\mathcal{K}\|_{L^\infty}$ and $C_3 = 2(\frac{\sinh(\gamma_1)\sinh(\gamma_M)+\cosh^2(\gamma_M)}{\sinh(\gamma_1)})$. Bounding (8.6.189) further, one gets

$$\begin{aligned} (\alpha_n, N_n^\alpha) \leq \; & \frac{C_2}{2}\|\alpha_n\|_{L^2(0,1)}\sum_{j\in\mathbb{Z}}\left\{2|\gamma_j|^2\|u_j\|^2_{L^2(0,1)} + 2\|u_{jy}\|^2_{L^2(0,1)}\right. \\ & \left. + \left[1 + C_3^2|\gamma_{n-j}|^2\right]\left[\|u_{(n-j)}\|^2_{L^2(0,1)} + \|V_{(n-j)}\|^2_{L^2(0,1)}\right]\right\} \\ \leq \; & C_4\|\alpha_n\|_{L^2(0,1)}\,\|\mathbf{w}\|^2_{\mathcal{K}H_{1h}(\Omega)}, \end{aligned} \tag{8.6.190}$$

for some positive C_4. Calculate now the $\mathcal{K}L^2$ norm of the velocity field for the controlled Navier-Stokes equation. As in (8.5.171),

$$\|\mathbf{w}\|^2_{\mathcal{K}L^2_{0h}(\Omega)} = \sum_{n\notin A} \|\mathbf{w}_n\|_{L^2(0,1)^2} + \sum_{n\in A} \|u_n\|^2_{K_n L^2(0,1)}. \tag{8.6.191}$$

We next compute the derivatives for each term in (8.6.191). We have that

$$\frac{d}{dt}\sum_{n\notin A} \|\mathbf{w}_n\|^2_{L^2(0,1)^2} \leq \sum_{n\notin A}\left[\frac{-2}{Re}\|\mathbf{w}_{ny}\|^2_{L^2(0,1)^2} - \frac{\gamma_n^2}{Re}\|\mathbf{w}_n\|^2_{L^2(0,1)^2} + (\mathbf{w}_n, \mathbf{N}_n)_{L^2(0,1)^2}\right], \tag{8.6.192}$$

and for $n \in A$, since $\|u_n\|_{K_n L^2(0,1)} = \|\alpha_n\|_{L^2(0,1)}$, one has

$$\frac{d}{dt}\|u_n\|^2_{K_n L^2(0,1)} = \frac{d}{dt}\|\alpha_n\|^2_{L^2(0,1)} \leq \frac{-2}{Re}\|\alpha_{ny}\|^2_{L^2(0,1)} - \frac{2\gamma_n^2}{Re}\|\alpha_n\|^2 + (\alpha_n, N_n^\alpha)_{L^2(0,1)}. \tag{8.6.193}$$

Then, summing (8.6.193) for $n \in A$, adding (8.6.192), and applying norm equivalences and the estimate (8.6.184), we get for some $C_0 > 0$

$$\begin{aligned}\frac{d}{dt}\|\mathbf{w}\|^2_{\mathcal{K}H_{0h}(\Omega)} &\leq -C_0\|\mathbf{w}\|^2_{\mathcal{K}H_{1h}(\Omega)} + \sum_{n\notin A}(\mathbf{w}_n, \mathbf{N}_n)_{L^2(0,1)^2} + \sum_{n\in A}(\alpha_n, N_n^\alpha)_{L^2(0,1)} \\ &\leq \|\mathbf{w}\|^2_{\mathcal{K}H_{1h}(\Omega)}\left(C_4\|\mathbf{w}\|_{\mathcal{K}H_{0h}(\Omega)} + \|\mathbf{w}\|_{\mathcal{K}H_{0h}(\Omega)} - C_0\right). \end{aligned} \tag{8.6.194}$$

Suppose that $\|\mathbf{w}\|_{\mathcal{K}H_{0h}(\Omega)} < \epsilon$. Then

$$\frac{d}{dt}\|\mathbf{w}\|^2_{\mathcal{K}H_{0h}(\Omega)} \leq \left((C_4+1)\epsilon - C_0\right)\|\mathbf{w}\|^2_{\mathcal{K}H_{1h}(\Omega)}, \tag{8.6.195}$$

and choosing ϵ such that $\epsilon < \frac{C_0}{2(C_4+1)}$,

$$\begin{aligned}\frac{d}{dt}\|\mathbf{w}\|^2_{\mathcal{K}H_{0h}(\Omega)} &\leq \frac{-C_0}{2}\|\mathbf{w}\|^2_{\mathcal{K}H_{1h}(\Omega)} \\ &\leq -C_5\|\mathbf{w}\|^2_{\mathcal{K}H_{0h}(\Omega)}, \end{aligned} \tag{8.6.196}$$

by Poincaré's inequality, where $C_5 > 0$. This proves local exponential stability in the $\mathcal{K}H_{0h}(\Omega)$ norm and therefore in the $H_{0h}(\Omega)$ norm.

A similar argument applies to the $H^1_{0h}(\Omega)$ and $H^2_{0h}(\Omega)$ norms, for proving local exponential stability; we skip the details since it is clear that the extra nonlinear convection terms that would appear in the proof (in a similar way to the proof for the $H_{0h}(\Omega)$ norm) can be bounded by the linear terms in $\mathbf{w}$, $\mathbf{w}_x$ and $\mathbf{w}_y$ for small $H^1_{0h}(\Omega)$ and $H^2_{0h}(\Omega)$ norms[6]. Well-posedness follows as in Section 8.5.4, as the argument in [57] applies to the nonlinear Navier-Stokes equations.

8.7 Proof of Proposition 8.21

In this section we prove a general result which includes Proposition 8.21 as a particular case.

We first recall the definition of the Gevrey class of functions, which plays an important role in studying solutions of the heat equation [31,58]. As shown later, solutions to kernel partial integro-differential equations that appear in unsteady backstepping problems are members of some Gevrey class.

Definition 8.23. *A smooth function $f(t)$ defined on $(0,T)$, for $T \in (0,\infty]$, is Gevrey of order α if there exists numbers $Q, R > 0$ such that, for all positive integers k,*

$$\sup_{t\in(0,T)} \left| \frac{d^k f}{dt^k} \right| \leq Q \frac{(k!)^\alpha}{R^k}. \tag{8.7.197}$$

We write $f \in \mathcal{G}^\alpha(0,T)$.

For functions of time and space, we define the following classes, denoting $H^{0,\infty}(0,1) = L^\infty(0,1)$.

Definition 8.24. *Given $m \geq 0$ integer, a function $f(t,y)$ is said to be Gevrey of order α in time $t \in (0,T)$, and $H^{m,\infty}(0,1)$ in space y, if $f(t,\cdot) \in H^{m,\infty}(0,1)$ for every time $t \in (0,T)$, $f(t,\cdot)$ possesses derivatives of all orders which also belong to $H^{m,\infty}(0,1)$, and there exist numbers $Q, R > 0$ such that, for all positive integers k,*

$$\sup_{t\in(0,T)} \left|\left| \frac{d^k f}{dt^k} \right|\right|_{H^{m,\infty}(0,1)} \leq Q \frac{(k!)^\alpha}{R^k}. \tag{8.7.198}$$

We write $f \in \mathcal{G}^\alpha((0,T), H^{m,\infty}(0,1))$.

[6] The only extra detail required would be a minor modification of Lemma 8.19 to account for the extra nonlinear terms in the pressure Poisson equation.

For functions having two or more space variables we similarly define $\mathcal{G}^\alpha((0,T),H^{m,\infty}(\Omega))$ where $\Omega \subset \mathbb{R}^2$ is any bounded set. Consider now the kernel equation

$$\begin{aligned} \epsilon K_{yy} - \epsilon K_{\eta\eta} - K_t(t,y,\eta) &= \lambda(t,\eta)K(t,y,\eta) - f(t,y,\eta) \\ &\quad + \int_\eta^y K(t,y,\xi)f(t,\xi,\eta)d\xi, \end{aligned} \tag{8.7.199}$$

with boundary conditions

$$K(t,y,y) = \frac{-1}{2\epsilon}\int_0^y \lambda(t,\sigma)d\sigma - \frac{g(t,0)}{\epsilon}, \tag{8.7.200}$$

$$K(t,y,0) = \int_0^y K(t,y,\sigma)\frac{g(t,\sigma)}{\epsilon}d\sigma - \frac{g(t,y)}{\epsilon}, \tag{8.7.201}$$

in the domain $(0,T)\times\mathcal{T}$, where $\epsilon, T > 0$, and the coefficients $f(t,y,\eta)$, $g(t,y)$ and $\lambda(t,y)$ verify

$$f \in \mathcal{G}^\alpha((0,T),H^{m-1,\infty}(\mathcal{T})), \tag{8.7.202}$$

$$\lambda \in \mathcal{G}^\alpha((0,T),H^{m,\infty}(0,1)), \tag{8.7.203}$$

$$g \in \mathcal{G}^\alpha((0,T),H^{m+1,\infty}(0,1)). \tag{8.7.204}$$

The following result regarding Equation (8.7.199) holds.

Theorem 8.25. *(Finite time) Assume $T \in (0,\infty)$. For coefficients f, g, λ as in (8.7.202)–(8.7.204), Equation (8.7.199) with boundary conditions (8.7.200)–(8.7.201) has a unique solution $K \in \mathcal{G}^\alpha((0,T),H^{m+1,\infty}(\mathcal{T}))$.*

For the infinite time interval, the result is similar.

Theorem 8.26. *(Infinite time) For coefficients f, g, λ verifying*

$$f \in \mathcal{G}^\alpha((0,\infty),H^{m-1,\infty}(\mathcal{T})) \cap L^\infty((0,\infty),H^{m-1,\infty}(\mathcal{T})), \tag{8.7.205}$$

$$\lambda \in \mathcal{G}^\alpha((0,\infty),H^{m,\infty}) \cap L^\infty((0,\infty),H^{m,\infty}(0,1)), \tag{8.7.206}$$

$$g \in \mathcal{G}^\alpha((0,\infty),H^{m+1,\infty}(0,1)) \cap L^\infty((0,\infty),H^{m+1,\infty}(0,1)), \tag{8.7.207}$$

it follows that Equation (8.7.199) with boundary conditions (8.7.200)–(8.7.201) has a unique solution

$$K \in \mathcal{G}^\alpha((0,\infty),H^{m+1,\infty}(\mathcal{T})) \cap L^\infty((0,\infty),H^{m+1,\infty}(\mathcal{T})). \tag{8.7.208}$$

Note that Theorem 8.26 includes Proposition 8.21 as a particular case, with $\alpha = 1$, and taking limit for m going to infinity.

8.7.1 Proof of Theorem 8.25

In the following it will be assumed that $1 \leq \alpha < 2$. For $\alpha < 1$ one has to substitute everywhere in the section α by 1.

We follow [101] to transform the PIDE into an integral equation. Applying the change of variables $\xi = y + \eta$ and $\beta = y - \eta$, and denoting

$$G(t, \xi, \beta) = K(t, y, \eta) = K\left(t, \frac{\xi + \beta}{2}, \frac{\xi - \beta}{2}\right), \tag{8.7.209}$$

the PIDE (8.7.199) is transformed into

$$\begin{aligned} 4\epsilon G_{\xi\beta} &= G_t(t, \xi, \beta) + A(t, \xi, \beta)G(t, \xi, \beta) - B(t, \xi, \beta) \\ &\quad + \int_{\frac{\xi-\beta}{2}}^{\frac{\xi+\beta}{2}} G\left(t, \frac{\xi + \beta}{2} + \sigma, \frac{\xi + \beta}{2} - \sigma\right) \\ &\quad \times f\left(t, \sigma + \frac{\xi - \beta}{2}, \sigma - \frac{\xi - \beta}{2}\right) d\sigma, \end{aligned} \tag{8.7.210}$$

with boundary conditions

$$G_\xi(t, \xi, 0) = \frac{-A(t, \xi, 0)}{4\epsilon}, \tag{8.7.211}$$

$$G(t, \xi, \xi) = \frac{-g(t, \xi)}{\epsilon} + \int_0^\xi G\left(t, \xi + \sigma, \xi - \sigma\right) \frac{g(t, \sigma)}{\epsilon} d\sigma, \tag{8.7.212}$$

in the domain $(0, T) \times \mathcal{T}_1$, where $\mathcal{T}_1 = \{(\xi, \beta) : 0 \leq \xi \leq 2, 0 \leq \beta \leq \min \xi, 2 - \xi\}$, and where now

$$A(t, \xi, \beta) = \lambda\left(t, \frac{\xi - \beta}{2}\right) \in \mathcal{G}^\alpha((0, T), H^{m,\infty}(\mathcal{T}_1)), \tag{8.7.213}$$

$$B(t, \xi, \beta) = f\left(t, \frac{\xi + \beta}{2}, \frac{\xi - \beta}{2}\right) \in \mathcal{G}^\alpha((0, T), H^{m-1,\infty}(\mathcal{T}_1)). \tag{8.7.214}$$

Changing the integration variable, we can rewrite Equation (8.7.210) as

$$\begin{aligned} 4\epsilon G_{\xi\beta} &= G_t(t, \xi, \beta) + A(t, \xi, \beta)G(t, \xi, \beta) - B(t, \xi, \beta) \\ &\quad + \int_0^\beta G\left(t, \xi + \sigma, \beta - \sigma\right) f\left(t, \sigma + (\xi - \beta), \sigma\right) d\sigma, \end{aligned} \tag{8.7.215}$$

and integrating (8.7.215) and making use of the boundary conditions (8.7.211)–(8.7.212) we reach

$$\begin{aligned}
G(t,\xi,\beta) &= \frac{1}{4\epsilon}\int_{\beta}^{\xi}\int_{0}^{\beta} G_t(t,\tau,\sigma)d\sigma d\tau \\
&+\frac{1}{4\epsilon}\int_{\beta}^{\xi}\int_{0}^{\beta} A(t,\tau,\sigma)G(t,\tau,\sigma)d\sigma d\tau - \frac{1}{4\epsilon}\int_{\beta}^{\xi}\int_{0}^{\beta} B(t,\tau,\sigma)d\sigma d\tau \\
&+\frac{1}{4\epsilon}\int_{\beta}^{\xi}\int_{0}^{\beta}\int_{0}^{\sigma} G\left(t,\tau+\mu,\sigma-\mu\right) f\left(t,\mu+(\tau-\sigma),\mu\right) d\mu d\sigma d\tau \\
&-\frac{1}{4\epsilon}\int_{\beta}^{\xi} A(t,\tau,0)d\tau - \frac{1}{\epsilon}g(t,\beta) \\
&+\frac{1}{\epsilon}\int_{0}^{\beta} g(t,\sigma)G\left(t,\beta+\sigma,\beta-\sigma\right)d\sigma,
\end{aligned} \tag{8.7.216}$$

an integro-differential equation that only contains time derivatives and spatial integrals.

Following the same method of proof as in [101], we look for a successive series approximation solution, such that

$$G = \sum_{n=0}^{\infty} G_n(t,\xi,\beta), \tag{8.7.217}$$

with

$$\begin{aligned}
G_0(t,\xi,\beta) &= -\frac{1}{4\epsilon}\int_{\beta}^{\xi}\int_{0}^{\beta} B(t,\tau,\sigma)d\sigma d\tau \\
&-\frac{1}{4\epsilon}\int_{\beta}^{\xi} A(t,\tau,0)d\tau - \frac{1}{\epsilon}g(t,\beta),
\end{aligned} \tag{8.7.218}$$

and for $n > 0$,

$$\begin{aligned}
G_n(t,\xi,\beta) &= \frac{1}{4\epsilon}\int_{\beta}^{\xi}\int_{0}^{\beta} (G_{n-1})_t(t,\tau,\sigma)d\sigma d\tau \\
&+\frac{1}{4\epsilon}\int_{\beta}^{\xi}\int_{0}^{\beta} A(t,\tau,\sigma)G_{n-1}(t,\tau,\sigma)d\sigma d\tau \\
&+\frac{1}{4\epsilon}\int_{\beta}^{\xi}\int_{0}^{\beta}\int_{0}^{\sigma} G_{n-1}\left(t,\tau+\mu,\sigma-\mu\right) f\left(t,\mu+(\tau-\sigma),\mu\right) d\mu d\sigma d\tau \\
&+\frac{1}{\epsilon}\int_{0}^{\beta} g(t,\sigma)G_{n-1}\left(t,\beta+\sigma,\beta-\sigma\right)d\sigma.
\end{aligned} \tag{8.7.219}$$

Since A, B and g are Gevrey in time and at least bounded in space (as $m \geq 1$), they can be simultaneously bounded[7] by a Gevrey function $Q(t)$, so $A \leq Q$, $B \leq Q$, $g \leq Q$, with Q a function such that there exist M, R such that for all $k \geq 0$, $t \in (0,T)$, one has

$$\frac{\partial^k Q(t)}{\partial t^k} \leq M \frac{(k!)^\alpha}{R^k}. \tag{8.7.220}$$

Define now

$$h(t,t_0) = \frac{1}{1 - \frac{t-t_0}{R^{1/\alpha}}}, \tag{8.7.221}$$

for $t_0 \in [0,T)$. Hence, when $t \in [t_0, \frac{R^{1/\alpha}}{2} + t_0)$, it follows that $1 \leq |h(t,t_0)|$. Since

$$\frac{\partial^k h(t,t_0)}{\partial t^k} = \frac{k!}{\left(1 - \frac{t-t_0}{R^{1/\alpha}}\right)^{k+1} R^{k/\alpha}} = \frac{k! h(t,t_0)^{k+1}}{R^{k/\alpha}}, \tag{8.7.222}$$

it is evident that for $t \in [t_0, \frac{R^{1/\alpha}}{2} + t_0)$, one has

$$\frac{k!}{R^{k/\alpha}} \leq \frac{\partial^k h(t,t_0)}{\partial t^k}, \tag{8.7.223}$$

hence

$$\frac{\partial^k Q(t)}{\partial t^k} \leq M \left(\frac{\partial^k h(t,t_0)}{\partial t^k}\right)^\alpha. \tag{8.7.224}$$

We partition the interval $(0,T)$ *uniformly* into a finite number m of subintervals, in the following way:

$$(0,T) = (0, \frac{R^{1/\alpha}}{2}) \cup [\frac{R^{1/\alpha}}{2}, R^{1/\alpha}) \cup \ldots \cup [(m-1)\frac{R^{1/\alpha}}{2}, T), \tag{8.7.225}$$

where m is chosen such that the length of the last subinterval is equal or less than $\frac{R^{1/\alpha}}{2}$. For each subinterval, set t_0 as the infimum of the subinterval. Then, for t in the subinterval, $h(t,t_0)$ bounds Q as in (8.7.224).

Consider first $t_0 = 0$. We show the proof for the subinterval $t \in (0, \frac{R^{1/\alpha}}{2})$; it proceeds equally for the rest of the subintervals because t_0 does not appear explicitly in the computations. This means that any bound obtained for the interval $(0, \frac{R^{1/\alpha}}{2})$ uniformly holds in the whole interval $(0,T)$. Hence, it suffices to prove the result for $t \in (0, \frac{R^{1/\alpha}}{2})$ and $t_0 = 0$.

[7] For example take $Q = A^2 + B^2 + g^2$.

Denote $h(t,0) = h(t)$ for simplicity. We prove the existence of the solution defined by the successive approximation series using a variant of the classical method of majorants. See [75] for a similar proof.

We claim that for all $n \geq 0$, $k \geq 0$, and $(t,\xi,\beta) \in (0, \frac{R^{1/\alpha}}{2}) \times \mathcal{T}_1$, one has

$$\left|\frac{\partial^k}{\partial t^k} G_n(t,\xi,\beta)\right| \leq \left(\frac{\partial^k}{\partial t^k} h(t)^{n+1}\right)^{\alpha} \frac{C^{n+1}\sqrt{\beta^n(\xi+\beta)^n}}{(n!)^{\gamma}}, \tag{8.7.226}$$

where $\gamma = 2-\alpha > 0$ and

$$C = \frac{2}{\epsilon R} + \frac{5M}{\epsilon}. \tag{8.7.227}$$

Assume the above formula is true (it is proved next). Then, substituting in the successive approximation series (8.7.217), one has, for $k \geq 0$,

$$\begin{aligned}
\left|\frac{\partial^k}{\partial t^k} G(t,\xi,\beta)\right| &\leq \sum_{n=0}^{\infty} \left(\frac{\partial^k}{\partial t^k} h(t)^{n+1}\right)^{\alpha} \frac{C^{n+1}\sqrt{\beta^n(\xi+\beta)^n}}{(n!)^{\gamma}} \\
&= \sum_{n=0}^{\infty} \left(\frac{\partial^k}{\partial t^k} h(t)^{n+1} \frac{C^{(n+1)/\alpha}\sqrt[2\alpha]{\beta^n(\xi+\beta)^n}}{(n!)^{\gamma/\alpha}}\right)^{\alpha} \\
&\leq \left(\frac{\partial^k}{\partial t^k} \sum_{n=0}^{\infty} h(t)^{n+1} \frac{C^{(n+1)/\alpha}\sqrt[2\alpha]{\beta^n(\xi+\beta)^n}}{(n!)^{\gamma/\alpha}}\right)^{\alpha} \\
&\leq \left(\frac{\partial^k}{\partial t^k} H(t,\xi,\beta)\right)^{\alpha},
\end{aligned} \tag{8.7.228}$$

where

$$H(t,\xi,\beta) = \sum_{n=0}^{\infty} h(t)^{n+1} \frac{C^{(n+1)/\alpha}\sqrt[2\alpha]{(1+\beta)^n(1+\xi+\beta)^n}}{(n!)^{\gamma/\alpha}}, \tag{8.7.229}$$

is an analytic function in all its variables in $(t,\xi,\beta) \in [0, \frac{R^{1/\alpha}}{2}] \times \mathcal{T}_1$, when $\alpha < 2$. This is easily seen for ξ and β. To see it for t, substitute ξ and β by their maximum (2 and 1 respectively). Then,

$$H(t,\xi,\beta) = \sum_{n=0}^{\infty} h(t)^{n+1} \frac{C^{(n+1)/\alpha}\sqrt[2\alpha]{12^n}}{(n!)^{\gamma/\alpha}} = \sum_{n=0}^{\infty} h(t)^{n+1} \frac{D^{n+1}}{(n!)^{\delta}}. \tag{8.7.230}$$

To check analyticity on $[0, \frac{R^{1/\alpha}}{2}]$, since all terms in the sum are already analytic, we extend H to a disk of radius $R^{1/\alpha}$ in the complex plane, i.e. $t \in \mathbb{C}$, $|t| \in [0, \frac{R^{1/\alpha}}{2}]$ and check convergence for t on compact subsets [91] of the disk. Set then $t = \frac{R^{1/\alpha}}{2}(1-\sigma)$, where $\sigma \in [0,1]$. Then,

$$H(t,\xi,\beta) \leq \sum_{n=0}^{\infty} \left(\frac{2D}{\sigma+1}\right)^{n+1} \frac{1}{(n!)^{\delta}}, \tag{8.7.231}$$

which converges for all values of D, σ, δ. Therefore H is also analytic in t. Then, by using (8.7.228), it follows that G is bounded in ξ and β, and Gevrey of order α in t. Note that, as was stated before, the proof holds as well when using $h(t,t_0)$ instead of $h(t,0)$, for $t \in [t_0, t_0 + \frac{R^{1/\alpha}}{2})$.

It remains to prove the estimate (8.7.226), by induction on n.

For $n = 0$ and $k = 0$, one has

$$\begin{aligned} |G_0(t,\xi,\beta)| &\leq \frac{1}{4\epsilon}\int_\beta^\xi \int_0^\beta Q(t) d\sigma d\tau \\ &\quad + \frac{1}{4\epsilon}\int_\beta^\xi Q(t) d\tau + \frac{1}{\epsilon} Q(t) \\ &= \frac{Q(t)}{\epsilon}\left(1 + \frac{1}{4}(\xi-\beta) + \frac{1}{4}\beta(\xi-\beta)\right) \\ &\leq h(t)^\alpha \frac{2M}{\epsilon} \leq h(t)^\alpha C, \end{aligned} \tag{8.7.232}$$

and for $n = 0$, $k > 0$,

$$\begin{aligned} \left|\frac{\partial^k G_0(t,\xi,\beta)}{\partial t^k}\right| &\leq \frac{1}{4\epsilon}\int_\beta^\xi \int_0^\beta \frac{\partial^k Q(t)}{\partial t^k} d\sigma d\tau \\ &\quad + \frac{1}{4\epsilon}\int_\beta^\xi \frac{\partial^k Q(t)}{\partial t^k} d\sigma + \frac{1}{\epsilon}\frac{\partial^k Q(t)}{\partial t^k} d\sigma d\tau \\ &\leq \left(\frac{\partial^k}{\partial t^k} h(t)\right)^\alpha \frac{2M}{\epsilon} \leq \left(\frac{\partial^k}{\partial t^k} h(t)\right)^\alpha C, \end{aligned} \tag{8.7.233}$$

so (8.7.226) is true for $n = 0$.

Suppose now it is true for $n - 1$. Then, for $k = 0$,

$$\begin{aligned} |G_n(t,\xi,\beta)| &\leq \frac{1}{4\epsilon}\int_\beta^\xi \int_0^\beta \left|\frac{\partial G_{n-1}}{\partial t}\right| (t,\tau,\sigma) d\sigma d\tau \\ &\quad + \frac{1}{4\epsilon}\int_\beta^\xi \int_0^\beta Q(t) \left|G_{n-1}\right| (t,\tau,\sigma) d\sigma d\tau \end{aligned}$$

$$+\frac{1}{4\epsilon}\int_{\beta}^{\xi}\int_{0}^{\beta}\int_{0}^{\sigma}|G_{n-1}|\,(t,\tau+\mu,\sigma-\mu)\,Q(t)d\mu d\sigma d\tau$$
$$+\frac{1}{\epsilon}\int_{0}^{\beta}Q(t)\,|G_{n-1}|\,(t,\beta+\sigma,\beta-\sigma)d\sigma, \qquad (8.7.234)$$

and using the induction hypothesis (8.7.226) and the bound on $Q(t)$ given in Equation (8.7.224),

$$\begin{aligned}|G_n(t,\xi,\beta)| \leq\ & \frac{1}{4\epsilon}\int_{\beta}^{\xi}\int_{0}^{\beta}\left(\frac{\partial}{\partial t}h(t)^n\right)^{\alpha}\frac{C^n\sqrt{\sigma^{n-1}(\tau+\sigma)^{n-1}}}{((n-1)!)^{\gamma}}d\sigma d\tau \\ & +\frac{1}{4\epsilon}\int_{\beta}^{\xi}\int_{0}^{\beta}M\left(h(t)^{n+1}\right)^{\alpha}\frac{C^n\sqrt{\sigma^{n-1}(\tau+\sigma)^{n-1}}}{((n-1)!)^{\gamma}}d\sigma d\tau \\ & +\frac{1}{4\epsilon}\int_{\beta}^{\xi}\int_{0}^{\beta}\int_{0}^{\sigma}M\left(h(t)^{n+1}\right)^{\alpha}\frac{C^n\sqrt{(\sigma-\mu)^{n-1}(\tau+\sigma)^{n-1}}}{((n-1)!)^{\gamma}}d\mu d\sigma d\tau \\ & +\frac{1}{\epsilon}\int_{0}^{\beta}M\left(h(t)^{n+1}\right)^{\alpha}\frac{C^n\sqrt{(\beta-\sigma)^{n-1}(2\beta)^{n-1}}}{((n-1)!)^{\gamma}}d\sigma. \qquad (8.7.235)\end{aligned}$$

Regarding the integrals, we have the following lemma.

Lemma 8.27. *For $(\xi,\beta)\in\mathcal{T}_1=\{(\xi,\beta):0\leq\xi\leq 2, 0\leq\beta\leq\min\{\xi,2-\xi\}\}$, we have that*

1. $\displaystyle\int_{\beta}^{\xi}\int_{0}^{\beta}\sqrt{\sigma^{n-1}(\tau+\sigma)^{n-1}}d\sigma d\tau\leq 8\frac{\sqrt{\beta^n(\xi+\beta)^n}}{(n+1)^2}$,
2. $\displaystyle\int_{\beta}^{\xi}\int_{0}^{\beta}\int_{0}^{\sigma}\sqrt{(\sigma-\mu)^{n-1}(\tau+\sigma)^{n-1}}d\mu d\sigma d\tau\leq 4\frac{\sqrt{\beta^n(\xi+\beta)^n}}{(n+1)^2}$,
3. $\displaystyle\int_{0}^{\beta}\sqrt{(\beta-\sigma)^{n-1}(2\beta)^{n-1}}d\sigma\leq 2\frac{\sqrt{(\beta+\xi)^n(\beta)^n}}{n+1}$.

Proof. For the integral in Point 1, the following chain of inequalities holds.

$$\begin{aligned}\int_{\beta}^{\xi}\int_{0}^{\beta}\sqrt{\sigma^{n-1}(\tau+\sigma)^{n-1}}d\sigma d\tau \leq\ & 2\int_{0}^{\beta}\frac{\sqrt{\sigma^{n-1}(\xi+\sigma)^{n+1}}}{n+1}d\sigma \\ \leq\ & 2\frac{\sqrt{(\xi+\beta)^{n+1}}\int_0^{\beta}\sqrt{\sigma^{n-1}}d\sigma}{n+1} \\ \leq\ & 4\frac{\sqrt{\beta^{n+1}(\xi+\beta)^{n+1}}}{(n+1)^2} \\ \leq\ & 8\frac{\sqrt{\beta^n(\xi+\beta)^n}}{(n+1)^2}. \qquad (8.7.236)\end{aligned}$$

Similarly, for the integral in Point 2, we have that

$$\begin{aligned}\int_\beta^\xi \int_0^\beta \int_0^\sigma \sqrt{(\sigma-\mu)^{n-1}(\tau+\sigma)^{n-1}}d\mu d\sigma d\tau &= \int_\beta^\xi \int_0^\beta 2\frac{\sqrt{(\sigma)^{n+1}(\tau+\sigma)^{n-1}}}{n+1}d\sigma d\tau \\ &= 8\frac{\sqrt{(\beta)^{n+3}(\xi+\beta)^{n+1}}}{(n+1)^2(n+3)} \\ &\leq 4\frac{\sqrt{\beta^n(\xi+\beta)^n}}{(n+1)^2}. \end{aligned} \tag{8.7.237}$$

Finally, Point 3 is deduced using the following reasoning:

$$\begin{aligned}\int_0^\beta \sqrt{(\beta-\sigma)^{n-1}(2\beta)^{n-1}}d\sigma &= 2\frac{\sqrt{(2\beta)^{n-1}(\beta)^{n+1}}}{n+1} \\ &\leq 2\frac{\sqrt{(\beta+\xi)^{n-1}(\beta)^{n+1}}}{n+1} \\ &\leq 2\frac{\sqrt{(\beta+\xi)^n(\beta)^n}}{n+1}. \end{aligned} \tag{8.7.238}$$

This proves the result. □

Using Lemma 8.27 in (8.7.235), we reach

$$\begin{aligned}|G_n(t,\xi,\beta)| &\leq \frac{2}{\epsilon}\left(h(t)^{n+1}\right)^\alpha \frac{n^\alpha}{R}\frac{C^n}{((n-1)!)^\gamma}\frac{\sqrt{\beta^n(\xi+\beta)^n}}{(n+1)^2} \\ &\quad +\frac{2M}{\epsilon}\left(h(t)^{n+1}\right)^\alpha \frac{C^n}{((n-1)!)^\gamma}\frac{\sqrt{\beta^n(\xi+\beta)^n}}{(n+1)^2} \\ &\quad +\frac{M}{\epsilon}\left(h(t)^{n+1}\right)^\alpha \frac{C^n}{((n-1)!)^\gamma}\frac{\sqrt{\beta^n(\xi+\beta)^n}}{(n+1)^2} \\ &\quad +\frac{2M}{\epsilon}\left(h(t)^{n+1}\right)^\alpha \frac{C^n}{((n-1)!)^\gamma}\frac{\sqrt{(\beta+\xi)^n(\beta)^n}}{n+1} \\ &\leq \left(\frac{2}{R}+5M\right)\left(h(t)^{n+1}\right)^\alpha \frac{C^n\sqrt{\beta^n(\xi+\beta)^n}}{\epsilon(n!)^\gamma} \\ &\leq \left(h(t)^{n+1}\right)^\alpha \frac{C^{n+1}\sqrt{\beta^n(\xi+\beta)^n}}{(n!)^\gamma} \end{aligned} \tag{8.7.239}$$

Similarly, for $k>0$, and using Leibnitz's formula,

$$\begin{aligned}\left|\frac{\partial^k G_n}{\partial t^k}\right| &\leq \frac{1}{4\epsilon}\int_\beta^\xi \int_0^\beta \left|\frac{\partial^{k+1}G_{n-1}}{\partial t^{k+1}}\right|(t,\tau,\sigma)d\sigma d\tau + \frac{1}{4\epsilon}\int_\beta^\xi \int_0^\beta \left[\sum_{i=0}^k \begin{pmatrix} k \\ i \end{pmatrix}\right. \\ &\quad \left. \times \left|\frac{\partial^i Q}{\partial t^i}\right| \left|\frac{\partial^{k-i}G_{n-1}}{\partial t^{k-i}}\right|(t,\tau,\sigma)\right] d\sigma d\tau + \frac{1}{4\epsilon}\int_\beta^\xi \int_0^\beta \int_0^\sigma \left[\sum_{i=0}^k \begin{pmatrix} k \\ i \end{pmatrix}\right. \end{aligned}$$

$$\times \left|\frac{\partial^i Q}{\partial t^i}\right| \left|\frac{\partial^{k-i} G_{n-1}}{\partial t^{k-i}}\right| (t, \tau+\mu, \sigma-\mu)\Bigg] d\mu d\sigma d\tau + \frac{1}{\epsilon}\int_0^\beta \left[\sum_{i=0}^k \begin{pmatrix} k \\ i \end{pmatrix}\right.$$

$$\times \left|\frac{\partial^i Q}{\partial t^i}\right| \left|\frac{\partial^{k-i} G_{n-1}}{\partial t^{k-i}}\right| (t, \beta+\sigma, \beta-\sigma)\Bigg] d\sigma, \tag{8.7.240}$$

and using the induction hypothesis (8.7.226) and (8.7.224),

$$\begin{aligned}
\left|\frac{\partial^k G_n}{\partial t^k}\right| \leq\ & \frac{1}{4\epsilon}\int_\beta^\xi \int_0^\beta \left(\frac{\partial^{k+1}}{\partial t^{k+1}} h(t)^n\right)^\alpha \frac{C^n\sqrt{\sigma^{n-1}(\tau+\sigma)^{n-1}}}{((n-1)!)^\gamma} d\sigma d\tau \\
& + \frac{1}{4\epsilon}\int_\beta^\xi \int_0^\beta \left[\sum_{i=0}^k \begin{pmatrix} k \\ i \end{pmatrix} M \left(\frac{\partial^i}{\partial t^i} h(t)\right)^\alpha \left(\frac{\partial^{k-i}}{\partial t^{k-i}} h(t)^n\right)^\alpha\right. \\
& \times \left.\frac{C^n\sqrt{\sigma^{n-1}(\tau+\sigma)^{n-1}}}{((n-1)!)^\gamma}\right] d\sigma d\tau + \frac{1}{4\epsilon}\int_\beta^\xi \int_0^\beta \int_0^\sigma \left[\sum_{i=0}^k \begin{pmatrix} k \\ i \end{pmatrix} M\right. \\
& \times \left.\left(\frac{\partial^i}{\partial t^i} h(t)\right)^\alpha \left(\frac{\partial^{k-i}}{\partial t^{k-i}} h(t)^n\right)^\alpha \frac{C^n\sqrt{(\sigma-\mu)^{n-1}(\tau+\sigma)^{n-1}}}{((n-1)!)^\gamma}\right] d\mu d\sigma d\tau \\
& + \frac{1}{\epsilon}\int_0^\beta \left[\sum_{i=0}^k \begin{pmatrix} k \\ i \end{pmatrix} M \left(\frac{\partial^i}{\partial t^i} h(t)\right)^\alpha \left(\frac{\partial^{k-i}}{\partial t^{k-i}} h(t)^n\right)^\alpha\right. \\
& \times \left.\frac{C^n\sqrt{(\beta-\sigma)^{n-1}(2\beta)^{n-1}}}{((n-1)!)^\gamma}\right] d\sigma,
\end{aligned} \tag{8.7.241}$$

The integrals appearing in (8.7.241) can be bounded applying Lemma 8.27, reaching

$$\begin{aligned}
\left|\frac{\partial^k G_n}{\partial t^k}\right| \leq\ & \frac{2}{\epsilon}\left(\frac{\partial^{k+1}}{\partial t^{k+1}} h(t)^n\right)^\alpha \frac{C^n\sqrt{\beta^n(\xi+\beta)^n}}{(n+1)^2((n-1)!)^\gamma} \\
& + \frac{M}{\epsilon}\left[\sum_{i=0}^k \begin{pmatrix} k \\ i \end{pmatrix} \left(\frac{\partial^i}{\partial t^i} h(t)\right)^\alpha \left(\frac{\partial^{k-i}}{\partial t^{k-i}} h(t)^n\right)^\alpha\right] \\
& \times (3+2(n+1))\frac{C^n\sqrt{\beta^n(\xi+\beta)^n}}{(n+1)^2(n-1)!)^\gamma}.
\end{aligned} \tag{8.7.242}$$

For the first line in (8.7.242) we use

$$\frac{\partial^i}{\partial t^i} h(t)^n = \frac{n}{R^{1/\alpha}}\frac{\partial^{i-1}}{\partial t^{i-1}} h(t)^{n+1}. \tag{8.7.243}$$

Using

$$\left(\frac{\partial^i}{\partial t^i}h(t)\right)\left(\frac{\partial^{k-i}}{\partial t^{k-i}}h(t)^n\right) = n\frac{i!(n+k-i-1)!}{(n+k)!}\left(\frac{\partial^k}{\partial t^k}h(t)^{n+1}\right)$$
$$= n\frac{i!}{(n+k)(n+k-1)\dots(n+k-i)} \times\left(\frac{\partial^k}{\partial t^k}h(t)^{n+1}\right), \tag{8.7.244}$$

we estimate the term in brackets that appears in the second line in (8.7.242), obtaining

$$\sum_{i=0}^{k}\begin{pmatrix} k \\ i \end{pmatrix}\left(\frac{\partial^i}{\partial t^i}h(t)\right)^{\alpha}\left(\frac{\partial^{k-i}}{\partial t^{k-i}}h(t)^n\right)^{\alpha}$$
$$= \left(\frac{\partial^k}{\partial t^k}h(t)^{n+1}\right)^{\alpha} n^{\alpha}\left\{\sum_{i=0}^{k}\begin{pmatrix} k \\ i \end{pmatrix}\left(\frac{i!}{(n+k)(n+k-1)\dots(n+k-i)}\right)^{\alpha}\right\}$$
$$= \left(\frac{\partial^k}{\partial t^k}h(t)^{n+1}\right)^{\alpha} n^{\alpha}\left\{\sum_{i=0}^{k}\frac{(i!)^{\alpha-1}k(k-1)\dots(k-i+1)}{(n+k)^{\alpha}\dots(n+k-i)^{\alpha}}\right\}. \tag{8.7.245}$$

The term in braces in (8.7.245) can be bound using the following lemma.

Lemma 8.28. *For $n, k \geq 1$ we have that*

$$\sum_{i=0}^{k}\frac{(i!)^{\alpha-1}k(k-1)\dots(k-i+1)}{(n+k)^{\alpha}\dots(n+k-i)^{\alpha}} \leq \frac{1}{n}. \tag{8.7.246}$$

Proof. We can rewrite the inequality as follows:

$$\frac{1}{(n+k)^{\alpha}}\sum_{i=0}^{k}\frac{\begin{pmatrix} k \\ i \end{pmatrix}}{\begin{pmatrix} n-1+k \\ i \end{pmatrix}^{\alpha}} \leq \frac{1}{n}. \tag{8.7.247}$$

Since for $1 \leq \alpha < 2$,

$$\frac{1}{(n+k)^{\alpha}}\sum_{i=0}^{k}\frac{\begin{pmatrix} k \\ i \end{pmatrix}}{\begin{pmatrix} n-1+k \\ i \end{pmatrix}^{\alpha}} \leq \frac{1}{n+k}\sum_{i=0}^{k}\frac{\begin{pmatrix} k \\ i \end{pmatrix}}{\begin{pmatrix} n-1+k \\ i \end{pmatrix}}, \tag{8.7.248}$$

it is enough to prove the lemma for $\alpha = 1$. We prove it by induction on n. For $n = 1$, it is obviously verified. For $n \geq 2$, it is convenient to write the inequality we want to prove as

$$\frac{1}{(n+k)} \sum_{i=0}^{k} \frac{k!(n-1+k-i)!}{(k-i)!(n-1+k)!} \leq \frac{1}{n}, \tag{8.7.249}$$

and cancelling some of the products, we arrive at the following inequality

$$\frac{\sum_{i=0}^{k} \left((n-1+k-i)(n-2+k-i)\dots(k-i+1)\right)}{(n+k)(n+k-1)\dots(k+1)} \leq \frac{1}{n}. \tag{8.7.250}$$

Assuming it true for n, we have for $n+1$ that

$$\begin{aligned}
&\frac{\sum_{i=0}^{k} \left((n+k-i)(n-1+k-i)\dots(k-i+1)\right)}{(n+1+k)(n+k)\dots(k+1)} \\
\leq\ & \left(\frac{n+k}{n+1+k}\right) \frac{\sum_{i=0}^{k} \left((n-1+k-i)(n-2+k-i)\dots(k-i+1)\right)}{(n+k)(n+k-1)\dots(k+1)} \\
\leq\ & \left(\frac{n+k}{n+1+k}\right) \frac{1}{n} \\
\leq\ & \frac{1}{n},
\end{aligned} \tag{8.7.251}$$

hence the inequality holds for all n. □

Using Lemma 8.28 in Equation (8.7.245), we reach

$$\begin{aligned}
&\sum_{i=0}^{k} \begin{pmatrix} k \\ i \end{pmatrix} \left(\frac{\partial^i}{\partial t^i} h(t)\right)^{\alpha} \left(\frac{\partial^{k-i}}{\partial t^{k-i}} h(t)^n\right)^{\alpha} \\
\leq\ & \left(\frac{\partial^k}{\partial t^k} h(t)^{n+1}\right)^{\alpha} n^{\alpha-1}.
\end{aligned} \tag{8.7.252}$$

Introducing (8.7.243) and (8.7.252) in (8.7.242), we obtain

$$\begin{aligned}
\left|\frac{\partial^k G_n}{\partial t^k}\right| \leq\ & \frac{2}{\epsilon R} \left(\frac{\partial^k}{\partial t^k} h(t)^{n+1}\right)^{\alpha} n^{\alpha} \frac{C^n \sqrt{\beta^n (\xi+\beta)^n}}{(n+1)^2((n-1)!)^{\gamma}} \\
&+ \frac{M}{\epsilon} \left(\frac{\partial^k}{\partial t^k} h(t)^{n+1}\right)^{\alpha} n^{\alpha-1} \left(3 + 2(n+1)\right) \\
&\times \frac{C^n \sqrt{\beta^n (\xi+\beta)^n}}{(n+1)^2 (n-1)!)^{\gamma}},
\end{aligned} \tag{8.7.253}$$

hence

$$\begin{aligned}
\left|\frac{\partial^k G_n}{\partial t^k}\right| &\leq \left(\frac{\partial^k}{\partial t^k}h(t)^{n+1}\right)^\alpha \left(\frac{2}{\epsilon R}+\frac{5M}{\epsilon}\right)\frac{C^n\sqrt{\beta^n(\xi+\beta)^n}}{(n!)^\gamma} \\
&= \left(\frac{\partial^k}{\partial t^k}h(t)^{n+1}\right)^\alpha \frac{C^{n+1}\sqrt{\beta^n(\xi+\beta)^n}}{(n!)^\gamma}, \qquad (8.7.254)
\end{aligned}$$

thus proving (8.7.226).

We have shown that $G \in \mathcal{G}^\alpha((0,T), L^\infty(\mathcal{T}_1))$. To get higher regularity in space, we differentiate in the ξ variable the integral equation (8.7.216), obtaining

$$\begin{aligned}
G_\xi(t,\xi,\beta) &= \frac{1}{4\epsilon}\int_0^\beta G_t(t,\xi,\sigma)d\sigma d\tau \\
&+\frac{1}{4\epsilon}\int_0^\beta A(t,\xi,\sigma)G(t,\xi,\sigma)d\sigma d\tau - \frac{1}{4\epsilon}\int_0^\beta B(t,\xi,\sigma)d\sigma d\tau \\
&+\frac{1}{4\epsilon}\int_0^\beta\int_0^\sigma G\left(t,\xi+\mu,\sigma-\mu\right)f\left(t,\mu+(\xi-\sigma),\mu\right)d\mu d\sigma d\tau \\
&-\frac{1}{4\epsilon}A(t,\xi,0)d\tau, \qquad (8.7.255)
\end{aligned}$$

which explicitly defines G_ξ. Next, we differentiate in the β variable the integral equation (8.7.216), reaching

$$\begin{aligned}
G_\beta(t,\xi,\beta) &= \frac{1}{4\epsilon}\int_\beta^\xi G_t(t,\tau,\beta)d\tau - \frac{1}{4\epsilon}\int_0^\beta G_t(t,\beta,\sigma)d\sigma \\
&+\frac{1}{4\epsilon}\int_\beta^\xi A(t,\tau,\beta)G(t,\tau,\beta)d\tau - \frac{1}{4\epsilon}\int_0^\beta A(t,\beta,\sigma)G(t,\beta,\sigma)d\sigma \\
&-\frac{1}{4\epsilon}\int_\beta^\xi B(t,\tau,\beta)d\tau + \frac{1}{4\epsilon}\int_0^\beta B(t,\beta,\sigma)d\sigma \\
&+\frac{1}{4\epsilon}\int_\beta^\xi\int_0^\beta G\left(t,\tau+\mu,\beta-\mu\right)f\left(t,\mu+(\tau-\beta),\mu\right)d\mu d\tau \\
&-\frac{1}{4\epsilon}\int_0^\beta\int_0^\sigma G\left(t,\beta+\mu,\sigma-\mu\right)f\left(t,\mu+(\beta-\sigma),\mu\right)d\mu d\sigma \\
&+\frac{1}{4\epsilon}A(t,\beta,0)d\tau - \frac{1}{\epsilon}g_\beta(t,\beta) + \frac{1}{\epsilon}g(t,\beta)G\left(t,2\beta,0\right) \\
&+\frac{1}{\epsilon}\int_0^\beta g(t,\sigma)G_\beta\left(t,\beta+\sigma,\beta-\sigma\right)d\sigma \\
&+\frac{1}{\epsilon}\int_0^\beta g(t,\sigma)G_\xi\left(t,\beta+\sigma,\beta-\sigma\right)d\sigma, \qquad (8.7.256)
\end{aligned}$$

an integral equation for G_β. Equation (8.7.256) can be written as

$$G_\beta(t,\xi,\beta) \;=\; \Phi(t,\xi,\beta) + \frac{1}{\epsilon}\int_0^\beta g(t,\sigma)G_\beta\left(t,\beta+\sigma,\beta-\sigma\right)d\sigma. \quad (8.7.257)$$

The function $\Phi(t,\xi,\beta)$ is computable from G and the coefficients A, B, and g. Then, Equation (8.7.257) is solved using a successive approximation scheme as before. We skip the details.

Hence, G_ξ and G_β are well-defined, as long as g_β, which was used in Equation (8.7.256), is well-defined. Iterating this process, higher order derivatives can be computed as long as the coefficients are differentiable. It follows that the regularity of G is determined by the regularity of the coefficients; it is proven by induction that the exact degree of regularity is exactly $G \in \mathcal{G}^\alpha((0,T), H^{m+1,\infty}(\mathcal{T}_1))$. This means that G has the same regularity as g, has one more derivative than λ, and two more derivatives than f. Moreover, repeating this argument for all values of m, if the coefficients are smooth in space, then the kernel is smooth in ξ and β.

8.7.2 Proof of Theorem 8.26

We proceed as in Section 8.25; covering the infinite interval $(0,\infty)$ with an infinite number of *uniform* subintervals of the form $[t_0, \frac{R^{1/\alpha}}{2}+t_0)$, the previous proof applies. We obtain always the same bounds for G. Hence a compactness argument is *not* required, as we obtain an uniform, finite bound for G, showing that the successive approximation series is well-defined for all times.

This chapter is a partial reprint of the material as it appears in
R. Vazquez, E. Trélat and J.-M. Coron, “Stable Poiseuille flow transfer for a Navier-Stokes system,” *Proc. of the 2006 ACC*, Minneapolis, 2006.
The dissertation author was the primary author and the coauthors listed in this publication directed and supervised the research, which is the basis for this chapter.

Chapter 9

Boundary Control of a Class of 1-D Nonlinear Parabolic PDEs

9.1 Introduction

Boundary control of linear parabolic PDEs is a well established subject with extensive literature. On the other hand, boundary control of *nonlinear* parabolic PDEs is still an open problem as far as general classes of systems are concerned. Applications of interest include not only fluids, thermal, chemically-reacting, and plasma systems, such as the systems presented in Chapters 2–7, but also flexible structures, atomic force microscopy [90,122], aeroelasticity, and quantum systems. The book [33] solves problems of nonlinear parabolic PDE control but for inside-the-domain actuation, rather than with boundary control. The problem of *motion planning* for boundary controlled nonlinear PDEs has been solved for parabolic systems [84] (using flatness and formal power series) and structural systems [74] (with a flatness/passivity approach).

When attempting to develop general methods for nonlinear PDEs, it is advisable to take a clue from finite dimensional nonlinear systems. Clearly, one should bet on methods that have emerged as successful there. This pretty much eliminates (direct) optimal control methods, because of the requirement to solve Hamilton-

Jacobi-Bellman PDEs, and leaves feedback linearization/backstepping/Lyapunov approaches [65, 69, 71, 98] as candidates for extension to PDEs.

The backstepping approach for *linear* PDEs has reached the level of maturity where a systematic design procedure [101] is available for a broad class of parabolic integro-differential equations in 1-D. This systematic procedure has found many applications [73, 112, 113] and is the starting point for our *nonlinear* developments here.

In [111] we presented some preliminary results and outlined our approach; in this chapter, we have shown the general method in full detail and present several examples. Our results are based on Volterra series. Previous similar nonlinear efforts [2, 24–26] were *discretization*-based and were successful in addressing some applications but in general cannot be expected to converge when the discretization step goes to zero, as shown in [11].

After presenting in full detail and with examples a method for designing stabilizing boundary controllers for a class of nonlinear 1-D parabolic PDEs, we study of some of the theoretical properties of the method. More specifically, we give some reasonable assumptions under which the feedback linearizing Volterra transformation and the control law, both defined by nonlinear operators involving infinite series, are well defined. We show that the transformation is at least locally invertible and include an explicit construction for computing the inverse of the transformation. Using the inverse, we show L^2 and H^1 local exponential stability and explicitly construct the exponentially decaying closed-loop solutions.

9.2 Class of Systems Under Study

We study the following class of parabolic systems,

$$u_t = u_{xx} + \lambda(x)u + F[u] + uH[u]\,, \quad x \in (0,1) \tag{9.2.1}$$

with the following boundary conditions

$$u_x(t,0) \;=\; qu(t,0), \quad u(t,1) = U(t), \tag{9.2.2}$$

where $U(t)$ is the control input and $F[u]$ and $H[u]$ are Volterra series nonlinearities as explained below. In (9.2.2), q is a number that can take any value. The particular cases $q = 0$ and $q = \infty$ can be used to model, respectively, Neumann and Dirichlet boundary conditions at $x = 0$. For simplicity we consider a Dirichlet boundary condition at $x = 1$, but different boundary conditions at the controlled end can be easily accommodated in our design.

A Volterra series is defined as a functional (i.e., a function that depends on another function), and has the form

$$F[u](t,x) = \sum_{n=1}^{\infty} F_n[u](t,x), \tag{9.2.3}$$

where the notation $F_n[u](t,x)$ emphasizes the fact that each $F_n[u](t,x)$ is defined as a functional of $u(t,x)$ and also depends on x and t. The precise definition of each term is

$$\begin{aligned} F_n[u](t,x) &= \int_0^x \int_0^{\xi_1} \cdots \int_0^{\xi_{n-1}} f_n(x,\xi_1,\ldots,\xi_n) \\ &\quad \times \left(\prod_{j=1}^{n} u(t,\xi_j) \right) d\xi_1 \ldots d\xi_n \end{aligned} \tag{9.2.4}$$

where f_n is called the n-th Volterra (triangular) kernel.

Volterra series [123] are widely known and studied in the control literature [27, 65, 76, 93]. They are causal functionals [51] that represent the general solution for nonlinear equations, generalizing the convolution solution for linear systems. An excellent exposition on Volterra series can be found in [92].

9.3 Motivating Examples

We give two examples of nonlinear plants that fall into the class of systems of Section 9.2.

9.3.1 Coupled nonlinear plant

Consider the following nonlinear plant

$$u_t = u_{xx} + \mu v, \tag{9.3.5}$$

$$0 = v_{xx} + \omega^2 v + uv + u, \tag{9.3.6}$$

where μ and ω are plant parameters, with boundary conditions

$$u(t,0) = v(t,0) = 0, \tag{9.3.7}$$

$$u(t,1) = U(t), \quad v(t,1) = V(t), \tag{9.3.8}$$

where $U(t)$ and $V(t)$ are actuation variables.

This kind of plant *structure*, consisting of a parabolic equation coupled with an elliptic equation, arises in some relevant applications, for example fluid mechanics, where the pressure verifies a nonlinear elliptic equation (4.2.5), structural problems [73], or singularly perturbed problems in chemical reactors [25] or in thermal fluid convection—the plant in Chapters 2–3 has a similar (but two-dimensional) structure.

To obtain a plant equation in the class of (9.2.1), we solve for v in terms of u from (9.3.6).Define

$$v(t,x) = \sum_{n=1}^{\infty} v_n(t,x), V(t) = \sum_{n=1}^{\infty} V_n(t), \tag{9.3.9}$$

where v_1 verifies,

$$0 = v_{1xx} + \omega^2 v_1 + u, \tag{9.3.10}$$

and for $n > 1$, v_n verifies

$$0 = v_{nxx} + \omega^2 v_i + uv_{n-1}, \tag{9.3.11}$$

with boundary conditions, for each n,

$$v_n(t,0) = 0, \quad v_n(t,1) = V_n(t). \tag{9.3.12}$$

We are free to choose $V_n(t)$ in any meaningful way if the series for V in (9.3.9) converges and the solution for (9.3.10)–(9.3.12) also makes (9.3.9) convergent.

In this case, it is possible to solve (9.3.10)–(9.3.11) explicitly. Denoting $v_0 = 1$, we get the following recursive solution for $i \geq 1$

$$\begin{aligned} v_n &= -\int_0^x \frac{\sin(\omega(x-\xi))}{\omega} v_{n-1}(\xi) u(t,\xi) d\xi \\ &\quad + \frac{\sin(\omega x)}{\sin\omega}\left(V_n(t) + \int_0^1 \frac{\sin(\omega(1-\xi))}{\omega} v_{n-1} u(t,\xi) d\xi\right). \qquad (9.3.13) \end{aligned}$$

Set the control law $V(t)$ as follows.

$$V_i(t) = -\int_0^1 \frac{\sin(\omega(1-\xi)}{\omega} v_{i-1} u(t,\xi) d\xi. \qquad (9.3.14)$$

The reason to choose this particular control law is to get a spatially strict-feedback system, as in (9.2.1).

With this control law the solution to the equation (9.3.6) is

$$v_n = \int_0^x \frac{\sin(\omega(x-\xi))}{\omega} v_{n-1}(\xi) u(t,\xi) d\xi. \qquad (9.3.15)$$

Denoting $\xi_0 = x$, we can solve the recursion in (9.3.15), getting

$$v_n = \frac{(-1)^n}{\omega^n} \int_0^{\xi_0} \cdots \int_0^{\xi_{n-1}} \prod_{j=1}^{n} \left[\sin(\omega(\xi_{j-1} - \xi_j))\, u(\xi_j)\right] d\xi_1 \ldots d\xi_n. (9.3.16)$$

Plugging (9.3.16) into (9.3.14), we obtain a general formula for V_n as follows:

$$\begin{aligned} V_n(t) &= \frac{(-1)^n}{\omega^n} \int_0^1 \int_0^{\xi_1} \cdots \int_0^{\xi_{n-1}} \sin(\omega(1-\xi_1))\, u(\xi_1) \\ &\quad \times \prod_{j=1}^{n-1} \big[\sin(\omega(\xi_j - \xi_{j+1}))\, u(\xi_{j+1})\big] d\xi_1 d\xi_2 \ldots d\xi_n. \qquad (9.3.17) \end{aligned}$$

Assuming that $u(t,x) \in L^2(0,1)$, both series in (9.3.9) converge in L^2 since using that $|\sin(\omega)/\omega| \leq 1$, one can bound $\|v_n\|_{L^2}^2$ as follows.

$$\begin{aligned} \|v_n\|_{L^2}^2 &\leq \left|\frac{\sin(\omega)}{\omega}\right|^{2n} \int_0^1 \left(\int_0^x \int_0^{\xi_1} \cdots \int_0^{\xi_{n-1}} \prod_{j=1}^{n} u(\xi_j) d\xi_1 \ldots d\xi_n\right)^2 dx \\ &\leq \left|\frac{\sin(\omega)}{\omega}\right|^{2n} \frac{1}{n!^2} \int_0^1 \left(\int_0^x u^2(\xi_1) d\xi_1\right)^n dx \leq \frac{\|u\|_{L^2}^{2n}}{n!^2}. \qquad (9.3.18) \end{aligned}$$

Hence, using the Cauchy-Schwartz inequality in ℓ_2,

$$\begin{aligned}\|v\|_{L^2}^2 &= \int_0^1 \left(\sum_{n=1}^{\infty} v_n(x)\right)^2 dx \le \left(\sum_{n=1}^{\infty} n^2 \|v_n(x)\|_{L^2}^2\right) \left(\sum_{n=1}^{\infty} \frac{1}{n^2}\right) \\ &\le 2\sum_{n=1}^{\infty} \frac{\|u\|_{L^2}^{2n}}{(n-1)!^2}, \end{aligned} \tag{9.3.19}$$

where we used $\sum_{n=1}^{\infty} \frac{1}{n^2} = \pi^2/6 \le 2$. Hence, $\|v\|_{L^2}^2 \le 2\|u\|_{L^2}^2 \exp\left(\|u\|_{L^2}^2\right)$. Similarly $|V| \le 2\|u\|_{L^2}^2 \exp\left(\|u\|_{L^2}^2\right)$.

Plugging the solution for v into (9.3.5), we reach

$$\begin{aligned} u_t &= u_{xx} + \mu \sum_{n=1}^{\infty} \frac{(-1)^n}{\omega^n} \\ &\times \int_0^{\xi_0} \cdots \int_0^{\xi_{n-1}} \prod_{j=1}^{n} \left(\sin\left(\omega(\xi_{j-1} - \xi_j)\right) u(\xi_j)\right) d\xi_1 \ldots d\xi_n, \end{aligned} \tag{9.3.20}$$

an autonomous system in u with boundary conditions

$$u(t,0) = 0, \quad u(t,1) = U(t), \tag{9.3.21}$$

and now the problem is reduced to designing U such that the above system is guaranteed to be stable in L^2.

Equation (9.3.20) is a particular example of (9.2.1) with

$$f_n = \mu \frac{(-1)^n}{\omega^n} \prod_{j=1}^{n} \sin\left(\omega(\xi_{j-1} - \xi_j)\right), \tag{9.3.22}$$

$\lambda = H = 0$, and $q = \infty$.

9.3.2 Parabolic semilinear equation

Consider the plant

$$v_t = v_{xx} + f(v), \tag{9.3.23}$$

where $f(v)$ is a nonlinear function *analytic at the origin*, verifying $f(0) = 0$, with boundary conditions

$$v(t,0) = 0, \quad v_x(t,0) = U(t), \tag{9.3.24}$$

where $U(t)$ is the actuation variable.

Remark 9.1. For the open-loop plant (9.3.23), finite-time blow up instabilities are likely to occur when $f(u)$ is superlinear. This was first studied in a classical paper [52] for power-like nonlinearities, and has been the subject of systematic study in subsequent years (see the reviews [43, 80]). More recently the question of *controllability* of this kind of equations has been considered. For superlinear functions which grow faster than $|u|\log^2(1+|u|)$ lack of global controllability is proved in [49]. Therefore, for many nonlinearities $f(v)$ only *local* or restricted results can be achieved; for example in [37] boundary control is used to move between sets of steady states for plants with superlinear nonlinearities.

To cast (9.3.23) into the form of (9.2.1) we differentiate (9.3.23) in x, getting

$$v_{xt} = v_{xxx} + f'(v)v_x. \tag{9.3.25}$$

Call $u = v_x$. Then, $v = \int_0^x u(t,\xi)d\xi$ and (9.3.25) yields

$$u_t = u_{xx} + f'(\int_0^x u(t,\xi)d\xi)u, \tag{9.3.26}$$

with boundary conditions

$$u_x(t,0) = 0, \quad u(t,0) = U(t). \tag{9.3.27}$$

The boundary condition at 0 was obtained evaluating (9.3.23) at $x = 0$ and using (9.3.24) and $f(0) = 0$. Expanding f' in its Taylor series at the origin, and calling

$$\lambda = f'(0), \tag{9.3.28}$$

$$h_n = f^{(n+1)}(0), \quad n > 1, \tag{9.3.29}$$

we can write (9.3.26) as

$$u_t = u_{xx} + \lambda u + u \sum_{n=1}^{\infty} \frac{h_n}{n!} \left(\int_0^x u(t,\xi)d\xi \right)^n, \tag{9.3.30}$$

and since

$$\left(\int_0^x u(t,\xi)d\xi \right)^n = n! \int_0^x \int_0^{\xi_1} \cdots \int_0^{\xi_{n-1}} \prod_{j=1}^n u(\xi_j)d\xi_1 d\xi_2 \dots d\xi_n, \tag{9.3.31}$$

we get

$$u_t = u_{xx} + \lambda u + u \sum_{n=2}^{\infty} \int_0^x \int_0^{\xi_1} \cdots \int_0^{\xi_{n-1}} h_n \prod_{j=1}^{n} u(\xi_j) d\xi_1 d\xi_2 \ldots d\xi_n, \qquad (9.3.32)$$

with boundary conditions (9.3.27). Equation (9.3.32) falls in the class of (9.2.1) with $F = 0$, $q = 0$, and λ and H given by (9.3.28)–(9.3.29). Note that stability of u in the L^2 norm implies stability of v in the H^1 norm, as $u(t, 0) = 0$.

9.4 Control Strategy

The objective is to find a Volterra feedback law $U(t)$, so the controlled system (9.2.1)–(9.2.2) is stable. To achieve that, a new PDE system is introduced, the *target system*, which is the following

$$w_t = w_{xx}, \qquad (9.4.33)$$

with homogeneous boundary conditions

$$w_x(t, 0) = \bar{q} w(t, 0), \quad , w(t, 1) = 0, \qquad (9.4.34)$$

where $\bar{q} = \max\{0, q\}$. The plant (9.4.33)–(9.4.34) is an L^2 and H^1 exponentially stable system by standard results from linear PDE theory.

The idea of the method is to transform (9.2.1) into (9.4.33). For this we use a change of variables based on a Volterra series,

$$\begin{aligned} w(t, x) &= u(t, x) - K[u](t, x) \\ &= u(t, x) - \sum_{n=1}^{\infty} K_n[u](t, x). \qquad (9.4.35) \end{aligned}$$

Evaluating (9.4.35) at $x = 1$ and using (9.2.2) and (9.4.34), we arrive at the control law

$$U(t) = \sum_{i=1}^{\infty} K_i[u](t, 1). \qquad (9.4.36)$$

Therefore, the control is computed using the Volterra kernels that define (9.4.35). Assuming that the series can be differentiated term by term in (9.4.35), and using (9.2.1) and (9.4.33) the following equation is obtained:

$$\lambda(x)u + \sum_{i=1}^{\infty} F_i[u] + u\sum_{i=1}^{\infty} H_i[u] = \sum_{i=1}^{\infty}\left(\frac{\partial}{\partial t}K_i[u] - \frac{\partial^2}{\partial x^2}K_i[u]\right). \qquad (9.4.37)$$

Using (9.4.37), the definition of each term in the Volterra series, integration by parts, and change of the order of integration in the multiple integrals, we obtain a set of partial integro-differential equations (PIDEs) for the kernels k_i that define the control (9.4.36). See Section 9.11.1 for a detailed derivation.

The PIDE verified by the n-th order kernel is

$$\begin{aligned}\partial_{xx}k_n &= \sum_{i=1}^{n}\partial_{\xi_i\xi_i}k_n + \sum_{i=1}^{n}\lambda(\xi_i)k_n + I_n[k_n, f_1] - f_n \\ &\quad + \sum_{m=2}^{n} B_n^m[k_{n-m+1}, f_m] + \sum_{m=1}^{n-1} C_n^m[k_{n-m}, h_m]. \qquad (9.4.38)\end{aligned}$$

The functions B_n^m, C_n^m and I_n in (9.4.38) have an involved definition that requires additional notation and the introduction of some intermediate functions. Hence for clarity we first finish stating and discussing the kernel equations and then introduce the concepts towards the precise definition of B_n^m, C_n^m and I_n, which is given respectively in (9.4.58), (9.4.59) and (9.4.60).

The solution to the PIDE (9.4.38) needs to satisfy the following boundary conditions. For $n = 1$,

$$\begin{aligned} k_1(x,x) &= \hat{q} - \frac{1}{2}\int_0^x \lambda(s)ds, \qquad (9.4.39)\\ k_{1\xi_1}(x,0) &= qk_1(x,0), \qquad (9.4.40)\end{aligned}$$

where $\hat{q} = \min\{0, q\}$, while for $n \geq 2$,

$$\begin{aligned} k_n(x,x,\xi_2,\xi_3,\ldots,\xi_n) &= -\frac{1}{2}\int_{\xi_2}^{x} h_{n-1}(s,\xi_2,\xi_3,\ldots,\xi_n)ds, \qquad (9.4.41)\\ k_{nx}(x,x,\xi_2,\xi_3,\ldots,\xi_n) &= \frac{1}{4}\left(h_{n-1}(\xi_2,\xi_2,\xi_3,\ldots,\xi_n) - h_{n-1}(x,\xi_2,\xi_3,\ldots,\xi_n)\right) \\ &\quad + \frac{1}{2}\int_{\xi_2}^{x}\phi_n(s,\xi_2,\xi_3,\ldots,\xi_n)ds, \qquad (9.4.42)\\ \partial_{\xi_{i-1}}k_n(x,\xi_1,\ldots,\xi_n)\Big|_{\xi_{i-1}=\xi_i} &= \partial_{\xi_i}k_n(x,\xi_1,\ldots,\xi_n)\Big|_{\xi_{i-1}=\xi_i}, \quad i = 2,..,n, \qquad (9.4.43)\\ k_{n\xi_n}(x,\xi_1,\ldots,\xi_{n-1},0) &= qk_n(x,\xi_1,\ldots,\xi_{n-1},0), \qquad (9.4.44)\end{aligned}$$

which are of mixed kind. In (9.4.42), the function ϕ_n is defined as

$$\begin{aligned}\phi_n \quad = \quad & \left[\sum_{i=2}^{n} \partial_{\xi_i \xi_i} k_n + \sum_{i=1}^{n} \lambda(\xi_i) k_n + I_n[k_n, f_1] - f_n \right. \\ & \left. + \sum_{m=2}^{n} B_n^m[k_{n-m+1}, f_m] + \sum_{m=1}^{n-1} C_n^m[k_{n-m}, h_m] \right]_{x=\xi_1} . \end{aligned} \tag{9.4.45}$$

Note that the bracket in (9.4.45) is evaluated at $x = \xi_1$ and thus can be computed from (9.4.41), without needing to know a priori k_n. We illustrate the value of ϕ_2 and ϕ_3 in (9.4.72) and (9.4.79) respectively. Equation (9.4.38) is a hyperbolic PIDE, for each k_n, evolving in the interior of a domain $\mathcal{T}_n = \{(x, \xi_1, \ldots, \xi_n) : 0 \leq \xi_n \leq \ldots \leq \xi_1 \leq x \leq 1\}$, a "hyper-pyramid" of dimension $n+1$ (in particular, a triangle for $n = 1$, and a pyramid for $n = 2$). Note that the volume of $\mathcal{T}_n$ decreases rapidly as the dimension n increases, as given by the following formula:

$$\mathrm{Vol}\,(\mathcal{T}_n) = \frac{1}{(n+1)!}. \tag{9.4.46}$$

Remark 9.2. The domain $\mathcal{T}_n$ has $n+2$ "sides" (which are n-dimensional hyperplanes) on its boundary. These are

$$\mathcal{R}_0 = \{(x, \xi_1, \ldots, \xi_n) : 0 < \xi_n < \ldots < \xi_1 < x = 1\}, \tag{9.4.47}$$

$$\mathcal{R}_1 = \{(x, \xi_1, \ldots, \xi_n) : 0 < \xi_n < \ldots < \xi_1 = x < 1\}, \tag{9.4.48}$$

$$\mathcal{R}_i = \{(x, \xi_1, \ldots, \xi_n) : 0 < \xi_n < \ldots < \xi_i = \xi_{i-1} < \ldots < x < 1\}, \tag{9.4.49}$$

$$\mathcal{R}_{n+1} = \{(x, \xi_1, \ldots, \xi_n) : 0 = \xi_n < \ldots < \xi_1 < x < 1\}, \tag{9.4.50}$$

where in (9.4.49), $i = 2, \ldots, n$. The boundary conditions (9.4.41)–(9.4.42) are non-homogeneous and given on $\mathcal{R}_1$. The boundary condition (9.4.43) is given on $\mathcal{R}_i$, for $i = 2, \ldots, n$ and represents the value of the normal derivative of k_n in the boundary $\mathcal{R}_i$, hence it is of Neumann type. The boundary condition (9.4.44) is of Robin type and given on $\mathcal{R}_{n+1}$. The value of the function k_n on $\mathcal{R}_0$ is what needs to be found for the control law (9.4.36).

Remark 9.3. Equation (9.4.38) with its boundary conditions can be reinterpreted as a wave equation in spacetime. If one thinks of x as time (time-like variable) and the other variables $\xi_1, \xi_2, \ldots, \xi_n$ as space coordinates (space-like variables), then the domain can be seen as a n-dimensional hyper-pyramid in $\mathbb{R}^n$ that *grows* (linearly in "time" x), with boundaries $\mathcal{R}_1, \mathcal{R}_2, \ldots, \mathcal{R}_{n+1}$ that are also growing in time. In particular, it can be seen that the boundaries $\mathcal{R}_2, \ldots, \mathcal{R}_{n+1}$ are time-like (they grow slower than the characteristic speed of wave propagation, lying inside the "causality" cone), but the boundary $\mathcal{R}_1$ is space-like, i.e., it grows faster than the characteristic speed of wave propagation (and lies outside the causality cone). For a wave equation to be well-posed [41], it is necessary that it has exactly one boundary condition on its time-like boundaries and two boundary conditions (initial data) on its space-like boundaries. That is the reason why the boundary $\mathcal{R}_1$ has two boundary conditions. The only exception is k_1, for which $\mathcal{R}_1$ is characteristic (i.e., the boundary condition is of Goursat type) and thus only needs one boundary condition, which is (9.4.39).

The term $I_n[k_n, f_1]$ is the homogenous integral term of the P*I*DE (Partial *Integro*-Differential Equation), while $B_n^m[k_{n-m+1}, f_m]$ and $C_n^m[k_{n-m}, h_m]$ are forcing terms, where only terms including previous kernels k_m with $m < n$ appear. This means the set of PIDE's can be solved *recursively* up to any desired order n, beginning with k_1.

We introduce now some additional definitions needed for writing the expressions for $B_n^m[k_{n-m+1}, f_m]$, $C_n^m[k_{n-m}, h_m]$ and $I[k_n, f_1]$ in (9.4.38).

Definition 9.4. *Given a set $\mathcal{S} = \{a_1, a_2, \ldots, a_k\}$ of k ordered variables and given m such that $0 \leq m \leq k$, we define $P_m(\mathcal{S})$ as the set of all posible ordered k-tuples that can be formed in the following way. The first m elements of the k-tuple are any m members of $\mathcal{S}$* ordered *by their indices. The last $k - m$ elements of the k-tuple are all the remaining members of $\mathcal{S}$, also ordered by their indices.*

Example 9.5. If $\mathcal{S} = \{a_1, a_2, a_3, a_4\}$, then:

$$P_0(\mathcal{S}) = \{(a_1, a_2, a_3, a_4)\}, \tag{9.4.51}$$

$$P_1(\mathcal{S}) = \{(a_1, a_2, a_3, a_4), (a_2, a_1, a_3, a_4), (a_3, a_1, a_2, a_4), (a_4, a_1, a_2, a_3)\}, \tag{9.4.52}$$

$$\begin{aligned} P_2(\mathcal{S}) &= \{(a_1,a_2,a_3,a_4),(a_1,a_3,a_2,a_4),(a_1,a_4,a_2,a_3),(a_2,a_3,a_1,a_4), \\ &\quad (a_2,a_4,a_1,a_3),(a_3,a_4,a_1,a_2)\}, \qquad (9.4.53) \\ P_3(\mathcal{S}) &= \{(a_1,a_2,a_3,a_4),(a_1,a_2,a_4,a_3),(a_1,a_3,a_4,a_2),(a_2,a_3,a_4,a_1)\}, \qquad (9.4.54) \\ P_4(\mathcal{S}) &= \{(a_1,a_2,a_3,a_4)\}. \qquad (9.4.55) \end{aligned}$$

Remark 9.6. If $\mathcal{S}$ has k elements, the number of elements of $P_m(\mathcal{S})$ is

$$\begin{pmatrix} k \\ m \end{pmatrix} = \frac{k!}{m!(k-m)!}. \qquad (9.4.56)$$

Define $\xi_0 = x$ and given $i \le n$, $\hat{\xi}_i^n = (\xi_i, \ldots, \xi_n)$ and $\hat{\gamma}_i^n = (\gamma_i, \ldots, \gamma_n)$. Set, for any function $g(x, \xi_1, \ldots, \xi_{n+m}) = g(\hat{\xi}_0^{n+m})$, and $1 \le j \le n$,

$$D_j^{n,m}[g(\hat{\xi}_0^{n+m})] = \sum_{\hat{\gamma}_1^{n-j+m} \in P_{n-j}(\hat{\xi}_{j+1}^{n+m})} g(\hat{\xi}_0^j, \hat{\gamma}_1^{n-j+m}). \qquad (9.4.57)$$

Then, the definition of the term $B_n^m[k_{n-m+1}, f_m]$ is

$$\begin{aligned} B_n^m[k_{n-m+1}, f_m] &= \sum_{j=1}^{n-m+1} \int_{\xi_j}^{\xi_{j-1}} D_j^{n-m+1,m} \Big[k_{n-m+1}(\hat{\xi}_0^{j-1}, s, \hat{\xi}_j^{n-m}) \\ &\quad \times f_m(s, \hat{\xi}_{n-m+1}^n) \Big] \, ds. \qquad (9.4.58) \end{aligned}$$

The term $C_n^m[k_{n-m}, h_m]$ is defined as

$$C_n^m[k_{n-m}, h_m] = \sum_{j=1}^{n-m} D_j^{n-m,m} \left[k_{n-m}(\hat{\xi}_0^{n-m}) h_m(\xi_j, \hat{\xi}_{n-m+1}^n) \right]. \qquad (9.4.59)$$

The definition of $I_n[k_n, f_1]$ is, using (9.4.58),

$$I_n[k_n, f_1] = B_n^1[k_n, f_1]. \qquad (9.4.60)$$

Remark 9.7. The number of terms of $B_n^m[k_{n-m+1}, f_m]$ is, using Remark 9.6,

$$\sum_{j=1}^{n-m+1} \begin{pmatrix} n-j+1 \\ n-j-m+1 \end{pmatrix}. \qquad (9.4.61)$$

The number of terms of $I_n[k_n, f_1]$ is

$$\sum_{j=1}^{n} \begin{pmatrix} n-j+1 \\ n-j \end{pmatrix} = \sum_{j=1}^{n} (n-j+1) = n(n+1)/2. \qquad (9.4.62)$$

Hence in the PIDE for k_n, the total number of integrals in I_n and B_n^m is

$$\begin{aligned}
\sum_{m=1}^{n}\sum_{j=1}^{n-m+1}\begin{pmatrix} n-j+1 \\ n-j-m+1 \end{pmatrix} &= \sum_{j=1}^{n}\sum_{m=1}^{n-j+1}\begin{pmatrix} n-j+1 \\ n-j-m+1 \end{pmatrix} \\
&= \sum_{j=1}^{n}\sum_{m=0}^{n-j}\begin{pmatrix} n-j+1 \\ m \end{pmatrix} \\
&= \sum_{j=1}^{n}(2^{n-j+1}-1) \\
&= 2^{n+1}\sum_{j=1}^{n}2^{-j}-n \\
&= 2^{n+1}(2(1-2^{-n-1})-1)-n \\
&= 2^{n+1}-n-2. \qquad (9.4.63)
\end{aligned}$$

Similarly, the number of terms in C_n^m is 2^n-n-1.

We next show, as an illustration of the general case, the PIDE equations that the first three kernels, k_1, k_2 and k_3, verify.

The PIDE equation for k_1 is

$$\partial_{xx}k_1 = \partial_{\xi_1\xi_1}k_1+\lambda(\xi_1)k_1-f_1(x,\xi_1)+\int_{\xi_1}^{x}k_1(x,s)f_1(s,\xi_1)ds, \quad (9.4.64)$$

with boundary conditions

$$\begin{aligned}
k_1(x,x) &= \hat{q}-\frac{1}{2}\int_0^x\lambda(s)ds, \qquad (9.4.65)\\
k_{1\xi_1}(x,0) &= qk_1(x,0). \qquad (9.4.66)
\end{aligned}$$

This equation evolves on the triangle $\mathcal{T}_1=\{(x,\xi_1):0\le\xi_1\le x\le 1\}$, which is drawn in Fig. 9.1(left).

Remark 9.8. Equation (9.4.64) is an autonomous equation in k_1. It is a particular case of the kernel equation for backstepping control of linear parabolic PDEs. Its well-posedness is already established [101], where symbolic and numerical methods of solution are proposed.

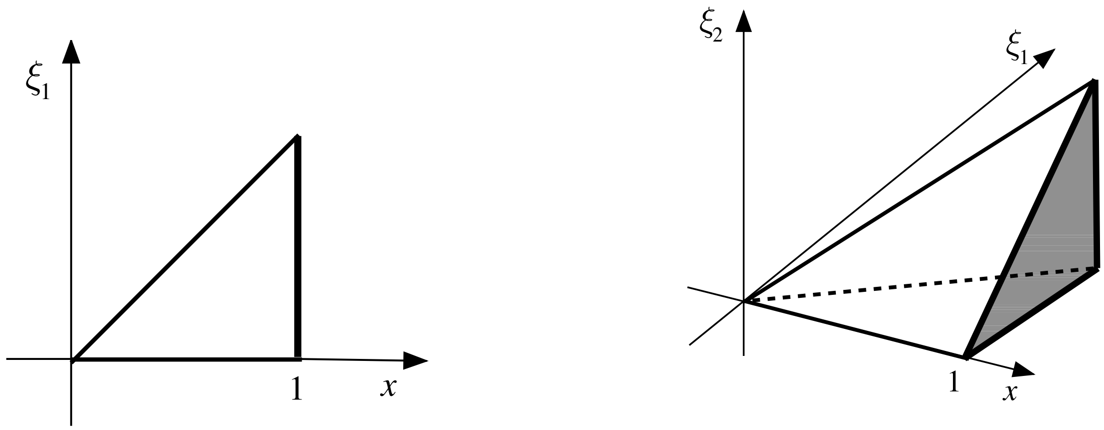

Figure 9.1: Left: The domain $\mathcal{T}_1$. Boundary conditions are given at $\xi_1 = 0$ and $x = \xi_1$ (lower and diagonal lines, respectively). The feedback law requires to compute the kernel k_1 at the boundary $x = 1$ (the vertical bold line). Right: The domain $\mathcal{T}_2$ shown in perspective. Robin boundary conditions are given at $\xi_2 = 0$ (the ground surface), while at $x = \xi_1$ (normal to the ground and hidden behind the figure due to the perspective) we have both Dirichlet and Neumann boundary conditions (initial-like conditions). A Neumann boundary condition is given at $\xi_1 = \xi_2$ (the surface that lies in front of a viewer looking in the ξ_1 direction). The feedback law requires to compute the kernel k_2 at the boundary $x = 1$ (the shaded surface).

The PIDE equation verified by k_2 is

$$\begin{aligned}
\partial_{xx} k_2 &= \partial_{\xi_1\xi_1} k_2 + \partial_{\xi_2\xi_2} k_2 + (\lambda(\xi_1) + \lambda(\xi_2))\, k_2 - f_2(x, \xi_1, \xi_2) \\
&\quad + \int_{\xi_1}^{x} k_1(x, s) f_2(s, \xi_1, \xi_2) ds + \int_{\xi_2}^{\xi_1} k_2(x, \xi_1, s) f_1(s, \xi_2) ds \\
&\quad + \int_{\xi_1}^{x} k_2(x, s, \xi_1) f_1(s, \xi_2) ds + \int_{\xi_1}^{x} k_2(x, s, \xi_2) f_1(s, \xi_1) ds \\
&\quad + k_1(x, \xi_1) h_1(\xi_1, \xi_2), \qquad (9.4.67)
\end{aligned}$$

with boundary conditions

$$\begin{aligned}
k_2(x, x, \xi_2) &= -\frac{1}{2} \int_{\xi_2}^{x} h_1(s, \xi_2) ds, \qquad (9.4.68) \\
k_{2x}(x, x, \xi_2) &= -\frac{1}{4} \left(3 h_1(\xi_2, \xi_2) + h_1(x, \xi_2)\right) \\
&\quad + \frac{1}{2} \int_{\xi_2}^{x} \phi_2(s, \xi_2) ds, \qquad (9.4.69) \\
k_{2\xi_2}(x, \xi_1, 0) &= q k_2(x, \xi_1, 0), \qquad (9.4.70) \\
\partial_{\xi_1} k_2(x, \xi_1, \xi_2)\Big|_{\xi_2 = \xi_1} &= \partial_{\xi_2} k_2(x, \xi_1, \xi_2)\Big|_{\xi_2 = \xi_1}, \qquad (9.4.71)
\end{aligned}$$

where

$$\begin{aligned}\phi_2(x,\xi_2) \;=\; & \int_{\xi_2}^{x} h_{1\xi_2\xi_2}(s,\xi_2)ds - 2h_{1\xi_2}(\xi_2,\xi_2) - h_{1\xi_1}(\xi_2,\xi_2) \\ & + (\lambda(x)+\lambda(\xi_2)) \int_{\xi_2}^{x} h_1(s,\xi_2)ds + 2f_2(x,x,\xi_2) \\ & + \int_{\xi_2}^{x}\int_{s}^{x} h_1(\sigma,s)f_1(s,\xi_2)d\sigma ds + h_1(x,\xi_2)\int_0^x \lambda(s)ds. \end{aligned} \tag{9.4.72}$$

This equation evolves on the pyramid $\mathcal{T}_2 = \{(x,\xi_1,\xi_2) : 0 \le \xi_2 \le \xi_1 \le x \le 1\}$, which is shown in Fig. 9.1(right). Once k_1 is solved from (9.4.64), it can be plugged into (9.4.67) which becomes an autonomous equation for k_2.

The equation verified by k_3 is the following.

$$\begin{aligned}\partial_{xx}k_3 \;=\; & \partial_{\xi_1\xi_1}k_3 + \partial_{\xi_2\xi_2}k_3 + \partial_{\xi_3\xi_3}k_3 + (\lambda(\xi_1)+\lambda(\xi_2)+\lambda(\xi_3))\,k_3 \\ & -f_3(x,\xi_1,\xi_2,\xi_3) + \int_{\xi_1}^{x} k_1(x,s)f_3(s,\xi_1,\xi_2,\xi_3)ds \\ & + \int_{\xi_2}^{\xi_1} k_2(x,\xi_1,s)f_2(s,\xi_2,\xi_3)ds + \int_{\xi_1}^{x} k_2(x,s,\xi_1)f_2(s,\xi_2,\xi_3)ds \\ & + \int_{\xi_1}^{x} k_2(x,s,\xi_2)f_2(s,\xi_1,\xi_3)ds + \int_{\xi_1}^{x} k_2(x,s,\xi_3)f_2(s,\xi_1,\xi_2)ds \\ & + \int_{\xi_3}^{\xi_2} k_3(x,\xi_1,\xi_2,s)f_1(s,\xi_3)ds + \int_{\xi_2}^{\xi_1} k_3(x,\xi_1,s,\xi_2)f_1(s,\xi_3)ds \\ & + \int_{\xi_2}^{\xi_1} k_3(x,\xi_1,s,\xi_3)f_1(s,\xi_2)ds + \int_{\xi_1}^{x} k_3(x,s,\xi_2,\xi_3)f_1(s,\xi_1)ds \\ & + \int_{\xi_1}^{x} k_3(x,s,\xi_1,\xi_3)f_1(s,\xi_2)ds + \int_{\xi_1}^{x} k_3(x,s,\xi_1,\xi_2)f_1(s,\xi_3)ds \\ & +k_2(x,\xi_1,\xi_2)h_1(\xi_2,\xi_3) + k_2(x,\xi_1,\xi_2)h_1(\xi_1,\xi_3) \\ & +k_2(x,\xi_1,\xi_3)h_1(\xi_1,\xi_2) + k_1(x,\xi_1)h_2(\xi_1,\xi_2,\xi_3), \end{aligned} \tag{9.4.73}$$

with boundary conditions

$$k_3(x,x,\xi_2,\xi_3) = -\frac{1}{2}\int_{\xi_2}^{x} h_2(s,\xi_2,\xi_3)ds, \tag{9.4.74}$$

$$\begin{aligned} k_{3x}(x,x,\xi_2,\xi_3) = & -\frac{1}{4}\left(3h_2(\xi_2,\xi_2,\xi_3) + h_2(x,\xi_2,\xi_3)\right) \\ & + \frac{1}{2}\int_{\xi_2}^{x} \phi_3(s,\xi_2,\xi_3)ds, \end{aligned} \tag{9.4.75}$$

$$k_{3\xi_3}(x,\xi_1,\xi_2,0) = qk_3(x,\xi_1,\xi_2,0), \tag{9.4.76}$$

$$\partial_{\xi_1} k_3(x,\xi_1,\xi_2,\xi_3)\Big|_{\xi_2=\xi_1} = \partial_{\xi_2} k_3(x,\xi_1,\xi_2,\xi_3)\Big|_{\xi_2=\xi_1}, \tag{9.4.77}$$

$$\partial_{\xi_2} k_3(x,\xi_1,\xi_2,\xi_3)\Big|_{\xi_3=\xi_2} = \partial_{\xi_3} k_3(x,\xi_1,\xi_2,\xi_3)\Big|_{\xi_3=\xi_2}, \tag{9.4.78}$$

where ϕ_3 is

$$\begin{aligned}
\phi_3(x,\xi_2,\xi_3) \;=\; & \int_{\xi_2}^{x} h_{2\xi_2\xi_2}(s,\xi_2,\xi_3)ds - 2h_{2\xi_2}(\xi_2,\xi_2,\xi_3) - h_{2\xi_1}(\xi_2,\xi_2,\xi_3) \\
& + \int_{\xi_2}^{x} h_{2\xi_3\xi_3}(s,\xi_2,\xi_3)ds + (\lambda(x)+\lambda(\xi_2)+\lambda(\xi_3)) \int_{\xi_2}^{x} h_2(s,\xi_2,\xi_3)ds \\
& + 2f_3(x,x,\xi_2,\xi_3) + \int_{\xi_2}^{x}\int_{s}^{x} h_1(\sigma,s) f_2(s,\xi_2,\xi_3) d\sigma ds \\
& + \int_{\xi_3}^{\xi_2}\int_{\xi_2}^{x} h_2(\sigma,\xi_2,s) f_1(s,\xi_3) d\sigma ds + \int_{\xi_2}^{x}\int_{s}^{x} h_2(\sigma,s,\xi_2) f_1(s,\xi_3) d\sigma ds \\
& + \int_{\xi_2}^{x}\int_{s}^{x} h_2(\sigma,s,\xi_3) f_1(s,\xi_2) d\sigma ds + h_1(\xi_2,\xi_3)\int_{\xi_2}^{x} h_1(s,\xi_2)ds \\
& + h_1(x,\xi_3)\int_{\xi_2}^{x} h_1(s,\xi_2)ds + h_1(x,\xi_2)\int_{\xi_2}^{x} h_1(s,\xi_3)ds \\
& + h_2(x,\xi_2,\xi_3)\int_{\xi_2}^{x}\lambda(s)ds
\end{aligned} \tag{9.4.79}$$

This equation evolves on the 4-dimensional hyper-pyramid $\mathcal{T}_3 = \{(x,\xi_1,\xi_2,\xi_3) : 0 \le \xi_3 \le \xi_2 \le \xi_1 \le x \le 1\}$. Once k_2 and k_1 are known from (9.4.64) and (9.4.67) the equation (9.4.73) becomes autonomous in k_3.

Note the increasing complexity of the kernel PIDEs but also the common recursive structure that underlies all the equations.

9.5 An Analytic Example of a Stabilizable Super-Linear System

Consider for this section the simpler case for which $\lambda = 0$ and $H = 0$, so only the F nonlinearity is present in (9.2.1), and $q = \infty$ (Dirichlet boundary conditions).

In Section 9.6 we discuss a numerical approach that would be used for solving for the controller gain kernels. However, at this point we don't have a proof of well posedness of the series of PIDEs for the gain kernels. For this reason, in this section we present an “inverse” where, instead of solving for the k-kernels with the f-kernels as given, we solve for the f-kernels with the k-kernels as given. This is not possible in general, however, in the case where $f_1 = 0$, i.e., the “purely nonlinear” case where the plant doesn't have a linear term in its Volterra series, it is possible to find the f-kernels when the k-kernels are given, i.e., it is possible to find the plant that is stabilized by a pre-assigned controller. This is easy to see by examining the equations (9.4.64)–(9.4.78). First, when $f_1 = 0$, then $k_1 = 0$. Second, for any k_2 that satisfies the boundary conditions (9.4.68)–(9.4.71), the kernel f_2 is obtained by direct evaluation of the derivatives of k_2 from (9.4.67). Third, for any k_3 that satisfies the boundary conditions (9.4.74)–(9.4.78), the kernel f_3 can be obtained by direct evaluation of certain integrals in (9.4.73). And so on for $f_4, f_5, \ldots$

So, starting with a controller as simple as possible—yet nonlinear—in this section we illustrate how it is possible to solve (9.4.38)–(9.4.44) to find the (nonlinear) plant which is stabilized by the preassigned controller

The simplest possible (nonlinear) controller we can think of comes from a single *second order* control kernel, $k_2 = \sigma_1\sigma_2(x-\sigma_1)(x-\sigma_2)$, whose particular form is chosen to satisfy (9.4.68)–(9.4.71). All other control kernels are set to zero, i.e., $k_1 = k_3 = \ldots = k_n = \ldots = 0$. Then the control input, $U(t) = K[u](t,1)$, is:

$$\begin{aligned} U(t) &= K[u](t,1) = \int_0^1 \int_0^{\xi_1} \xi_1\xi_2(x-\xi_1)(x-\xi_2) \\ &\quad \times u(t,\xi_1)u(t,\xi_2)d\xi_1 d\xi_2, \end{aligned} \tag{9.5.80}$$

which can be written shorter thanks to the symmetry of the kernel:

$$U(t) = \tfrac{1}{2}\left(\int_0^1 \xi(x-\xi)u(t,\xi)d\xi\right)^2. \tag{9.5.81}$$

The plant kernels derived from (9.4.38) are $f_1 = 0$,

$$\begin{aligned} f_2 &= 2\xi_2\xi_1 + 2\xi_2 x - 2\xi_2^2 + 2\xi_1 x - 2\xi_1^2, \qquad (9.5.82) \\ f_3 &= \xi_1\xi_2 x\left(\frac{x\xi_2}{3}(\xi_2^2+\xi_1 x) - \frac{\xi_2^4}{6} - \frac{\xi_1^4}{6} - \frac{x^3}{2}(\xi_1+\xi_2) + \frac{\xi_1^3}{3}(x-\xi_2)\right. \end{aligned}$$

$$
\begin{aligned}
& +\frac{\xi_2\xi_1}{3}(x^2-\xi_2^2)+\frac{x^4}{3}\Bigg)+\xi_1\xi_3 x\left(\frac{x^4}{3}+\frac{\xi_1^3}{3}(x-\xi_3)+\frac{2\xi_3\xi_1x^2}{3}\right. \\
& \left.-\frac{\xi_1^4}{6}-\frac{x^3}{2}(\xi_1+\xi_3)\right)+\frac{\xi_1^2}{6}\left(\xi_2^5+\xi_1^3(\xi_3^2+\xi_2^2)\right)+\xi_2\xi_3x^2\left(\frac{x^2}{3}\right. \\
& \left.-\frac{x}{2}(\xi_2-\xi_3)+\frac{2\xi_2\xi_3}{3}\right)+\frac{\xi_1^2\xi_2\xi_3}{6}\left(4\xi_3\xi_2(2\xi_1+\xi_2)-7\xi_2^3\right. \\
& \left.-7\xi_1^2(\xi_2+\xi_3)\right)+\frac{x\xi_1\xi_2\xi_3}{6}\left(6x\xi_3\xi_1+7\xi_2^3+14\xi_1^3-20\xi_1^2x\right. \\
& +6x\xi_3\xi_2+\xi_2^2(10\xi_1-4\xi_3-10x)+2x^2(3x-\xi_1-\xi_2-\xi_3) \\
& \left.+6\xi_1(\xi_3\xi_1+\xi_2\xi_1+x\xi_2-3\xi_2\xi_3)\right), \qquad (9.5.83)
\end{aligned}
$$

$$
f_n = B_n^{n-1}[k_2, f_{n-1}], \qquad (9.5.84)
$$

where we can write (9.5.84) using definition (9.4.58) as

$$
\begin{aligned}
f_n = & \int_{\xi_2}^{\xi_1} k_2(x,\xi_1,s) f_{n-1}(s,\xi_2,\dots,\xi_n)ds \\
& + \int_{\xi_1}^{x} \sum_{\hat{\gamma}_1^n \in P_1(\hat{\xi}_1^n)} k_2(x,s,\gamma_1) f_{n-1}(s,\gamma_2,\dots,\gamma_n)ds. \qquad (9.5.85)
\end{aligned}
$$

Using this definition and employing a symbolic calculation program, it is possible to get all the kernels up to a desired order. Higher order kernels get smaller and smaller, and their influence becomes almost negligible. This is stated in the following lemma, that guarantees convergence of the Volterra series of the plant defined by (9.5.82)–(9.5.84).

Proposition 9.9. *The kernels $f_2,\dots,f_n,\dots$ defined by (9.5.82)–(9.5.84) verify the following bound.*

$$
|f_n(x,\xi_1,\dots,\xi_n)| \le \frac{x^{5n-8}}{4}. \qquad (9.5.86)
$$

Hence, the Volterra series defined by $\sum_{i=2}^{\infty} F_i[u](t,x)$ converges for $u \in L^2(0,1)$.

Proof. For every n one has that $\xi_n \le \xi_{n-1} \le \dots \le \xi_1 \le x$. Note that

$$
|k_2| = |\xi_1\xi_2(x-\xi_1)(x-\xi_2)| \le \frac{x^4}{16}. \qquad (9.5.87)
$$

For $n = 2$,

$$\begin{aligned} |f_2| &= \left|2\xi_2\xi_1 + 2\xi_2 x - 2\xi_2^2 + 2\xi_1 x - 2\xi_1^2\right| \\ &= |2\xi_2\xi_1 + 2\xi_2(x-\xi_2) + 2\xi_1(x-\xi_1)| \\ &\leq x^2(2 + 1/2 + 1/2) = 3x^2. \end{aligned} \tag{9.5.88}$$

Assume now the claim of the theorem is true for $n-1$. Then, for n,

$$\begin{aligned} |f_n| &= \left|\int_{\xi_2}^{\xi_1} k_2(x,\xi_1,s) f_{n-1}(s,\xi_2,\ldots,\xi_n)ds \right. \\ &\quad \left. + \int_{\xi_1}^{x} \sum_{\hat{\gamma}_1^n \in P_1(\hat{\xi}_1^n)} k_2(x,s,\gamma_1) f_{n-1}(s,\gamma_2,\ldots,\gamma_n)ds \right| \\ &\leq \frac{x^4}{16}\left(\int_{\xi_2}^{\xi_1} 3s^{5n-13}ds + \int_{\xi_1}^{x} \sum_{\hat{\gamma}_1^n \in P_1(\hat{\xi}_1^n)} 3s^{5n-13}ds\right) \\ &= \frac{x^4}{16}\left(3\frac{n+1}{5n-12}x^{5n-12}\right) \\ &= 3x^{5n-8}\frac{n+1}{16(5n-12)} \\ &\leq \frac{x^{5n-8}}{4}, \end{aligned} \tag{9.5.89}$$

since for $n \geq 3$, $\frac{n+1}{16(5n-12)} \leq 1/12$. This gives us (9.5.86).

Since $x \in (0,1)$, we have that $|f_n| \leq \frac{1}{4}$. Hence if $u \in L^2(0,1)$,

$$\begin{aligned} \int_0^1 \left(\sum_{n=2}^{\infty} F_n[u](t,x)\right)^2 dx &= \int_0^1 \left(\sum_{n=2}^{\infty} \int_0^x \int_0^{\xi_1} \cdots \int_0^{\xi_{n-1}} f_n(x,\xi_1,\ldots,\xi_n)\right. \\ &\quad \left. \times \left(\prod_{j=1}^{n} u(t,\xi_j)\right) d\xi_1 \ldots d\xi_n\right)^2 dx \\ &\leq \frac{1}{16}\int_0^1 \left(\sum_{n=2}^{\infty} \frac{\left(\int_0^x u(t,\xi)d\xi\right)^n}{n!}\right)^2 \\ &\leq \frac{\|u\|_{L^2}^2 \exp\left(\|u\|_{L^2}^2 - 1\right)}{8}, \end{aligned} \tag{9.5.90}$$

where we have followed similar steps as in (9.3.18). This completes the proof. $\square$

For the purpose of illustrating the effect of the functional operators K and F, we plot the effect of both of them on an example function, $u(t,x) =$

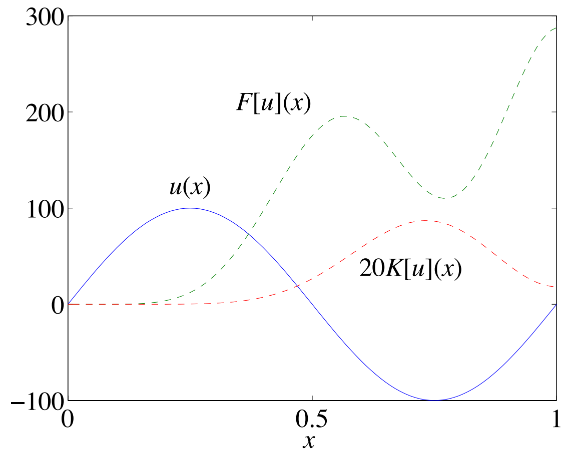

Figure 9.2: Effect of K and F on $u(t,x) = 100\sin(2\pi x)$

$100\sin(2\pi x)$, in Figure 9.2. The order of magnitude of K is much less than the order of magnitude of F, so we plot $20K$ for the sake of clarity.

9.6 Numerical Simulations

In general it is not possible to obtain analytic expressions for the Volterra kernels. Thus we have to rely on numerical simulations to compute the k_n's. The first-order kernel is computed with a finite differences scheme from [101]. Using a similar finite difference scheme, we were able to compute the second-order kernels for the examples of Section 9.3 and then used them for closed-loop simulations of the system. The main additions to the method of [101] were the use of the extra boundary condition (9.4.69) and using a smaller discretization step for x than for the ξ variables, which is essential for stability [81].

9.6.1 Coupled nonlinear plant

Consider the example plant given in Section 9.3.1. Its Volterra nonlinearity is explicitly written in Equation (9.3.20). We set the numerical values for the parameters of the plant as $\mu = 50$, $\omega = 2.5$. A simple linear stability analysis shows that the equilibrium at the origin is unstable for these values.

To find a control law to stabilize the system, we apply the design method outlined in Section 9.4, and numerically solved for the kernels. In Fig. 9.3 we show the numerical value of the first two kernels, k_1 and k_2, at $x = 1$, which is the value appearing in the control formula (9.4.36). We found that using just the linear kernel k_1 in the feedback law (9.4.36)[1], stabilized the system for a wide range of initial conditions. However, for initial conditions of large enough size (with a peak of the order of 1000), the linear controller fails to stabilize the system, as shown in Fig. 9.4. In Fig. 9.5 we show how the same initial condition is stabilized when the second-order kernel is used in (9.4.36), i.e., truncating the control law to second order is enough for stabilization for that size of initial conditions.

9.6.2 Quadratic nonlinearity

Consider the plant

$$u_t = u_{xx} + u^2, \tag{9.6.91}$$

with boundary conditions

$$u(t, 0) = 0, \quad u_x(t, 1) = U(t). \tag{9.6.92}$$

This plant is in the class of the example of Section 9.3.2, with $f(u) = u^2$. Then, in (9.3.32), $\lambda = 0$, $h_1 = 2$, and for $n > 1$, $h_n = 0$. In this case, $k_1 = 0$ as the plant does not have linear terms. In Fig 9.6 we show the numerical value of the second order control kernel k_2. We tested numerically the control law (9.4.36) using only k_2. We found that, for initial conditions of size large enough (with a peak value approximately more than 4), the open-loop system blows up (in finite time), as shown in Fig. 9.7 (left). In Fig. 9.7 (right), we show how the second-order controller is able to prevent the blow-up and stabilize the system for the same initial conditions. However, the same controller fails to stabilize u for larger initial conditions (with peaks over 8). This restricted local result is not only due to truncation of (9.4.36), but to the fact that (9.6.91) is *not* globally stabilizable

[1] This is equivalent to applying the result of [101] to the *linearized* system.

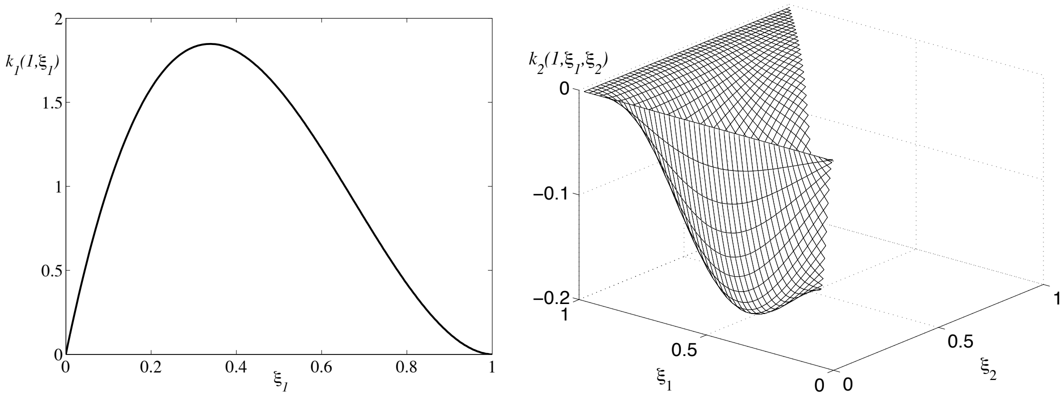

Figure 9.3: Control kernels $k_1(1, \xi_1)$ (left) and $k_2(1, \xi_1, \xi_2)$ (right) for the example of Section 9.3.1, with $\mu = 50$, $\omega = 2.5$. Note that the kernel $k_2(1, \xi_1, \xi_2)$ is only defined for $\xi_2 \leq \xi_1$.

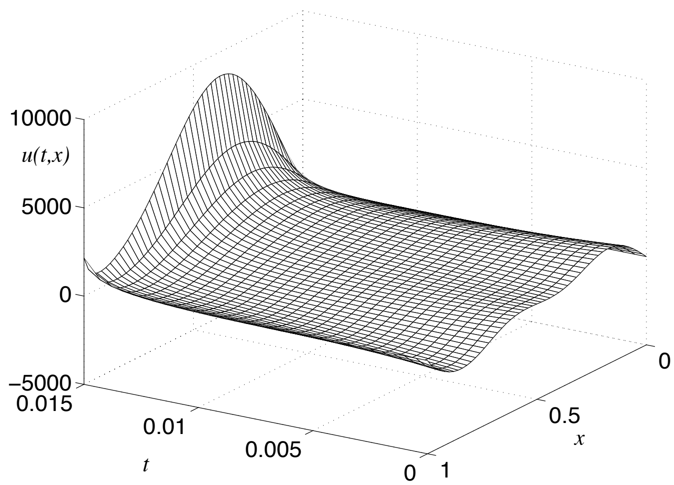

Figure 9.4: Closed-loop simulation for $u(t, x)$ using only the first (linear) order kernel k_1, in the example of Section 9.3.1.

(see Remark 9.1). Thus increasing the controller-order may enlarge the basin of attraction of the origin for the closed-loop system, but only up to a certain limit.

9.6.3 Simulations results for the example of Section 9.5

We made numerical simulations of the nonlinear plant introduced in Section 9.5. Starting with a large enough initial condition (of the order of 200), the uncontrolled system diverges to infinity in finite time, as seen in Figure 9.8. With the controller (9.5.80), this behavior is suppressed and the system is stabilized, as

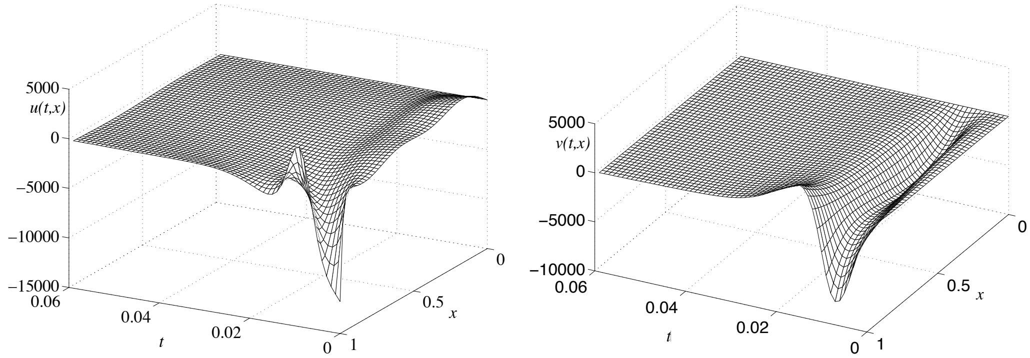

Figure 9.5: Closed-loop simulation for $u(t,x)$ (left) and $v(t,x)$ (right) in the example of Section 9.3.1. The control law is approximated to second order using control kernels k_1 and k_2.

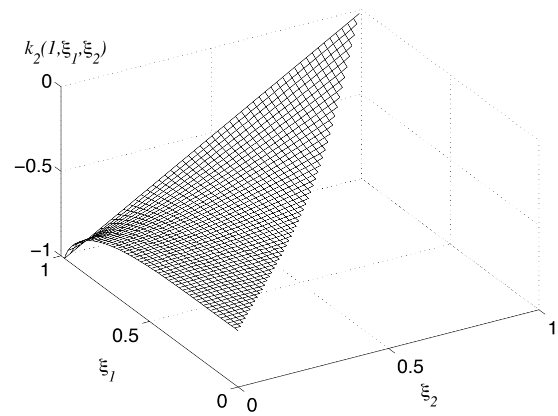

Figure 9.6: Second-order control kernel $k_2(1, \xi_1, \xi 2)$ for the example of Section 9.3.2 with $f(u) = u^2$ (quadratic nonlinearity). Note that the kernel $k_2(1, \xi_1, \xi_2)$ is only defined for $\xi_2 \leq \xi_1$.

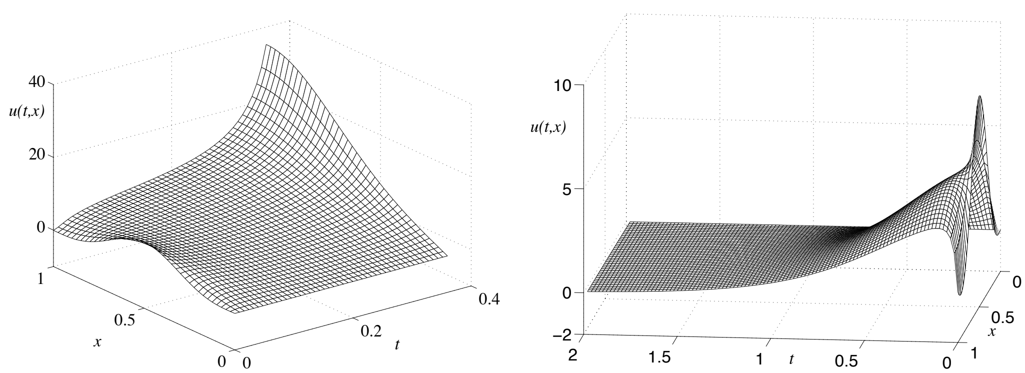

Figure 9.7: Uncontrolled (left) and controlled system (right) for the example of Section 9.3.2 with $f(u) = u^2$ (quadratic nonlinearity). The control law is truncated to second order. The solution of the uncontrolled system blows up in finite time, while the controlled system converges to the origin.

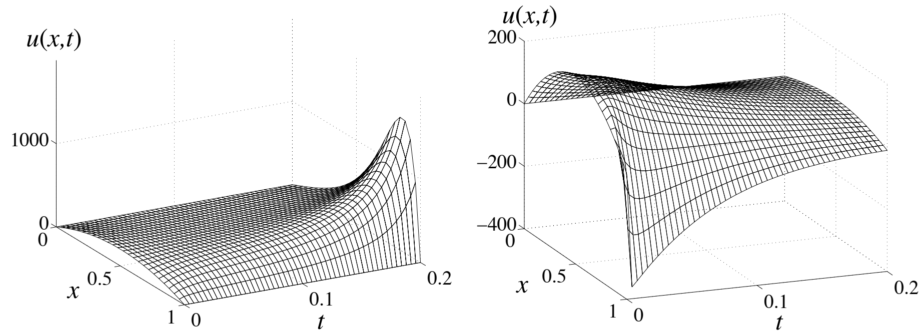

Figure 9.8: Uncontrolled (left) and controlled system (right) for the example of Section 9.5. The solution of the uncontrolled system blows up in finite time. The trayectory of the control input (right) is $u(t, 1)$. The size of the control effort (-400) is reasonable given the size of the initial condition (with a peak about 200).

shown in Figure 9.8.

9.7 Convergence Analysis for the Transformation

In this section we study the convergence of (9.4.35) and (9.4.36).

9.7.1 Mathematical Preliminaries

First we establish some notation and state some results about Volterra series.

Define $\mathcal{T}_n(x,\xi) = \left\{(\hat{\xi}_1^n) : 0 \leq \xi_n \leq \ldots \leq \xi_1 \leq x \leq 1\right\}$. Note that $\mathcal{T}_n = \mathcal{T}_n(1,\xi)$. Define also

$$\prod^{i} u = \prod_{j=1}^{i} u(t,\xi_j), \quad \prod^{i,k} u = \prod_{\substack{j=1 \\ j\neq k}}^{i} u(t,\xi_j), \tag{9.7.93}$$

$$\int_{\mathcal{T}_n(x,\xi)} f(\hat{\xi}_0^n) d\hat{\xi}_1^n = \int_0^x \int_0^{\xi_1} \cdots \int_0^{\xi_{n-1}} f(x,\xi_1 \ldots \xi_n) d\xi_1 \ldots d\xi_n. \tag{9.7.94}$$

We formalize the concept of convergence of Volterra series with $L^2(\mathcal{T}_n)$ kernels. Consider a Volterra series $F[u]$ with kernels $f_n(\hat{\xi}_0^n)$, i.e.,

$$F[u](t,x) = \sum_{n=1}^{\infty} F_n[u](t,x) = \sum_{n=1}^{\infty} \int_{\mathcal{T}_n(x,\xi)} f_n(\hat{\xi}_0^n) \prod^{i} u d\hat{\xi}_1^n, \tag{9.7.95}$$

The following definition quantifies the convergence of (9.7.95) in $L^2(0,1)$ (in the sequel we will write just L^2 for simplicity).

Definition 9.10. *Given (9.7.95) with kernels $f_n \in L^2(\mathcal{T}_n)$, we define the radius of convergence ρ as*

$$\rho = \left(\limsup_{n\to\infty} \left(\frac{\|f_n\|^2_{L^2(\mathcal{T}_n)}}{n!} \right)^{1/n} \right)^{-1}, \tag{9.7.96}$$

and the gain bound function $f(s) : [0,\rho) \to [0,\infty)$ as

$$f(s) = 2 \sum_{n=1}^{\infty} \frac{n^2 \|f_n\|^2_{L^2(\mathcal{T}_n)}}{n!} s^n. \tag{9.7.97}$$

Using ρ and f from Definition 9.10 we can state a result that guarantees convergence of the Volterra series (9.7.95).

Theorem 9.11 (Gain Bound Theorem). *Given a Volterra series $F[u]$ as in (9.7.95), with kernels $f_n \in L^2(\mathcal{T}_n)$, radius of convergence ρ and gain bound function f, the following results hold.*

1. *The integrals and sums in (9.7.95) converge for $u \in L^2$ verifying that $\|u\|^2_{L^2} < \rho$.*
2. *$F[u]$ satisfies $\|F[u]\|^2_{L^2} \le f(\|u\|^2_{L^2})$ and consequently F maps balls of L^2 into balls of L^2.*

Proof. From the definition (9.7.95), and using the Cauchy-Schwartz inequality,

$$F_n[u]^2 \;\le\; \|f_n\|^2_{L^2(\mathcal{T}_n)} \left(\int_{\mathcal{T}_n(x,\xi)} \prod^{n} u^2 d\hat{\xi}_1^n \right) = \frac{\|f_n\|^2_{L^2(\mathcal{T}_n)} \|u\|^{2n}_{L^2}}{n!}, \tag{9.7.98}$$

hence,

$$\begin{aligned} F[u]^2 &= \int_0^1 \left(\sum_{n=1}^{\infty} F_n[u] \right)^2 dx \\ &\le \left(\sum_{n=1}^{\infty} n^2 F_n[u]^2 \right) \left(\sum_{n=1}^{\infty} \frac{1}{n^2} \right) \\ &\le 2 \sum_{i=1}^{\infty} \frac{n^2 \|f_n\|^2_{L^2(\mathcal{T}_n)} \|u\|^{2n}_{L^2}}{n!}, \end{aligned} \tag{9.7.99}$$

where we used that $\sum_{n=1}^{\infty}\frac{1}{n^2}=\frac{\pi^2}{6}\leq 2$. Thus we obtain

$$\|F[u]\|_\infty^2=\max_{x\in(0,1)}F[u]^2\leq 2\sum_{i=1}^{\infty}\frac{n^2\|f_n\|^2_{L^2(\mathcal{T}_n)}\|u\|_{L^2}^{2n}}{n!}. \tag{9.7.100}$$

Then from elementary theory of power series and noting that $\lim_{n\to\infty}\sqrt[n]{n^2}=1$ and that $\|F[u]\|^2_{L^2}\leq\|F[u]\|^2_\infty$, the result follows. $\square$

We give now some examples illustrating Theorem 9.11.

Example 9.12. Let $F[u]$ be a Volterra series with kernels f_n and let C and D be generic positive constants.

1. If the kernels f_n verify an uniform bound $\|f_n\|^2_{L^2(\mathcal{T}_n)}\leq D$, then $\rho=\infty$ and the series is everywhere convergent for $u\in L^2$. We also have that $f(s)=2s(s+1)D\exp(s)$. Note also that $f(s)\leq 2D\left(\exp(3s)-1\right)$.

2. If the kernels f_n grow exponentially like $\|f_n\|^2_{L^2(\mathcal{T}_n)}\leq DC^n$, then again $\rho=\infty$ and the series is everywhere convergent. We have in this case that $f(s)=2sC(sC+1)D\exp(Cs)$. Note also that $f(s)\leq 2D\left(\exp(3Cs)-1\right)$.

3. If the kernels f_n grow as fast as $\|f_n\|^2_{L^2(\mathcal{T}_n)}\leq n!DC^n$, then $\rho=1/C$ and the series convergence can only be guaranteed if $\|u\|_{L^2}\leq 1/C$. We have in this case that $f(s)=\frac{2sC(sC+1)D}{(1-sC)^3}$. Note that $f(s)\leq\frac{2D(sC)^2}{(1-sC)^4}$

Remark 9.13. Since $\|f_n\|^2_{L^2(\mathcal{T}_n)}\leq\frac{\|f_n\|^2_\infty}{n!}$, if $f_n\in L^\infty(\mathcal{T}_n)$, similar results to Theorem 9.11 can be stated in terms of the L^∞ norms of the f_n's. Note also that by (9.7.100) the L^∞ norm of $F[u]$ is well defined for $u\in L^2$.

Remark 9.14. From (9.4.35),

$$\begin{aligned} w_x &= u_x-k_1(x,x)u(x)-u(x)\sum_{n=1}^{\infty}\int_{\mathcal{T}_n(x,\xi)}k_{n+1}(x,x,\hat{\xi}_1^n)\prod_n u\,d\hat{\xi}_1^n \\ &\quad -\sum_{n=1}^{\infty}\int_{\mathcal{T}_n(1,\xi)}k_{nx}(x,\hat{\xi}_1^n)\prod_n u\,d\hat{\xi}_1^n \\ &= u_x-\bar{k}(x)u(x)-u(x)\bar{K}[u]-\tilde{K}[u], \end{aligned} \tag{9.7.101}$$

where $\bar{K}[u]$ and $\tilde{K}[u]$ are Volterra series in u (not in u_x) with kernels $\bar{k}_n = k_{n+1}(x, x, \hat{\xi}_1^n)$ and $\tilde{k}_n = k_{nx}(x, \hat{\xi}_1^n)$. Note that from the boundary condition (9.4.41), we have that

$$\bar{k} = \hat{q} - \frac{1}{2}\int_0^x \lambda(s)ds, \quad \bar{k}_n = -\frac{1}{2}\int_{\xi_1}^x h_n(s, \hat{\xi}_1^n)ds, \tag{9.7.102}$$

where $\hat{q} = \min\{0, q\}$. Hence,

$$\|w_x\|_{L^2}^2 \leq 4\left(\|u_x\|_{L^2}^2 + \|u\|_{L^2}^2\|\bar{k}\|_\infty^2 + \|u\|_{L^2}^2\|\bar{K}[u]\|_\infty^2 + \|\tilde{K}[u]\|_{L^2}^2\right), \tag{9.7.103}$$

which means that the H_1 norm of w can be computed from the H^1 norm of u.

9.7.2 Assumptions

In the sequel, we assume the following hypothesis are true.

Assumption 9.15. *We assume the following holds.*

1. $\lambda(x) \in \mathcal{C}^1[0,1]$, $h_n \in \mathcal{C}^1[\mathcal{T}_n]$, $f_n \in \mathcal{C}^0[\mathcal{T}_n]$.

2. *The sequence $h_n(\hat{\xi}_0^{n+1})$ verifies the following bound*

$$\max_{(\hat{\xi}_0^n)\in\mathcal{T}_n}\left\{\left|h_n(\hat{\xi}_0^n)\right| + \sum_{i=0}^n \left|h_{n\xi_i}(\hat{\xi}_0^n)\right|\right\} \leq D_h\left(\frac{1}{\rho_h}\right)^{n-1} n!. \tag{9.7.104}$$

3. *The parameter $\lambda(x)$ verifies*

$$\max_{x\in[0,1]}\{|\lambda(x)|\} \leq D_h. \tag{9.7.105}$$

4. *The sequence $f_n(\hat{\xi}_0^{n+1})$ verifies the following bound*

$$\max_{(\hat{\xi}_0^n)\in\mathcal{T}_n}\left\{\left|f_n(\hat{\xi}_0^n)\right|\right\} \leq D_f\left(\frac{1}{\rho_f}\right)^{n-1} n!. \tag{9.7.106}$$

5. *Under the above assumptions, for each n, there exists a $H^1(\mathcal{T}_n)$ solution k_n of the kernel PIDE equations (9.4.38)–(9.4.44).*

Remark 9.16. In Assumption 9.15, point 1 specify some continuity and differentiability requirements for the parameters of the plant. Points 2 and 4 quantify the convergence of the plant nonlinearities H and F. Point 5 ensures that the set of kernel PIDE equations is well-posed.

9.7.3 Main Convergence Result

We next show a result that relates the convergence of the transformation and the feedback law series, respectively (9.4.35) and (9.4.36), to the convergence of the plant nonlinearities $F[u]$ and $H[u]$. The result also studies the convergence of the transformation (9.7.101) for w_x.

Theorem 9.17. *Under Assumption 9.15, the Volterra series in the transformation (9.4.35), the control law (9.4.36) and the w_x transformation (9.7.101) are convergent with radius of convergence*

$$\rho_k = \left(\frac{\min\{\rho_f, \rho_h\}}{2}\right)^2 \exp\left(-2\sqrt{\gamma}\right), \tag{9.7.107}$$

where $\gamma = \max\{1, \|f_1\|_\infty + \|\lambda\|_\infty\}$. Moreover, k_n verifies

$$\|k_n\|^2_{L^2(\mathcal{T}_n)} \leq (n-1)! 4 D^2 C^{2n-2} \exp\left(2n\sqrt{\gamma} + 2\Upsilon + |\hat{q}|\right), \tag{9.7.108}$$

$$\|k_{nx}\|^2_{L^2(\mathcal{T}_n)} \leq n! 2 D^2 C^{2n-2} \exp\left(2n\sqrt{\gamma} + 2\Upsilon + |\hat{q}|\right), \tag{9.7.109}$$

where $D = D_f + \rho_h D_h + 2((1+\rho_h)D_h)(|q|+1)\exp(1+|\hat{q}|)\sqrt{(1+\rho_h)^2 D_h^2 + D_f^2}$, $C = \left(\frac{\min\{\rho_f,\rho_h\}}{2}\right)^{-1}$ and $\Upsilon = 4\frac{D^2(1+2\sqrt[4]{\gamma})^2}{\gamma^2}$.

See Section 9.11.2 for the proof.

Remark 9.18. In the above theorem, if $q = \infty$ (meaning the plant has a Dirichlet boundary condition at the uncontrolled end), then the above bounds hold setting $q = 0$.

Corollary 9.19. *Under the same assumptions of the theorem, if the Volterra series nonlinearity of the plant is globally convergent in L^2, then the transformation Volterra series (9.4.35), the control (9.4.36) and the w_x transformation (9.7.101) converge globally in L^2 as well.*

Proof. If the Volterra series nonlinearity of the plant F and H are everywhere convergent, then by the limit (9.7.96) being infinity, for any $\epsilon > 0$ (possibly very small), there exists $D_\epsilon > 0$ (possibly very large) such that both f_n and h_n verify

$$\max\{|h_n|, |f_n|\} \leq n! B_\epsilon \epsilon^{n-1}. \tag{9.7.110}$$

Hence under the assumptions of Theorem 9.17, the kernel solution k_n verifies

$$\|k_n\|^2_{L^2(\mathcal{T}_n)} \leq (n-1)! 4 D_\epsilon^2 \left(\frac{\epsilon}{2}\right)^{2n-2} \exp\left(2n\sqrt{\gamma_\epsilon} + 2\Upsilon_\epsilon + |\hat{q}|\right), \tag{9.7.111}$$

where D_ϵ and Υ_ϵ are defined as in Theorem 9.17 replacing $D_h = D_f = B_\epsilon$ and $\rho_h = \rho_f = 1/\epsilon$, but note that $\gamma = \max\{1, \|f_1\|_\infty + \|\lambda\|_\infty + c\}$ does not depend on ϵ. Then the radius of convergence of the Volterra series defined by k_n is $\rho_k \geq \frac{4\exp(2\sqrt{\gamma})}{\epsilon^2}$. Since this holds for any positive ϵ, we must have $\rho_k = \infty$. $\square$

9.8 Stability Analysis

We now study the properties of the closed-loop system (9.2.1)–(9.2.2), (9.4.36). To analyze the behavior of this system, we study the invertibility of the change of variables (9.4.35). It is natural to seek also a Volterra formulation for this inverse change of variables, which is assumed as having the following form

$$u = w + L[w], \tag{9.8.112}$$

which is expanded as

$$u(t,x) \quad = \quad w(t,x) + \sum_{n=1}^{\infty} \int_{\mathcal{T}_n(x,\xi)} l_n(\hat{\xi}_0^n) \prod_n w d\hat{\xi}_1^n. \tag{9.8.113}$$

The existence of this inverse change of variables can be guaranteed employing the theorem for inversion of Volterra series, which is proved in [27, Theorem 3.3.1.].

Theorem 9.20 (**Volterra series inversion**). *A Volterra series has a local inverse at the origin if and only if its first (linear) kernel is invertible.*

In that context, the word "local' means that a unique Volterra series representation can be found for the inverse transformation, which has the form specified by (9.8.113), and whose radius of convergence (in the sense of Definition 9.10 and Theorem 9.11) is possible finite, even if the transformation is globally convergent.

The direct and inverse transformations give a relation between u and w that can be exploited to obtain properties of u (governed by a complex nonlinear equation) from properties of w (that verifies an easy to analyze heat equation). The commutative diagram of Fig. 9.9 illustrates our strategy. We have denoted the initial conditions for u and w as $u(0,x) = u_0$ and $w(0,x) = w_0$, respectively. In the left, $\mathcal{T}_u(t)$ is the semigroup that governs the behavior of u when the loop is closed, so that $u(t) = T_u(t)u_0$; its generator can be obtained homogenizing (9.2.1) and taking (9.4.36) into account. In the right, $\mathcal{T}_w(t)$ is the semigroup generated by the laplacian operator in (9.4.33), so that $w(t) = \mathcal{T}_w(t)w_0$. Above and below are respectively the direct and inverse transformation, $\mathrm{Id} - K$ and $\mathrm{Id} + L$ that relate u and w. We are interested in the properties of u, but direct analysis of $\mathcal{T}_u(t)$ is very difficult—it is generated by a nonlinear operator. Instead, from Fig. 9.9, we use that $\mathcal{T}_u(t) = (\mathrm{Id} + L) \circ \mathcal{T}_w(t) \circ (\mathrm{Id} - K)$, dividing the analysis into smaller, more tractable pieces. The transformations $\mathrm{Id} + L$ and $\mathrm{Id} - K$ are still nonlinear but time invariant, and are analyzed within the framework of Volterra series, whereas the heat equation semigroup $\mathcal{T}_w(t)$ is linear and simple, producing even explicit solutions. We begin by analyzing $\mathcal{T}_w$, whose behavior is summarized in the following lemma, which follows from standard estimates for the heat equation [45, 82].

Lemma 9.21. *Consider the system (9.4.33) with boundary conditions (9.4.34). Then, the equilibrium $w \equiv 0$ is exponentially stable in the L^2 and H^1 norms, i.e., $\forall t \geq 0$*

$$\|w(t)\|_{\mathcal{L}}^2 \leq \mathrm{e}^{-t} \|w_0\|_{\mathcal{L}}^2, \tag{9.8.114}$$

where $\mathcal{L}$ is either L^2 or H^1.

$$\begin{tikzcd} u_0(x) \arrow[r, "\mathrm{Id} - K"] \arrow[d, "\mathcal{T}_u(t)"] & w_0(x) \arrow[d, "\mathcal{T}_w(t)"] \\ u(t,x) & w(t,x) \arrow[l, "\mathrm{Id} + L"'] \end{tikzcd}$$

Figure 9.9: Commutative diagram for the closed-loop system.

Using Lemma 9.21 and the relations illustrated by Fig. 9.9, we get the following result about the stability properties of the closed-loop system.

Theorem 9.22. *Let Assumption 9.15 hold and assume that there is a L^2 (resp. H^1) solution u to the closed loop system (9.2.1) with boundary conditions (9.2.2) and control law (9.4.36). Then, the origin $u \equiv 0$ of the closed loop system is locally exponentially stable in the L^2 (resp. H^1) norm, i.e., denoting the initial condition for u as $u(0,x) = u_0(x)$, there exists $C_1, C_2 > 0$ such that, if $\|u_0\|^2_{\mathcal{L}} \leq C_1$, then $\forall t \geq 0$*

$$\|u(t)\|^2_{\mathcal{L}} \leq C_2 \mathrm{e}^{-t} \|u_0\|^2_{\mathcal{L}}, \tag{9.8.115}$$

where $\mathcal{L}$ is either L^2 or H^1, and C_1, C_2 depend on the plant parameters, but not on u_0.

Proof. Under Assumption 9.15, the transformation (9.4.35) exists and converges for $\|u(t)\|^2_{L^2} \leq \rho_K$, where ρ_K denotes the radius of convergence of the transformation Volterra series. The first kernel of (9.4.35) is $\mathrm{Id} - K_1$ and constitute the linear part of the transformation. In [101] it is shown that this linear part is *always* invertible. Hence, using Theorem 9.20, the whole transformation is locally invertible and the inverse transformation has the form specified by (9.8.113). Therefore there exists $\rho_L > 0$ such that, if $\|w(t)\|^2_{L^2} < \rho_L$, then (9.8.113) converges.

Denote by $k(s)$ and $l(s)$ the gain bound functions of the direct and inverse Volterra series transformation respectively, as defined in (9.7.97).

From (9.4.35), we have that

$$w_0 = u_0 - K[u_0]. \tag{9.8.116}$$

Set $C_1 = k^{-1}(\rho_L)/2 < \rho_K$. Hence, if $u_0 \leq C_1$ we get that

$$\|w(t)\|_{L^2}^2 \leq \|w_0\|_{L^2}^2 \leq k(\|u_0\|_{L^2}^2) \leq k(C_1) < \rho_l \tag{9.8.117}$$

for all time t. Therefore, the inverse (9.8.112) converges and the relations of Fig. 9.9 hold for all time $t \geq 0$. Set now $C_3 = \frac{k(C_1)}{C_1}$ and $C_4 = \frac{l(C_1C_3)}{C_1C_3}$. Then, for $\|u_0\|_{L^2}^2 < C_1$, since $\|w(t)\|_{L^2}^2 \leq C_3C_1$ and both $k(s)$ and $l(s)$ are class $\mathcal{K}$ functions [69], we have that

$$\|u(t)\|_{L^2}^2 \leq l(\|w(t)\|_{L^2}^2) \leq C_4\|w(t)\|_{L^2}^2 \leq C_4\mathrm{e}^{-t}\|w_0\|_{L^2}^2 \leq C_3C_4\mathrm{e}^{-t}\|u_0\|_{L^2}^2, \tag{9.8.118}$$

so setting $C_2 = C_3C_4$, (9.8.115) follows for the L^2 norm. To obtain the bound for the H^1 norm we use (9.7.101) and (9.7.103), and note that

$$u_x = w_x - (w + L[w])(\bar{k}(x) + \bar{K}[w + L[w]]) - \tilde{K}[w + L[w]]. \tag{9.8.119}$$

Hence u_x can be recovered from w_x when the Volterra series in (9.8.119) converge. If $\|u_0\|_{H^1}^2 \leq C_1$, then obviously $\|u_0\|_{L^2}^2 \leq C_1$, and since the radius of convergence of both $\bar{K}$ and $\tilde{K}$ is at least ρ_K, all the series in the right hand side in (9.8.119) converge. Then we use Lemma 9.21 and proceed in the same way as in (9.8.118) for the H^1 norm (using the gain bound functions for $\bar{K}$ and $\tilde{K}$), obtaining possibly a different C_2; to get the same C_2 for both L^2 and H^1 we pick the maximum of the two. Then the result follows. $\square$

Remark 9.23. In Theorem 9.22 we have assumed well-posedness of the closed-loop system. For the case $q = \infty$ (Dirichlet boundary condition at $x = 0$), since (9.4.33)–(9.4.34) is well-posed in H^1 and since (9.7.101), (9.8.119) allow to prove local equivalence of the H^1 norms of u and w, the assumption can be dropped, provided u_0 verifies some compatibility conditions [101] (see Proposition 9.29 for an example). For other values of q, (9.4.33)–(9.4.34) is well-posed in H^2 and this argument is not enough.

Remark 9.24. Note that (9.4.33) can be solved explicitly. This means that, when $\|u_0\|_{\mathcal{L}} < C_1$, u can be obtained explicitly for all times. We give an illustration for the simplest case, when $q = \infty$. Then, u is given as

$$\begin{aligned} u &= 2\sum_{n=1}^{\infty} \mathrm{e}^{-\pi^2 n^2 t} \sin(\pi n x) \int_0^1 \sin(\pi n \xi)\,[u_0(\xi) - K[u_0](\xi)]\,d\xi \\ & +L\left[2\sum_{n=1}^{\infty} \mathrm{e}^{-\pi^2 n^2 t} \sin(\pi n x) \int_0^1 \sin(\pi n \xi)\,[u_0(\xi) - K[u_0](\xi)]\,d\xi\right]. \end{aligned} \quad (9.8.120)$$

For other values of q similar formulas can be written.

The constant C_1 for which Theorem 9.22 holds determines the "basin of attraction" of the equilibrium at the origin for the closed-loop system. Since $C_1 = k^{-1}(\rho_L)$, if ρ_L and some bound on the k_n's is known then C_1 can be more precisely quantified. We state a Corollary for Theorem 9.22 for some particular cases, introduced in Example 9.12, that occur frequently in practice.

Corollary 9.25. *Let $\rho_K, \rho_L > 0$ denote the radii of convergence of the direct and inverse Volterra transformation, (9.4.35) and (9.8.113), respectively. Let C and D denote generic positive constants.*

1. *If $\rho_K = \rho_L = \infty$, then Theorem 9.22 holds globally, i.e., for all $u \in L^2$.*

2. *If the kernels k_n verify $\|k_n\|^2_{L^2(\mathcal{T}_n)} \leq D$, then $\rho_K = \infty$ and Theorem 9.22 holds at least for $\|u\|^2_{L^2} \leq \frac{1}{3}\log\left(1 + \frac{\rho_L}{2D}\right)$.*

3. *If the kernels k_n grow like $\|k_n\|^2_{L^2(\mathcal{T}_n)} \leq DC^n$, then $\rho_K = \infty$ and Theorem 9.22 holds at least for $\|u\|^2_{L^2} \leq \frac{1}{3C}\log\left(1 + \frac{\rho_L}{2D}\right)$.*

4. *If the kernels k_n grow as $|k_n\|^2_{L^2(\mathcal{T}_n)} \leq n!DC^n$, then $\rho_K = 1/C$ and Theorem 9.22 holds for $\|u\|^2_\infty \leq \frac{1}{C}\left(\sqrt{1+\sqrt{\frac{D}{2\rho_L}}}\right)\left(\sqrt{1+\sqrt{\frac{D}{2\rho_L}}} - \sqrt[4]{\frac{D}{2\rho_L}}\right) > 0$.*

9.9 Inverse Transformation

Theorem 9.22 depends critically on the inverse transformation and its properties. Next we give explicit formulas that allow to compute the inverse from the kernels k_n.

Define l_1 as the unique function that verifies the following well-posed [101] PIDE

$$\begin{aligned}\partial_{xx} l_1(x,\xi_1) &= \partial_{\xi_1\xi_1} l_1(x,\xi_1) - \lambda(x) l_1 - f_1(x,\xi_1) \\ &\quad - \int_{\xi_1}^{x} l_1(s,\xi_1) f_1(x,s) ds, \end{aligned} \tag{9.9.121}$$

with boundary conditions

$$l_1(x,x) = \hat{q} - \frac{1}{2}\int_0^x \lambda(s) ds, \tag{9.9.122}$$

$$l_{1\xi_1}(x,0) = q l_1(x,0). \tag{9.9.123}$$

The following result holds.

Proposition 9.26. *The first kernel l_1 of the inverse (9.8.112) is given by the solution of (9.9.121)–(9.9.123), whereas for $n \geq 2$, l_n is given by the following formula*

$$l_n(\hat{\xi}_0^n) = g_n(\hat{\xi}_0^n) + \int_{\xi_1}^{x} l_1(x,s) g_n(s,\hat{\xi}_1^n) ds. \tag{9.9.124}$$

In (9.9.124), the g_n are functions defined as follows:

$$g_n = \sum_{\substack{i_1,\dots,i_j \geq 1, j\geq 2 \\ i_1+\cdots+i_j = n}} p_j[k_j; l_{i_1},\dots,l_{i_j}], \tag{9.9.125}$$

where the function $p_j[k_j; l_{i_1},\dots,l_{i_j}]$ is recursively computed in the following way. Let

$$p_1[k_j; l_{i_1},\dots,l_{i_j}] = \begin{cases} k_j(\hat{\xi}_0^j) + \int_{\xi_j}^{\xi_{j-1}} k_j(\hat{\xi}_0^{j-1}, s) l_1(s,\xi_j) ds, & i_j = 1, \\ \int_{\xi_j}^{\xi_{j-1}} k_j(\hat{\xi}_0^{j-1}, s) l_{i_j}(s, \hat{\xi}_j^{j+i_j-1}) ds, & i_j > 1, \end{cases} \tag{9.9.126}$$

and for $1 \leq m \leq j-1$, $p_{m+1}[k_j; l_{i_1},\dots,l_{i_j}]$ is computed from $p_m[k_j; l_{i_1},\dots,l_{i_j}]$ as follows:

$$p_{m+1}[k_j; l_{i_1},\dots,l_{i_j}] = \begin{cases} p_m[k_j; l_{i_1},\dots,l_{i_j}] + q_m[p_m], & i_{j-m} = 1, \\ q_m[p_m], & i_{j-m} > 1. \end{cases} \tag{9.9.127}$$

In (9.9.127),

$$q_m[p_m] = \int_{\xi_{j-m}}^{\xi_{j-m-1}} D_{j-m}^{\alpha_m, i_{j-m}} \Big[p_m[k_j; l_{i_1}, \ldots, l_{i_j}](\hat{\xi}_0^{j-m-1}, s, \hat{\xi}_{j-m}^{\alpha_m - 1}) \times l_{i_{j-m}}(s, \hat{\xi}_{\alpha_m}^{\alpha_m + i_{j-m} - 1}) \Big] \, ds, \tag{9.9.128}$$

where $\alpha_m = j - m + \sum_{\beta=j-m+1}^{j} i_\beta$ *and the function* $D_{j-m}^{\alpha_m, i_{j-m}}$ *is given in (9.4.57).*

Proof. Consider the transformation (9.4.35) and the inverse (9.8.113),

$$w = u - K[u], \tag{9.9.129}$$

$$u = w + L[w]. \tag{9.9.130}$$

We expand (9.9.129) as a sum of K_1 (the linear transformation) and the rest of the transformation (which is nonlinear). Then, we get

$$w = u - K_1[u] - \hat{K}[u], \tag{9.9.131}$$

where $\hat{K}[u] = \sum_{n=2}^{\infty} K_n[u]$. Calling $z = w + \hat{K}[u]$, we get

$$z = u - K_1[u], \tag{9.9.132}$$

which is the equation of a linear Volterra transformation; hence, we can use the result of [101] to show that it is invertible and explicitly compute the kernel l_1 of the (linear) inverse L_1, obtaining

$$u = z + L_1[z]. \tag{9.9.133}$$

Substituting now the definition of z in (9.9.133),

$$u = w + \hat{K}[u] + L_1[w + \hat{K}[u]], \tag{9.9.134}$$

and using the linearity of L_1,

$$u = w + L_1[w] + \hat{K}[u] + L_1[\hat{K}[u]]. \tag{9.9.135}$$

Replace now (9.9.130) in (9.9.135). Then,

$$u = w + L_1[w] + \hat{K}[w + L[w]] + L_1[\hat{K}[w + L[w]]]. \tag{9.9.136}$$

We define $G[w] = \hat{K}[w+L[w]]$, the composition of two Volterra series. Introducing G in (9.9.136) and using the definition of the inverse series (9.9.130) we get

$$L[w] = L_1[w] + G[w] + L_1[G[w]], \tag{9.9.137}$$

which expanded for each $n \geq 2$, gives (9.9.124). The expression for g given by (9.9.125)–(9.9.128) follows from repeatedly applying Lemma 9.30 in Section 9.11.1 to the definition of G as the composition of two Volterra series. $\square$

Remark 9.27. From (9.9.125)–(9.9.128) we get that the n-th kernel g_n depends only on the kernels $k_1, \ldots, k_{n-1}$ and $l_1, \ldots, l_{n-1}$. Hence, Equation (9.9.124) gives a recursive, *explicit* formula to compute the kernels l_n beginning at $n = 2$ (l_1 is computed directly from (9.9.121)–(9.9.123)) up to any desired order.

9.9.1 Analytic example

For the analytic example of Section 9.5, we have $K[u] = K_2[u] = \hat{K}[u]$ and $l_1 = 0$ because $k_1 = f_1 = 0$. These facts greatly simplify the formulas for l_n in Proposition 9.26. We have that $l_2 = k_2$ and for $n > 2$,

$$\begin{aligned} l_n &= \int_{\xi_2}^{\xi_1} k_2(x, \xi_1, s) l_{n-1}(s, \xi_2, \ldots, \xi_n) ds \\ &\quad + \sum_{i=2}^{n-2} \int_{\xi_1}^{x} D_1^{n-i+1,i} \left[\left(\int_{\xi_1}^{\sigma} k_2(x, \sigma, s) l_{n-i}(s, \hat{\xi}_1^{n-i}) ds \right) l_i(\sigma, \hat{\xi}_{n-i+1}^{n}) \right] d\sigma \\ &\quad + \int_{\xi_1}^{x} D_1^{2,n-1} [k_2(x, s, \xi_1) l_{n-1}(s, \hat{\xi}_2^{n})] ds. \end{aligned} \tag{9.9.138}$$

Using formula (9.9.138) and symbolical software, we explicitly find the first three kernels as $l_1 = 0$ and

$$l_2 = \xi_1 \xi_2 (x - \xi_1)(x - \xi_2), \tag{9.9.139}$$

$$\begin{aligned} l_3 &= \xi_1 \xi_2 \xi_3 \left[(2x - \xi_2 - \xi_3) \left(\frac{\xi_1^5 - x^5}{5} + \frac{x^4 - \xi_1^4}{4}(x + \xi_1) + \frac{\xi_1^3 - x^3}{3} x \xi_1 \right) \right. \\ &\quad + (x(\xi_2 + \xi_3) - \xi_2 \xi_3) \left(\frac{x^4 + \xi_1^4}{4} + \frac{\xi_1^3 - x^3}{3}(x + \xi_1) + \frac{x^2 + \xi_1^2}{2} x \xi_1 \right) \\ &\quad + (x - \xi_1) \left(\frac{\xi_2^5 - x^5}{5} + \frac{x^4 + \xi_2^4}{4}(x + \xi_2 + \xi_3) + \frac{\xi_2^3 - x^3}{3}(x(\xi_2 + \xi_3) \right. \end{aligned}$$

$$+\xi_2\xi_3) + \frac{x^2+\xi_2^2}{2}x\xi_2\xi_3\Big)\Big]. \tag{9.9.140}$$

Using (9.9.138) we can study the convergence of the inverse Volterra series for the example. First we analyze the growth of the kernels.

Lemma 9.28. *For l_n defined as in (9.9.139) and (9.9.138), it holds that for $n \geq 2$,*

$$|l_n(x,\xi_1,\ldots,\xi_n)| \leq n!\frac{1}{16^{n-1}}x^{5n-6}. \tag{9.9.141}$$

Proof. For $n = 2$, the claim of (9.9.141) is true since $l_2 = k_2 \leq \frac{1}{16}x^4$ as we found in (9.5.87). We now assume (9.9.141) for $n-1, n-2, \ldots, 2$ and prove it holds for $n \geq 3$. Taking absolute values in (9.9.138), using (9.4.57) and (9.9.141) for $n-1, n-2, \ldots, 2$, we get

$$\begin{aligned}|l_n| \;\leq\; & \frac{x^4}{16}\left(\frac{(n-1)!}{16^{n-2}}\int_0^x s^{5n-11}ds + \sum_{i=2}^{n-2}\begin{pmatrix} n \\ i \end{pmatrix}\frac{(n-i)!i!}{16^{n-i-1+i-1}}\int_0^x s^{5(n-i)-6}ds\right. \\ & \left.\times\int_0^x s^{5i-6}ds + \frac{n(n-1)!}{16^{n-2}}\int_0^x s^{5n-11}ds\right),\end{aligned} \tag{9.9.142}$$

where the binomial coefficients come from using Remark 9.6. Hence,

$$\begin{aligned}|l_n| \;&\leq\; n!\frac{x^4}{16^{n-1}}\left(\frac{n+1}{n}\int_0^x s^{5n-11}ds + \sum_{i=2}^{n-2}\int_0^x s^{5(n-i)-6}ds\int_0^x s^{5i-6}ds\right) \\ &\leq\; n!\frac{x^4}{16^{n-1}}\left(\frac{n+1}{n(5n-10)}x^{5n-10} + x^{5(n-i)-5+5i-5}\sum_{i=2}^{n-2}\frac{1}{(5(n-i)-5)(5i-5)}\right) \\ &\leq\; n!\frac{x^{5n-6}}{16^{n-1}}\left(\frac{n+1}{n(5n-10)} + \frac{1}{5n-10}\sum_{i=2}^{n-2}\left(\frac{1}{(5(n-i)-5)} + \frac{1}{5i-5}\right)\right) \\ &\leq\; n!\frac{x^{5n-6}}{16^{n-1}}\left(\frac{n+1}{n(5n-10)} + \frac{n-3}{5n-10}\left(\frac{1}{5}+\frac{1}{5}\right)\right) \\ &\leq\; n!\frac{x^{5n-6}}{16^{n-1}}\left(\frac{5+n(n+2)}{5n(5n-10)}\right),\end{aligned} \tag{9.9.143}$$

and since $5 + n(n+2) \leq 5n(5n-10)$ for $n \geq 3$, inequality (9.9.141) follows for n. ∎

We now state the result of Theorem 9.22 for the example, illustrating how to prove well-posedness for Dirichlet boundary conditions.

Proposition 9.29. *Consider the closed-loop plant (9.2.1)–(9.2.2) where* $H = 0$, $\lambda = 0$, $q = \infty$, *and* F *is given by* $f_1 = 0$, *(9.5.82)–(9.5.85) and control law (9.5.80). Let* $u_0 \in H^1(0,1)$ *be the initial condition for* u *verifying the compatibility conditions*

$$u_0(0) = 0, \quad u_0(1) = \frac{1}{2}\left(\int_0^1 \xi(x-\xi)u(\xi)d\xi\right)^2. \tag{9.9.144}$$

Then, there is a unique solution $u(t,x)$ *such that* $u \in L^2((0,\infty), H^1(0,1))$ *and the origin* $u \equiv 0$ *of the closed loop system is locally exponentially stable in the* L^2 *and* H^1 *norm, i.e., there exists* $C_2 > 0$ *such that, if* $\|u_0\|^2_{\mathcal{L}} \leq 32$, *then* $\forall t \geq 0$

$$\|u(t)\|^2_{\mathcal{L}} \leq C_2 \mathrm{e}^{-t}\|u_0\|^2_{\mathcal{L}}, \tag{9.9.145}$$

where $\mathcal{L}$ *is either* L^2 *or* H^1 *and* $C_2 > 0$ *does not depend on* u_0. *Moreover, we can write the closed-loop solution for* $u(t,x)$ *as*

$$\begin{aligned} u &= 2\sum_{n=1}^{\infty} \mathrm{e}^{-\pi^2 n^2 t}\sin(\pi n x)\int_0^1 \sin(\pi n\xi)\left[u_0(\xi) - \frac{1}{2}\left(\int_0^\xi \eta(\xi-\eta)u_0(\eta)d\eta\right)^2\right]d\xi \\ &\quad + L\left[2\sum_{n=1}^{\infty} \mathrm{e}^{-\pi^2 n^2 t}\sin(\pi n x)\int_0^1 \sin(\pi n\xi)\left[u_0(\xi) - \frac{1}{2}\right.\right. \\ &\quad \left.\left. \times\left(\int_0^\xi \eta(\xi-\eta)u_0(\eta)d\eta\right)^2\right]d\xi\right]. \end{aligned} \tag{9.9.146}$$

Proof. Using Lemma 9.28, since $x \leq 1$ we get that, for all n, $|l_n| \leq \frac{n!}{16^{n-1}}$. Hence, from Definition 9.10 and Example 9.12, we have that for the inverse Volterra series defined by $l_2 = k_2$ and (9.9.138), the radius of convergence is $\rho_L = 16^2 = 256$. The gain bound function for the transformation (9.4.35), since k is finite, can be written as $k(s) = 2s + s^2/32$. Using ρ_L and $k(s)$, and proceeding as in Corollary 9.25, we get the L^2 and H^1 results of Theorem 9.22 for initial conditions u_0 verifying $\|u_0\|^2_{L^2} \leq C_1 = k^{-1}(\rho_L)/2 = 32$. Moreover, (9.9.144) implies that $w_0(0) = w_0(1) = 0$ and since $w_0 \in H^1$, the equation (9.4.33) has a unique solution in $L^2((0,\infty), H^1(0,1))$ [45, Theorems 3 and 4, pages 356–358] (in fact more regularity is obtained, but we skip the details). Using that

$$w_x = u_x - \frac{1}{2}\left(\int_0^x (2x-\xi)u(t,\xi)d\xi\right)^2, \tag{9.9.147}$$

$$u_x = w_x + \frac{1}{2}\left(\int_0^x (2x-\xi)\left(w+L[w]\right)(t,\xi)d\xi\right)^2, \tag{9.9.148}$$

is valid ($L[w]$ converges) if $\|u\|_{L^2}^2 \leq 32$ (which is also implied in the $\mathcal{L} = H^1$ case if $\|u\|_{H^1}^2 \leq 32$), then u also has a $L^2((0,\infty), H^1(0,1))$ solution. The explicit solutions are obtained solving the heat equation. $\square$

As simulation results in Section 9.5 show for the example, where $u_0 = 400x(1-x)$ implying that $\|u_0\|_{L^2}^2 \approx 5000$, the result is far from limited to such a small neighborhood of the origin. This illustrates the rather conservative nature of Theorem 9.22.

9.10 Open Problems

The efforts on nonlinear *boundary* control of PDEs of parabolic type have so far resulted primarily in negative results—results that show that control cannot prevent finite time blow up. While in this chapter we formulate the first general framework in which the problem is tractable, there are some missing pieces in the analysis that prevent our solution to be complete.

In our formulation, finding the controller's Volterra kernels is the main design task. We have derived the set of equations that the kernels need to verify, a recursive set of linear hyperbolic PDEs on domains of increasing dimension and decreasing volume, with moving boundaries. In Section 9.5 we present a particular solution in detail, and then we show numerical examples in Section 9.6. However, beyond numerical evidence we have not provided any general well-posedness proof for the kernel equations and just assumed it. Nevertheless in Section 9.7 we derived a priori estimates to show that the existence of an H^1 solution to the kernel equations is enough to define a convergent Volterra series in the transformation and the control feedback law.

In Section 9.8 we provided a result of L^2 and H^1 exponential stability. We have not pursued the study of stability in higher regularity functional spaces, like the H^2 space—which would be useful to establish well-posedness of the closed-loop system. Such spaces are endowed with norms whose study under our framework require some manipulation (term by term second-order differentiation) of the transformation Volterra series. Before justifying such an operation we need more insight into the regularity of the kernel equation solutions.

The stability result is *local* in nature because it relies critically on the properties of the inverse transformation (9.8.113). Even if the transformation (9.4.35) is globally convergent in L^2, it is not possible to generically guarantee that it has an everywhere defined inverse. We have shown through an example that this result is too conservative and there is room for improvement. However, there are plants falling in the class of (9.2.1) that are not globally stabilizable (see Sections 9.3.2 and 9.6.2), therefore a global stability result is not possible for the whole class. Thus, to obtain a global result, we need to refine (9.2.1) and identify a subclass of systems for which the Volterra series transformation (9.4.35) is globally invertible. This implies, by Corollary 9.25, that those plants are globally stabilized by feedback law (9.4.36).

9.11 Auxiliary Technical Results

9.11.1 Derivation of the general kernel equations

Here we show the derivation of the general kernel PIDE equation for any order n.

We first state a technical result.

Lemma 9.30. *Given n positive, $1 \leq j \leq n$ and an arbitrary function $f_n(\hat{\xi}_0^n)$, it holds that*

$$\int_{\mathcal{T}_n(x,\xi)} f_n(\hat{\xi}_0^n) d\hat{\xi}_1^n = \int_{\mathcal{T}_{n-1}(x,\xi)} \int_{\xi_j}^{\xi_{j-1}} f_n(\hat{\xi}_0^{j-1}, s, \hat{\xi}_j^{n-1}) ds d\hat{\xi}_1^{n-1}. \quad (9.11.149)$$

If m is positive and $g_m(\hat{\xi}_0^m)$ is another arbitrary function, then

$$\begin{aligned}
&\int_{\mathcal{T}_n(x,\xi)} f_n(\hat{\xi}_0^n) \int_{\mathcal{T}_m(\xi_j,\sigma)} g_m(\xi_j, \hat{\sigma}_1^m) d\hat{\sigma}_1^m d\hat{\xi}_1^n \\
= &\int_{\mathcal{T}_{n+m}(x,\xi)} D_j^{n,m}[f_n(\hat{\xi}_0^n) g_m(\xi_j, \hat{\xi}_{n+1}^{n+m})] d\hat{\xi}_1^{n+m}. \qquad (9.11.150)
\end{aligned}$$

Proof. Identity (9.11.149) is derived directly from Fubini's theorem. For (9.11.150), write

$$\begin{aligned}
&\int_{\mathcal{T}_n(x,\xi)} f_n(\hat{\xi}_0^n) \left(\int_{\mathcal{T}_m(\xi_j,\sigma)} g_m(\xi_j, \hat{\sigma}_1^m) d\hat{\sigma}_1^m \right) d\hat{\xi}_1^n \\
= &\int_{\Omega_j^m(\hat{\xi}_1^{n+m})} f_n(\hat{\xi}_0^n) g_m(\xi_j, \hat{\xi}_{n+1}^{n+m}) d\hat{\xi}_1^{n+m}, \qquad (9.11.151)
\end{aligned}$$

where

$$\Omega_j^m(\hat{\xi}_1^{n+m}) = \{x \geq \xi_1 \geq \ldots \geq \xi_n \geq 0; \xi_j \geq \xi_{n+1} \geq \ldots \geq \xi_{n+m} \geq 0\}. \qquad (9.11.152)$$

For any m and $1 \leq j \leq n$, it holds that

$$\Omega_j^m(\hat{\xi}_1^{n+m}) = \bigcup_{\hat{\gamma}_1^{n-j+m} \in \mathcal{P}_{n-j}(\hat{\xi}_{j+1}^{n+m})} \{\xi_1 \geq \xi_2 \geq \ldots \geq \xi_j \geq \gamma_1 \geq \ldots \geq \gamma_{n+m-j} \geq 0\}. \qquad (9.11.153)$$

To prove (9.11.153), we first note that if $j = n$ or $m = 0$, $\Omega_j^m(\hat{\xi}_1^{n+m}) = \mathcal{T}_n(x,\xi)$, while if $j < n$ and $m \geq 1$, since

$$\begin{aligned}
\{\xi_j \geq \xi_{j+1} \geq 0\} \;=\; &\{\xi_j \geq \xi_{j+1} \geq \xi_{n+1}\} \cup \left(\bigcup_{l=2}^{n-1} \{\xi_{n+l} \geq \xi_{j+1} \geq \xi_{n+l+1}\} \right) \\
&\cup \{\xi_{n+m} \geq \xi_{j+1} \geq 0\}, \qquad (9.11.154)
\end{aligned}$$

we get

$$\begin{aligned}
\Omega_j^m(\hat{\xi}_1^{n+m}) \;=\; &\Omega_{j+1}^m(\hat{\xi}_1^{n+m}) \cup \left(\bigcup_{l=2}^{m-1} \Omega_{j+1}^{m-l}(\hat{\xi}_1^j, \hat{\xi}_{n+1}^{n+l-1}, \hat{\xi}_{j+1}^n, \hat{\xi}_{n+l}^{n+m}) \right) \\
&\cup \Omega_{j+1}^0(\hat{\xi}_1^j, \hat{\xi}_{n+1}^{n+m}, \hat{\xi}_{j+1}^n). \qquad (9.11.155)
\end{aligned}$$

Similarly, for $j = n$ or $m = 0$, the symbol $\mathcal{P}_{n-j}(\hat{\xi}_{j+1}^{n+m}) = \{\hat{\xi}_{j+1}^{n+m}\}$, and if $j < n$ and $m \geq 1$, verifies that

$$\begin{aligned}
\mathcal{P}_{n-j}(\hat{\xi}_{j+1}^{n+m}) \;=\; &\{\xi_{j+1}, P_{n-j-1}(\hat{\xi}_{j+2}^{n+m})\} \cup \left(\bigcup_{l=2}^{m-1} \{\hat{\xi}_{n+1}^{n+l-1}, \xi_{j+1}, P_{n-j-1}(\hat{\xi}_{j+2}^n, \hat{\xi}_{n+l}^{n+m})\} \right) \\
&\cup \{\hat{\xi}_{n+1}^{n+m} \hat{\xi}_{j+1}^n\}. \qquad (9.11.156)
\end{aligned}$$

Note (9.11.156) and (9.11.155) is essentially the same identity (the former expressed as a combinatorial identity and the later given as a geometric identity). This fact allows to easily prove (9.11.153) by double induction on j and m.

With (9.11.153) established, we have that

$$\begin{aligned}
&\int_{\mathcal{T}_n(x,\xi)} f_n(\hat{\xi}_0^n)\left(\int_{\mathcal{T}_m(\xi_j,\sigma)} g_m(\xi_j,\hat{\sigma}_1^m)d\hat{\sigma}_1^m\right)d\hat{\xi}_1^n \\
= &\sum_{\hat{\gamma}_1^{n-j+1}\in\mathcal{P}_{n-j}(\hat{\xi}_{j+1}^{n+m})}\int_{\mathcal{T}_{n+m}(x,\xi)} f_n(\hat{\xi}_0^j,\hat{\gamma}_1^{n-j})g_m(\xi_j,\hat{\gamma}_{n-j+1}^{n-j+m})d\hat{\xi}_1^{n+i} \\
= &\int_{\mathcal{T}_{n+m}(x,\xi)} D_j^{n,m}[f_n(\hat{\xi}_0^n)g_m(\hat{\xi}_j,\hat{\xi}_{n+1}^{n+m})]d\hat{\xi}_1^{n+m}, \qquad (9.11.157)
\end{aligned}$$

where we have used (9.4.57). Then, (9.11.150) follows. □

We next derive the general kernel equation for $n\geq 2$ (the case $n=1$ is covered in [101]). We start from Equation (9.4.37),

$$\begin{aligned}
0 = &\sum_{n=1}^{\infty}\left(\lambda(x)u+u(t,x)\int_{\mathcal{T}_n(x,\xi)} h_n(\hat{\xi}_0^n)\prod^n ud\hat{\xi}_1^n+\int_{\mathcal{T}_n(x,\xi)} f_n(\hat{\xi}_0^n)\prod^n ud\hat{\xi}_1^n\right. \\
&\left.+\left(\frac{\partial^2}{\partial x^2}-\frac{\partial}{\partial t}\right)\int_{\mathcal{T}_n(x,\xi)} k_n(\hat{\xi}_0^n)\prod^n ud\hat{\xi}_1^n\right). \qquad (9.11.158)
\end{aligned}$$

The second spatial derivative in (9.11.158) is

$$\begin{aligned}
&\frac{\partial^2}{\partial x^2}\int_{\mathcal{T}_n(x,\xi)} k_n(\hat{\xi}_0^n)\prod^n ud\hat{\xi}_1^n \\
= &\int_{\mathcal{T}_n(x,\xi)}\partial_{xx}k_n(\hat{\xi}_0^n)\prod^n ud\hat{\xi}_1^n+u_x(t,x)\int_{\mathcal{T}_{n-1}(x,\xi)} k_n(x,\hat{\xi}_0^{n-1})\prod^{n-1} ud\hat{\xi}_1^{n-1} \\
&+u(t,x)\int_{\mathcal{T}_{n-1}(x,\xi)}\left(2\partial_x k_n(x,\hat{\xi}_0^{n-1})+\partial_{\xi_1}k_n(x,\hat{\xi}_0^{n-1})\right)\prod^{n-1} ud\hat{\xi}_1^{n-1} \\
&+u(t,x)^2\int_{\mathcal{T}_{n-2}(x,\xi)} k_n(x,x,\hat{\xi}_0^{n-2})\prod^{n-2} ud\hat{\xi}_1^{n-2}, \qquad (9.11.159)
\end{aligned}$$

whereas the time derivative in (9.11.158) is as follows

$$\frac{\partial}{\partial t}\int_{\mathcal{T}_n(x,\xi)} k_n(\hat{\xi}_0^n)\prod^n ud\hat{\xi}_1^n$$

$$= \sum_{j=1}^{n} \int_{\mathcal{T}_n(x,\xi)} k_n(\hat{\xi}_0^n) u_{xx}(t,\xi_j) \prod^{n,j} u d\hat{\xi}_1^n + \sum_{j=1}^{n} \int_{\mathcal{T}_n(x,\xi)} \lambda(\xi_j) k_n(\hat{\xi}_0^n) \prod^{n} u d\hat{\xi}_1^n$$
$$+ \sum_{j=1}^{n} \int_{\mathcal{T}_n(x,\xi)} k_n(\hat{\xi}_0^n) H[u](\xi_j,t) \prod^{n} u d\hat{\xi}_1^n$$
$$+ \sum_{j=1}^{n} \int_{\mathcal{T}_n(x,\xi)} k_n(\hat{\xi}_0^n) F[u](\xi_j,t) \prod^{n,j} u d\hat{\xi}_1^n. \tag{9.11.160}$$

Using (9.11.149) for the first term in (9.11.160),

$$\sum_{j=1}^{n} \int_{\mathcal{T}_n(x,\xi)} k_n(\hat{\xi}_0^n) u_{xx}(t,\xi_j) \prod^{n,j} u d\hat{\xi}_1^n$$
$$= \sum_{j=1}^{n-1} \int_{\mathcal{T}_{n-1}(x,\xi)} \int_{\xi_j}^{\xi_{j-1}} k_n(\hat{\xi}_0^{j-1}, s, \hat{\xi}_j^{n-1}) u_{xx}(s,t) \prod^{n-1} u d\hat{\xi}_1^{n-1}$$
$$+ \int_{\mathcal{T}_{n-1}(x,\xi)} \int_{0}^{\xi_{n-1}} k_n(\hat{\xi}_0^{n-1}, s) u_{xx}(s,t) \prod^{n-1} u d\hat{\xi}_1^{n-1}, \tag{9.11.161}$$

and integrating by parts,

$$\sum_{j=1}^{n} \int_{\mathcal{T}_n(x,\xi)} k_n(\hat{\xi}_0^n) u_{xx}(t,\xi_j) \prod^{n,j} u d\hat{\xi}_1^n$$
$$= \sum_{j=1}^{n} \int_{\mathcal{T}_n(x,\xi)} \partial_{\xi_j\xi_j} k_n(\hat{\xi}_0^n) \prod^{n} u d\hat{\xi}_1^n$$
$$+ \sum_{j=1}^{n} \int_{\mathcal{T}_{n-1}(x,\xi)} k_n(\hat{\xi}_0^{j-1}, \xi_{j-1}, \hat{\xi}_j^{n-1}) u_x(t,\xi_{j-1}) \prod^{n-1} u d\hat{\xi}_1^{n-1}$$
$$- \sum_{j=1}^{n-1} \int_{\mathcal{T}_{n-1}(x,\xi)} k_n(\hat{\xi}_0^{j-1}, \xi_j, \hat{\xi}_j^{n-1}) u_x(t,\xi_j) \prod^{n-1} u d\hat{\xi}_1^{n-1}$$
$$- \sum_{j=1}^{n} \int_{\mathcal{T}_{n-1}(x,\xi)} \int_{\xi_j}^{\xi_{j-1}} \partial_{\xi_j} k_n(\hat{\xi}_0^{j-1}, \xi_{j-1}, \hat{\xi}_j^{n-1}) u(t,\xi_{j-1}) \prod^{n-1} u d\hat{\xi}_1^{n-1}$$
$$+ \sum_{j=1}^{n-1} \int_{\mathcal{T}_{n-1}(x,\xi)} \int_{\xi_j}^{\xi_{j-1}} \partial_{\xi_j} k_n(\hat{\xi}_0^{j-1}, \xi_j, \hat{\xi}_j^{n-1}) u(t,\xi_j) \prod^{n-1} u d\hat{\xi}_1^{n-1}$$
$$- u_x(t,0) \int_{\mathcal{T}_{n-1}(x,\xi)} k_n(\hat{\xi}_0^{n-1}, 0) \prod^{n-1} u d\hat{\xi}_1^{n-1}$$
$$+ u(t,0) \int_{\mathcal{T}_{n-1}(x,\xi)} k_{n\xi_n}(\hat{\xi}_0^{n-1}, 0) \prod^{n-1} u d\hat{\xi}_1^{n-1}. \tag{9.11.162}$$

In (9.11.162), some terms cancel out, yielding

$$\begin{aligned}
&\sum_{j=1}^{n}\int_{\mathcal{T}_n(x,\xi)} k_n(\hat{\xi}_0^n)u_{xx}(t,\xi_j)\prod^{n,j} ud\hat{\xi}_1^n \\
= &\sum_{j=1}^{n}\int_{\mathcal{T}_n(x,\xi)} \partial_{\xi_j\xi_j}k_n(\hat{\xi}_0^n)\prod^{n} ud\hat{\xi}_1^n + u_x(t,x)\int_{\mathcal{T}_{n-1}(x,\xi)} k_n(x,x,\hat{\xi}_1^{n-1})\prod^{n-1} ud\hat{\xi}_1^{n-1} \\
&-u(t,x)\int_{\mathcal{T}_{n-1}(x,\xi)} \partial_{\xi_1}k_n(x,x,\hat{\xi}_1^{n-1})\prod^{n-1} ud\hat{\xi}_1^{n-1} \\
&+\sum_{j=1}^{n-1}\int_{\mathcal{T}_{n-1}(x,\xi)}\int_{\xi_j}^{\xi_{j-1}} \Big(\partial_{\xi_j}k_n(\hat{\xi}_0^{j-1},\xi_j,\hat{\xi}_j^{n-1}) \\
&-\partial_{\xi_j+1}k_n(\hat{\xi}_0^{j-1},\xi_j,\hat{\xi}_j^{n-1})\Big)\,u(t,\xi_j)\prod^{n-1} ud\hat{\xi}_1^{n-1} \\
&+u(t,0)\int_{\mathcal{T}_{n-1}(x,\xi)} \Big(k_{n\xi_n}(\hat{\xi}_0^{n-1},0) - qk_n(\hat{\xi}_0^{n-1},0)\Big)\prod^{n-1} ud\hat{\xi}_1^{n-1}. \qquad (9.11.163)
\end{aligned}$$

In the last line of (9.11.163) we have used the Robin boundary condition for u at $x = 0$. The third term in (9.11.160) can be written as

$$\begin{aligned}
&\sum_{j=1}^{n}\int_{\mathcal{T}_n(x,\xi)} k_n(\hat{\xi}_0^n)H[u](\xi_j,t)\prod^{n} ud\hat{\xi}_1^n \\
= &\sum_{j=1}^{n}\sum_{m=1}^{\infty}\int_{\mathcal{T}_n(x,\xi)} k_n(\hat{\xi}_0^n)\left(\int_{\mathcal{T}_i(\xi_j,\sigma)} h_m(\xi_j,\hat{\sigma}_1^m)\prod^{m} ud\hat{\sigma}_1^m\right)\prod^{n} ud\hat{\xi}_1^n \\
= &\sum_{j=1}^{n}\sum_{m=1}^{\infty}\int_{\mathcal{T}_{n+m-1}(x,\xi)} D_j^{n,m}[k_n(\hat{\xi}_0^n)h_m(\xi_j,\hat{\xi}_{n+1}^{m+n})]\prod^{n+m} ud\hat{\xi}_1^{n+m}, \quad (9.11.164)
\end{aligned}$$

where we have applied (9.11.150). Then, we can write

$$\begin{aligned}
&\sum_{n=1}^{\infty}\sum_{j=1}^{n}\sum_{m=1}^{\infty}\int_{\mathcal{T}_{n+m}(x,\xi)} D_j^{n,m}[k_n(\hat{\xi}_0^n)h_m(\xi_j,\hat{\xi}_{n+1}^{m+n})]\prod^{n+m} ud\hat{\xi}_1^{n+m} \\
= &\sum_{n=1}^{\infty}\sum_{m=1}^{n-1}\sum_{j=1}^{n-m+1}\int_{\mathcal{T}_n(x,\xi)} D_j^{n-m,m}[k_{n-m}(\hat{\xi}_0^{n-m})h_m(\xi_j,\hat{\xi}_{n-m+1}^{n})]\prod^{n} ud\hat{\xi}_1^n \\
= &\sum_{n=1}^{\infty}\int_{\mathcal{T}_n(x,\xi)}\sum_{m=1}^{n-1} C_n^m[k_{n-m},h_m]\prod^{n} ud\hat{\xi}_1^n \qquad (9.11.165)
\end{aligned}$$

Similarly, the fourth term in (9.11.160) can be written as

$$
\begin{aligned}
&\sum_{j=1}^{n}\int_{\mathcal{T}_n(x,\xi)} k_n(\hat{\xi}_0^n)F[u](\xi_j,t)\prod^{n,j} ud\hat{\xi}_1^n \\
=\ &\sum_{j=1}^{n}\sum_{m=1}^{\infty}\int_{\mathcal{T}_{n+m-1}(x,\xi)} D_j^{n,m}[k_n(\hat{\xi}_0^n)f_m(\xi_j,\hat{\xi}_{n+1}^{m+n}]\prod^{n+m,j} ud\hat{\xi}_1^{n+m} \\
=\ &\sum_{j=1}^{n}\sum_{m=1}^{\infty}\int_{\mathcal{T}_{n+m-1}(x,\xi)}\int_{\xi_j}^{\xi_{j-1}} D_j^{n,m}[k_n(\hat{\xi}_{j-1}^n,s,\hat{\xi}_j^{n-1})f_m(s,\hat{\xi}_n^{m+n-1})]ds \\
&\times\prod^{n+m-1} ud\hat{\xi}_1^{n+m-1}, \qquad (9.11.166)
\end{aligned}
$$

where we have applied (9.11.150) and (9.11.149). Then, as in (9.11.165),

$$
\begin{aligned}
&\sum_{n=1}^{\infty}\sum_{j=1}^{n}\sum_{m=1}^{\infty}\int_{\mathcal{T}_{n+m-1}(x,\xi)}\int_{\xi_j}^{\xi_{j-1}} D_j^{n,m}[k_n(\hat{\xi}_{j-1}^n,s,\hat{\xi}_j^{n-1})f_m(s,\hat{\xi}_n^{m+n-1})]ds \\
&\times\prod^{n+m-1} ud\hat{\xi}_1^{n+m-1} \\
=\ &\sum_{n=1}^{\infty}\int_{\mathcal{T}_n(x,\xi)}\left(I[k_n,f_1]+\sum_{m=2}^{n}B_n^m[k_{n-m+1},f_m]\right)\prod^{n} ud\hat{\xi}_1^n. \qquad (9.11.167)
\end{aligned}
$$

Collecting all the terms (9.11.159), (9.11.163), (9.11.165) and (9.11.167) into (9.11.158), we get

$$
\begin{aligned}
0\ =\ &\sum_{n=1}^{\infty}\int_{\mathcal{T}_n(x,\xi)}\Bigg[f_n+\partial_{xx}k_n-\sum_{j=1}^{n}\partial_{\xi_j\xi_j}k_n-\sum_{j=1}^{n}\lambda(\xi_j)k_n-I[k_n,f_1]` \\
&-\sum_{m=2}^{n}B_n^i[k_{n-m+1},f_m]-\sum_{m=1}^{n-1}C_n^m[k_{n-m},h_m]\Bigg]\prod^{n} ud\hat{\xi}_1^n \\
&+u(t,0)\sum_{n=1}^{\infty}\int_{\mathcal{T}_{n-1}(x,\xi)}\left(k_{n\xi_n}(\hat{\xi}_0^{n-1},0)-qk_n(\hat{\xi}_0^{n-1},0)\right)\prod^{n-1} ud\hat{\xi}_1^{n-1} \\
&+\sum_{n=1}^{\infty}\sum_{j=1}^{n-1}\int_{\mathcal{T}_{n-1}(x,\xi)}\int_{\xi_j}^{\xi_{j-1}}\left(\partial_{\xi_j}k_n(\hat{\xi}_0^{j-1},\xi_j,\hat{\xi}_j^{n-1})-\partial_{\xi_j+1}k_n(\hat{\xi}_0^{j-1},\xi_j,\hat{\xi}_j^{n-1})\right) \\
&\times u(t,\xi_j)\prod^{n-1} ud\hat{\xi}_1^{n-1} \\
&+u(t,x)\left[\lambda(x)+\sum_{n=1}^{\infty}\int_{\mathcal{T}_{n-1}(x,\xi)}\left(h_{n-1}+2\frac{d}{dx}k_n(x,x,\hat{\xi}_1^{n-1})\right)\prod^{n-1} ud\hat{\xi}_1^{n-1}\right] \\
&+u^2(t,x)\sum_{n=2}^{\infty}\int_{\mathcal{T}_{n-2}(x,\xi)} k_n(x,x,x,\hat{\xi}_1^{n-2})\prod^{n-2} ud\hat{\xi}_1^{n-2}, \qquad (9.11.168)
\end{aligned}
$$

where we define the total derivative $\frac{d}{dx}$ of the kernel k_n as

$$\frac{d}{dx}k_n(x,x,\hat{\xi}_1^{n-1}) = k_{nx}(x,x,\hat{\xi}_1^{n-1}) + k_{n\xi_1}(x,x,\hat{\xi}_1^{n-1}). \tag{9.11.169}$$

Since (9.11.168) has to be verified for arbitrary u, we get that the terms inside the integrals must be zero. Hence, we get

$$\begin{aligned} \partial_{xx}k_n &= \sum_{i=1}^{n} \partial_{\xi_i\xi_i}k_n + \sum_{j=1}^{n}\lambda(\xi_j)k_n - f_n + I_n[k_n, f_1] \\ &\quad + \sum_{m=2}^{n} B_n^m[k_{n-m+1}, f_m] + \sum_{m=1}^{n-1} C_n^m[k_{n-m}, h_m], \end{aligned} \tag{9.11.170}$$

and

$$\partial_{\xi_{i-1}}k_n(\hat{\xi}_0^n)\Big|_{\xi_{i-1}=\xi_i} = \partial_{\xi_i}k_n(\hat{\xi}_0^n)\Big|_{\xi_{i-1}=\xi_i}, i = 2,..,n, \tag{9.11.171}$$

$$k_{n\xi_n}(\hat{\xi}_0^{n-1}, 0) = qk_n(\hat{\xi}_0^{n-1}, 0), \tag{9.11.172}$$

$$\frac{d}{dx}k_n(x,x,\hat{\xi}_2^n) = -\frac{1}{2}h_{n-1}(x,\hat{\xi}_2^n), \tag{9.11.173}$$

$$k_n(x,x,x,\hat{\xi}_3^n) = 0. \tag{9.11.174}$$

Equations (9.11.170)–(9.11.174) are the general kernel equations, but we still need to derive boundary conditions (9.4.41) and (9.4.42)

Integrating (9.11.173) and using (9.11.174) to determine the constant of integration, we get (9.4.41):

$$k_n(x,x,\hat{\xi}_2^n) = -\frac{1}{2}\int_{\xi_2}^{x} h_{n-1}(s,\hat{\xi}_2^n)ds. \tag{9.11.175}$$

Boundary condition (9.4.42) is built into (9.11.170). Defining ϕ_n as in (9.4.45), when $\xi_1 = x$ (9.11.170) reduces to

$$\partial_{xx}k_n(x,x,\hat{\xi}_2^n) = \partial_{\xi_1\xi_1}k_n(x,x,\hat{\xi}_2^n) + \phi_n(x,\hat{\xi}_2^n). \tag{9.11.176}$$

Taking derivative with respect to x in (9.11.173),

$$\left(\partial_{xx}k_n + \partial_{\xi_1\xi_1}k_n + 2\partial_{x\xi_1}k_n\right)(x,x,\hat{\xi}_2^n) = -\frac{1}{2}\partial_x h_{n-1}(x,\hat{\xi}_2^n), \tag{9.11.177}$$

which substituted in (9.11.176) gives

$$2\left(\partial_{xx}k_n + \partial_{x\xi_1}k_n\right)(x, x, \hat{\xi}_2^n) = -\frac{1}{2}\partial_x h_{n-1}(x, \hat{\xi}_2^n) + \phi_n(x, \hat{\xi}_2^n), \qquad (9.11.178)$$

hence

$$\frac{d}{dx}k_{nx}(x, x, \hat{\xi}_2^n) = -\frac{1}{4}\partial_x h_{n-1}(x, \hat{\xi}_2^n) + \frac{1}{2}\phi_n(x, \hat{\xi}_2^n). \qquad (9.11.179)$$

From (9.11.171) at $i = 2$, $\xi_1 = x$, we get that

$$k_{n\xi_1}(x, x, x, \hat{\xi}_3^n) = k_{n\xi_2}(x, x, x, \hat{\xi}_3^n) \qquad (9.11.180)$$

and since (9.11.174) implies

$$\left(k_{nx} + k_{n\xi_1} + k_{n\xi_2}\right)(x, x, x, \hat{\xi}_3^n) = 0, \qquad (9.11.181)$$

we get, from (9.11.173), that

$$k_{nx}(x, x, x, \hat{\xi}_3^n) = -h_{n-1}(x, \hat{\xi}_2^n). \qquad (9.11.182)$$

Integrating (9.11.179) and using (9.11.182) to find the constant of integration, we get

$$\begin{aligned} k_{nx}(x, x, \hat{\xi}_2^n) &= -\frac{1}{4}h_{n-1}(x, \hat{\xi}_2^n) - \frac{3}{4}h_{n-1}(\xi_2, \hat{\xi}_2^n) \\ &\quad + \frac{1}{2}\int_{\xi_2}^{x} \phi_n(s, \hat{\xi}_2^n)ds. \end{aligned} \qquad (9.11.183)$$

9.11.2 Proof of Theorem 9.17

Define the (x-dependent) $L^2(\mathcal{T}_n)$ norm of $k_n(\hat{\xi}_0^n)$ as

$$\|k_n(x)\|^2_{L^2(\mathcal{T}_n(x))} = \int_{\mathcal{T}_n(x,\xi)} k_n^2(\hat{\xi}_0^n)d\hat{\xi}_1^n \qquad (9.11.184)$$

For simplicity we will write $\|k_n(x)\|^2_{L^2(\mathcal{T}_n)}$.

The proof of the theorem requires a number of technical results. The first result is used to get a simpler expression for the number of terms in the right hand side of the kernel PIDE equation.

Lemma 9.31. *For $n \geq m \geq 0$, we have that*

$$\sum_{j=0}^{n-m} \begin{pmatrix} m+j \\ j \end{pmatrix} = \frac{(n+1)!}{(m+1)!(n-m)!}. \tag{9.11.185}$$

Proof. We have that

$$\begin{aligned} & \sum_{j=0}^{n-m} \begin{pmatrix} m+j+1 \\ j \end{pmatrix} \\ = & \begin{pmatrix} m+1 \\ 0 \end{pmatrix} + \sum_{j=1}^{n-m} \begin{pmatrix} m+j+1 \\ j \end{pmatrix} \\ = & \ 1 + \sum_{j=1}^{n-m} \begin{pmatrix} m+j \\ j \end{pmatrix} + \sum_{j=1}^{n-m} \begin{pmatrix} m+j \\ j-1 \end{pmatrix} \\ = & \sum_{j=0}^{n-m} \begin{pmatrix} m+j \\ j \end{pmatrix} + \sum_{j=0}^{n-m-1} \begin{pmatrix} m+j+1 \\ j \end{pmatrix}, \end{aligned} \tag{9.11.186}$$

where we have used the fact that

$$\begin{pmatrix} n+1 \\ k+1 \end{pmatrix} = \begin{pmatrix} n \\ k+1 \end{pmatrix} + \begin{pmatrix} n \\ k \end{pmatrix}. \tag{9.11.187}$$

Hence, solving in (9.11.186) for the left hand side of (9.11.185), we get

$$\begin{aligned} \sum_{j=0}^{n-m} \begin{pmatrix} m+j \\ j \end{pmatrix} &= \sum_{j=0}^{n-m} \begin{pmatrix} m+j+1 \\ j \end{pmatrix} - \sum_{j=0}^{n-m-1} \begin{pmatrix} m+j+1 \\ j \end{pmatrix} \\ &= \begin{pmatrix} n+1 \\ n-m \end{pmatrix}, \end{aligned} \tag{9.11.188}$$

and the result follows. □

The next result allows to estimate the various norms arising in the proof of the theorem.

Lemma 9.32. *The following estimates hold.*

1. For D defined in (9.4.57), we have that for any function $g_n(\xi_0^n)$,

$$\begin{aligned}\|D_j^{n,m}[g_n f_m](x)\|^2_{L^2(\mathcal{T}_{n+m})} &\leq x^m \frac{\|f_m\|^2_\infty}{m!} \frac{(m+n-j)!}{m!(n-j)!} \\ &\quad \times \|g_n(x)\|^2_{L^2(\mathcal{T}_n)}. \qquad (9.11.189)\end{aligned}$$

2. For B defined in (9.4.58), we have that

$$\begin{aligned}\|B_n^m[k_{n-m+1}, f_m](x)\|^2_{L^2(\mathcal{T}_n)} &\leq x^m \frac{(n+1)!(n-m+1)}{(m+1)!(n-m)!} \frac{\|f_m\|^2_\infty}{m!} \\ &\quad \times \|k_{n-m+1}(x)\|^2_{L^2(\mathcal{T}_{n-m+1})}. \qquad (9.11.190)\end{aligned}$$

3. For C defined in (9.4.59), we have that

$$\begin{aligned}\|C_n^m[k_{n-m}, h_m](x)\|^2_{L^2(\mathcal{T}_n)} &\leq x^m \frac{n!(n-m)}{(m+1)!(n-m-1)!} \frac{\|h_m\|^2_\infty}{m!} \\ &\quad \times \|k_{n-m}(x)\|^2_{L^2(\mathcal{T}_{n-m})}. \qquad (9.11.191)\end{aligned}$$

Proof. Using the definition of D, we have that

$$\begin{aligned}\|D_j^{n,m}[g_n, f_m](x)\|^2_{L^2(\mathcal{T}_{n+m})} &= \int_{\mathcal{T}_{n+m}(x,\xi)} D_j^{n,m}[g_n, f_m]^2(\hat{\xi}_0^{n+m-1}) d\hat{\xi}_1^{n+m} \\ &= \int_{\mathcal{T}_{n+m}(x,\xi)} \left(\sum_{\hat{\gamma}_1^{n-j+m} \in P_{n-j}(\hat{\xi}_{j+1}^{n+m})} g_n(\hat{\xi}_0^j, \hat{\gamma}_1^{n-j}) \right. \\ &\quad \left. \times f_m(\xi_j, \hat{\gamma}_{n-j+1}^{n+m-j}) ds \right)^2 d\hat{\xi}_1^{n+m}. \qquad (9.11.192)\end{aligned}$$

Since $P_{n-j}(\hat{\xi}_{j+1}^{n+m})$ has $\frac{(n+m-j)!}{m!(n-j)!}$ elements and as $\left(\sum_{k=1}^n p_k\right)^2 \leq n \sum_{k=1}^n p_k^2$, (9.11.192) yields

$$\begin{aligned}&\|D[g_n, f_m, j](x)\|^2_{L^2(\mathcal{T}_{n+m})} \\ \leq\ & \frac{(n+m-j)!}{m!(n-j)!} \int_{\mathcal{T}_{n+m-1}(x,\xi)} \sum_{\hat{\gamma}_1^{n-j+m} \in P_{n-j}(\hat{\xi}_{j+1}^{n+m})} \left(g_n^2(\hat{\xi}_0^j, \hat{\gamma}_1^{n-j}) \right. \\ &\left. \times f_m^2(\xi_j, \hat{\gamma}_{n-j+1}^{n+m-j}) \right) d\hat{\xi}_1^{n+m} \\ =\ & \frac{(n+m-j)!}{m!(n-j)!} \int_{\mathcal{T}_{n+m-1}(x,\xi)} D_j^{n,m}[g_n^2, f_m^2](\hat{\xi}_0^{n+m}) d\hat{\xi}_1^{n+m}. \qquad (9.11.193)\end{aligned}$$

From Lemma 9.30,

$$\begin{aligned}
&\int_{\mathcal{T}_{n+m}(x,\xi)} D_j^{n,m}[g_n^2, f_m^2, j](\hat{\xi}_0^{n+m})d\hat{\xi}_1^{n+m} \\
&= \int_{\mathcal{T}_n(x,\xi)} g_n^2(\hat{\xi}_0^n)\left(\int_{\mathcal{T}_m(\xi_j,\sigma)} f_m^2(\xi_j,\hat{\sigma}_1^m)d\hat{\sigma}_1^m\right)d\hat{\xi}_1^n \\
&\leq \frac{\|f_m\|_\infty^2 x^m}{m!}\int_{\mathcal{T}_n(x,\xi)} g_n^2(\hat{\xi}_0^n)d\hat{\xi}_1^n, \qquad (9.11.194)
\end{aligned}$$

hence

$$\|D_j^{n,m}[g_n, f_m, j](x)\|_{L^2(\mathcal{T}_{n+m})}^2 \leq \frac{(n+m-j)!}{m!(n-j)!}\frac{\|f_m\|_\infty^2 x^m}{m!}\|g_n(x)\|_{L^2(\mathcal{T}_n)}^2, \quad (9.11.195)$$

which gives (9.11.189). For (9.11.190), and using Lemma 9.30

$$\begin{aligned}
&\|B_n^m[k_{n-m+1}, f_m](x)\|_{L^2(\mathcal{T}_n)}^2 \\
&= \int_{\mathcal{T}_n(x,\xi)}\left(\sum_{j=1}^{n-m+1}\int_{\xi_j}^{\xi_{j-1}} D_j^{n-m+1,m}\left[k_{n-m+1}(\hat{\xi}_0^{j-1}, s, \hat{\xi}_{n-m}^j)f_m(s,\hat{\xi}_{n-m+1}^n)\right]\right)^2 d\hat{\xi}_1^n \\
&\leq (n-m+1)\sum_{j=1}^{n-m+1}\int_{\mathcal{T}_n(x,\xi)}\int_{\xi_j}^{\xi_{j-1}} D_j^{n-m+1,m}\Big[k_{n-m+1}(\hat{\xi}_0^{j-1}, s, \hat{\xi}_{n-m}^j) \\
&\quad \times f_m(s,\hat{\xi}_{n-m+1}^n)\Big]^2 d\hat{\xi}_1^n \\
&= (n-m+1)\sum_{j=1}^{n-m+1}\int_{\mathcal{T}_{n+1}(x,\xi)} D_j^{n-m+1,m}[k_{n-m+1}(\hat{\xi}_0^{n-m+1})f_m(\xi_j,\hat{\xi}_{n-m}^{n+1})]^2 d\hat{\xi}_1^n \\
&= (n-m+1)\sum_{j=1}^{n-m+1}\|D_j^{n-m+1,m}[k_{n-m+1}f_m](x)\|_{L^2(\mathcal{T}_{n+1})}^2, \qquad (9.11.196)
\end{aligned}$$

and using (9.11.189) we get

$$\begin{aligned}
\|B_n^m[k_{n-m+1}, f_m](x)\|_{L^2(\mathcal{T}_n)}^2 &\leq (n-m+1)\left(\sum_{j=1}^{n-m+1}\frac{(n+1-j)!}{m!(n-m+1-j)!}\right) \\
&\quad \times x^m\frac{\|f_m\|_\infty^2}{m!}\|k_{n-m+1}(x)\|_{L^2(\mathcal{T}_{n-m+1})}^2. \quad (9.11.197)
\end{aligned}$$

and using Lemma 9.31 on the sum in (9.11.197), we obtain

$$\sum_{j=1}^{n-m+1}\frac{(n+1-j)!}{m!(n-m+1-j)!} = \sum_{j=0}^{n-m}\begin{pmatrix} m+j \\ j \end{pmatrix} = \frac{(n+1)!}{(m+1)!(n-m)!}, \quad (9.11.198)$$

hence, we get (9.11.190). The estimate for C is obtained in the same way as the estimate for B. The result then follows. □

Remark 9.33. Since $I[k_n, f_1] = B_1^n[k_n, f_1]$, we get

$$\|I[k_n, f_1](x)\|^2_{L^2(\mathcal{T}_n)} \leq \frac{n^2(n+1)}{2}\|f_1\|^2_{\xi_\infty}\|k_n(x)\|^2_{L^2(\mathcal{T}_n)}. \tag{9.11.199}$$

The next lemma is useful to treat the Robin boundary condition.

Lemma 9.34. *Let $n \geq 1$, $q > 0$, $k_n(\hat{\xi}_0^n) \in H^1(\mathcal{T}_n)$. Then*

$$\begin{aligned} q\int_{\mathcal{T}_{n-1}(x,\xi)} k_n^2(\hat{\xi}_0^{n-1}, 0)d\hat{\xi}_1^{n-1} \ &\leq \ q\int_{\mathcal{T}_{n-1}(x,\xi)} k_n^2(x, x, \hat{\xi}_1^{n-1})d\hat{\xi}_1^{n-1} \\ &\quad +q^2\|k_n^2(x)\|_{L^2(\mathcal{T}_n)} \\ &\quad +\sum_{j=1}^{n}\|k^2_{n\xi_j}(x)\|_{L^2(\mathcal{T}_n)}. \end{aligned} \tag{9.11.200}$$

Proof. By the fundamental theorem of calculus,

$$\begin{aligned} &q\int_{\mathcal{T}_{n-1}(x,\xi)} k_n^2(\hat{\xi}_0^{n-1}, 0)d\hat{\xi}_1^{n-1} - q\int_{\mathcal{T}_{n-1}(x,\xi)} k_n^2(\hat{\xi}_0^{n-1}, \xi_{n-1})d\hat{\xi}_1^{n-1} \\ = \ &-q\int_{\mathcal{T}_n(x,\xi)} \partial_{\xi_n} k_n^2(\hat{\xi}_0^n)d\hat{\xi}_1^n = -2q\int_{\mathcal{T}_n(x,\xi)} k_n k_{n\xi_n}(\hat{\xi}_0^n)d\hat{\xi}_1^n. \end{aligned} \tag{9.11.201}$$

Similarly, using Lemma 9.30, for $j = 0, \ldots, n-2$,

$$\begin{aligned} &q\int_{\mathcal{T}_{n-1}(x,\xi)} k_n^2(\hat{\xi}_0^j, \xi_{j+1}, \hat{\xi}_{j+1}^{n-1})d\hat{\xi}_1^{n-1} - q\int_{\mathcal{T}_{n-1}(x,\xi)} k_n^2(\hat{\xi}_0^j, \xi_j, \hat{\xi}_{j+1}^{n-1})d\hat{\xi}_1^{n-1} \\ = \ &-q\int_{\mathcal{T}_n(x,\xi)} \partial_{\xi_j} k_n^2(\hat{\xi}_0^n)d\hat{\xi}_1^n = -2q\int_{\mathcal{T}_n(x,\xi)} k_n k_{n\xi_{j+1}}(\hat{\xi}_0^n)d\hat{\xi}_1^n, \end{aligned} \tag{9.11.202}$$

hence

$$\begin{aligned} &q\int_{\mathcal{T}_{n-1}(x,\xi)} k_n^2(\hat{\xi}_0^{n-1}, 0)d\hat{\xi}_1^{n-1} - q\int_{\mathcal{T}_{n-1}(x,\xi)} k_n^2(x, x, \hat{\xi}_1^{n-1})d\hat{\xi}_1^{n-1} \\ = \ &-2q\int_{\mathcal{T}_n(x,\xi)} k_n\left(\sum_{j=1}^{n} k_{n\xi_j}\right)(\hat{\xi}_0^n)d\hat{\xi}_1^n \\ \leq \ &q^2\|k_n^2(x)\|_{L^2(\mathcal{T}_n)} + \sum_{j=1}^{n}\|k^2_{n\xi_j}(x)\|_{L^2(\mathcal{T}_n)}, \end{aligned} \tag{9.11.203}$$

and the result follows. □

The next lemma is used to get a precise estimate of the kernel growth.

Lemma 9.35. *Let $n > 2$, $x \in [0,1]$ and $\Upsilon > 0$. Then*

$$\int_0^x \xi^{\frac{n-1}{2}} \exp(\Upsilon\xi)\, d\xi \leq \frac{x^{\frac{n}{2}} \exp(\Upsilon x)}{\sqrt{n+1}\sqrt{D}} \tag{9.11.204}$$

Proof. Using the Cauchy-Schwartz inequality,

$$\begin{aligned}
\int_0^x \xi^{\frac{n-1}{2}} \exp(\Upsilon\xi)\, d\xi &\leq \sqrt{\left(\int_0^x \xi^{n-1} d\xi\right)\left(\int_0^x \exp\left(\frac{\Upsilon}{2}\xi\right) d\xi\right)} \\
&= \sqrt{\frac{x^n \left(\exp\left(\frac{\Upsilon}{2}x\right) - 1\right)}{2n\Upsilon}} \\
&\leq \frac{x^{\frac{n}{2}} \exp(\Upsilon x)}{\sqrt{n+1}\sqrt{\Upsilon}}, \qquad (9.11.205)
\end{aligned}$$

where we have used that $n+1 \leq 2n$. Hence the result follows. $\square$

The next result is the main ingredient in the proof of Theorem 9.17.

Proposition 9.36. *Let $g_n(x) \geq 0$ be a sequence of differentiable functions defined for $n \geq 1$, $x \in [0,1]$, and verifying $g_n(0) = 0$. Assume the following estimate holds for $n \geq 1$,*

$$\begin{aligned}
\frac{d}{dx} g_n(x) &\leq (nB+E)g_n(x) + C^{n-1}D\sqrt{\frac{x^n n!}{2}} + \frac{\sqrt{(n+1)!}}{B}\sum_{m=2}^{n} C^{m-1} \\
&\quad \times D g_{n-m+1}(x)\sqrt{\frac{x^m}{m(n-m+1)!}}\left(1 + \frac{2}{\sqrt{(n+1)x}}\right), \qquad (9.11.206)
\end{aligned}$$

where $B, C, E > 0$ and $D \geq B^2$. Then, $g_n(x)$ verifies the following bound:

$$g_n(x) \leq \sqrt{n!}DC^{n-1}x^{n/2}\exp\left((nB+E+\Upsilon)x\right), \tag{9.11.207}$$

where $\Upsilon = 4\frac{D^2(1+2\sqrt{B})^2}{B^4} > 1$.

Proof. We prove the claim by complete induction. For $n = 1$, the bound for g_1 is not dependent on other g_n's:

$$\frac{d}{dx} g_1(x) \leq (B+E)g_1 + D\sqrt{\frac{x}{2}}. \tag{9.11.208}$$

Using the comparison principle (Khalil), since $g_1(0) = 0$,

$$\begin{aligned} g_1(x) &\leq D\frac{1}{\sqrt{2}}\int_0^x \sqrt{\xi}\exp\left((B+E)(x-\xi)\right)d\xi \\ &\leq D\sqrt{x}\exp\left((B+E)x\right) \\ &\leq D\sqrt{x}\exp\left((B+E+\Upsilon)x\right), \end{aligned} \tag{9.11.209}$$

so the result follows for $n = 1$. For $n \geq 2$, we assume that the claim holds for g_j if $j = 1, \ldots, n-1$. Then $g_n'(x)$ is bounded as follows

$$\begin{aligned} \frac{d}{dx}g_n(x) &\leq (nB+E)g_n(x) + C^{n-1}D\sqrt{\frac{x^n n!}{2}} + \frac{\sqrt{(n+1)!x^{n+1}}}{B}\sum_{m=2}^{n}\frac{C^{n-1}D^2}{\sqrt{m}} \\ &\quad \times \exp\left((B(n-m+1)+E+\Upsilon)x\right)\left(1+\frac{2}{\sqrt{(n+1)x}}\right) \\ &= nBg_n(x) + C^{n-1}D\sqrt{\frac{x^n n!}{2}} + C^{n-1}\frac{D^2}{B}\sqrt{(n+1)!x^{n+1}}\exp\left((\Upsilon+E)x\right) \\ &\quad \times \sum_{m=2}^{n}\frac{\exp\left(B(n-m+1)x\right)}{\sqrt{m}}\left(1+\frac{2}{\sqrt{(n+1)x}}\right). \end{aligned} \tag{9.11.210}$$

Now, call $z = \exp(Bx)$. Note that the sum in the last line of (9.11.210) can be written as

$$\begin{aligned} \sum_{m=2}^{n}\exp\left(B(n-m+1)x\right)\frac{1}{\sqrt{m}} &= \sum_{m=2}^{n}\frac{z^{n-m+1}}{\sqrt{m}} \\ &\leq \frac{1}{\sqrt{2}}\sum_{m=1}^{n-1}z^m \\ &= \frac{1}{\sqrt{2}}\frac{z^n - z}{z-1}. \end{aligned} \tag{9.11.211}$$

Since $z = \exp(Bx)$, we have that $z - 1 \geq Bx$, which implies that

$$\begin{aligned} \sum_{m=2}^{n}\exp\left(B(n-m+1)x\right) &\leq \frac{\exp(Bnx) - \exp(Bx)}{\exp(Bx) - 1} \\ &\leq \frac{\exp(Bnx)}{Bx}. \end{aligned} \tag{9.11.212}$$

Similarly, we can also write

$$\begin{aligned}\sum_{m=2}^{n} \exp\left(B(n-m+1)x\right) &= \left(\sqrt{\sum_{m=2}^{n} \exp\left(B(n-m+1)x\right)}\right)^2 \\ &\le \sqrt{\frac{\exp\left(Bnx\right)}{Bx}}\sqrt{(n-1)\exp\left(B(n-1)x\right)} \\ &= \sqrt{\frac{n+1}{Bx}}\exp\left(Bnx\right). \qquad (9.11.213)\end{aligned}$$

We use (9.11.213) for the part of (9.11.210) affected by $\frac{2}{\sqrt{(n+1)x}}$, and (9.11.212) for the rest. Then (9.11.210) yields

$$\begin{aligned}\frac{d}{dx}g_n(x) &\le (nB+E)g_n(x) + C^{n-1}D\sqrt{\frac{x^n n!}{2}} + C^{n-1}\frac{D^2}{B^2}\sqrt{(n+1)!}\sqrt{x^{n-1}} \\ &\quad \times \frac{1}{\sqrt{2}}\exp\left(Bnx + Ex + \Upsilon x\right)\left(1+2\sqrt{B}\right) \qquad (9.11.214)\end{aligned}$$

Integrating and since $g_n(0) = 0$,

$$\begin{aligned}g_n(x) &\le C^{n-1}D\sqrt{\frac{n!}{2}}\int_0^x \exp\left((Bn+E)(x-\xi)\right)\xi^{n/2}d\xi + C^{n-1}\sqrt{(n+1)!} \\ &\quad \times \frac{D^2}{B^2\sqrt{2}}\left(1+2\sqrt{B}\right)\int_0^x \exp\left((Bn+E)x\right)\xi^{\frac{n-1}{2}}\exp\left(\Upsilon\xi\right)d\xi \\ &\le C^{n-1}D\sqrt{\frac{n!}{2}}\exp\left((Bn+E)x\right)\int_0^x \xi^{n/2}d\xi + C^{n-1}\sqrt{(n+1)!}\frac{D^2}{B^2\sqrt{2}} \\ &\quad \times \left(1+2\sqrt{B}\right)\exp\left((Bn+E)x\right)\int_0^x \xi^{\frac{n-1}{2}}\exp\left(\Upsilon\xi\right)d\xi \\ &\le C^{n-1}D\sqrt{\frac{n!}{2}}x^{n/2+1}\frac{2}{n+2}\exp\left((Bn+E)x\right) + C^{n-1}\sqrt{(n+1)!}\frac{D^2}{B^2\sqrt{2}} \\ &\quad \times \left(1+2\sqrt{B}\right)\exp\left((Bn+E)x\right)\frac{x^{\frac{n}{2}}}{\sqrt{n+1}}\frac{\exp\left(\Upsilon\xi\right)}{2\frac{D(1+2\sqrt{B})}{B^2}} \\ &\le \sqrt{n!}x^{n/2}C^{n-1}D\exp\left(Bnx+Ex+\Upsilon x\right)\frac{1}{\sqrt{2}}\left(\frac{2}{n+2}+\frac{1}{2}\right) \\ &\le \sqrt{n!}x^{n/2}C^{n-1}D\exp\left(Bnx+Ex+\Upsilon x\right), \qquad (9.11.215)\end{aligned}$$

where we have used Lemma 9.35 and the definition of $\Upsilon = 4\frac{D^2(1+2\sqrt{B})^2}{B^4}$. This completes the proof. $\square$

Proposition 9.37. *Let Assumption 9.15 hold. Define for each $n \geq 1$ the function $\psi_n(\xi_0^n)$ as the solution of the wave equation*

$$\psi_{nxx} = \sum_{i=1}^{n} \psi_{n\xi_i\xi_i}, \tag{9.11.216}$$

with boundary conditions

$$\begin{aligned}
\psi_n(x, x, \xi_2^n) &= \hat{\phi}_n(x, \xi_2^n), && (9.11.217)\\
\partial_{\xi_{i-1}}\psi_n(\xi_0^n)\Big|_{\xi_{i-1}=\xi_i} &= \partial_{\xi_i}\psi_n(\xi_0^n)\Big|_{\xi_{i-1}=\xi_i}, \quad i = 2, .., n, && (9.11.218)\\
\psi_{n\xi_n}(\xi_0^{n-1}, 0) &= q\psi_n(\xi_0^{n-1}, 0), && (9.11.219)
\end{aligned}$$

where $\hat{\phi}_1(x) = \hat{q} - 1/2\int_0^x \lambda(s)ds$, and for $n \geq 2$, $\hat{\phi}_n(x, \xi_2^n) = -1/2\int_{\xi_2}^x h_{n-1}(s, \xi_2^n)$. Then

$$\begin{aligned}
\|\psi_n(x)\|^2_{L^2(\mathcal{T}_n)} + \|\psi_{nx}(x)\|^2_{L^2(\mathcal{T}_n)} &\leq 4((\rho_h+1)D_h)^2 x^n (1+|q|)^2 \exp(1+|\hat{q}|)(n-1)!\\
&\quad \times \left(\frac{1}{\rho_h}\right)^{2(n-1)}, && (9.11.220)\\
\|\varphi_n\|^2_{L^2(\mathcal{T}_n)} &\leq D_\varphi^2 \left(\frac{1}{\rho_\varphi}\right)^{2(n-1)} n! x^n, && (9.11.221)
\end{aligned}$$

where

$$\begin{aligned}
\varphi_n &= -\sum_{i=1}^{n} \lambda(\xi_i)\psi_n - I_n[\psi_n, f_1] - c\psi_n\\
&\quad -\sum_{m=2}^{n} B_n^m[\psi_{n-m+1}, f_m] - \sum_{m=1}^{n-1} C_n^m[\psi_{n-m}, h_m] && (9.11.222)
\end{aligned}$$

and $\rho_\varphi = \frac{\min\{\rho_f, \rho_h\}}{2}$, $D_\varphi = 2((\rho_h+1)D_h)(|q|+1)\exp(1+|\hat{q}|)\sqrt{(\rho_h+1)^2 D_h^2 + D_f^2}$.

Proof. Under Assumption 9.15, there is a H_1 solution to (9.11.216)–(9.11.219). Consider

$$\begin{aligned}
L_{\psi_n}(x) &= \int_{\mathcal{T}_n(x,\xi)} \frac{(1+\hat{q}^2)\psi_n^2 + \psi_{nx}^2 + \sum_{j=1}^n \psi_{n\xi_j}^2}{2}(x, \hat{\xi}_1^n) d\hat{\xi}_1^n\\
&\quad + \frac{q}{2}\int_{\mathcal{T}_{n-1}(x,\xi)} \psi_n^2(x, \hat{\xi}_1^{n-1}, 0) d\hat{\xi}_1^{n-1}\\
&\quad + \frac{|\hat{q}|}{2}\int_{\mathcal{T}_{n-1}(x,\xi)} \hat{\phi}_n^2(x, \hat{\xi}_1^{n-1}) d\hat{\xi}_1^{n-1}. && (9.11.223)
\end{aligned}$$

By Lemma 9.34, $L_{\psi_n}(x) \geq 0$. It is straightforward to show (see Proof of Theorem 9.17 below), using (9.11.216)–(9.11.219), that for $n \geq 2$,

$$\begin{aligned}
L'_{\psi_n}(x) &= (1+\hat{q}^2)\int_{\mathcal{T}_n(x,\xi)} \psi_n\psi_{nx}(x,\hat{\xi}_1^n)d\hat{\xi}_1^n + |\hat{q}|\int_{\mathcal{T}_{n-1}(x,\xi)} \hat{\phi}_n\hat{\phi}_{nx}(x,\hat{\xi}_1^{n-1})d\hat{\xi}_1^{n-1} \\
&\quad + \int_{\mathcal{T}_{n-1}(x,\xi)} \frac{(1+\hat{q}^2)\hat{\phi}_n^2 + \hat{\phi}_{nx}^2 + \sum_{j=2}^n \hat{\phi}_{n\xi_j}^2}{2}(x,\hat{\xi}_2^n)d\hat{\xi}_2^n \\
&\quad + \frac{q}{2}\int_{\mathcal{T}_{n-2}(x,\xi)} \hat{\phi}_n^2(x,\hat{\xi}_1^{n-2},0)d\hat{\xi}_1^{n-2} + \frac{|\hat{q}|}{2}\int_{\mathcal{T}_{n-2}(x,\xi)} \hat{\phi}_n^2(x,x,\hat{\xi}_1^{n-2})d\hat{\xi}_1^{n-2} \\
&\leq (1+|\hat{q}|)L_{\psi_n}(x) + (n-1)!^2 D_h^2 \left(\frac{1}{\rho_h}\right)^{2(n-2)} \\
&\quad \times \left(\frac{x^{n-1}(1+|\hat{q}|)^2}{(n-1)!}\frac{n+2}{8} + \frac{|q|}{2}\frac{x^{n-2}}{(n-2)!}\frac{x^2}{8}\right) \\
&\leq (1+|\hat{q}|)L_{\psi_n}(x) + (n-1)!x^{n-1}D_h^2 \\
&\quad \times \left(\frac{1}{\rho_h}\right)^{2(n-2)} (1+|\hat{q}|)^2(1+|q|)\frac{n+2}{8}.
\end{aligned} \tag{9.11.224}$$

Since $L_{\psi_n}(0) = 0$, integrating (9.11.224) and using that

$$\|\psi_n(x)\|^2_{L^2(\mathcal{T}_n)} + \|\psi_{nx}(x)\|^2_{L^2(\mathcal{T}_n)} \leq 2L_{\psi_n}(x), \tag{9.11.225}$$

we get (9.11.220) for $n \geq 2$. For $n = 1$, (9.11.220) follows similarly.

Finally, to get the estimate on φ we use (9.11.220) and Lemma 9.32 in the definition of φ, obtaining (9.11.221). This finishes the proof. □

Now we prove the main Theorem.

Proof of Theorem 9.17. We obtain the estimates (9.7.108) by a Lyapunov method. First, we homogenize the equation defining $\hat{k}_n(\xi_0^n) = k_n(\xi_0^n) - \psi_n(\xi_0^n)$, where ψ_n was defined in Proposition 9.37.

Then the kernels $\hat{k}_n$ verify (9.4.38)–(9.4.45) with (9.4.41) replaced by $\hat{k}_n(x,x,\xi_2^n) = 0$ and an additional right-hand side term, φ_n, as defined in Proposition 9.37, in (9.4.38). For simplicity, we drop hats and define $\gamma = \max\{1, \|f_1\|_\infty + \|\lambda\|_\infty\}$.

Consider, for each $n \geq 1$, the following Lyapunov function

$$\begin{aligned} L_n(x) &= \int_{\mathcal{T}_n(x,\xi)} \frac{(n^2\gamma + \hat{q}^2)k_n^2(x,\hat{\xi}_1^n) + k_{nx}^2(x,\hat{\xi}_1^n) + \sum_{j=1}^n k_{n\xi_j}^2(x,\hat{\xi}_1^n)}{2} d\hat{\xi}_1^n \\ &\quad + \frac{q}{2}\int_{\mathcal{T}_{n-1}(x,\xi)} k_n^2(x,\hat{\xi}_1^{n-1},0)d\hat{\xi}_1^{n-1}, \end{aligned} \tag{9.11.226}$$

which is positive definite by application of Lemma 9.34. Note that (9.11.226) is equivalent to the H^1 norm in $\mathcal{T}_n(x)$:

$$L_n(x) = \frac{n^2\gamma\|k_n(x)\|_{L^2(\mathcal{T}_n)}^2 + \|k_{nx}(x)\|_{L^2(\mathcal{T}_n)}^2 + \sum_{j=1}^n \|k_{n\xi_j}(x)\|_{L^2(\mathcal{T}_n)}^2}{2}. \tag{9.11.227}$$

If $q = \infty$ (Dirichlet boundary condition at $x = 0$), then set $q = 0$ in (9.11.226) and the rest of the proof.

Taking the x derivative of (9.11.226), we get

$$\begin{aligned} L_n'(x) &= (n^2\gamma + \hat{q}^2)\int_{\mathcal{T}_n(x,\xi)} k_n k_{nx}(x,\hat{\xi}_1^n)d\hat{\xi}_1^n \\ &\quad + \int_{\mathcal{T}_n(x,\xi)} \left(k_{nx}k_{nxx}(x,\hat{\xi}_1^n) + \sum_{j=1}^n k_{n\xi_j}k_{n\xi_j x}(x,\hat{\xi}_1^n) \right) d\hat{\xi}_1^n \\ &\quad + \int_{\mathcal{T}_{n-1}(x,\xi)} \frac{\gamma k_n^2(x,x,\hat{\xi}_1^{n-1}) + k_{nx}^2(x,x,\hat{\xi}_1^{n-1}) + \sum_{j=1}^n k_{n\xi_j}^2(x,x,\hat{\xi}_1^{n-1})}{2} d\hat{\xi}_1^{n-1} \\ &\quad + q\int_{\mathcal{T}_{n-1}(x,\xi)} k_n k_{nx}(x,\hat{\xi}_1^{n-1},0)d\hat{\xi}_1^{n-1} \\ &\quad + \frac{q}{2}\int_{\mathcal{T}_{n-2}(x,\xi)} k_n^2(x,x,\hat{\xi}_1^{n-2},0)d\hat{\xi}_1^{n-1}. \end{aligned} \tag{9.11.228}$$

From the boundary conditions, $k_n^2(x,x,\hat{\xi}_1^{n-1}) = 0$, so $k_{n\xi_j}^2(x,x,\hat{\xi}_1^{n-1}) = 0$ for $j \geq 2$, and $k_{nx}(x,x,\hat{\xi}_1^{n-1}) = -k_{n\xi_1}(x,x,\hat{\xi}_1^{n-1})$. Hence, the third line of (9.11.228) is greatly simplified as follows.

$$\begin{aligned} &\int_{\mathcal{T}_{n-1}(x,\xi)} \frac{(n^2\gamma + \hat{q}^2)k_n^2(x,x,\hat{\xi}_1^{n-1}) + k_{nx}^2(x,x,\hat{\xi}_1^{n-1}) + \sum_{j=1}^n k_{n\xi_j}^2(x,x,\hat{\xi}_1^{n-1})}{2} d\hat{\xi}_1^{n-1} \\ &= \int_{\mathcal{T}_{n-1}(x,\xi)} k_{nx}^2(x,x,\hat{\xi}_1^{n-1})d\hat{\xi}_1^{n-1}. \end{aligned} \tag{9.11.229}$$

Using the kernel PIDE equation for the first term in the second line of

(9.11.228) we get

$$
\begin{aligned}
&\int_{\mathcal{T}_n(x,\xi)} k_{nx}k_{nxx}(x,\hat{\xi}_1^n)d\hat{\xi}_1^n \\
= \;& \sum_{j=1}^{n}\int_{\mathcal{T}_n(x,\xi)} k_{nx}k_{n\xi_j\xi_j}(x,\hat{\xi}_1^n)d\hat{\xi}_1^n + \int_{\mathcal{T}_n(x,\xi)}\left(\sum_{j=1}^{n}\lambda(\xi_j)\right)k_{nx}k(x,\hat{\xi}_1^n)d\hat{\xi}_1^n \\
& - \int_{\mathcal{T}_n(x,\xi)}(k_{nx}f_n(x,\hat{\xi}_1^n)d\hat{\xi}_1^n + \int_{\mathcal{T}_n(x,\xi)}(k_{nx}\varphi_n(x,\hat{\xi}_1^n)d\hat{\xi}_1^n \\
& + \int_{\mathcal{T}_n(x,\xi)} k_{nx}I[k_n,f_1](x,\hat{\xi}_1^n)d\hat{\xi}_1^n \\
& + \sum_{m=2}^{n}\int_{\mathcal{T}_n(x,\xi)} k_{nx}B_n^m[k_{n-m+1},f_m](x,\hat{\xi}_1^n)d\hat{\xi}_1^n \\
& + \sum_{m=1}^{n-1}\int_{\mathcal{T}_n(x,\xi)} k_{nx}C_n^m[k_{n-m},h_m](x,\hat{\xi}_1^n)d\hat{\xi}_1^n. \qquad (9.11.230)
\end{aligned}
$$

Now the first integral in the second line of (9.11.230) can be expressed as

$$
\begin{aligned}
&\sum_{j=1}^{n}\int_{\mathcal{T}_n(x,\xi)} k_{nx}k_{n\xi_j\xi_j}(x,\hat{\xi}_1^n)d\hat{\xi}_1^n \\
= \;& \sum_{j=1}^{n-1}\int_{\mathcal{T}_{n-1}(x,\xi)}\int_{\xi_j}^{\xi_{j-1}} k_{nx}k_{n\xi_j\xi_j}(x,\hat{\xi}_1^{j-1},s,\hat{\xi}_j^{n-1})dsd\hat{\xi}_1^{n-1} \\
& + \int_{\mathcal{T}_n(x,\xi)} k_{nx}k_{n\xi_n\xi_n}(x,\hat{\xi}_1^n)d\hat{\xi}_1^n. \qquad (9.11.231)
\end{aligned}
$$

Integrating by parts in ξ_j in (9.11.231),

$$
\begin{aligned}
&\sum_{j=1}^{n}\int_{\mathcal{T}_n(x,\xi)} k_{nx}k_{n\xi_j\xi_j}(x,\hat{\xi}_1^n)d\hat{\xi}_1^n \\
= \;& -\sum_{j=1}^{n-1}\int_{\mathcal{T}_{n-1}(x,\xi)}\int_{\xi_j}^{\xi_{j-1}} k_{nx\xi_j}k_{n\xi_j}(x,\hat{\xi}_1^{j-1},s,\xi_j^{n-1})dsd\hat{\xi}_1^{n-1} \\
& - \int_{\mathcal{T}_n(x,\xi)} k_{nx\xi_n}k_{n\xi_n}(x,\hat{\xi}_1^n)d\hat{\xi}_1^n \\
& + \sum_{j=1}^{n-1}\int_{\mathcal{T}_{n-1}(x,\xi)}\Big(k_{nx}k_{n\xi_j}(x,\hat{\xi}_1^{j-1},\xi_{j-1},\hat{\xi}_j^{n-1}) - k_{nx}k_{n\xi_j}(x,\hat{\xi}_1^{j-1},\xi_j,\xi_j^{n-1})\Big)d\hat{\xi}_1^{n-1} \\
& + \int_{\mathcal{T}_n(x,\xi)}\Big(k_{nx}k_{n\xi_n}(x,\hat{\xi}_1^{n-1},\xi_{n-1}) - k_{nx}k_{n\xi_n}(x,\hat{\xi}_1^{n-1},0)\Big)d\hat{\xi}_1^{n-1} \\
= \;& -\sum_{j=1}^{n}\int_{\mathcal{T}_n(x,\xi)} k_{nx\xi_j}k_{n\xi_j}(x,\hat{\xi}_1^n)d\hat{\xi}_1^n + \int_{\mathcal{T}_{n-1}(x,\xi)} k_{nx}k_{n\xi_1}(x,x,\hat{\xi}_1^{n-1})d\hat{\xi}_1^{n-1}
\end{aligned}
$$

$$
\begin{aligned}
&+\sum_{j=1}^{n-1}\int_{\mathcal{T}_{n-1}(x,\xi)}\left(k_{nx}k_{n\xi_{j+1}}(x,\hat{\xi}_1^j,\xi_j,\hat{\xi}_j^{n-1})-k_{nx}k_{n\xi_j}(x,\hat{\xi}_1^{j-1},\xi_j,\xi_j^{n-1})\right)d\hat{\xi}_1^{n-1}\\
&-\int_{\mathcal{T}_{n-1}(x,\xi)}k_{nx}k_{n\xi_n}(x,\hat{\xi}_1^{n-1},0)d\hat{\xi}_1^{n-1}, \qquad (9.11.232)
\end{aligned}
$$

and using the Neumann boundary conditions for $\xi_j=\xi_{j+1}$ and the Robin boundary conditions for $\xi_n=0$, we get

$$
\begin{aligned}
&\sum_{j=1}^{n}\int_{\mathcal{T}_n(x,\xi)}k_{nx}k_{n\xi_j\xi_j}(x,\hat{\xi}_1^n)d\hat{\xi}_1^n\\
=\;&-\sum_{j=1}^{n}\int_{\mathcal{T}_n(x,\xi)}k_{nx\xi_j}k_{n\xi_j}(x,\hat{\xi}_1^n)d\hat{\xi}_1^n-\int_{\mathcal{T}_{n-1}(x,\xi)}k_{nx}^2(x,x,\hat{\xi}_1^{n-1})d\hat{\xi}_1^{n-1}\\
&-q\int_{\mathcal{T}_{n-1}(x,\xi)}k_{nx}k_n(x,\hat{\xi}_1^{n-1},0)d\hat{\xi}_1^{n-1}, \qquad (9.11.233)
\end{aligned}
$$

where we have used again that $k_{n\xi_1}(x,x,\hat{\xi}_1^{n-1})=-k_{nx}(x,x,\hat{\xi}_1^{n-1})$. Then some terms cancel out, leaving

$$
\begin{aligned}
\frac{d}{dx}L_n \;=\;&(n^2\gamma+\hat{q}^2)\int_{\mathcal{T}_n(x,\xi)}k_nk_{nx}(x,\hat{\xi}_1^n)d\hat{\xi}_1^n+\int_{\mathcal{T}_n(x,\xi)}\left(\sum_{j=1}^{n}\lambda(\xi_j)\right)k_{nx}k(x,\hat{\xi}_1^n)d\hat{\xi}_1^n\\
&-\int_{\mathcal{T}_n(x,\xi)}k_{nx}f_n(x,\hat{\xi}_1^n)d\hat{\xi}_1^n+\int_{\mathcal{T}_n(x,\xi)}(k_{nx}\varphi_n(x,\hat{\xi}_1^n)d\hat{\xi}_1^n\\
&+\int_{\mathcal{T}_n(x,\xi)}k_{nx}I[k_n,f_1](x,\hat{\xi}_1^n)d\hat{\xi}_1^n\\
&+\sum_{m=2}^{n}\int_{\mathcal{T}_n(x,\xi)}k_{nx}B_n^m[k_{n-m+1},f_m](x,\hat{\xi}_1^n)d\hat{\xi}_1^n\\
&+\sum_{m=1}^{n-1}\int_{\mathcal{T}_n(x,\xi)}k_{nx}C_n^m[k_{n-m},h_m](x,\hat{\xi}_1^n)d\hat{\xi}_1^n, \qquad (9.11.234)
\end{aligned}
$$

and using Cauchy-Schwartz and Young's inequalities, and the definition of γ (note that if $f_1=0$ then $I[k_n,f_1]=0$),

$$
\begin{aligned}
\frac{d}{dx}L_n \;\leq\;&(n\sqrt{\gamma}+|\hat{q}|)\int_{\mathcal{T}_n(x,\xi)}\frac{(n^2\gamma+\hat{q}^2)k_n^2(x,\hat{\xi}_1^n)+k_{nx}^2(x,\hat{\xi}_1^n)}{2}d\hat{\xi}_1^n\\
&+\sqrt{\int_{\mathcal{T}_n(x,\xi)}k_{nx}^2(x,\hat{\xi}_1^n)d\hat{\xi}_1^n}\left(\|f_n\|_\infty\sqrt{\frac{x^n}{n!}}+\sqrt{\int_{\mathcal{T}_n(x,\xi)}\varphi_n^2(x,\hat{\xi}_1^n)d\hat{\xi}_1^n}\right)\\
&+\sum_{m=2}^{n}\sqrt{\int_{\mathcal{T}_n(x,\xi)}k_{nx}^2(x,\hat{\xi}_1^n)d\hat{\xi}_1^n}\sqrt{\int_{\mathcal{T}_n(x,\xi)}\left(B_n^m[k_{n-m+1},f_m](x,\hat{\xi}_1^n)\right)^2d\hat{\xi}_1^n}
\end{aligned}
$$

$$+\sum_{m=1}^{n-1}\sqrt{\int_{\mathcal{T}_n(x,\xi)} k_{nx}^2(x,\hat{\xi}_1^n)d\hat{\xi}_1^n}\sqrt{\int_{\mathcal{T}_n(x,\xi)}\left(C_n^m[k_{n-m},h_m](x,\hat{\xi}_1^n)\right)^2 d\hat{\xi}_1^n}$$
$$+n\sqrt{\gamma}\int_{\mathcal{T}_n(x,\xi)}\frac{k_{nx}^2+\frac{I^2[k_n,f_1](x,\hat{\xi}_1^n)}{n^2\|f_1\|_\infty}}{2}d\hat{\xi}_1^n, \tag{9.11.235}$$

and using Lemma 9.32,

$$\begin{aligned}
\frac{d}{dx}L_n &\leq (2n\sqrt{\gamma}+|\hat{q}|)\int_{\mathcal{T}_n(x,\xi)}\frac{(n^2\gamma+\hat{q}^2)k_n^2(x,\hat{\xi}_1^n)+k_{nx}^2(x,\hat{\xi}_1^n)}{2}d\hat{\xi}_1^n \\
&\quad+\sqrt{\int_{\mathcal{T}_n(x,\xi)} k_{nx}^2(x,\hat{\xi}_1^n)d\hat{\xi}_1^n}\left(\|f_n\|_\infty\sqrt{\frac{x^n}{n!}}+\sqrt{\int_{\mathcal{T}_n(x,\xi)}\varphi_n^2(x,\hat{\xi}_1^n)d\hat{\xi}_1^n}\right) \\
&\quad+\sqrt{\int_{\mathcal{T}_n(x,\xi)} k_{nx}^2(x,\hat{\xi}_1^n)d\hat{\xi}_1^n}\sqrt{(n+1)!}\left[\sum_{m=2}^{n}\frac{\|f_m\|_\infty\sqrt{x^m}}{m!}\sqrt{\frac{n-m+1}{m(n-m)!}}\right. \\
&\quad\times\sqrt{\int_{\mathcal{T}_{n-m+1}(x,\xi)} k_{n-m+1}^2(x,\hat{\xi}_1^{n-m+1})d\hat{\xi}_1^{n-m+1}}+\frac{1}{\sqrt{n+1}}\sum_{m=1}^{n-1}\frac{\|h_m\|_\infty\sqrt{x^m}}{m!} \\
&\quad\left.\times\sqrt{\frac{n-m}{m(n-m-1)!}}\sqrt{\int_{\mathcal{T}_{n-m}(x,\xi)} k_{n-m}^2(x,\hat{\xi}_1^{n-m})d\hat{\xi}_1^{n-m}}\right] \\
&\leq (2n\sqrt{\gamma}+|\hat{q}|)L_n(x)+\sqrt{2L_n(x)}\left(\|f_n\|_\infty\sqrt{\frac{x^n}{n!}}+\|\varphi_n\|_{L^2(\mathcal{T}_n)}\right) \\
&\quad+2\sqrt{\frac{(n+1)!L_n(x)}{\gamma}}\sum_{m=2}^{n}\frac{\|f_m\|_\infty}{m!}\sqrt{\frac{x^m L_{n-m+1}(x)}{m(n-m+1)!}} \\
&\quad+2\sqrt{\frac{n!L_n(x)}{\gamma}}\sum_{m=1}^{n-1}\frac{\|h_m\|_\infty}{m!}\sqrt{\frac{x^m L_{n-m}(x)}{m(n-m)!}}.
\end{aligned} \tag{9.11.236}$$

Using Assumption 9.15 and Proposition 9.37,

$$\begin{aligned}
\frac{d}{dx}L_n &\leq (2n\sqrt{\gamma}+|\hat{q}|)L_n(x)+\sqrt{2L_n(x)}\left(\left(\frac{1}{\rho_f}\right)^{n-1}D_f+\left(\frac{1}{\rho_\varphi}\right)^{n-1}D_\varphi\right)\sqrt{x^n n!} \\
&\quad+2\sqrt{\frac{(n+1)!L_n(x)}{\gamma}}\sum_{m=2}^{n}\left(\frac{1}{\rho_f}\right)^{m-1}D_f\sqrt{\frac{x^m L_{n-m+1}(x)}{m(n-m+1)!}} \\
&\quad+2\sqrt{\frac{n!L_n(x)}{\gamma}}\sum_{m=1}^{n-1}\left(\frac{1}{\rho_h}\right)^{m-1}\rho_h D_h\sqrt{\frac{x^m L_{n-m}(x)}{m(n-m)!}}.
\end{aligned} \tag{9.11.237}$$

Call $C = 1/\rho_\varphi$. Then $1/\rho_f \leq C$ and $1/\rho_h \leq C$. Call $D = D_f + \rho_h D_h + D_\varphi$.

Dividing (9.11.237) by $2\sqrt{L_n(x)}$, getting

$$\begin{aligned} \frac{d}{dx}\sqrt{L_n(x)} &\leq (n\sqrt{\gamma}+\frac{|\hat{q}|}{2})\sqrt{L_n(x)}+C^{n-1}D\sqrt{\frac{x^n n!}{2}}+\sqrt{\frac{(n+1)!}{\gamma}}\sum_{m=2}^{n}C^{m-1}D \\ &\times\sqrt{\frac{x^m L_{n-m+1}(x)}{m(n-m+1)!}}\left(1+\frac{2}{\sqrt{x(n+1)}}\right). \end{aligned} \tag{9.11.238}$$

Calling $g_n(x)=\sqrt{L_n(x)}$ in (9.11.238), we get

$$\begin{aligned} \frac{d}{dx}g_n(x) &\leq (n\sqrt{\gamma}+\frac{|\hat{q}|}{2})g_n(x)+C^{n-1}D\sqrt{\frac{x^n n!}{2}}+\sqrt{\frac{(n+1)!}{\gamma}}\sum_{m=2}^{n}C^{m-1}D \\ &\times g_{n-m+1}(x)\sqrt{\frac{x^m}{m(n-m+1)!}}\left(1+\frac{2}{\sqrt{x(n+1)}}\right). \end{aligned} \tag{9.11.239}$$

Since $g_n>0$ and $g_n(0)=\sqrt{L_n(0)}=0$, we can use Proposition 9.36 with $B=\sqrt{\gamma}$, $E=\frac{|\hat{q}|}{2}$. Thus we obtain

$$\sqrt{L_n(x)}\leq\sqrt{n!}DC^{n-1}x^{n/2}\exp\left(n\sqrt{\gamma}x+\frac{|\hat{q}|}{2}x+\Upsilon x\right), \tag{9.11.240}$$

where $\Upsilon=4\frac{D^2(1+2\sqrt[4]{\gamma})^2}{\gamma^2}>1$. Squaring (9.11.240) yields

$$L_n(x)\leq n!D^2C^{2n-2}x^n\exp\left(2n\sqrt{\gamma}x+|\hat{q}|x+2\Upsilon x\right). \tag{9.11.241}$$

Hence, recovering the hat notation,

$$\frac{n^2\gamma}{2}\|\hat{k}_n(x)\|^2_{L^2(\mathcal{T}_n)}\leq L_n(x)\leq n!D^2C^{2n-2}\exp\left(2n\sqrt{\gamma}+|\hat{q}|+2\Upsilon\right), \tag{9.11.242}$$

and since $\gamma^{-1}\leq 1$,

$$\|k_n(x)+\psi_n(x)\|^2_{L^2(\mathcal{T}_n)}\leq(n-1)!2D^2C^{2n-2}\exp\left(2n\sqrt{\gamma}+|\hat{q}|+2\Upsilon\right), \tag{9.11.243}$$

where ψ_n was defined in Proposition 9.37. Then, using the definition of C and D,

$$\begin{aligned} \|k_n(x)\|^2_{L^2(\mathcal{T}_n)} &= \|k_n(x)+\psi_n(x)-\psi_n(x)\|^2_{L^2(\mathcal{T}_n)} \\ &\leq (n-1)!4D^2C^{2n-2}\exp\left(2\left(n\sqrt{\gamma}+\Upsilon\right)+|\hat{q}|\right), \end{aligned} \tag{9.11.244}$$

and we get that the Volterra series defined by k_n is convergent with radius of convergence

$$\rho_k=C^{-2}\exp\left(-2\sqrt{\gamma}\right)=\left(\frac{\min\{\rho_f,\rho_h\}}{2}\right)^2\exp\left(-2\sqrt{\gamma}\right). \tag{9.11.245}$$

Similarly we get

$$\|k_{nx}(x)\|^2_{L^2(\mathcal{T}_n)} \leq n!2D^2C^{2n-2}\exp\left(2\left(n\sqrt{\gamma}+\Upsilon\right)+|\hat{q}|\right), \tag{9.11.246}$$

which used in (9.7.101) gives the convergence of the transformation for w_x, thus proving the theorem. □

This chapter is a partial reprint of the material as it appears in
R. Vazquez and M. Krstic, "Control of 1-D parabolic PDEs with Volterra nonlinearities —Part I: Design," in preparation, 2006.
R. Vazquez and M. Krstic, "Control of 1-D parabolic PDEs with Volterra nonlinearities —Part II: Analysis," in preparation, 2006.
The dissertation author was the primary author and the coauthor listed in these publications directed and supervised the research, which is the basis for this chapter.

Chapter 10

Future Work

The results presented in this dissertation provide a starting point towards more complex and realistic boundary control and observer problems for convective, turbulent and magnetohydrodynamic flows and other nonlinear distributed parameter systems modeling physical systems.

We present several open questions and possible directions of future research that extend our results in a natural way.

1. We proved closed-loop stability and estimator convergence for the Navier-Stokes and MHD control laws and observers of Chapters 4–8, however we did not show simulation results. To verify the theory and give further insight into the properties of our controllers and estimators, DNS simulations need to be done. The numerical tests need to focus on turbulence-critical issues like the behavior of the controller at small k_x for moderate-to-large k_z.

2. While the problems solved in Chapters 2–8 were tractable due to their simple (spatially-invariant) geometry, many engineering problems of interest are formulated in non-spatially-invariant geometries, for instance finite or irregular channels, or the problem of vortex shedding stabilization. However the extension of the backstepping method to a 2-D or 3-D *general geometry* is still an open problem; preliminary results lead to challenging ultra-hyperbolic equations for the kernels.

3. Our methods were successful in handling problems with one boundary actuator/measurement for each infinite-dimensional state of the system. We did not consider "underactuated" systems (in the sense of having less actuators/sensors than infinite-dimensional states), but such systems are very likely to arise in practice. For example, one would like to achieve channel flow relaminarization by means of injection/suction actuators (i.e., using only the normal component of the velocity) and pressure sensors at the wall, or, for the case of the convection loop of Chapter 2, stop the convective instability just by rotating the outer cylinder. Under such conditions, the plant becomes *non-strict-feedback* and the backstepping method, based on a linear, strict-feedback Volterra operator, fails to address them. A promising tool for extending the method is the theory of Fredholm operators, which are non-strict-feedback in form, however the Fredholm approach leads to many new difficult technical questions (non-causal equations, operator invertibility, kernel solvability) and is yet to be explored.

4. In this dissertation we have always considered incompressible fluid, for both Navier-Stokes and MHD flows; however in many situations compressibility effects cannot be neglected. Then, the physical and mathematical nature of the equations changes radically, as the system becomes hyperbolic. Our design relies critically on the parabolicity of the equations (once the pressure is taken care of) and does not extend in a simple manner to the compressible equations, even in the inviscid case. Nevertheless, recent breakthroughs have allowed to extend the backstepping method to simple hyperbolic systems and offer some new possibilities in the area of compressible flows.

5. If the assumption of a low magnetic Reynolds number is dropped, the inductionless MHD equations become the full-blown MHD equations, and instead of the simple additional electric field *static* equation, there are three additional *dynamic* equations, one for each component of the magnetic field. The

problem becomes then extremely challenging, and at the same time opens up new possibilities, such electromagnetic-only actuators. Those will be more implementable in practice than mechanical actuators, allowing, for instance, the design of "electromagnetic pumps" which would find application for cooling systems.

6. The problems solved in Chapters 2–8 were all nonlinear; however, we linearized the plant equations in order to apply the infinite-dimensional linear backstepping technique. In Chapter 9 we provide a method to solve nonlinear problems, however the class of systems considered is not broad enough to include the Navier-Stokes or MHD systems. Future work includes extending the class of systems to include convective nonlinearities and higher-dimensional coupled systems in spatially-invariant geometries.

7. New developments in the linear backstepping method have successfully addressed a wide range of *linear* problems such as cylinder wake, strings, elastic beams, and infinite-dimensional delay systems. Since our nonlinear design naturally extends the linear method for the parabolic case, similar developments are possible for the *nonlinear* versions of those problems.

8. While we addressed nonlinear control of parabolic PDEs, the problem of *observer design* is amenable to the same treatment and presents some pioneering opportunities in state estimation for nonlinear PDEs.

9. In Section 9.10 we provided a number of open questions for the nonlinear method. Those include the very important unanswered question of global stabilization. Since the nonlinear plants we consider include some which are not globally stabilizable, we need to refine the class of systems to be controlled. Such a refinement will possibly need a result establishing a connection between the global invertibility of the Volterra series transformation for a given plant (since global invertibility leads to global stabilization) and the plant parameters (which determine controllability properties of the plant).

Bibliography

[1] O. M. Aamo and M. Krstic, *Flow Control by Feedback: Stabilization and Mixing*, Berlin, Springer, 2002.

[2] O.M. Aamo and M. Krstic, "Global stabilization of a nonlinear Ginzburg-Landau model of vortex shedding," *European Journal of Control*, vol. 10, pp. 105-116, 2004.

[3] O. M. Aamo, A. Smyshlyaev and M. Krstic, "Boundary control of the linearized Ginzburg-Landau model of vortex shedding," *SIAM Journal of Control and Optimization*, vol. 43, pp. 1953–1971, 2005.

[4] M.-R. Alam, W.-J. Liu and G. Haller, "Closed-loop separation control: an analytic approach," *Phys. Fluids*, vol. 18, 043601, 2006.

[5] A. Aliseda, K. Ariyur, O. Sarrazin, J. C. Lasheras, and M. Krstic, "Tailored fuel injection for pulsed detonation engines via feedback control," *AIAA Journal of Propulsion and Power*, vol. 19, pp. 917–921, 2003.

[6] A. Armaou and P.D. Christofides, "Dynamic optimization of dissipative PDE systems using nonlinear order reduction," *Chemical Engineering Science*, vol. 57, pp. 5083–5114, 2002.

[7] J. Baker, A. Armaou and P.D. Christofides, "Nonlinear control of incompressible fluid flow: application to Burgers' equation and 2D channel flow," *J. Math. Anal. Appl.*, vol. 252, pp. 230–255, 2000.

[8] J. Baker, A. Armaou and P.D. Christofides, "Drag reduction in incompressible channel flow using electromagnetic forcing," *Proceedings of the 2000 ACC*, Chicago, pp. 4269–4273, 2000.

[9] J. Baker and P.D. Christofides "Finite-dimensional approximation and control of non-linear parabolic systems," *Int. J. Control*, vol. 73, no. 5, pp. 439-456, 2000.

[10] A. Balogh, W.-J. Liu and M. Krstic M, "Stability enhancement by boundary control in 2D channel flow," *IEEE Transactions on Automatic Control*, vol. 46, pp. 1696–1711, 2001.

[11] A. Balogh and M. Krstic, "Infinite dimensional backstepping for nonlinear parabolic PDEs," in: *Sixty Open Problems in the Mathematics of Systems and Control* (V. Blondel and A. Megretski, Eds.), Princeton University Press, Princeton, NJ, 2003.

[12] B. Bamieh, F. Paganini and M.A. Dahleh M. A. , "Distributed control of spatially-invariant systems," *IEEE Trans. Automatic Control*, vol 45, pp. 1091–1107, 2000.

[13] V. Barbu, "Feedback stabilization of Navier-Stokes equations," *ESAIM: Control, Optim. Cal. Var.*, vol. 9, pp. 197–205, 2003.

[14] V. Barbu, C. Popa, T. Havarneanu and S.S. Sritharan, "Exact controllability of magneto-hydrodynamic equations," *Communications on Pure and Applied Mathematics*, vol. 56(6), pp. 732–783, 2003

[15] V. Barbu, "Stabilization of a plane channel flow by wall normal controllers" Preprint, 2006.

[16] V. Barbu and R. Triggiani, "Internal stabilization of Navier-Stokes equations with finite-dimensional controllers," *Indiana University Mathematics Journal*, vol. 53, pp. 1443–1494, 2004.

[17] V. Barbu, I. Lasiecka and R. Triggiani, "Tangential boundary stabilization of Navier-Stokes equations," *Memoirs of the American Mathematical Society*, vol. 181, no. 852, 2006.

[18] G.K. Batchelor, *An Introduction to Fluid Mechanics*, London, Cambridge University Press, 1967.

[19] K. Beauchard, "Local controllability of a 1-D Schrödinger equation," *J. Math Pures Appl. (9)*, vol. 84(7), pp. 851–956, 2005.

[20] T.W. Berger, J. Kim, C. Lee and J. Lim, "Turbulent boundary layer control utilizing the Lorentz force," *Phys. Fluids*, vol. 12, p. 631, 2000.

[21] T. R. Bewley. "Flow control: new challenges for a new Renaissance," *Progress in Aerospace Sciences*, 37, pp. 21–58, 2001.

[22] T. R. Bewley and B. Protas, "Skin friction and pressure: the 'footprints' of turbulence," *Physica D*, 196, 28–44, 2004.

[23] K.S. Breuer and J. Park, "Actuation and control of a turbulent channel flow using Lorentz forces," *Phys. Fluids*, vol. 16(4), p. 897, 2004.

[24] D. Boskovic and M. Krstic, "Nonlinear stabilization of a thermal convection loop by state feedback," *Automatica*, vol. 37, pp. 2033–2040, 2001.

[25] D. Boskovic and M. Krstic, "Backstepping control of chemical tubular reactors," *Computers and Chemical Engineering*, vol. 26, pp. 1077–1085, 2002.

[26] D. Boskovic and M. Krstic, "Stabilization of a solid propellant rocket instability by state feedback," *lnternational Journal of Robust and Nonlinear Control*, vol. 13, pp. 483–495, 2003.

[27] S. Boyd, L.O. Chua and C.A. Desoer, "Analytical foundations of Volterra series," *Journal of Mathematical Control and Information*, vol. 1, pp. 243–282, 1984.

[28] R. Bracewell, *The Fourier Transform and its Aplications*, 3rd. ed., McGraw-Hill, 1999.

[29] J.W. Brown and R.V. Churchill, *Fourier Series and Boundary Value Problems*, 6th Ed., McGraw-Hill, 2001.

[30] J. A. Burns, B. B. King and D. Rubio, "Feedback control of a thermal fluid using state estimation," *International Journal of Computational Fluid Dynamics*, vol. 11, pp. 93–112, 1998.

[31] H. Chen and L. Rodino, "General theory of PDE and Gevrey classes," in *General theory of partial differential equations and microlocal analysis*, Pitman Res. Notes Math. Ser., vol. 349, pp. 6–81, Longman, 1996.

[32] M. Chevalier, J. Hoepffner, T. R. Bewley and D. S. Henningson, "State estimation in wall-bounded flow systems. Part 2. Turbulent flows," *Journal of Fluid Mechanics*, to appear, 2006.

[33] P.D. Christofides, *Nonlinear and Robust Control of Partial Differential Equation Systems: Methods and Applications to Transport-Reaction Processes*, Birkhauser, Boston, 2001.

[34] J. Cochran, R. Vazquez and M. Krstic, "Backstepping boundary control of Navier-Stokes channel flow: a 3D extension," *Proceedings of the 25th American Control Conference (ACC)*, Minneapolis, 2006.

[35] J.-M. Coron, "On the controllability of the 2D incompressible Navier-Stokes equations with the Navier slip boundary conditions," *ESAIM: Control, Optim. Cal. Var.*, vol. 1, pp. 35–75, 1996.

[36] J.M. Coron, "Local controllability of a 1-D tank containing a fluid modeled by the shallow water equations", *ESAIM: Contr. Optim. Calc. Variat.*, vol. 8, pp. 513–554, 2002.

[37] J.M. Coron and E. Trelat, "Global steady-state controllability of 1-D semilinear heat equation", *SIAM J. Cont. Opt.*, vol. 43(2), pp. 549–569, 2004.

[38] J.M. Coron and E. Trelat, "Global steady-state stabilization and controllability of 1-D semilinear wave equation", *Comun. Contemp. Math.*, vol. 8(4), pp. 1–33, 2006.

[39] K. Beauchard and J.M. Coron, "Controllability of a quantum particle in a moving potential well", *J. Functional Analysis*, vol. 232, pp. 328–389, 2006.

[40] D. Colton, "The solution of initial-boundary value problems for parabolic equations by the method of integral operators," *Journal of Differential Equations*, vol. 26, pp. 181-190, 1977.

[41] R. Courant and D. Hilbert, *Methods of Mathematical Physics*, vol. 2, Interscience Publishers, New York, 1955.

[42] K. Debbagh, P. Cathalifaud and C. Airiau, "Optimal and robust control of small disturbances in a channel flow with a normal magnetic field," preprint, 2006.

[43] K. Deng and H.A. Levine, "The role of critical exponents in blow-up theorems: the sequel," *Journal of Mathematical Analysis and Applications*, vol. 243, pp. 85–126, 2000.

[44] P. G. Drazin, *Introduction to Hydrodynamic Stability*, Cambridge, UK, Cambridge University Press, 2002.

[45] L. C. Evans, *Partial Differential Equations*, American Mathematical Society, Providence, Rhode Island,1998.

[46] C. Fabre, "Uniqueness results for Stokes equations and their consequences in linear and nonlinear control problems," *ESAIM: Control, Optim. Cal. Var.*, vol. 1, pp. 267–302, 1996.

[47] H. Fattorini and D.L. Russell, "Exact controllability theorems for linear parabolic equations in one space dimension," *Arch. Rat. Mech. Anal.*, vol. 43, pp. 272–292, 1971.

[48] C. Fefferman, "Existence and smoothness of the Navier-Stokes equation," *The Clay Mathematics Institute*, `http://www.claymath.org/millennium/Navier-Stokes_Equations/navierstokes.pdf`, 2000.

[49] E. Fernandez-Cara and E. Zuazua, "Null and approximate controllability for weakly blowing up semilinear heat equations," *Annales de l'IHP. Analyse non Linéaire*, vol. 17, pp. 583–616, 2000.

[50] E. Fernandez-Cara, S. Guerrero, O. Y. Imanuvilov, J. P. Puel, "On the controllability of the n-dimensional Navier-Stokes and Boussinesq systems with $n-1$ scalar controls," *Comptes Rendus Mathematique*, vol. 340, pp. 275–280, 2005.

[51] M. Fliess, "Fonctionnelles causales non lineaires et indeterminees non commutatives," *Bull. Soc. Math. France*, 109, pp. 3–40, 1981.

[52] H. Fujita, "On the blowing up of solutions of the cauchy problem for $u_t = \triangle u + u^{1+\alpha}$," *Journal of the Faculty of Sciences, University of Tokyo, Section IA Mathematics*, vol. 13, pp. 105–113, 1966.

[53] A. V. Fursikov, "Stabilization of two-dimensional Navier-Stokes equations with help of a boundary feedback control," *J. Math. Fluid Mech.*, vol. 3(3), pp. 259–301, 2001.

[54] A. V. Fursikov, "Stabilization for the 3-D Navier-Stokes system by feedback boundary control," *Discrete Contin. Dyn. Syst.*, vol. 10, pp. 289–314, 2004.

[55] A. V. Fursikov and M. D. Gunzburger, "Boundary value problems and optimal boundary control for the Navier-Stokes system: the two-dimensional case," *SIAM J. Control Optim.*, vol. 36(3), pp. 852–894, 1998.

[56] J. Guckenheimer and P. Holmes, *Nonlinear Oscillations, Dynamical Systems, and Bifurcations of Vector Fields*, 3rd ed. New York, Springer-Verlag, 1997.

[57] M. D. Gunzburger and S. Manservisi, "The velocity tracking problem for Navier-Stokes flows with boundary control," *SIAM J. Control Optim.*, vol. 39(2), pp. 594–634, 2000.

[58] M. Gevrey, "La nature analytique des solutions des équations aux dérivées partielles," *Ann. Sc. Ecole Norm. Sup.*, vol. 25, pp. 129–190, 1918.

[59] R. Haberman, *Elementary Applied Partial Differential Equations*, Prentice-Hall, Englewood Cliffs, NJ, 1987.

[60] J. Hartmann, "Theory of the laminar flow of an electrically conductive liquid in a homogeneous magnetic field," *Det Kgl. Danske Videnskabernes Selskab. Mathematisk-fysiske Meddelelser*, XV(6), pp. 1–27.

[61] H. Hochstadt, *Integral Equations*, New York, Wiles, 1973.

[62] J. Hoepffner, M. Chevalier, T.R. Bewley and D.S. Henningson, "State estimation in wall-bounded flow systems. Part 1. Perturbed laminar flows." *Journal of Fluid Mechanics*, vol. 534, pp. 263–294, 2005.

[63] M. Hogberg, T.R. Bewley and D.S. Henningson, "Linear feedback control and estimation of transition in plane channel flow," *Journal of Fluid Mechanics*, vol. 481, pp.149–175, 2003.

[64] O.Y. Imanuvilov, "On exact controllability for the Navier-Stokes equations," *ESAIM: Control, Optim. Cal. Var.*, vol. 3, pp. 97–131, 1998.

[65] A. Isidori, *Nonlinear Control Systems*, Springer-Verlag, Berlin, 1995.

[66] M.R. Jovanovic and B. Bamieh, "Componentwise energy amplification in channel flows," *J. Fluid Mech.*, vol. 543, pp. 145–183, 2005.

[67] Y. Kannai, "Nonexistence for a boundary value problem arising in parabolic theory," *Israel Journal of Mathematics*, vol. 71, pp. 349–351, 1990.

[68] C. H. Von Kerczek, "The instability of oscillatory plane Poiseuille flow," *J. Fluid Mech.*, vol. 116, pp. 91–114, 1982.

[69] H. K. Khalil, *Nonlinear Systems*, 3rd edition, Prentice-Hall, Englewood Cliffs, NJ, 2002.

[70] P. V. Kokotovic, H. K. Khalil and J. O'Reilly, *Singular Perturbation Methods in Control*, Philadelphia, SIAM Classics in Applied Mathematics, 1999.

[71] M. Krstic, I. Kanellakopoulos, and P. V. Kokotovic, *Nonlinear and Adaptive Control Design*, Wiley, 1995.

[72] M. Krstic, "On global stabilization of Burgers' equation by boundary control," *Systems and Control Letters*, vol. 37, pp. 123–141, 1999.

[73] M. Krstic, A. Smyshlyaev, and A. Siranosian, "Backtepping boundary controllers and observers for the slender Timoshenko beam: Part I Design, *Proceedings of the 2006 American Control Conference*, Minneapolis, 2006.

[74] A. Kugi, D. Thull, and K. Kuhnen, "An infinite-dimensional control concept for piezoelectric structures with complex hysteresis," *Structural Control and Health Monitoring*, 13, pp. 1099–1119, 2006.

[75] B. Laroche, P. Martin and P. Rouchon, "Motion planning for the heat equation," *International Journal of Robust and Nonlinear Control*, vol. 10, pp. 629–643, 2000.

[76] F. Lamnabhi-Lagarrigue, "Volterra and Fliess series expansions for nonlinear systems," in: *The Control Handbook* (W.S. Levine, Ed.), pp.879–888, CRC Press, Boca Raton, FL, 1996.

[77] E. Lauga, T. R. Bewley, " The decay of stabilizability with Reynolds number in a linear model of spatially developing flows," *Proc. R. Soc. Lond. A*, vol. 459, pp. 2077–2095, 2003.

[78] E. Lauga, T. R. Bewley, "Modern control of linear global instability in a cylinder wake model," *International Journal of Heat and Fluid Flow*, vol. 23, pp. 671–677, 2002.

[79] D. Lee and H. Choi, "Magnetohydrodynamic turbulent flow in a channel at low magnetic Reynolds number," *Journal of Fluid Mechanics*, vol. 439, pp. 367–394, 2001.

[80] H.A. Levine, "The role of critical exponents in blow-up theorems," *SIAM Review*, vol. 32, pp. 262–288, 1990.

[81] L.R Lines, R. Slawinski and R.P. Bording, "A recipe for stability of finite-difference wave-equation computations," *Geophysics*, vol. 64, pp. 967–969, 1999.

[82] W. J. Liu, "Boundary feedback stabilization of an unstable heat equation," *SIAM J. Control Optim.*, vol. 42, no. 3, pp. 1033–1043.

[83] E. N. Lorenz, "Deterministic non-periodic flow," *J. Atmos. Sci.*, vol. 20, pp. 130–141,1963.

[84] T. Meurer, *Feedforward and Feedback Tracking Control of Diffusion-Convection-Reaction Systems using Summability Methods*, Doctoral Dissertation, Stuttgart University, 2005.

[85] U. Muller and L. Buhler, *Magnetofluiddynamics in Channels and Containers*, Berlin, Springer, 2001.

[86] J. Pang and K.-S. Choi, "Turbulent drag reduction by Lorentz force oscillation," *Phys. Fluids*, vol. 16(5), L35, 2004.

[87] B. Protas and A. Styczek, "Optimal control of the cylinder wake in the laminar regime," *Physics of Fluids*, vol. 14, no. 7, pp. 2073–2087, 2002.

[88] J.-P. Raymond, "Feedback boundary stabilization of the two dimensional Navier-Stokes equations," *SIAM Journal on Control and Optimization*, vol. 45, pp. 790–828, 2006.

[89] S. C. Reddy, P.J. Schmid, and D.S. Henningson, "Pseudospectra of the Orr-Sommerfeld operator," *SIAM J. Appl. Math.*, vol. 53, no. 1, pp. 15–47, 1993.

[90] F. J. Rubio-Sierra, R. Vazquez and R. Stark, "Transfer function analysis of the micro cantilever used in atomic force microscopy," *IEEE Transactions on Nanotechnology*, vol. 5, pp. 692–700, 2006.

[91] W. Rudin, *Real and Complex Analysis* , 3rd ed., New York, McGraw-Hill, 1986.

[92] W.J. Rugh, *Nonlinear Sytem Theory: The Volterra/Wiener Approach*, Web version, `http://www.ece.jhu.edu/~rugh/volterra/book.pdf`, 1981.

[93] S. Sastry, *Nonlinear Systems: Analysis, Stability and Control*, Springer-Verlag, New York, 1999.

[94] E. Schuster and M. Kristic, "Inverse optimal boundary control for mixing in magnetohydrodynamic channel flows," *Proceedings of the 2003 CDC*, Maui, Hawaii USA, 2003.

[95] P.J. Schmid and D.S. Henningson, *Stability and Transition in Shear Flows*, Berlin, Springer, 2001.

[96] M. Schmidt and E. Trélat, "Controllability of Couette-Taylor flows by rotating cylinders," *Comm. Pure Applied Analysis*, vol. 5(1), pp. 201–211, 2006.

[97] T. I. Seidman, "Two results on exact boundary control of parabolic equations," *Applied Mathematics and Optimization*, vol. 11, pp. 145-152, 1984.

[98] R. Sepulchre, M. Jankovic and P.V. Kokotovic, *Constructive Nonlinear Control*, Springer-Verlag, New York, 1997.

[99] M. Sermange and R. Temam, "Some mathematical questions related to the MHD equations," *Communications on Pure and Applied Mathematics*, vol. 36, pp. 635–664, 1983.

[100] G. F. Simmons, *Differential Equations With Applications and Historical Notes*, New York, McGraw-Hill, 1991.

[101] A. Smyshlyaev and M. Krstic, "Closed form boundary state feedbacks for a class of partial integro-differential equations," *IEEE Transactions on Automatic Control*, vol. 49, pp. 2185–2202, 2004.

[102] A. Smyshlyaev and M. Krstic, "Backstepping observers for parabolic PDEs," *Systems and Control Letters*, vol. 54, pp. 1953–1971, 2005.

[103] A. Smyshlyaev and M. Krstic, "On control design for PDEs with space-dependent diffusivity or time-dependent reactivity," *Automatica*, 41, pp. 1601-1608, 2005.

[104] S.S. Sritharan, "Stochastic Navier-Stokes equations: solvability, control and filtering," in *Stochastic Partial Differential Equations and Applications - VII*, G. Da Prato and L. Tubaro eds., pp. 273–280, Chapman & Hall/CRC, 2006.

[105] S.S. Sritharan, "On the acceleration of viscous fluid through an unbounded channel," *Journal of Mathematical Analysis and Applications*, vol. 168(1), pp. 255–283, 1992.

[106] S.S. Sritharan, V. Barbu, T. Havarneanu and C. Popa, "Local controllability for the magnetohydrodynamic equations revisited," *Advances in Differential Equations*, vol. 10(5), pp. 481–504, 2005.

[107] R. Temam, *Navier-Stokes Equations and Nonlinear Functional Analysis*, Second edition, SIAM, Philadelphia,1995.

[108] R. Temam, *Navier-Stokes Equations*, Studies in Mathematics and its Applications, vol. 2, North-Holland Publishing Co., Amsterdam, 1984.

[109] J.-P. Thibault and L. Rossi, "Electromagnetic flow control: characteristic numbers and flow regimes of a wall-normal actuator," *J. Phys. D: Appl. Phys.*, vol. 36, pp. 2559–2568, 2003.

[110] R. Triggiani, "Exponential feedback stabilization of a 2-D linearized Navier-Stokes channel flow by finite-dimensional, wall-normal boundary controllers, with arbitrarily small support," preprint, 2006

[111] R. Vazquez and M. Krstic, "Volterra Boundary Control Laws for a Class of Nonlinear Parabolic Partial Differential Equations," *Proc. of the NOLCOS 2004*, Stuttgart, Germany, 2004.

[112] R. Vazquez and M. Krstic, "Explicit integral operator feedback for local stabilization of nonlinear thermal convection loop PDEs," *Systems and Control Letters*, vol. 55, pp. 624–632, 2006.

[113] R. Vazquez and M. Krstic, "A closed-form feedback controller for stabilization of linearized Navier-Stokes equations: the 2D Poiseuille flow," *Proc. of the 2005 CDC*, Sevilla, Spain, 2005.

[114] R. Vazquez and M. Krstic, "A closed-form observer for the channel flow Navier-Stokes system," *Proc. of the 2005 CDC*, Sevilla, Spain, 2005.

[115] R. Vazquez and M. Krstic, "Higher order stability properties of a 2D Navier-Stokes system with an explicit boundary controller," *Proc. of the 2006 ACC*, Minneapolis, 2006.

[116] R. Vazquez, E. Trélat and J.-M. Coron, "Stable Poiseuille flow transfer for a Navier-Stokes system," *Proc. of the 2006 ACC*, Minneapolis, 2006.

[117] R. Vazquez, E. Schuster and M. Krstic, "A closed-form observer for the 3D inductionless MHD and Navier-Stokes channel flow," *Proc. of the 2006 CDC*, San Diego, 2006.

[118] R. Vazquez and M. Krstic, "Control of 1-D parabolic PDEs with Volterra nonlinearities—Part I: Design," in preparation, 2006.

[119] R. Vazquez and M. Krstic, "Control of 1-D parabolic PDEs with Volterra nonlinearities—Part II: Analysis," in preparation, 2006.

[120] R. Vazquez and M. Krstic, "Explicit output feedback stabilization of a thermal convection loop by continuous backstepping and singular perturbations," submitted, *2007 American Control Conference*, New York, 2007.

[121] R. Vazquez, E. Schuster and M. Krstic, "A closed-form feedback controller for stabilization of magnetohydrodynamic channel flow," submitted, *2007 European Control Conference*, Kos, Greece, 2007.

[122] R. Vazquez, F. J. Rubio-Sierra and R. Stark, "Transfer function analysis of a surface coupled atomic force microscope cantilever system," *Proc. of the 2006 ACC*, Minneapolis, 2006.

[123] V. Volterra, *Theory Of Functionals And Of Integral And Integro-Differential Equations*, Dover, New York, 1959.

[124] E. Zuazua, "Propagation, observation, control and numerical approximation of waves," *SIAM Review*, 47, pp. 197–243.